

Identifying regulators of lung epithelial cell differentiation by using a forward genetic screening approach in mouse



Dissertation
zur Erlangung des Doktorgrades
der Naturwissenschaften

vorgelegt beim Fachbereich 15
der Goethe-Universität
in Frankfurt am Main

von
Ziba Jaberansari
Aus Tehran, Iran

Frankfurt am Main (2016)

(D30)

Vom Fachbereich der
Goethe Universität als Dissertation angenommen.

Dekan: Prof. Dr. Meike Piepenbring

Gutachter: Prof. Dr. Didier Stainier

Prof. Dr. Anna Starzinski-Powitz

Datum der Disputation:

EIDESSTATTLICHE ERKLÄRUNG

Hiermit versichere ich, dass ich die vorliegende Dissertation selbständig und nur unter zu Hilfe-nahme der hier angegebenen Quellen und Hilfsmitteln verfasst habe.

Die Dissertation wurde bisher keiner anderen Fakultät vorgelegt. Ich erkläre, dass ich bisher kein Promotionsverfahren erfolglos beendet habe und dass keine Aberkennung eines bereits erworbenen Doktorgrades vorliegt.

Frankfurt, den 01.02.2016

Ziba Jaberansari

Abstract:

Identifying regulators of lung epithelial cell differentiation by using a forward genetic screening approach in mouse

The lung comprises more than 40 different cell types, from epithelial cells to resident mesenchymal cells. These cells arise from the foregut endoderm and differentiate into specialized cell types that form the respiratory and conducting airways, and the trachea. However, the molecular pathways underlying these differentiation processes are poorly understood, and may be relevant to pathological conditions. According to the World Health Organization (WHO), while the respiratory disease rate is increasing, limited treatment and therapies are available. Thus, there is a growing need for new treatment strategies and alternative therapies. Various *in vivo* and *in vitro* studies in the model organism *mus musculus* have already provided valuable information on lung cell lineages and their differentiation and/ or dedifferentiation during development and pathological conditions. However, there remain many questions regarding the key regulators and molecular machinery driving lung cell differentiation and underlying lung progenitor/stem cell biology.

Aiming to develop new animal models for lung diseases, we used a forward genetic screening approach, which provides an unbiased method for identifying genes with important roles in lung cell differentiation, and thus probable contributors to pathological conditions. We conducted an *N*-ethyl-*N*-nitrosourea (ENU) mutagenesis screen in mice and used several histological and immunohistochemical approaches to identify and isolate mutants, focusing on mutations associated with cell differentiation rather than those affecting early development and patterning of the respiratory system. Thus, we screened for phenotypes in the respiratory system of pups from the F2 generation at postnatal day 7 and 0 (P7; P0). I specifically screened 114 families. Each F1 male animal is the founder of 5 to 6 F2 female daughters. For each family, at least 4 F2 females per male founder were analyzed. In total, I screened 630 litters at P7 and P0 with 7 pups on average for each litter. As a result of this extensive screening, 11 different phenotypes in 42 different F2s were discovered at primary screen and later just 2 phenotypes recovered in F3 generation of identified carriers. To identify the causative genes for each of these phenotypes, whole exome sequencing will be conducted in the future to identify recurring SNPs; these can subsequently be linked causatively to the resultant phenotype(s) via complementation studies. In turn, these linkages would enable the

creation of mutant mice using CRISPR/Cas9 genomic engineering, which would be invaluable to the further study of respiratory development and disease.

Table of Contents

Eidesstattliche Erklärung:.....	i
Abstract.....	ii

Chapter 1

1.Introduction	10
<u>1.1. Lung development and function</u>	10
<u>1.2. Overview of lung development</u>	12
<u>1.3.Lung structure and cells types</u>	15

Chapter 2

Designing a study model for <i>in-vivo</i> lung cell differentiation and histopathology research.....	30
2.1. Pulmonary fibrosis and Interstitial Lung Diseases (ILD) models.....	31
<u>2.1.1 Inherited Interstitial Lung Disease Surfactant Protein C Mutations</u>	31
<u>2.1.2. Pulmonary Fibrosis models</u>	33
<u>2.1.3. Cystic fibrosis models</u>	35
<u>2.1.4. Other mouse models for lung disease</u>	35
<u>Neoplastic lung disease and Lung cancer</u>	36
2.2. Experimental approach.....	38
<u>2.2.1. - Forward genetic screen background</u>	38
<u>2.2.2. ENU mutagenizing in animal models</u>	42
<u>2.2.3. Previous ENU forward genetic screen work on mouse</u>	47
2.3. Discovering of the causative gene in identified phenotype.....	50
<u>2.3.1. Isolation of phenotypes</u>	50
<u>2.3.2. Mapping and whole exome sequencing</u>	51

Chapter 3

Materials and methods.....	53
3.1. <u>Equipment</u>	53
Disposable	53
Non-disposables	54
3.2. <u>Buffer and solutions</u>	56
Antibodies	57
Primary Antibodies.....	57
Hybridoma bank antibodies.....	57
Secondary antibodies.....	58
Methods	59
1. <u>Mice</u>	59
1.2. <u>ENU mutagenesis and Breeding strategy</u>	59
1.3. <u>Lung and trachea isolation</u>	60
2. <u>Staining</u>	63

Chapter 4

Results

4.1. Inflammation, bronchiolitis, collapse lobe phenotypes.....	75
4.1.1. <u>Most significant founder:</u>	75
4.1.2. <u>Second most significant founder</u>	89
4.2. Identified phenotype with F3 generation.....	97
4.2.1. <u>Founder 1(ID#398443); carriers with alveolar interstitial inflammation</u>	97
4.2-2- <u>Founder 2 (ID#404656); carriers with alveolar interstitial inflammation</u>	102
4.3. Phenotypes without recovered F3 carrier or with different characteristics in recovered phenotype from primary phenotype	107
4.3.1. <u>lung nodule</u>	107

<u>4.3.2. Abnormal AECI distribution and interstitial inflammatory cell mass and sub cutaneous hemorrhage</u>	117
<u>4.3.3. Leaking vessel phenotype</u>	122
<u>4.3.4. Tracheal Goblet cells hyperplasia and accumulation of mucus in distal airways</u>	123
<u>4.3.5. Alveolar collapse, Neonatal respiratory distress syndrome (NRDS)</u>	126

Chapter 5

Discussion and outlooks	128
The possible mechanisms associated with phenotype.....	129
Conclusion.....	138
Future direction	143
Mapping Whole Exome Sequencing.....	143
ZUSAMMENFASSUNG.....	146
References.....	152
Acknowledgment.....	159
Curriculum Vitae.....	160

Abbreviation

α -SMA: Alpha-smooth muscle actin

AECI: Alveolar epithelial cells type 1

AECII: Alveolar epithelial cells type 2

BADJ: Bronchioalveolar duct junction

BSA: Bovine serum albumin

BASCs: Bronchioalveolar stem cells

CCSP: Clara cell secretory protein

° C: Degree Celsius

DAPI: 4', 6-Diamidino-2-phenylindole

DASC: distal airway club stem cells

ENU: *N*-ethyl-*N*-nitrosourea

EpCAM: Epithelial cell adhesion molecule

MSCs: Mesenchymal stem cells

ml: Milliliter

μ l: Microliter

mM: Millimolar

mm: Millimeter

min: Minute

mRNA: Messenger RNA

MUC5AC: Mucin-5AC

PBS: Phosphate buffered saline

PCNA: Proliferating-cell-nuclear-antigen

PDGFR- α : Platelet-derived growth factor receptor-alpha

PDGFR- β : Platelet-derived growth factor receptor-beta

PFA: Paraformaldehyde

RT: Room temperature

SPC: Surfactant protein C

SMGs: Submucosal glands

VEGF: Vascular endothelial growth factor

v/v: Volume to volume

w/v: Weight/volume

Chapter1

1.Introduction

1.1. Lung development and function

The respiratory system represents an important innovation for terrestrial animal evolution. In fact, this organ is one of the most recent organs to have evolved in mammals. The cardiovascular and pulmonary systems co-developed through the evolution to adopt life outside of water from ancient fish descendants. Therefore, embryonic lung development represents a useful model to study complex tissue interactions during organ development. According to the World Health Organization (WHO), while the respiratory diseases rate is increasing, limited treatment and therapies are available for lung diseases. The lung transplantation usually is the one and only option for patients. Approximately only in the United States 1,000–1,500 lung transplant operation perform yearly. Due to a significant shortage of suitable donors and complications of lung transplantation such as lifelong immunosuppression and approximately 50% mortality rate due to chronic rejection, new approaches and therapies are required. Most lethal respiratory diseases are lung cancer, adenocarcinoma and Idiopathic Pulmonary Fibrosis (IPF). Thus, there is a growing need for new drugs and alternative therapies. The development of new therapies is boosted by the discovery of novel factors involved in processes of initiation and development of pathological condition. Indeed, underlying mechanisms of respiratory diseases is not clear.

In this regard, various *in vivo* and *in vitro* studies in the mouse model have already developed and provided valuable information on lung cell lineages, molecular and cellular mechanisms that involve in processes of lung development. However, there is still much more to learn about lung cell differentiation and dedifferentiation regulators and lung progenitor/ stem cells during development and pathological conditions. For example there is not any available animal model for lethal respiratory disease such as IPF.

In addition, many of the intercellular signaling networks in morphogenesis of the respiratory system are conserved. Thus, studying them can help us to understand the development

of other branched tubular organs such as the kidney, mammary gland, and prostate (Morrisey & Hogan, 2010).

A complete respiratory system is composed of the proximal conducting airways and the distal gas-exchanging alveolar space. The development of respiratory organ is composed of 5 stages: embryonic, pseudoglandular, canalicular, saccular, and alveolar. In Figure 1, the steps of lung development illustrated. In this figure, summary of lung development five stages and main signaling factors presented.

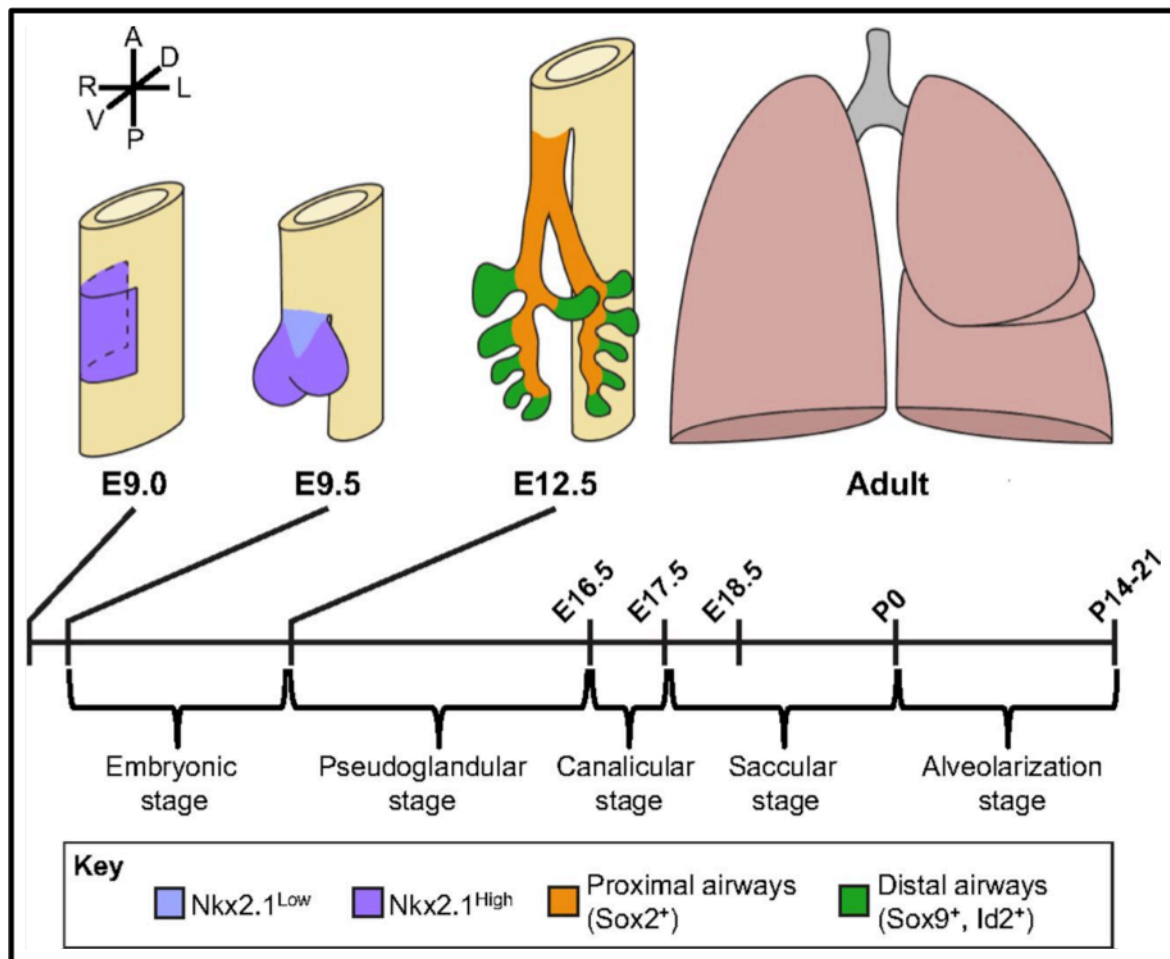


Figure 1. Overview of lung development five stages time points and most important signaling factors (Morrisey & Hogan, 2010)

1.2. Overview of lung development:

In mice the respiratory system (the trachea and lungs) develops from precursors at ventral wall of anterior foregut endoderm at embryonic age 9.5 (~22 somite stage), indeed at area of *Nkx2.1* expression initiation. By E9.5-E10.0, the formation of the trachea is observed and the embryonic stage of lung development begins and ends at E12.5. The single foregut tube divided into two tubes. First, ventral part with expression of *Nkx2-1* (*Ttf1*) forms trachea. Then, esophagus derive from dorsal part with *Sox2* expression. In addition, surrounding mesenchyme with *Bmps*, *Noggin*, *Fgfs* and *Wnts* signaling are involving in foregut separation. The lung tissue has double origin and many processes of lung development are dependent on the interaction between epithelium and mesenchyme. The previous *in vitro* transplantation experiments shown a cross-talk between the endodermal epithelium and the mesodermal mesenchyme for branching morphogenesis and cytodifferentiation (Shannon & Hyatt, 2004). For example, removal of mesenchyme from the branching tips; prevents the epithelial tubules formation. However; if mesenchyme of the growing tips were transplant adjacent to the prospective trachea, bronchial branches outgrowth abnormally from trachea's domain (Schittny & Burri, 2008). The branching process is a particular process and similar with the other branched organs. It has been reported, airways and formation of tree like lung branches play a fundamental role in arterial and smooth muscle patterning in respiratory organ. Many works has done to decode the airway branching. In this regard, Metzger et al reported that *Spry2* regulates the site of initiation and number of branches in specific domains in lung (Metzger, Klein, Martin, & Krasnow, 2008).

The lung morphogenesis dependent on a cross-talk between the endodermal-derived epithelium and the mesodermal-derived lung mesenchyme. A major signaling pathway in this communication is *Shh* and highly expressed by embryonic lung epithelium. In addition, the *Patched* (*Ptc*) which is the receptor for *Shh*, is expressed by the lung mesenchyme that highly focalized *Fgf10* production. The *Fgf10* is prominent player of directing epithelial morphogenesis to lung development (Shannon & Hyatt, 2004). By end of the embryonic stage mesenchymal cells around the prospective trachea condense focally and differentiate into cartilage precursors. Cartilage formation moves from proximal to distal along with the future airways. Cartilage formation continues until the end of the canalicular stage and it completes around the smallest bronchi (Schittny & Burri, 2008).

Previous research studies has shown deficiencies in Shh, Gli1/Gli3, RARs, Fgfr2, Fgf10, Foxf1, Sox2, Nkx2-1, Bmp4, Noggin, and Wnts lead to defects in foregut development such as tracheoesophageal fistula and esophageal atresia (EA/TEF) (Morrisey & Hogan, 2010). Some transcription factors are required for regulating whole transcriptional programs in epithelial cells of the respiratory system such as Gata and Foxa transcription factors. Indeed, Foxa, Gata6, and Nkx2-1 provide an environment in endoderm to transcription of respiratory system-specific genes, at the time of trachea specification and throughout the lung development. The detail of most current information on patterning and morphogenesis of foregut endoderm presented in Figure2.

As is shown at specification of the future trachea and lungs; Nkx2-1 and Wnt2/2b and FGF signals express highly from the mesoderm. In addition, from anterior of endoderm Shh through Foxf1, Gli1 and Gli3 triggers Bmp4 signaling. It induces bifurcation of this domain. The Fgf10 signaling requires retinoic acid (RA) signaling and involves inhibition of Tgf β . In the other word, the endogenous RA maintains low levels of Tgf β signaling in the mesoderm of the lung field to allow *Fgf10* expression and lung bud generation (F. Chen et al., 2007).

By E12 the organogenesis of major airways finish. From E12-E16.5 the bronchial morphogenesis happens. This is “pseudoglandular stage” and highly depend on Fgf10 and Fgfr2 expression in the mesoderm and endoderm respectively. The next step is formation and spreading out of conducting airways. During canalicular stage (E16.5- E17.5) distal epithelium and mesenchyme differentiates and form the early gas-exchange units. In addition, the cuboidal epithelial cells differentiates into type I and type II alveolar epithelial cells and surfactants produce. Indeed, at this stage lung parenchyma canalized by capillaries. Therefore, this stage has been named Canalicular. Meanwhile, widening and lengthening at distal of bronchiole forms air sacs. Each of these air sacs called alveolus which means little cavity in Latin. During the alveolarization stage (E17.5-P4) the future airways expands. In addition, inside the alveoli a crest or edge ingrowth and an inter-saccular septa forms. However, the morphology of alveoli changes until the end of postnatal period at alveolar stage (P4-P14). In this step secondary septum develops (Schittny & Burri, 2008). Furthermore, myofibroblast progenitor cells and endothelial cells migrate to these crests. These structures are high in elastin content, especially at their tips.

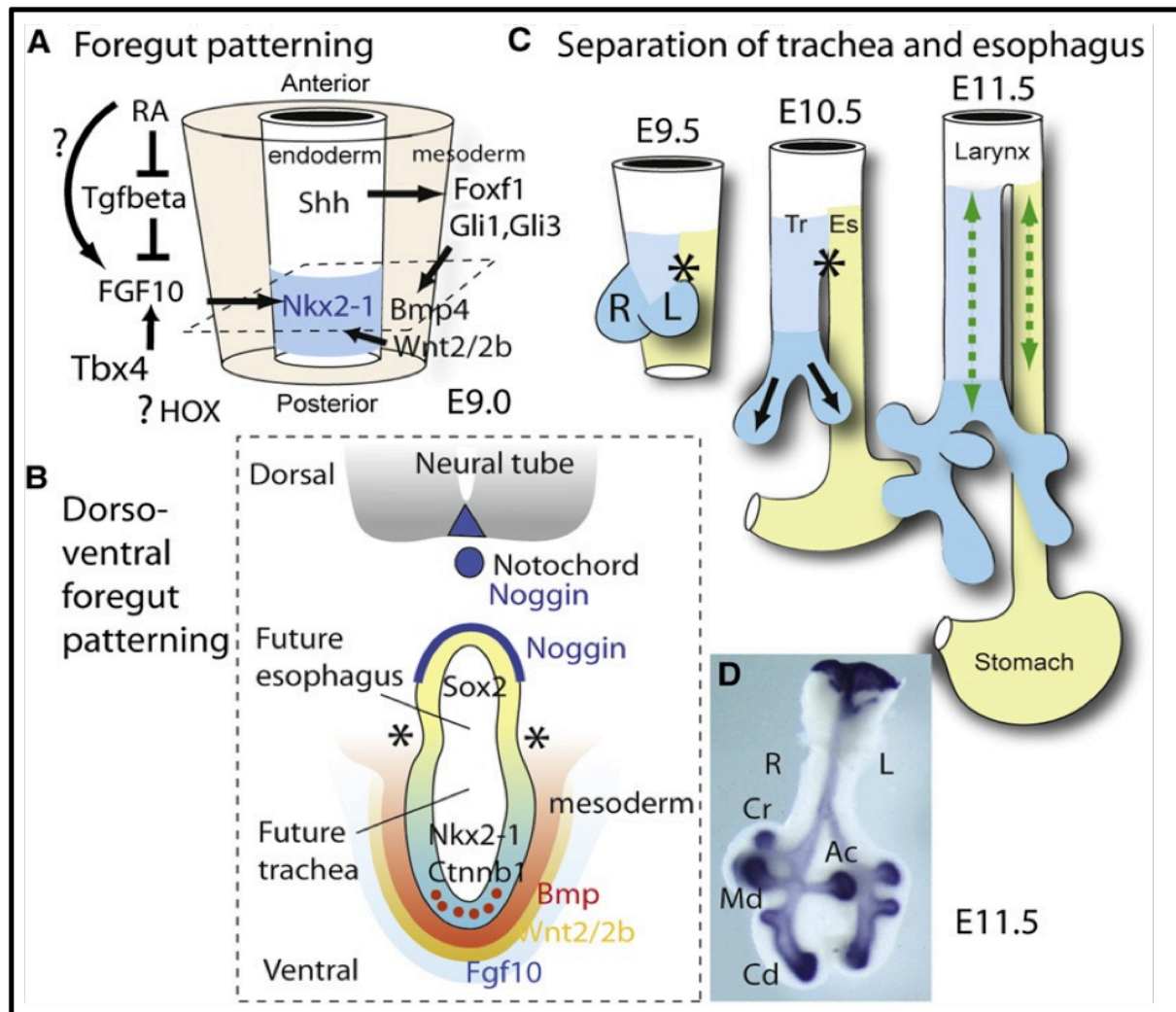


Figure 2. Patterning and Morphogenesis of the anterior foregut and relevant signals. Early specification of the future trachea and lungs with high expression of Nkx2-1 and Wnt2/2b and FGF signals from the mesoderm. From anterior of endoderm Shh through Foxf1 and Gli1 and Gli3 triggers Bmp4 signaling and induce bifurcation of this domain. The Fgf10 signaling requires retinoic acid (RA) signaling and involves inhibition of Tgfb. The endogenous RA controls Tgfb activity in the prospective lung field to allow local expression of *Fgf10* and induction of lung buds (F. Chen et al., 2007). (B) Schematic section through undivided foregut at the level of the dotted box in (A) showing the highest Sox2 levels dorsally, and Nkx2-1, ventrally. The action of Bmp4 is antagonized by noggin (Domyan et al., 2011). Asterisks mark the site of separation of foregut into two tubes. (C) Embryonic ages and separation of the foregut tube into trachea and esophagus begins at anterior of the lung buds (asterisk). There is also extensive elongation of the two tubes (green arrows) as well as outgrowth of primary lung buds. (D) Whole-mount in situ hybridization for Shh showing expression in the endoderm with highest levels in distal tips. Domain branching gives rise to the primordial buds of the right cranial (Cr), medial (Md), caudal (Cd), and accessory (Ac) lobes. Figure 2, adopted from (Morrissey & Hogan, 2010).

1.3.Lung structure and cells types:

Lung organ has a very complex three dimensional structure and composed of various cell types with very divers physiological function throughout proximal to dorsal of lung.

At the proximal part of lung organ, the trachea and main bronchi consists of pseudostratified epithelium. This pseudostratified mucociliary epithelium of the lung composed of Basal cells; approximately 30% J. R. Rock et al. (2009). These basal cells are fairly undifferentiated. In addition, ciliated cells, club cells so called Clara cells and a few mucus/goblet cells form pseudostratified mucociliary epithelium. The most important cell types in trachea and lung epithelium and their main locations illustrated in Figure3. As is indicated in Figure.3 lung organized into three anatomical regions; trachea and main bronchi, intralobar airways and alveoli. These three area totally contains 5 different parts and presumably consists stem cell niches. According to normal homeostasis model presented at Figure 3; three cell types are lung progenitor cells and all lung epithelial cells derived from them.

Throughout the lung organ, the intercartilage regions in the proximal trachea assumed as first stem/ progenitor cells niche (Volckaert & De Langhe, 2014). Secondly, intralobar airway epithelium composed of club, ciliated and clusters of neuroendocrine (NE) cells called NE bodies (NEBs), Figure3(2). Third, bronchioalveolar duct junctions (BADJs) that located at branching points, BADJs containing a population of naphthalene-resistant (variant) club cells. These cells play role in lung regeneration process Figure3 (3). In fact, club cells are known to have stemness and capable of self-renewal for the maintenance and repair of bronchioles. A subset of club cells called as variant club /Club^v cells. They are resistant to naphthalene treatment. Club^v cells exist at either the bronchioalveolar duct junctions (BADJs) or neuroendocrine bodies (NEBs) (Rawlins & Hogan, 2006). At BADJs some Club^v cells expressing Scgb1a1 (secretoglobin, family 1A, member 1/ CCSP:clara cells secretory protein) as well as Pro SP-C. These cells, termed as bronchioalveolar stem cells (BASCs: Scgb1a1+/Sftpc+) and differentiate into both Club cells and AT2s in vitro (Zheng et al., 2013). The Club cells do not give rise to AEC2 and AEC1 cells after injury to the alveoli by hyperoxia. Therefore, while Club cells can be considered a stem cell population; they don't have stemness in all injury/repair models (Hogan et al., 2014). The NEBs also can be a niche for the Clara^V cells as well as very innervated. Moreover, BADJ region

contains putative BASCs (Giangreco, Reynolds, & Stripp, 2002; Reynolds, Giangreco, Power, & Stripp, 2000). These two regions are full of blood vessels.

In the most distal part of lung, alveolar epithelium consist of two type of alveolar/ pneumocyte cells. Alveolar type II cells called alveolar progenitor cells. These cells are long-term self-renewing stem cells and give rise to ATI cells Figure3 (5).

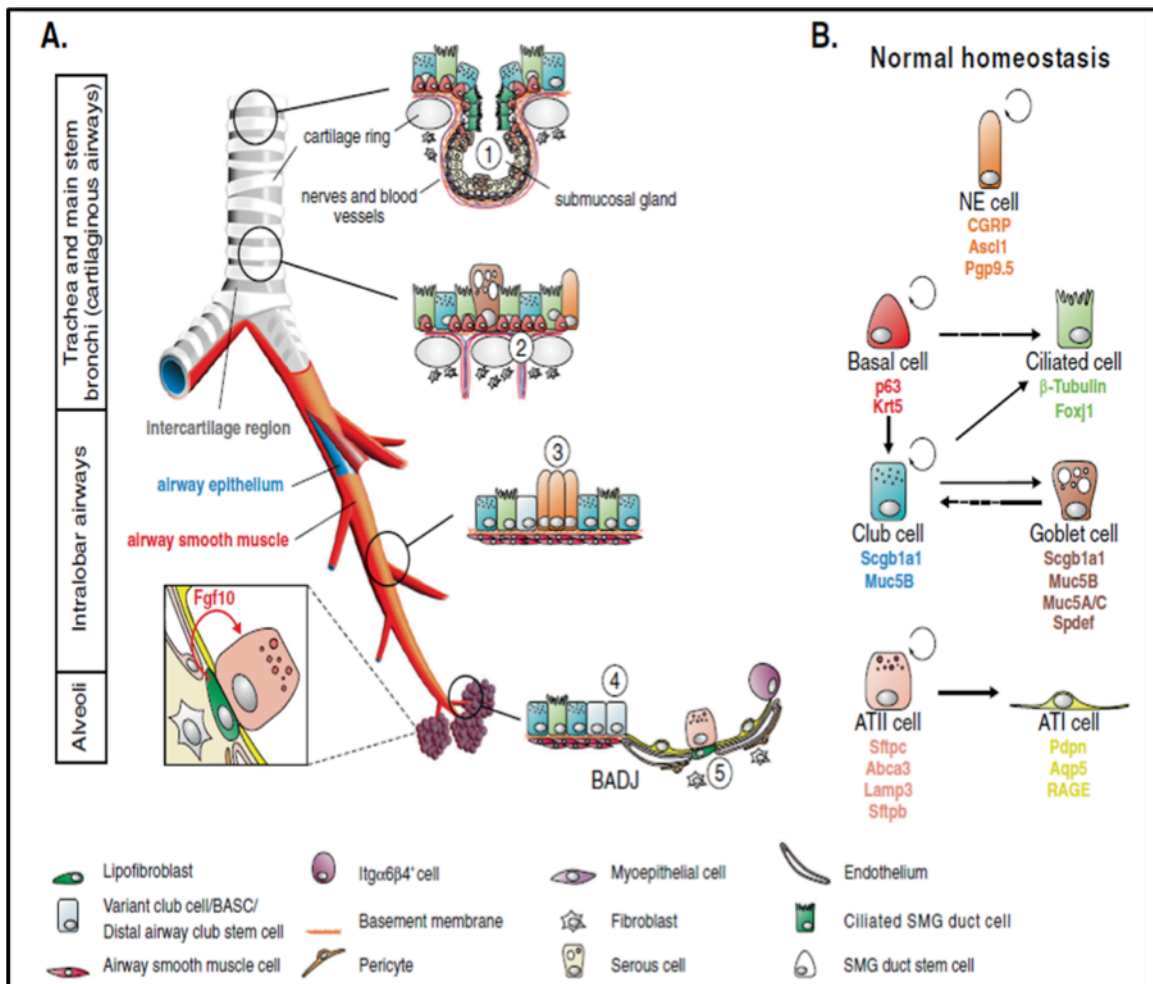


Figure 3. The adult mouse lung epithelium with various cells types and normal homeostasis. (A) The mouse lung organization into three anatomical regions: The cartilaginous airways trachea and main stem bronchi are lined by a pseudostratified epithelium consisting of secretory (club and goblet), ciliated, basal and a few scattered neuroendocrine (NE) cells. Submucosal glands (SMGs) are located between cartilage rings of the proximal trachea and contain a stem cell population in their ducts (1) basal stem cells in the intercartilage regions (2). The intra lobar airway epithelium contains club, ciliated and clusters of NE cells called NE bodies (NEBs), (3) Naphthalene-resistant (variant) club cells are located adjacent to the NEBs and at the bronchioalveolar duct junctions (BADJs). (4) bronchioalveolar stem cells (BASCs) and distal airway club stem cells (DASCs) which are activated after injury. (5). The alveolar epithelium consists a niche that controls the behavior of ATII cells during normal homeostasis and after injury. Lipofibroblasts in the lung interstitium express Fgf10 and are found juxtaposed to ATII stem cells. (B) Lineage relationships of lung epithelial stem cells and their progeny during normal homeostasis. Dashed arrows represent lineage relationships, that not yet been definitively established (Volckaert & De Langhe, 2014)

Although, many work has done to identify the lineage relationships of lung epithelial stem cells and their progeny during normal homeostasis and pathological conditions. Still it needs to define how the undifferentiated epithelial cells that presented in the primary buds, give rise to all of the specialized cells of the postnatal lung (Morrisey & Hogan, 2010).

The available epithelial cell lineage models also need to clarify meticulously. In this regard, Figure 4, represent the recent model and unknown facts which need to be investigated. The recent cell lineages studies (Rawlins, Clark, Xue, & Hogan, 2009) shows that between E11.5 and E13.5, a cell population at distal tip give rise to club, ciliated, and NE cells as well as to AEC1 and AEC2. However, these cells at E17.5 only populate the alveoli. Though this study was very informative on epithelial development; the mechanisms that regulate the number and developmental potential of the distal progenitor populations need to investigate at different stages. Moreover, it is not clear what controls the allocation of their descendants to different lineages.

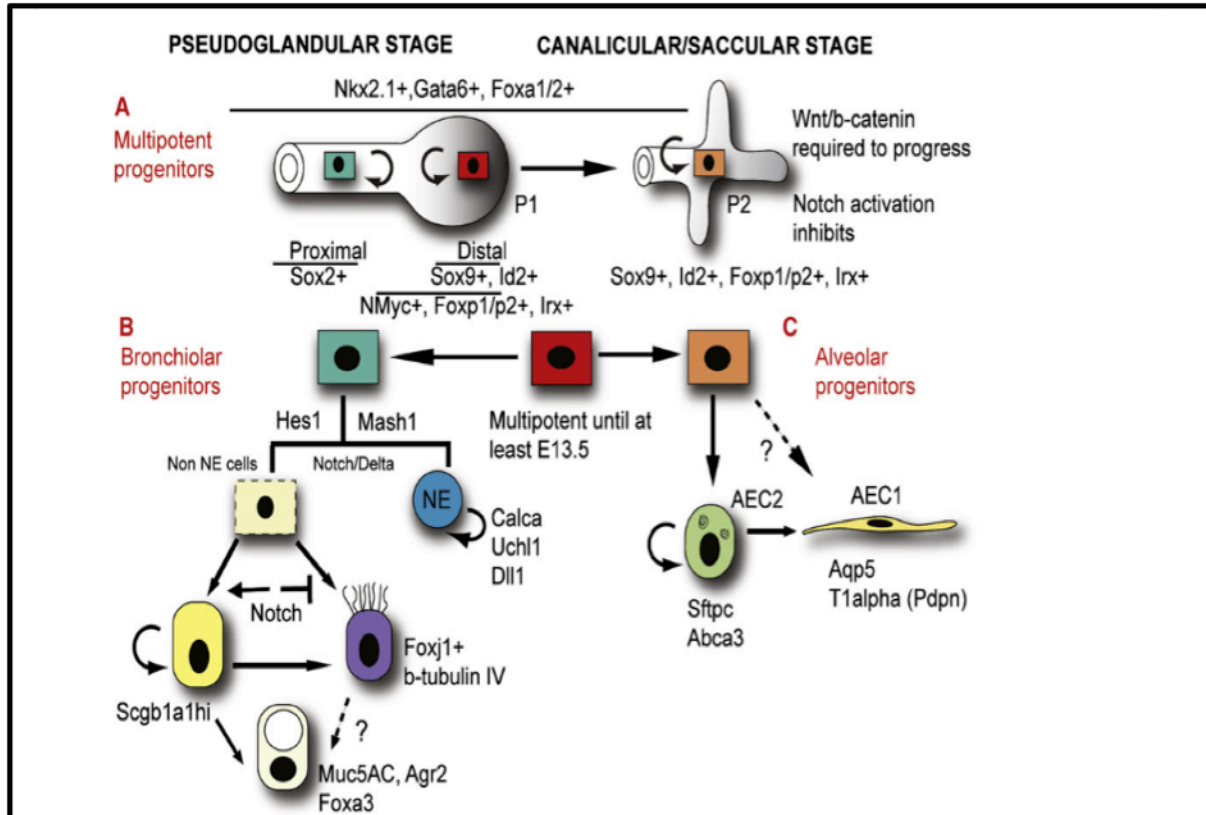


Figure 4. Epithelial cell lineages in the lung. (A) Multipotent progenitor cells at the pseudoglandular stage (E11–16.5), progenitor cells (P1, red) within the distal tip epithelium both self-renew and generate descendants (green). They populate the conducting airways. At least up to E13.5 the P1 cells are multipotent. P1 cells persist to the canalicular stage when they generate cells (P2, orange) that populate the future alveoli. There is evidence that Wnt and Notch signaling regulate the switch from production of bronchiolar to alveolar. (B) Putative airway progenitors (green) expressing Sox2. Bronchiolar lineage decision mediated by Notch signaling via Hes1 and is between an NE (blue) and putative non-NE fate (light green). Mash1 expression is required for NE cell commitment and differentiation. The non-NE cells subsequently undergo a second Notch-mediated decision to commit to the secretory cell (yellow, Scgb1a1hi) or ciliated cell (purple, FoxJ1+, β-tubulin IV+) lineages. It is believed that once Scgb1a1+ cells are formed, they are able to self-renew over the long term and to give rise to ciliated cells in the postnatal lung. Also, mucus-producing cells can be derived from Club cells directly; however, other sources are possible. (C) Alveolar epithelial progenitor giving rise to AEC1 (Aqp5+, T1alpha+) and AEC2 (Sftpc+) cells, or AEC2 cells themselves generating AEC1. The genetic mechanism of that is not clear completely (Morrissey & Hogan, 2010).

Therefore, the aim of this research project was to specifically study the differentiation of following cell types as golden standard to investigate lung cell differentiation during development and regeneration. Most focused cell types in this work are bronchiolar and alveolar progenitor cells.

1.3.1 Basal cells

Basal cells (BCs) are so called lung stem cells. They express the transcription factor *Trp-63* (*p63*) and *Cytokeratins 5* and *14* (*Krt5/14*). They are responsible for the establishment of structural organization of epithelium inside respiratory system. In the rodent, BCs are restricted to the trachea and spread out among the ciliated, secretory, and neuroendocrine cells. By contrast, in the human lung, BCs are present throughout the airways, including small bronchioles. As is shown in Figure 3.B. and Figure 4. in normal hemostasis; basal cells comprise two subpopulations: stem cells and basal luminal progenitors. In addition, few scattered neuroendocrine (NE) cells and submucosal glands (SMGs) located adjacent to BCs and form a stem cell niche.

According to a lineage tracing study on transgenic mice; Tg (KRT5-CreER); BCs are indeed self-renewing stem cells and involved in tracheal growth and homeostasis (at least for up to 16 weeks), and repair (J. R. Rock et al., 2009). It is not clear if BCs are a functionally heterogeneous population. It has been observed a subset of tracheal BCs (<20%) expressing Krt14 (Keratin 14) and are unipotent self-renewing subpopulation at homeostasis (Ghosh et al., 2011) (Watson et al.).

1.3.2 Club cells

Club cells or so called Clara cells are bronchiolar exocrine cells. They are cuboidal, non-ciliated secretory cells; and dome shape apically. They lined through all small airways and trachea. Clara cells are central players in protection of airways from environmental exposures. These cells produce Clara cell secretory protein (CCSP/CC10) which is secretoglobin 1A1 (SCGB1A1) member of the SCGB protein. In human it referred as uteroglobin (Ug). In addition, they produce surfactant apoproteins A, B, and D, proteases, antimicrobial peptides, several cytokines, chemokines, and mucin to the extracellular fluid that lining airspaces. Therefore, they play a role in detoxifying and controlling the extent of inflammation in lung. Moreover, club cells have progenitor activity in postnatal growth of the bronchioles, but not the trachea (Rawlins, Okubo, et al., 2009). In addition, their well known role is participating in mucociliary clearance of airways in collaboration with ciliated cells. This mechanism help the lungs to trapped the inhaled

microorganisms and foreign particles by help of mucin and secretoglobin and brush out these particles with help of ciliated cells cilia. It has been shown that, Scgb1a1⁺ Clara cells play role in postnatal growth, homeostasis, and repair of lung epithelium. The majority of club cells in the bronchioles both self-renews and generates ciliated cells. In the trachea, Club cells contribute to tracheal repair but do not self-renew extensively.

The lineage tracing studies with a Secretoglobin 1A member 1 (Scgb1a1/CC10)- CreER allele shown that a population of Club cells (Scgb1a1positive) give rise to alveolar lineages in response to some injuries, including bleomycin. However, in steady state conditions or in response to naphthalene or hyperoxia these club cells cannot differentiate to alveolar cells (Rawlins, Okubo, et al., 2009).

The distribution of club cells in a normal P0 lung is shown in Figure 5. B and 5.C. As is demonstrated; Club cells lined through the airway. The whole mount staining for club cells clearly visualized the structure of normal distal branches and distribution of club cells as well as alveolar epithelial type 2 cells. The structure of normal lung with five lobes shown at Figure 5.A. The particular branching pattern of lung has investigated carefully by Metzger group (Metzger et al., 2008).

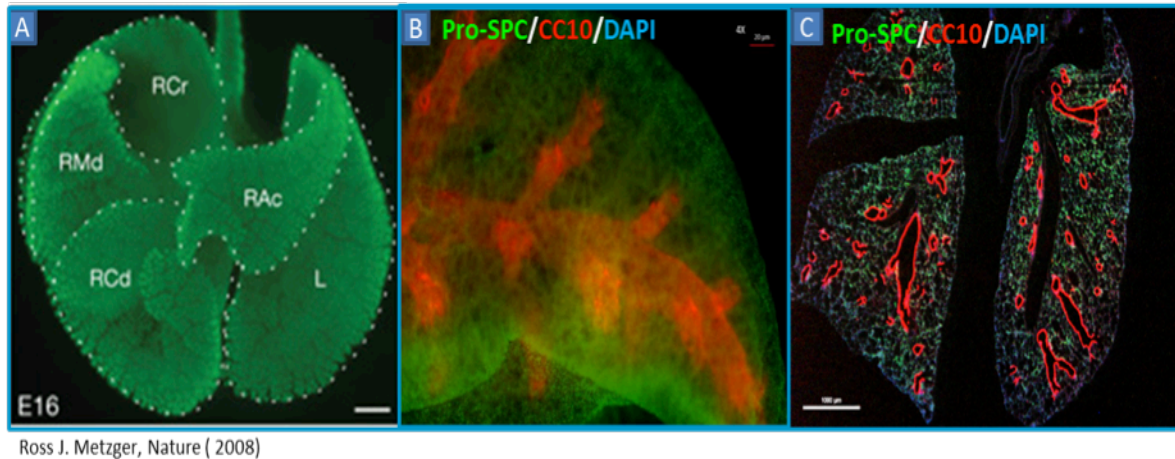


Figure 5. Lung lobes and structure of airways branches and cell distribution by and after branching formation. (A) Structure of a fully formed lung with 5 lobes. The ventral view of lung whole mount staining for E-cadherin (green) to show the airway epithelium. The five different lobes distinguished with dotted lines right cranial (RCr), right middle (RMd), accessory (RAc), right caudal (RCd) and left (L) lobes. Scale bar, 500 mm (Metzger et al., 2008). (B) The ventral view of the RAc of a P7 mouse. The whole mount staining for club cells (CC10 in red) and Alveolar type II cells/ AECII (Pro-SPC in green). (C) Represents the normal distribution and structure of L, RCr and RCd lobes of a P7 lung. It stained for AECII (green) and club cells (red).

1.3.3 Ciliated cells

As mentioned before, ciliated cells are part of ciliated pseudostratified columnar epithelium. These cells express Foxj1 and acetylated tubulin IV. The Foxj1 expressing cells are detected in the proximal epithelium in a “salt and pepper” pattern as early as E14.5 (Rawlins, Ostrowski, Randell, & Hogan, 2007). The Figure 6 shows the distribution of ciliated cells and basal cell in trachea and proximal airways.

The proportion of multiciliated cells are in balance with secretory luminal cells. It is fairly 50:50; however, their number decrease towards the end of the bronchioles in distal lung. Ciliated cells are unilayered columnar cells and keep the airways clear of mucus and dirt. Previous study on a clonal 3D organoid assay showed that that IL-6/Stat3 signaling promotes ciliogenesis at multiple levels (Tadokoro et al., 2014).

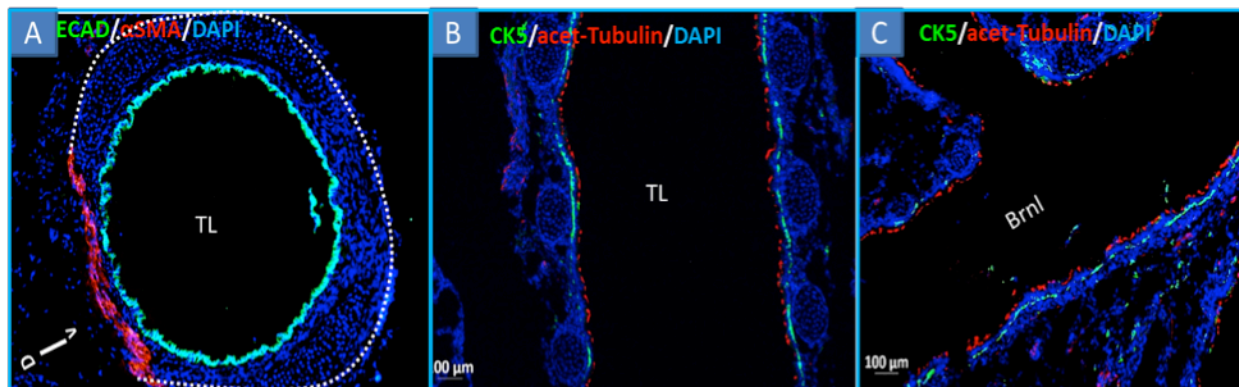


Figure 6. Immunofluorescence images of tissue sections of trachea and proximal lung airways. (A) Transverse section of a P7 pup trachea. At the posterior of tracheal C-shaped cartilage rings, smooth muscles located, labeled for alpha smooth muscle (red), the cartilage ring marked by dashed line and nucleus stained with 4'-6-diamidino-2-phenylindole (DAPI; blue), and epithelial cells at tracheal lumen stained with Ecadherin(green). (B) Longitudinal section of trachea stained for basal cell-specific protein (CK5; green), ciliated cells marker (Acetylated tubulin; red) and nuclei. (C) The distal part of a bronchi and branching to a smaller bronchiole.

1.3.4. Alveolar Epithelial cells

1.3.4.1-Alveolar Epithelial cells type I

More than 99% of the internal surface area of the lungs composed of the alveolar surface. Almost 90% of the alveolar epithelium contain flattened alveolar epithelial cell type I (AECI) (Dobbs & Johnson, 2007). These cells are squamous and branched with multiple apical surfaces. The apical surface area of AETI cells is large (*i.e.* $\sim 5,000 \mu\text{m}^2$ for human AETI cells), and they are very thin cells (*i.e.* $0.2 \mu\text{m}$ in depth). The gas exchange barrier is composed of AETI and endothelial cells joined by fused basement membranes (Sutherland, Edwards, & Murray, 2001). Figure 7 showing the alveolar epithelium. The structure of alveoli units that formed by AECI visualized by immunohistochemistry staining for AECI and AECII. AECs type I form alveoli walls and minimizing the diffusion distance between alveolar gas in alveoli and the blood in the pulmonary vasculatures. Therefore, facilitate gas exchange. They express ion channels (Aqp5 and Cfr), and Podoplanin/ type I cell alpha protein (T1 α) which is an apical membrane protein and exclusive for AECI. The biological functions of T1 α in the alveolar epithelium are unknown. However, previously the raft-associated distribution of T1 α / podoplanin in mouse alveolar epithelium reported (Barth, Bläsche, & Kasper, 2010).

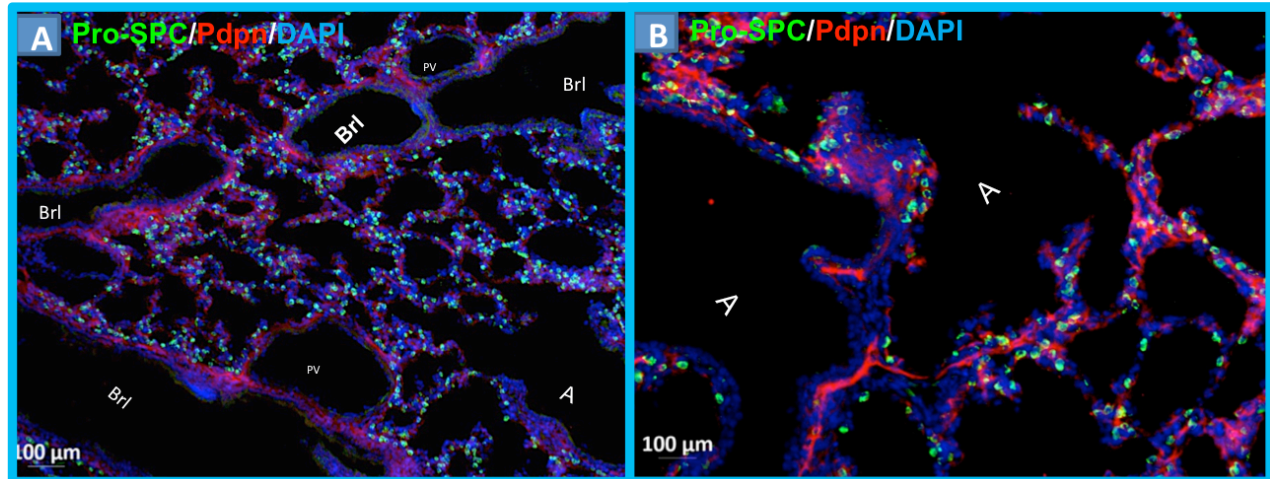


Figure 7. Alveolar epithelial cells and their location in alveoli wall structure. **(A, B)** Alveolar epithelial cells type I (AECI) in red stained with podoplanin /T1alpha (Anti t1 α ; DSHB- 8.1.1; Hamster, 1:20). AEC II in green located at corner of alveoli walls, marked by Anti-Pro surfactant Protein C /pro SP-C (Merck/ Millipore; Rabbit; 1:600). The lymphatic vessels also stained in red. Abbreviations: A: Alveoli; Brl: Bronchiole, PV: pulmonary Vessel

1.3.4.2- Alveolar Epithelial cells type II

AEC II cells are cuboidal with rounded nuclei and have many cytoplasmic organelles, including lamellar bodies. These cells located at the corners of alveolar walls. They produce surfactant proteins such as surfactant protein C (ProSP-C), Figure 7. In addition, AECII are able to both proliferate and giving rise to new AECII cells as well as differentiates into AECI cells.

The proportion of ATI cells and AECII cells within the alveolus is critical for maintaining normal lung function. These cells synthesis and secret of immunomodulatory proteins that play role in host defense. Type II cells secrete surfactant to prevent partial collapse or incomplete inflation of the lung. They keep the alveolus almost fluid free, and participate in innate immunity to fight infection and minimize inflammation (Mason, 2006). These functions are important in lung regeneration. Moreover, lung expansion and mechanical factors induces both AECII proliferation and differentiation into ATI cells. However, mechanical strain has also been reported to induce apoptosis in ATII cells. Therefore, role of mechanical stress in regulating of AECII is not clear. Also, in AECII's differentiation; extracellular matrix factors can play a very significant role.

1.3.5 Other cell type in lung

1.3.5.1-Mucus producing goblet cells

The goblet cells with ciliated cells compose the respiratory mucosa. Goblet cells express Muc5ac, Foxa3, and are found in the trachea and proximal airways. The number of goblet cells is low in the mouse compared with human (G. Chen et al., 2009). Goblet cells synthesize, store, and secrete large mucopolysaccharide-rich mucins. In fact, they influence mucociliary clearance and innate defense of the lung. Recent lineage tracing experiments show that club cells can give rise to goblet cells without cell proliferation, by a process that requires the transcription factor Spdef (G. Chen et al., 2009). In addition, whether other cell types, such as ciliated cells, can give rise to goblet cells is not known (Morrissey & Hogan, 2010).

1.3.5.2- Neuroendocrine cells (NE)

At the intralobar airway epithelium besides club and ciliated cells clusters of another cell type exist. These cells are Neuroendocrine cells (NE) and their innervated clusters called neuroepithelial bodies (NEBs). They are airway O₂ sensors and express calcitonin (Calca or Cgrp) and Pgp9.5 (Uchl1)(Morrissey & Hogan, 2010). Figure 8. presents the distribution of NEBs.

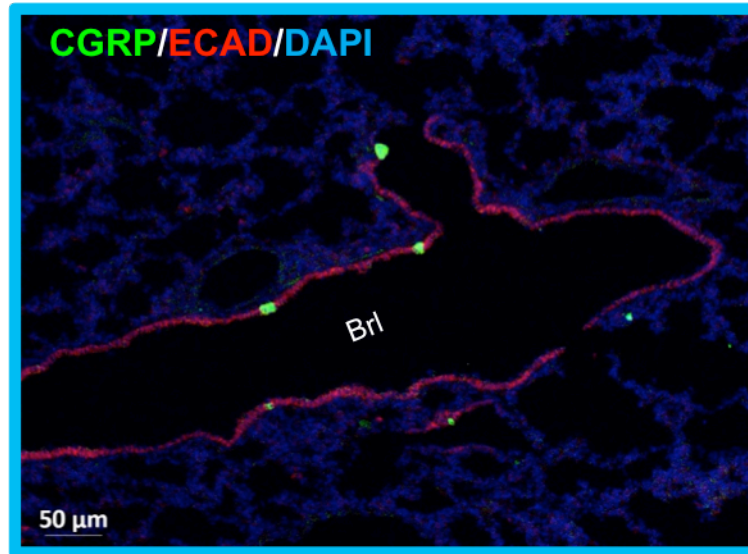


Figure 8. lung epithelium and neuroendocrine cells clusters. The NEBs spreads out in distal bronchioles. Neuroendocrine cells stained in green by anti CGRP (Sigma, Rabbit, 1:5000) and epithelial cells in bronchial lumen visualized by anti E-cadherin/ Decma-1 (abcam; Rat; 1:1000) antibody.

1.3.5.3-Putative bronchio-alveolar stem cells (BASCs) and distal airway club stem cells (DASCs)

In addition, two more cell population recently introduced as lung progenitor cells in dorsal lung. First, bronchioalveolar stem cells (BASCs). This cell population located at bronchioalveolar duct junctions (BADJs) and express both Club cells and AECII marker. Second, at distal airway club stem cells (DASCs) located; which their self renewal capacity activated after injury. These cell types classified in the group of endogenous epithelial progenitor cells of the lung (J. Rock & Königshoff, 2012). The Figure 9 A and B illustrate detailed characteristics and relationship of identified epithelial progenitor cells.

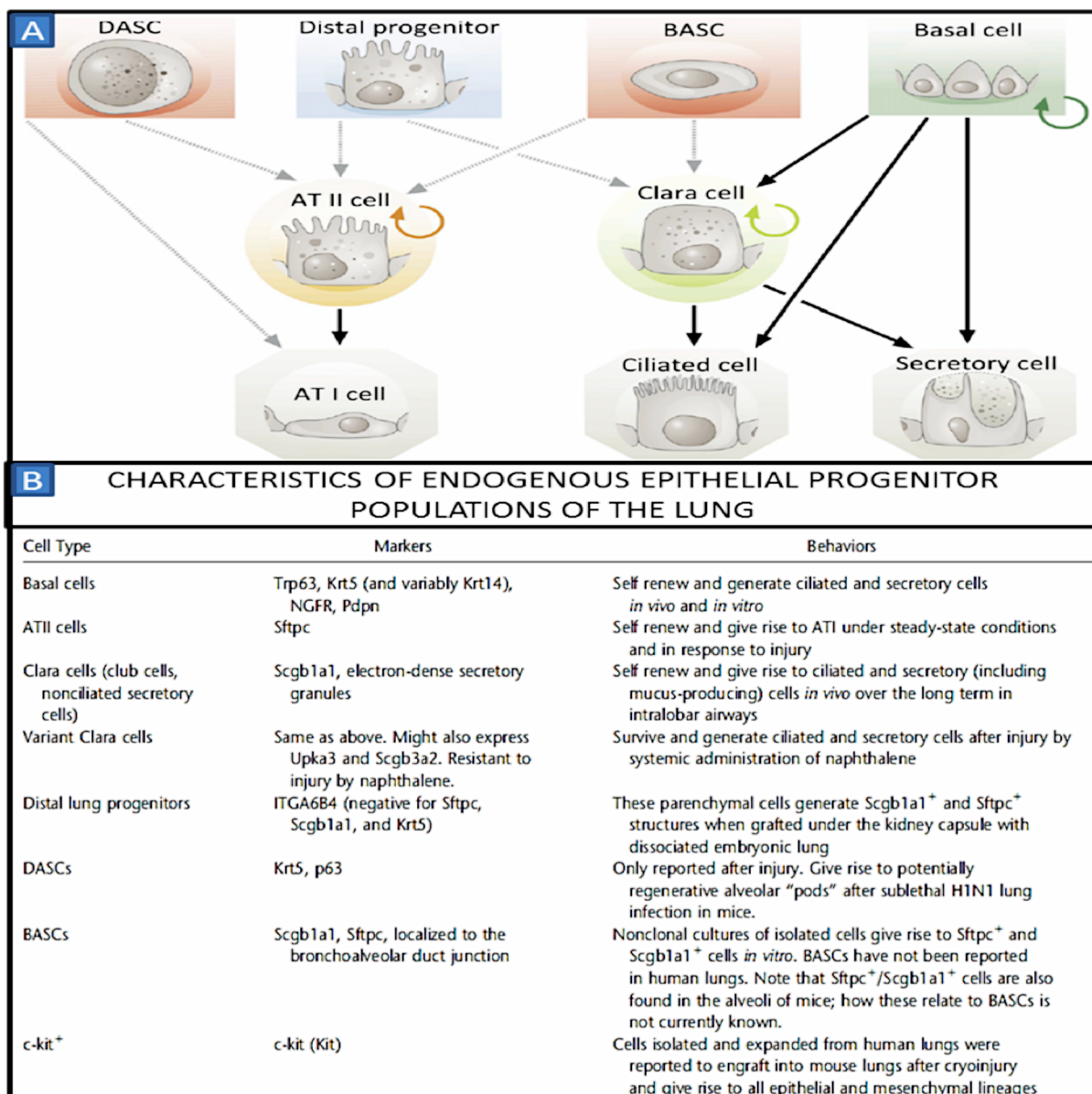


Figure 9. Endogenous epithelial progenitor cells of the lung. (A) The relationship of endogenous epithelial progenitor cells according to *in vivo* and *in vitro* study models. The dashed lines used for cell lineages that still is not clear. (B) Detailed characteristics of identified epithelial progenitor cells are given in Table. The cell type markers and their cell behavior has summarized in this table (J. Rock & Königshoff, 2012). ATII cells: alveolar epithelial cell type II cells; BASC: bronchioalveolar stem cell; DASC: distal airway stem cell.

1.3.6. Lung mesenchyme

The cellular composition of the mesenchyme is complex. The lung mesenchyme induces specification and morphogenetic signals to the epithelium throughout development. Indeed; mesenchyme plays a significant role during respiratory lineage specification, branching morphogenesis, vascular development, and alveolar maturation (McCulley, Wienhold, & Sun, 2015). The lung mesenchyme composed of matrix and various cell types such as smooth muscles, pericytes, myofibroblasts, fibroblasts, endothelium of blood vessels and mesothelium.

The mesenchyme gives rise to endothelial cells of blood vessels and pericytes by the process of vasculogenesis. At the main bronchi, smooth muscle covers the dorsal surface of the endoderm and cartilaginous rings encompass the ventral airways. In all proximal airways, smooth muscle cells encircle the entire endoderm, but are absent at tips of distal airways during branching morphogenesis. In postnatal stage, the distal mesoderm generates myofibroblasts in the tips of the alveolar walls. Other cell types in lung mesenchyme; are interstitial immune cells such as alveolar macrophages and lymphocytes. The ratio of alveolar macrophages to lymphocytes is 1:5 to 1:10. The most common lymphocyte in the normal human alveolar interstitium is the T-cell. Indeed, they composed more than 95% of the lymphocyte population. Alveolar macrophages play a role in 1) defense against pathogens, 2) destruction of potential allergens; 3) presentation of antigens to T-lymphocytes; and 4) clearing of antigens to regional lymph nodes.

In interstitial lung disease, alveolar macrophage become activated by an immune complex. Through mediators, termed chemokine, the macrophage attracts polymorphs and other cells from the circulation to the alveolar space, or it can initiate fibrosis with various mediators that stimulate fibroblasts and muscle cells to proliferate. This leads to interstitial fibrosis.

In general, smooth muscle, pericytes, myofibroblasts associated with capillaries and fibroblasts; are other mesenchymal cell types. The fibroblasts engage in fibrogenesis and secretion of collagen and proteoglycans. In fact the fibrous system, fibronectin, proteoglycans and basement membranes form the matrix of alveolar mesenchyme. The backbone of the lung is a continuous system of fibers anchored at the hilum and put under tension by negative intrapleural pressure. Fibrous system provides the lung an appropriate structural integrity. The fiber-system along with surfactant, maintains the stability of the alveoli from collapsing. Thus, the alveoli are mechanically independent.

The fibronectin molecule forms fibrils associated with matrix components and mesenchymal cells in the interstitium. Through specific binding sites on the fibronectin molecules, it promotes cell adhesion and migration, cytodifferentiation, phagocytosis, and cell growth. While collagen fibers provide tensile strength and elastic fibers provides elastic recoil. The proteoglycans influence lung compliance and fluid balance.

The epithelial and endothelial basement membranes (BM) are continuous and form barriers defining the outer borders of the interstitium. BM composed of Collagen IV, laminin, heparan sulfate and Entactin. BM support for epithelial and endothelial cells and prevents passage of non inflammatory cells. In addition, BM induces angiogenesis.

1.3.7 Lung interstitium

In general, the interstitium in lung characterized as part of the interalveolar septal wall. The interstitium made of collagen and elastin fibers, as wells fibroblasts, myofibroblasts, histiocytes, mast cells and slight nerves. Indeed, interstitial myofibroblasts adjacent to capillaries, control perfusion of the alveoli. Interstitium also includes mast cells and a histiocytes which is an transitional model of blood monocytes and alveolar macrophage. Moreover, lymphoid elements and langerhans cells, are within the interstitium. Interstitium located between the alveolar epithelial and capillary endothelial basement membranes. In fact, it is abundant around the airways and arteries in the centers of the lobules (Dani S. Zander MD, 2008).

1.3.8. Macrophage in lung

Last but not least component of lung organ are macrophages. Macrophages are required for normal and pathological processes in tissue. They play role in clearing apoptotic cells and cellular debris in immunological responses. In fact, macrophages in parallel of other white blood cells involve in initiation and progression of most lethal lung diseases.

Alveolar macrophages reside in the airspaces and adjacent with AECI cells and II alveolar epithelial cells. Macrophages found in the larger airways within the mucous layer and in the interstitial space between the alveoli and the blood vessels. The tissue macrophages are either classically activated M1 macrophages or alternatively activated M2 macrophages and play role in wound healing and immune regulation. Alveolar macrophages are regulated by the airway epithelium through their interactions with AECII, and transforming growth factor- β (TGF β). In Figure 10, resident leukocytes in healthy lung and their interaction with alveolar epithelium suggested. Alveolar macrophages can produce TGF β and retinoic acid and induce forkhead box P3 (FOXP3) expression in both naive and activated CD4⁺ T cells which are present in the lumen of the airways (Hussell & Bell, 2014).

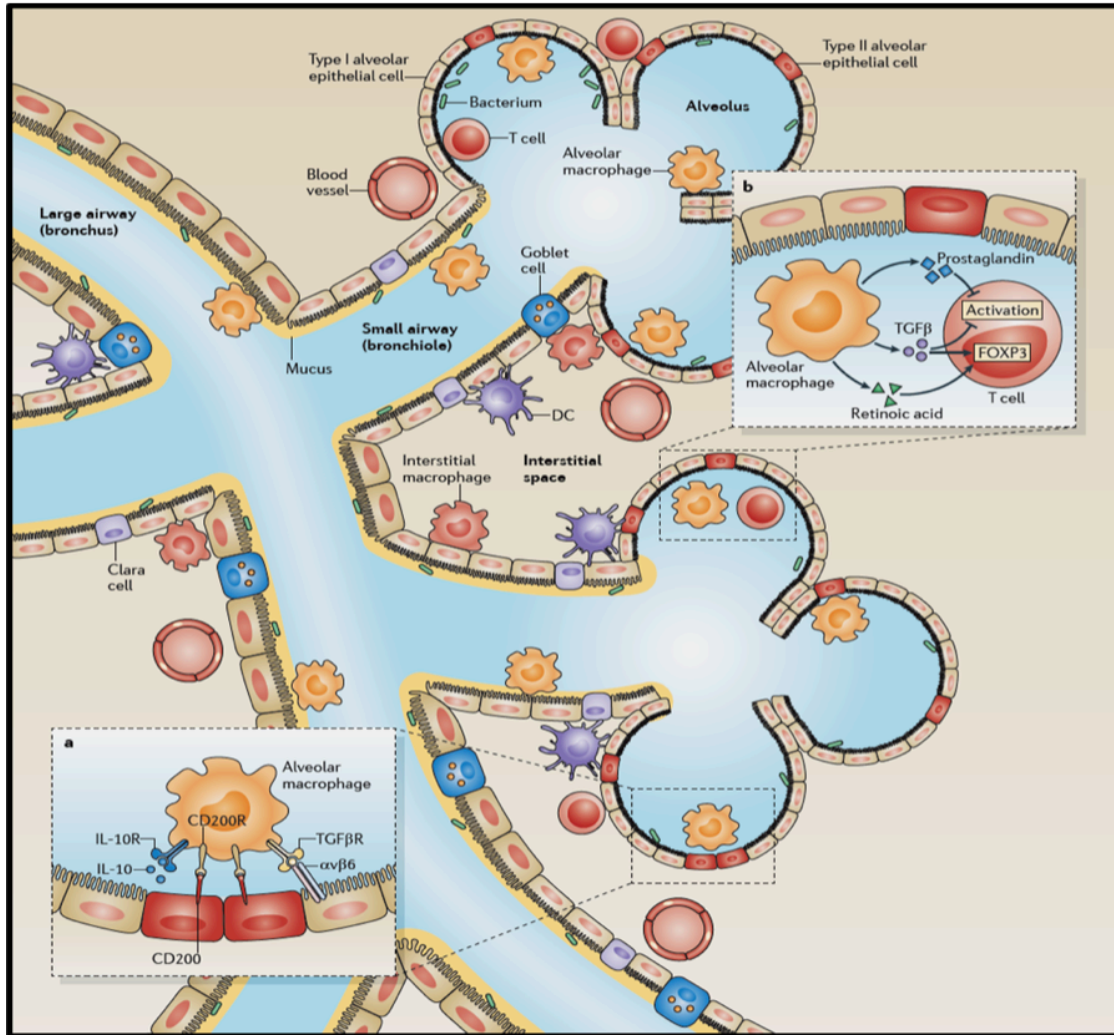


Figure 10. Leukocyte interactions in the healthy lungs. Alveolar macrophages reside in the airspaces juxtaposed with AECI and II. Mucus-producing goblet cells are present in both large and small airways. The secretory non-ciliated Club cells are more common in the bronchioles. Macrophages are also found in the interstitial space between the alveoli and the blood vessels where T cells, dendritic cells (DCs) and a sparse population of B cells also reside. Commensal and pathogenic bacteria reside within the airway mucosa and in the alveoli. a | Alveolar macrophages are regulated by the airway epithelium through their interactions with CD200, which is expressed by AEC II alveolar cells, and expressing growth factor- β (TGF β) to the epithelial cell surface by α v β 6 integrin. Also, secreted interleukin-10 (IL-10) and its receptor involve in inducing signals to macrophages. These interactions can also take place in the larger airways, where CD200 and α v β 6 integrin are also expressed by the bronchial epithelium. b | The secretion of TGF β and retinoic acid by alveolar macrophages can induce forkhead box P3 (FOXP3) expression in both naive and activated CD4⁺ T cells that are present in the lumen of the airways. In addition, TGF β and prostaglandins suppress T cell activation. CD200R, CD200 receptor; IL-10R, IL-10 receptor; TGF β R, TGF β receptor. Adopted from (Hussell & Bell, 2014)

Chapter 2

Designing a study model for *in-vivo* lung cell differentiation and histopathology research

Given to the complex anatomical structure of lung organ and lack of efficient tools to recapitulate the physiological structure and providing lung regeneration and dedifferentiation cues; *in vivo* study on animal models still is mandatory. To develop a new animal model to identify novel genes and regulators of lung cell differentiation during physiological and pathological conditions, a phenotype driven forward genetic screening approach choose.

In general, lung disease can be first: bacterial, viral and parasitic lung disease, second: neoplastic lung diseases and third, non-neoplastic lung diseases. Enormous amount of research done on investigating molecular pathogenesis of lung disease. Although, limited animal models for non-neoplastic and neoplastic lung disease has established. Due to lack of enough knowledge and information about molecular pathogenesis of non-neoplastic lung disease; designing a model which completely replicate pathological conditions have not been done yet. Designing genetically engineered mice are slow, costly and do not always recapitulate human biology. Nonetheless, developing rodent models and integration of these model systems will benefit the genomic revolution and refining our understanding and treatment of human diseases (Kwon & Berns, 2013).

Regarding designed mouse models, mainly for most fatal heritable lung disease such as Cystic fibrosis (CF), and other interstitial lung disease such as pulmonary fibrosis and COPD some study models designed.

In fact, about 100 pathological sever condition in the lung classified under interstitial lung diseases category. In this category usually the interstitium is target and slow collagen (fibrosis) accumulation occurs. However, inflammatory cells involve in interstitial lung diseases are variable from lymphocytes in nonspecific interstitial pneumonia to neutrophils as in usual interstitial pneumonia (UIP). The **UIP**, according to pulmonologists and radiologists also known **Idiopathic Pulmonary Fibrosis (IPF)**, is indeed an inflammatory interstitial process. IPF results in progressive fibrosis and honeycombing. According to previous work on IPF, inflammation does

not play a major role, and development of the disease is successive of epithelial cell injury, alteration in regeneration of parenchymal tissue and abnormal reparative processes.

However, the mechanisms of epithelial damage in IPF are currently unknown, as is the etiology of this disease. Also, classical viral interstitial pneumonias, hypersensitivity pneumonia, and autoimmune disease such as rheumatoid arthritis, systemic lupus erythematosus are included in this category.

2.1. Pulmonary fibrosis and Interstitial Lung Diseases (ILD) models

2.1.1 Inherited Interstitial Lung Disease Surfactant Protein C Mutations

One of IPF-like lung disease in interstitium is due to Surfactant protein C (SP-C) mutations. Patients with these mutations fail to secrete mature SP-C. The mutations occur in the luminal part of the surfactant protein C precursor protein; BRICHOS domain (≈ 100 amino acid C-terminal region), it affects targeting, processing, and folding of proteins. Thus, causes protein aggregation, proteasome dysfunction, and caspase 3 activation (Mulugeta, Nguyen, Russo, Muniswamy, & Beers, 2005). The Figure 1 is a structure of pro surfactant protein C, BRICHOS domain and mutations that cause interstitial lung disease (Dani S. Zander MD, **2008**).

In a “gain-of-function” study model toxic effects of mutant proteins investigated in epithelial cells. In this model expression of inflammatory mediators increased and epithelial cells undergone apoptosis.

2.1.2. Pulmonary Fibrosis models

Given to this fact that pathogenesis of fibrosis is associated with a couple of conditions, such as infections, collagen vascular disease, allergic alveolitis, and trauma. Therefore, designing a model that re-creates all the structural, biochemical, and molecular characteristics of human disease has not been accomplished yet.

By genetic manipulation and external induction the pulmonary fibrosis models has created.

The most common methods to induce pulmonary fibrotic reactions is by using exogenous agents; include direct instillation of fibrogenic agents and exposure to thoracic irradiation (Table 1) (Chua, Gauldie, & Laurent, 2005).

Table 1. Approaches for inducing fibrosis in animal models

Exogenous Agent/Approach	Nature of Tissue Damage	Animal Species Used
Bleomycin	Oxidant-mediated DNA scission leading to fibrogenic cytokine release	Mice, rats, hamsters, rabbits, dogs, primates, pheasants
Inorganic particles (silica, asbestos)	Type IV hypersensitivity reactions with or without granuloma formation	Mice, rats, hamsters, sheep, rabbits
Irradiation	Free radical-mediated DNA damage	Mice, rats, rabbits, dogs, hamsters, sheep, primates
Gene transfer (TGF- β , IL-1 β , GM-CSF)	Downstream activation of specific cytokine pathway/s	Mice, rats
Fluorescein isothiocyanate	Incompletely understood. Presumed T-cell-independent.	Mice
Vanadium pentoxide	Incompletely understood. An inorganic metal oxide.	Mice, rats
Haptenic antigens (e.g. trinitrobenzene sulphonic acid compounds)	Recall cell-mediated immune response	Mice, hamsters

The bleomycin is most used fibrogenic agent. It is antineoplastic and have oxidant effect which cleaving DNA and increase the levels of fibrogenic mediators. It can be administered endotracheally, intraperitoneally, or intravenously, and very occasionally by intramuscular or

subcutaneous injection. The profibrotic effect of bleomycine has observed in dogs and later on standardized in rats and mice. The lesions induced by this agent are patchy inflammation, epithelial damage with reactive hyperplasia and apoptosis. In addition, the basement membrane will change as well as spindle-shaped mesenchymal cells similar to the myofibroblast accumulates in lung.

Although the bleomycin instillation model is easily reproducible, it should be remembered that it is a model involving rapid onset of the lesion. Thus it has a defined duration.

The merit of the bleomycin model is its robust reproducibility and versatility. Indeed, bleomycin reproduces the general morphology of interstitial lung fibrosis without copying any particular and lung disorder. Thus, this model cannot be an experimental equivalent of IPF due to first; fast lung remodeling in bleomycin induced pulmonary fibrosis. Secondly, developing focal emphysema-like changes in lung tissue.

Another material to induce fibrosis is amiodarone in mouse, and hamster. This drug has administered endotracheally and orally to produce profibrotic effect. Moreover, inhalation of particles such as asbestos or silica induce progressive fibrosis accompanied by a granulomatous inflammatory reaction in humans and rodents. In fact, these models are especially useful for the study of macrophages and other phagocytes. Furthermore, other materials inhalation such as cobalt and cadmium chloride, isocyanates and nitrous ureas, has been used to induce fibrosis.

Moreover, lung researcher widely has used Naphtalen injury models to understand the pathogenesis and potential treatment of airway fibrotic disorders. This technique is simple and reproducible. The naphthalene has administered intraperitoneal and triggers regional hyperproliferation of epithelial progenitor cells. In fact, this technique targets club cells and loss of club cells and defect local epithelial repair mechanisms. Thus, the peribronchial and fibroblast proliferation and airway fibrosis occurs (Aoshiba et al., 2014).

Irradiation is another fibrosis inducer. Given to various drawbacks of this technique, such as spacious equipment, and conducting a series of radiation sessions, it is not the most common method to produce animal models to study fibrosis.

The last but not least is genetic manipulation of experimental animals. In this regard, researchers has developed many Knock in and knock out animals with alteration in cytokines and growth factors genes and proteases that associated with extracellular matrix, and other components of the interstitium and alveolar epithelium (Dani S. Zander MD, 2008).

2.1.3. Cystic fibrosis models

Cystic fibrosis is caused by mutations in the *CFTR* gene. The most common lethal and morbid consequence of *CFTR* mutations is a lung disease that evolves from small-airway obstruction with mucus plugging and air trapping, airway inflammation and intermittent infection, into chronic bacterial infection, bronchiectasis and ultimately death.

Based on these findings, there is general agreement that the pathogenesis of cystic fibrosis lung disease reflects a defect in the innate defense of airway surfaces against bacterial infection. For Cystic Fibrosis (CF) approximately 11 CF mouse models have been made. This disease is the most common genetic disease among Caucasians. Most of these models has made for the cystic fibrosis transmembrane conductance regulator (*CFTR*) gene. However; these models are not optimum models. The *CFTR* null mice did not develop CF lesions similar with human CF cases. Among developed CF models, the Mall et al's CF mouse model is an ideal disease model. Mall and et al mutated the cystic fibrosis transmembrane conductance regulator (*CFTR*) gene. Therefore, airway Na⁺ absorption increased and epithelial Na⁺ channels (ENaC) overexpresses in airways. As a result, defective mucus depletion, mucus obstruction, goblet cell metaplasia, neutrophilic inflammation and poor bacterial clearance will provided a disease model similar with human CF cases (Mall, Grubb, Harkema, O'Neal, & Boucher, 2004).

2.1.4. Other mouse models for lung disease

Chronic obstructive pulmonary disease (COPD)

Emphysema and chronic bronchitis, classified together as COPD. The airflow limitation, and abnormal inflammatory response of the airways and lungs to toxic particles and gases (Brusselle et al., 2006). COPD listed as the fifth leading cause of death in the world and represents a major economic and social burden worldwide (Pauwels & Rabe, 2004). It has been known that smoking is the most important risk factor for COPD. It is indeed an incurable disease with chronic inflammation, progressive destruction of alveoli and progressive respiratory dysfunction leading to death. The only treatment for that is lung transplantation.

To investigate cellular and molecular mechanisms of COPD various murine models were designed (Brusselle et al., 2006). First group of COPD models prepared by administrating of tissue-degrading enzymes I to trachea (Karlinsky & Snider, 1978). It causes emphysema-like lesions in the lung parenchyma, and imbalances the protease-anti protease enzymes in alveolar epithelium. In the second approach, toxic stimuli creates COPD-like lesions in mice. For this purpose inhalation of tobacco smoke, sulfur dioxide, nitrogen dioxide, or oxidants such as ozone used.

The third method is designing transgenic mice such as **Marlboro mouse** in which Macrophage elastase (MMP-12) is knock out (Shapiro, 2000).

To recapitulated COPD pathological condition, exposure to cigarette smoke is a most common model. Although there is difference between mice and human lungs after chronic cigarette smoke exposure. In addition, Cigarette smoke-related changes reported as a strain-dependent phenomena.

In mice generally, ciliated epithelium extends throughout the airway with increasing proximal density, a few submucosal glands generally are available in mouse and they are located exclusively in the trachea. Mouse airways are less than human are branched out.

Although, inflammatory cell recruitment to alveolar spaces and air-space enlargement are similar to the response in humans (Shapiro, 2000).

Neoplastic lung disease and Lung cancer

Lung cancers including two different subtypes, first small cell lung cancer (**SCLC**) and second non small cell lung cancer (**NSCLC**).

The **SCLC** also known as *oat cell carcinoma or small cell undifferentiated carcinoma*. This type is highly associated with tobacco smoking and is an aggressive type and usually metastases to lymph nodes, bone, brain, adrenal glands, and the liver. It is believed derive from neuroendocrine cells in lung. The large variety of lesions has found as players of SCLC. Thus, to design good models to study neoplastic lung disease various combinations of concurrent oncogenic mutations should be consider. (Huijbers, Krimpenfort, Berns, & Jonkers, 2011) (Dow & Lowe, 2012)

The loss-of-function mutations in the retinoblastoma, p53 genes and PI3K pathway, Notch, Hedgehog, glutamate receptors, Sox genes, DNA repair genes and several receptor kinases reported as genes involve in lung cancer (Peifer et al., 2012). The correlation of SOX2 expression and SCLC stages and maintaining has been reported before. In addition, to design SCLC mouse models, amplification of distinct chromosomal regions such as L-MYC, C-MYC, SOX2 and SOX4 used (Rudin et al., 2012).

According to the American Cancer Society, approximately 85-90% of lung cancer cases are NSCLC. The NSCLC include three types; **Adenocarcinoma**; slow growing lung cancer at outer area of the lung, **Squamous cell carcinoma** generally forms in the center of the lung; and **Large cell carcinoma** occurs anywhere in the lung epithelium.

According to previous research on NSCLC and discovered causative mutation in relevant genes; various models designed to study lung cancers. In this regard, Kras, Braf, Egfr, Lkb1, Rac1, NfkappaB, and p53 used to develop these models (Kwon & Berns, 2013). The summary of these models presented in (Tables 2); (Peifer et al., 2012).

In summery, according to available knowledge and lung disease models, the mechanism of IPF and other fetal lung disease is not well understood. Also, animal models with very similar human idiopathic pulmonary fibrosis and interstitial lung disease phenotypes haven't develop yet. Thus, it is required to develop new lung disease models. In this regard, approaches without any pre assumption are fundamental to provide knowledge on lung disease. Given to this fact that many signaling pathways and genes are collaborating in formation of lung pathological conditions. Therefore, by investigating only one signaling pathway and gene researchers cannot reach to a comprehensive lung disease model.

Table 1. Mouse models for NSCLS adapted from (Kwon & Berns, 2013)

Mouse models for NSCLC			
Mouse mutant	Tumor induction	Phenotype	Reference
LSL-KrasG12D endogenous control	Sporadic infection of lung cells with Adeno-Cre virus	Adenomas & adenocarcinomas Long latency	(Jackson et al., 2001)
KrasG12D LA1 and LA2 in wt or p53 deficiency	Spontaneous lung tumor development due to sporadic switching of LA allele	Adenomas & adenocarcinomas A variety of tumor types	(Johnson et al., 2001)
Tet-op-KrasG12D in wt or p53 and P19Arf deficiency	CCSP-rtTA transgene, treatment with doxycyclin. Transgene directs rtTA expression in alveolar type II cells	Fast tumor growth, accelerated in p53 and Ink4A/Arf def. background.	(Fisher et al., 2001)
LSL-KrasG12D	Tamoxifen Cre-ERT2 knockins in SPC and CC10 (AT2 and Clara cells)	Adenomas & adenocarcinomas with SPC-Cre.	(Xu et al., 2012)
Beta-Actin loxGFPlox -Kras	Ad5-CMV-Cre	Adenomas & adenocarcinomas Short latency	(Meuwissen et al., 2001)
LSL-KrasG12D; p53lox/lox	Sporadic switching of lung cells with Lenti Cre virus	Accelerated tumor development. Metastasis. Role for Nkx2-1 and Hmga2	(Winslow et al., 2011)
PTENlox/lox	Clara cell specific CCSP-Cre.	No tumors	(Iwanaga et al., 2008)
LSL-KrasG12D; PTENlox/lox	Clara cell specific CCSP-Cre.	Accelerated tumor development. Metastasis	(Li et al., 2008) (Iwanaga et al., 2008)
LSL-KrasG12D; Lkb1lox/lox	Ad5-CMV-Cre	Strongly augmented tumor growth and metastasis both Adenocarcinomas and Squamous cell carcinomas	(Ji et al., 2007)
LSL-KrasG12Vgeo	Cre-ERT2 (RERT-ert) + Tamoxifen	Adenomas & adenocarcinomas. Not all KrasV12 expressing cells proliferate	(Guerra et al., 2003)
LL-BrafV600E	Ad5-CMV-Cre	Adenomas & rarely progress to adenocarcinoma	(Dankort et al., 2007)
Inducible-cRaf mutant	Clara and Alveolar type II cell specific expression	Only expression in alveolar type II cells gives rise to macroscopic tumors. De-induction causes reversion	(Ceteci et al., 2011)
TRE-Egfr L858R/T790M/Del exon 19 mutants	CCSP-rtTA doxycyclin inducible	Adenocarcinomas. T790M and L858R/T790M double mutant show less aggressive growth	(Politi et al., 2006; Regales et al., 2007)
Tet-op-PIK3CA H1047R; CCSP-rtTA	CCSP-rtTA doxycycline inducible	Adenocarcinoma with bronchioalveolar features	(Engelman et al. 2008)

2.2. Experimental approach

2.2.1. - Forward genetic screen background

Historically the classical genetics studies were phenotype-based. The goal of these studies was to find all of the genes involved in a trait. This approach is known as a “genetic screen”. The forward genetic screen is an old and well established approach. The causative genes responsible for phenotypic traits and new mutant alleles will discover by morphological and histological analysis. Forward genetic screens may uncover novel and unexpected genes without any pre assumptions.

This technique used in various microorganisms: yeast, worms, flies, Arabidopsis, drosophila; Zebrafish and mouse model. Actually, this approach has been used mostly in zebrafish

and drosophila. Due to optical transparency of zebrafish and drosophila, high number of embryos production in a single mating; genetics has used these two organisms extensively in forward genetic screen. In fact, high number of embryos production in these models are crucial to have more robust statistics. Although, to study the respiratory system development and lung cell differentiation, the closest possible model to human is mouse.

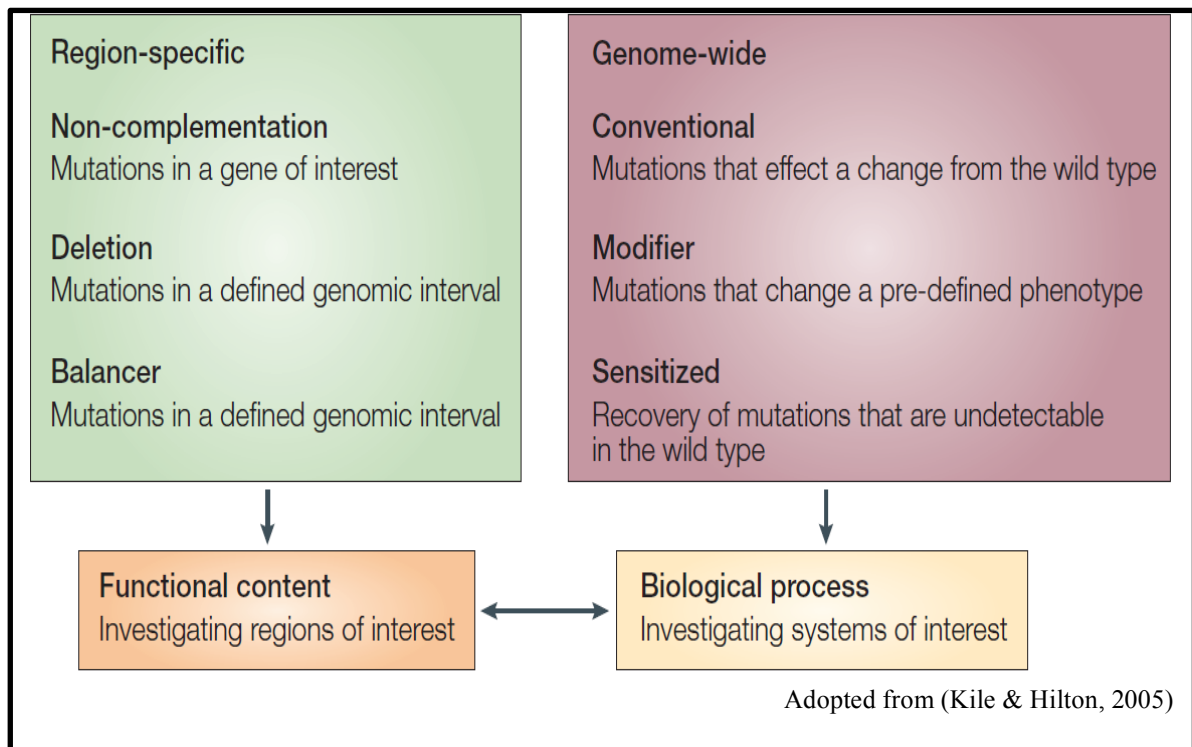


Figure 2. Genetic screens classification, various techniques are available to induce mutation.

Moreover, since a century ago it has been confirmed that the Mendel's laws are applicable to animals as well as plants. After that mouse model has become the key experimental tool in the human's physiology and disease research. Indeed, the advances in sequencing of the mouse genome clarify that approximately 25,000 genes in human have direct mouse counterparts. (Kile & Hilton, 2005). In fact, 99% of mouse genes have a homologue in the human genome and 96% of the homologue in human genome; lies within a similar conserved syntenic interval ("Initial sequencing and comparative analysis of the mouse genome," 2002). In addition, zebrafish generation time of fertilization and sexual maturity is very similar with mouse, which is about 3 months.

The forward genetic approaches in the mouse has limitations such as realistic mutation rates, size of available mouse colonies and the generation time of the mouse. However; the forward genetics in mice became feasible due to two reason.

First, development of high-throughput genome sequencing technologies and available draft of the C57BL/J6 mouse genome and sequencing of other mouse strain variants. Second, develop of large mouse genetics laboratories, such as the Jackson Laboratories that created a database of polymorphisms between various strains of mice. Thus, with the completion of the mouse genome and the characterization of strain-specific polymorphisms, the identification of potent point mutagens seems a feasible approach. According to available various reproductive mouse mutant strains it is reasonable to create mutant phenotypes and map their underlying genetic cause. All these findings lead scientist to use mouse animal for in vivo studies on lung organ.

In forward genetic screen, first of all, mutants will generate by various mutagenizing methods such as radiation, chemicals, or insertional mutagenesis (e.g. transposable elements). So the next step in any forward genetic screen after choosing a right model, is mutagenizing.

The following are name of available and commonly used mutagenesis methods and materials in forward genetic screening history.

Radiation

The radiation with X-rays, breaks the double-stranded DNA and result in large deletions of pieces of chromosome or chromosomal re-arrangements. These mutations are easier to map by cytological examination of chromosomes. The frequency of X-ray mutagenesis (13×10^{-5} to 50×10^{-5} per locus) it means 20 to 100 times of spontaneous mutants. Mutagenizing with X ray produce a wide variety of chromosomal rearrangements, such as inversion, deletions, and translocations and usually affect multiple genes(Cordes, 2005). However, they are not limited to single genes. Therefore, radiation is not a good approach for fine-scale mutagenesis. Irradiation with x-rays (Dove, 1987) produce large deletions and in practice it is difficult to recover large numbers of mutant animals. Thus, the mapping of such mutations is very difficult.

Chemicals

The chemicals such as ethylmethanesulfonate (EMS) causes point mutations or may be nonsense or mis-sense. Also, it can be in non-coding sequence, affecting splicing signals or regulatory elements that control gene expression. Agents such as chlorambucil which targets post-meiotic cells. Mutagenizing with chemicals produce many different mutations within gene regions. Chemicals induce a range of chromosomal rearrangements with great frequency (Russell et al., 1989). In this regard, chemicals such as alkylating agents ethyl methane sulfonate (EMS) and *N*-ethyl-*N*-nitrosourea (ENU) also has used. This alkylating agents induce hundreds of thousands random point mutation in whole genome (Cordes, 2005).

Transposable elements (TEs)

Transposable elements (TEs) or insertional mutagenesis containing a marker gene(s) that mobilized in the genome. The TE can insert in a coding region and disrupt the amino acid sequence. Also, it may insert into a neighboring non-coding DNA and affect intron splicing or gene expression. The most advantage of the TE insertion is that it can easily be mapped and cloned the region of genome. In this technique, after identifying mutants, they can be separated into complementation groups and mapped to general chromosomal location by linkage with known markers.

The forward genetic screen can apply on a single gene or on the entire genome. In one hand, there is region-specific screen in which the functional content of a particular genomic interval is investigated. There are two different approaches to induce mutation in genome. In the sequence-based approach, allelic series in selected genes generates. On the other hand, in genome-wide screens; the genetic regulation of a specific biological process will study. In Figure.2 shows current strategies in forward genetic screen. The mutagenesis screens in mouse can design in different ways. As is presented in Figure 2, there are several approaches to the identification of new mutations.

In this work the ENU chose to induce mutation in mouse model. After inducing the mutation in the animals, the breeding will take place to prepare mutant individuals. By phenotypes analysis the mutants isolated, and then the gene is mapped.

2.2.2. ENU mutagenizing in animal models

ENU

The *N*-ethyl-*N*-nitrosourea (ENU) induces mostly random single-base-pair mutations and mainly recessive loss-of-function mutations with random distribution throughout the genome. The (ENU) is an alkylating agent that generates hypomorphic mutations which often found in human disease. During DNA replication, the ethylated base pairs result in mistaken identity and introduction of a point mutations (Cordes, 2005). Mostly transversion of A to T and less frequently G/C-to-C/G or small deletions, in the DNA. Dosage and repetition of ENU treatment can be adjusted to induce on average one mutation in every 1–1.5 mega bases (Mb) or about 3,000 changes per haploid genome. In fact, about 1.6% of which are in coding regions (Concepcion, Seburn, Wen, Frankel, & Hamilton, 2004). ENU mutagenizing unlike irradiation affects single loci (Kile & Hilton, 2005).

According to a survey done by Noveroske et al, on ENU mutagenizing reports, 63% of mutations are missense and 26% cause abnormal splicing. The rest 10%; resulted in nonsense mutations, and 1% caused “make-sense” mutations by converting a stop codon to an amino-acid-coding codon (Noveroske, Weber, & Justice, 2000).

Previous ENU mutagenizing efforts reported G1 animals carry ~25 mutations with functional consequences. Also, these mutations occurs mostly in hypomorphic alleles rather than in alleles with hypermorphic (increased), neomorphic (novel), or antimorphic (dominant negative) function (Cordes, 2005).

To mutagenized animals; particularly in mouse models, adult male animals are better candidates given to active DNA repair rate in female animal's oocytes. The ENU mutagenize spermatogonial stem cells in male and ova in female animals. During lifetime of a male mammalian, sperm undergone division and differentiation continuously. However, Ova in female mammals produced by oocytes in perinatal period. Oocytes are undergone meiosisI, DNA miss match repair and DNA damage check points (W.E. Crusio 1999). Therefore, mutagenizing adult males is more successful. The mutated genes in their progenies are located only on paternally derived chromosomes (W.E. Crusio 1999).

It is expected to have mutation rate of approximately one mutation per 1.5 mega base pairs (Mbp) in an optimal ENU induction experiment in mouse (Weber, Salinger, & Justice, 2000). The rate of mutation by ENU is ~100-fold higher than the spontaneous mutation rate and 3-fold higher than X-irradiation approach (Kile & Hilton, 2005).

The ENU mutagenizing can produce approximately 32 loss-of-function mutations per genetic line. Therefore, the number of mutants would be much more than reverse-genetic approach. Most identified human molecular mutations are not null but function largely in hypomorphic manner or dominant and semi-dominant. Therefore, less polymorphisms in mutagenesis screens will allow us to identify novel proteins and perhaps classification of human allelic series. Thus, forward genetic is better approach to discover genes which are relevant with human disease (Weber et al., 2000). Generally, for the forward genetic screen two different type of screen strategy is available; conventional screens and modifier screens.

General ENU breeding strategy

To prepare a population of animal models to study and screen for induced mutations, treated male mice crossed with wild type female animals. Each F1 progeny will receive one mutagenized gamete and presumably would be Heterozygote regarding mutated genes throughout of whole genome. In fact, for total length of mouse genome (approx. 2998) Mb, 1 bp change per million bp induce. Thus, each F1 male carries approx. 3000 bp changes in whole genome (Kile & Hilton, 2005). As a result, each F1 mouse will carry about 30 coding changes. The ENU-induced mutations are recessive or co-dominant and in the best case scenario phenotypes only observed only in homozygotes.

Generally the ENU breeding can use in either conventional or modifier method. The conventional scheme is for discovering either dominant or recessive phenotypes. To study dominant phenotype mostly F1 progenies and for recessive mutants F3 progenies will be analyzed. In the other word, F1 animals will crossed out or breed with wild type animals and will screen for the phenotype of interest with dominant segregation (Figure.3). On the other hand, in case of

screening for phenotypes with recessive segregation, F1 male animals breed out with wild type animals and produce F2 generation progenies.

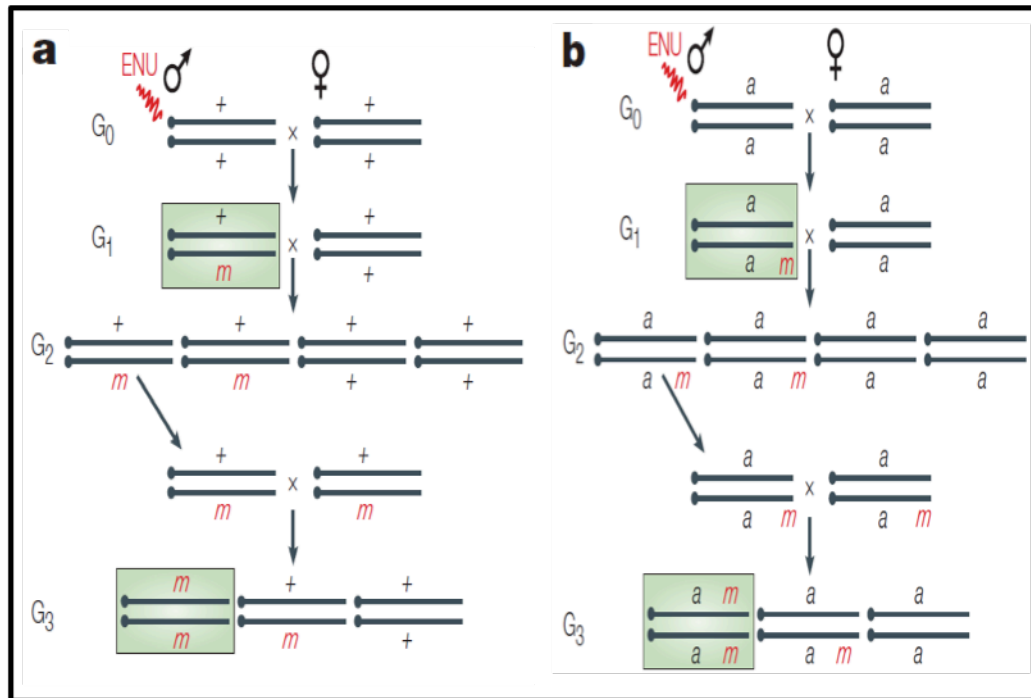


Figure 3. Conventional strategy and modifier strategy in conventional screen. The shaded box indicates animals to be examined for novel phenotypes in each screen strategy. In both panels, *m* represents a new ENU induced mutation and + indicates the wild-type allele. a. Conventional strategy in which mutants with deviation from normal wild-type phenotype is isolated. The isolated mutations can be either recessive or dominant. For dominantly functioning mutations the G1 generation will screen, and recessively functioning mutations being isolated in the G3 generation. b. In modifier screen *a* represents a pre-existing recessive allele that causes a phenotype of interest. ENU-induced mutation in this example is linked to the recessive allele *a*. In this screen, mutants with the pre-existing phenotype of interest will be isolated. This phenotype is enhanced or suppressed in modifier screen. In addition, genes that function in the same pathway as *a* can be identified. Adopted image from (Kile & Hilton, 2005).

In my part of screen, 4 G0 (C57Bl/67) ENU treated mice used to establish colony. From these G0, 114 F1 male animal produced by breeding with C57BL/6J or FVB female wild type animals and at least 4 female and 2 male produced from each F1 male. Each F1 male named the founder of a family of F2 generation animals. The F2 male animals were stored as substitutions of F1 founders.

As an alternative breeding strategy, in case of aging, death and sterility of F1 founder fathers, each F2 female could use for interbreeding with F2 females. Regarding of required time

to screen one F2 female per F1 male, total 21 to 22 weeks should take in consideration. In detail, 10 weeks is required to produce F1 mature (7 week old male) animals from each G0. Then if F1 males bred exactly at 7 weeks old, WT female partners yield F2 generation animals in 4 weeks. By 2 months these F2 animals were mature and back crossed with F1 founder. Then, after three or four weeks, the P0 pups were ready for screen. In case of P7 screening one more week took to finish screening of one F2 female.

In this case by crossing back of each F2 female with F1 founder, scientist expect to detect a recessive phenotype in $\frac{1}{4}$ of progenies. This hypothesis is according with segregation mandelian law; ‘‘ the alleles for each gene segregate from each other; hence, each gamete carries only one allele for each gene’’. The Figure.4 presents a breeding scheme model.

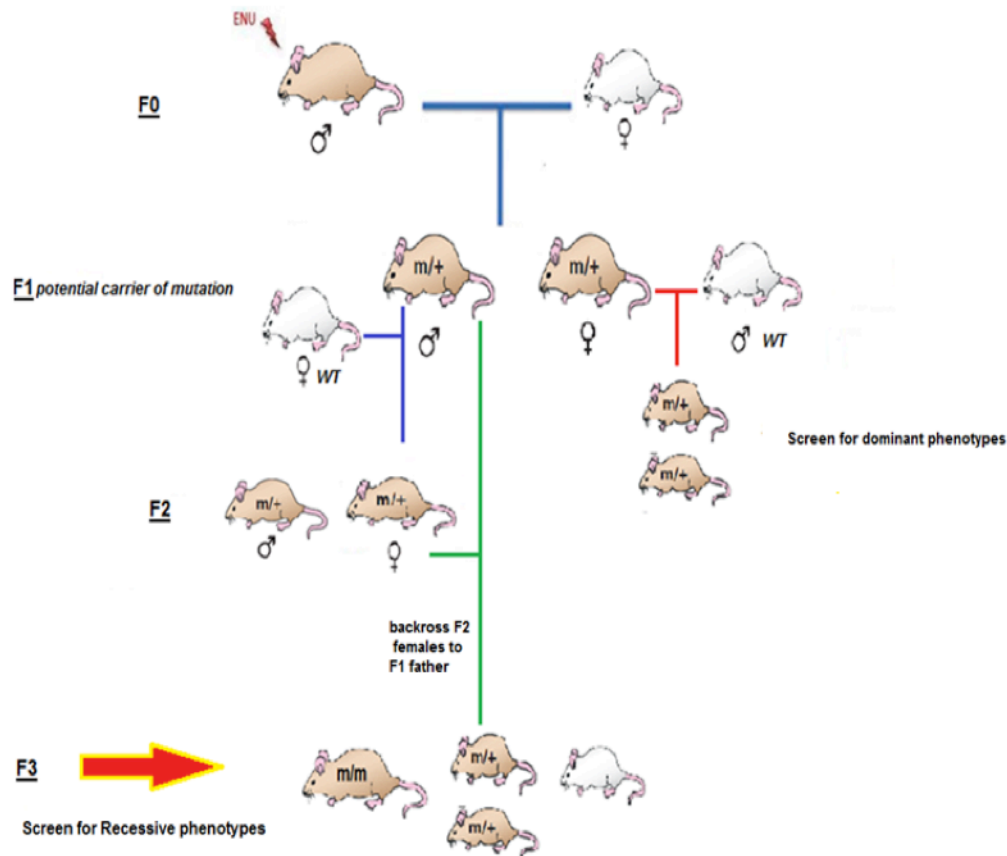


Figure 4. Breeding scheme for conventional forward screen

In this work the conventional screening for recessive phenotypes carried. According to ‘Efficiency of scanning’’ index; advent by Shedlovsky group, probability of finding one homozygote in F3 generation of a F1 founder calculated as follow.

In case of; screening 4 F2 female per 1 F and per cross screening of 5 the efficiency is 85% .

$$E = 1 - [0.5 + (0.75^n)]^k$$

K: number of G2 females and n: number of progeny tested per G2

In this work for each F1 male; at least 4 F2 female screened and the average litter size was 7.

Therefore, the efficiency of this screen was 83%. Thus, ¾ of progenies (75%) would carry none or only one allele of mutated gene. As a result, no phenotype with recessive segregation would identify. In other 25% of F3 progenies; in which will receive the mutated gene from both parents; the recessive phenotype will manifest.

In order to assess the probability of transmission of each F1 mutation to F3, following formula suggests by Georgel et al (Jonathan Ewbank, 2008).

$$P = 1 - [0.5 + (0.5) * (3/4)^{g3}]^{g2}$$

g2= number of F2

g3= F3 offspring per F2 mother.

For example if two F2 daughters per F1 male produce and three F3 pups per F2 daughter screen, approximately 50% of F1 mutations will transmit into F3 homozygous (Jonathan Ewbank, 2008). For recessive screen the mutagenized male mate with untreated females to produce the F1 progeny. Furthermore, recessive screening requires additional breeding to establish the F2 generation and crossing each F1 father to achieve homozygosity for expression of the recessive mutation.

Modifier screen

In modifier screens, scientist analyze the modification of a pre-existing phenotype. Therefore, they isolate mutants with enhanced or suppressed previous phenotype. In conventional screen, The G0 ENU-treated males breed to wild type females to produce F1 offspring. The F1 mice are heterozygous for these mutations. Then depends on dominant or recessive type of screen breeding protocols are different.

Most of previous ENU forward genetic screens done to identify dominant mutations. For example, two important genes in development of inner ear such as *beethoven* and *headturner* identified through this type of screen. Although, screening for dominant phenotypes are easier and shorter in terms of the time of generation production. The rate of recovery of phenotypes is around 2% (Nolan et al., 2000). Thus, many genes would have been missed in these types of screens (Brown & Nolan, 1998).

Each progeny of G0 male mouse, contains about 25 mutations that affect protein sequence. This hypothesis is true if the 1.5% of the genome encodes a protein (Weber et al., 2000).

For any single locus, one can expect to recover a point mutation among approximately 1000 mutagenized gametes. Therefore, ENU mutagenesis has a potential to generate an allelic series, which can exhibit a variety of phenotypes reflecting the divergent functional aspects of the encoded protein.

2.2.3. Previous ENU forward genetic screen work on mouse

Indeed, ENU forward genetic screen is technique to identify novel phenotypes and genes for developmental biology research.

The largest mouse mutagenesis program in the world located at Scripps research institute and developed by Dr. Beutler, the Nobel prize winner 2011 ("Beutler laboratory"). The main goal of this ENU forward genetic screen project is identifying genes that are essential for the mammalian innate immune. Many genes involve in immune response has discovered through this work. For example, *Yipf6* that induce a spontaneous intestinal inflammation in mice model (Brandl et al., 2012); missense mutation in the gene encoding the protease *iRhom2* and disrupts the secretion of mouse TNF alpha (Siggs et al., 2012); a dominant mutation called ***Possum*** with neurobehavioral abnormality (Kearney et al., 2001). The summary of discovered novel mutant strains is available on <http://mutagenetix.scripps.edu>; ("UT Mutagenetix center,").

Some other successful previous ENU forward genetic screening in mouse carried on at GSF in Munich, Germany, and the Medical Research Council center in Harwell, UK can successful previous work. In the both groups the screens conduct to identify dominant mutations. At GSF, 182 confirmed mutants, from 14,000 F1, was isolated. These phenotypes were changes in visible,

clinical–chemical, biochemical, immunological, haematological and behavioral parameters. The Harwell screen focused on visible, clinical–chemical and neurobehavioural phenotypes. They reported 196 heritable traits from 35,000 F1 mice.

In addition, at the Australian Phenomics Facility has provided a large library of discovered and available phenotypes and their causative genes under name of Australia phenome bank at <http://www.apf.edu.au/> ("APF,") .

Some of other identified phenotypes by ENU forward screening are: anemic *hem8* mouse model in which can be used in the study of iron metabolism (Bartnikas et al., 2013). The cleft palate as a result of a dominant point mutation; cardiac and nuchal edema, neural tube defects, situs inversus of the heart, posterior truncation and the absence of limbs and lungs.

In another ENU forward genetic screen by Carolien Wansleebe and et al, (2011) on mouse embryo in different embryonic stages, various phenotypes isolated. Among those two homozygous mutants (E17.5) with the neural tube defect craniorachischisis , *Sec24b*^{Krabbel} and *Scrib*^{5120-6B} , identified with lung development defect. Lungs of both mutants were smaller than those of wildtypes and the lobes are irregularly shaped (Wansleebe et al., 2011). They reported the phenotype is due to inadequate intracellular trafficking of *Vangl2*. In mouse, Planar Cell Polarity (PCP) gene, *Vangl2*, encoding core PCP proteins and plays role in embryonic convergent extension (CE), polarized cell division, cilia orientation and mammalian kidney-branching morphogenesis (Wansleebe et al., 2011).

This, mutation of *Vangl2* in mutant *Sec 24- b* creates neural tube defects (NTDs) and impair branching of embryonic mouse lung airways. The identified phenotypes by Wansleebe et al presented at Figure5.

Regarding other identified phenotypes by ENU forward genetic screening, cardiac and nuchal edema, neural tube defects, situs inversus of the heart, posterior truncation and the absence of limbs and lungs. Totally they identified novel mutant alleles for *Dll1*, *Ptprb*, *Plexin-B2*, *Fgf10*, *Wnt3a*, *Ncx1*, *Scrib* (*Scrib*, Scribbled homolog of *Drosophila* and *Sec24b* (Wansleebe et al., 2011). This work was one of best examples of a successful ENU forward genetic screening; however, this study done in embryonic stages of F1 offspring; dominant segregated phenotypes.

In addition, previous ENU forward genetic screen reported some phenotypes in lung such as mutants with thickened lung mesenchyme at E18.5. This phenotype observed in distal airspaces and mesenchyme become thin in order to enhance the gas exchange. If the lung mesenchyme fails to become thin, it impairs gas exchange after birth (Cole et al., 1995) (Hooper & Wallace, 2006). Two lines reported for this phenotype, 12BCC-013 and 12BCC-016 (Caruana et al., 2013). However, this phenotype was not reproducible due to carrier males in line 12BCC-013 and another line failed to produce further progeny. They suggested either weak penetrant phenotype or the introduction of a modifier alleles could be the reasons of negative recovery. The table 3 presented the summary of ENU- induced mouse mutants in this reported work.

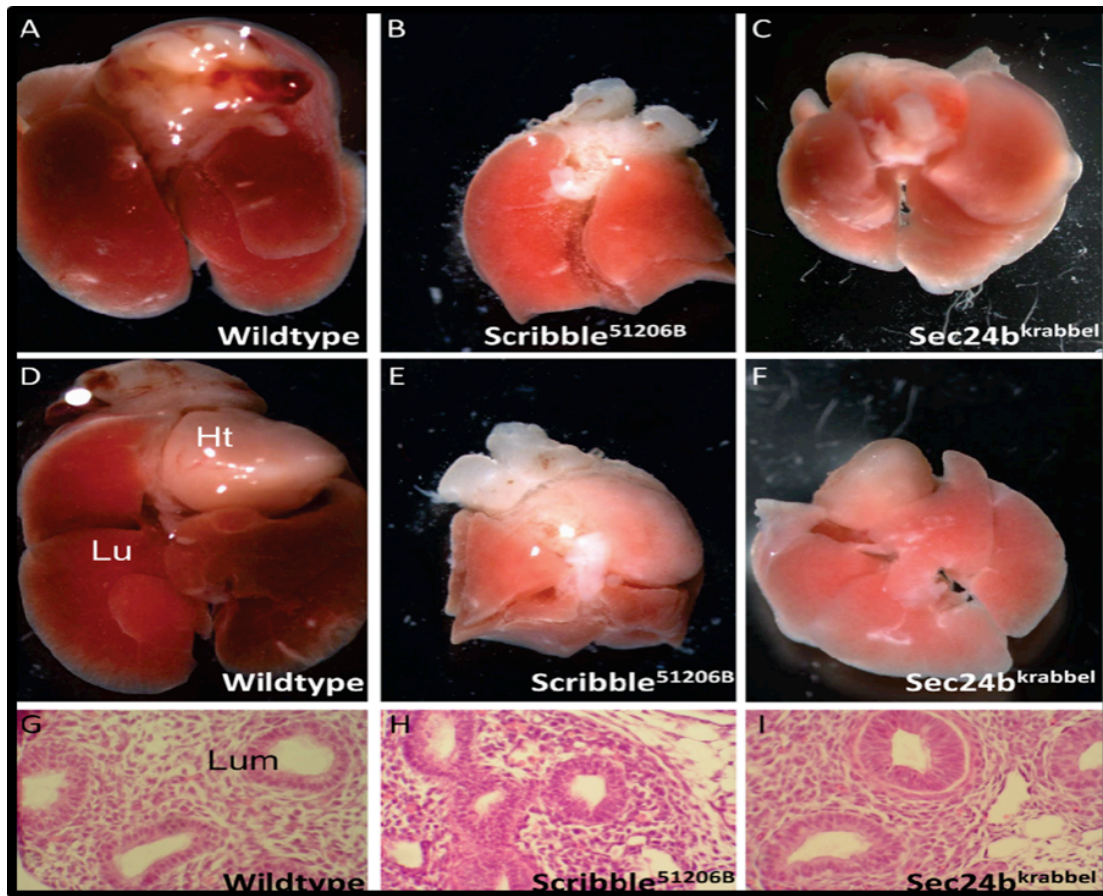


Figure 5. Affected lung development obtained in Wansleebe et al. screen report. (A–C) Dorsal and (D–E) ventral views of the lungs and hearts of (A,D) wildtype (B,E) Scribble and (C,F) Sec24b mutant embryos. Note the reduction in size of the mutant lung, in particular that of Scribble. (G–I) Sections of wildtype (G), Scribble mutant (H) and Sec24b mutant (I) lungs at E13.5. Ht and Lu (D) mark the heart and Lungs respectively, lumina (G) are labeled 'Lum'. Adapted figure from (Wansleebe et al., 2011).

According to previous phenotype screening studies most of recovered phenotypes have been discovered in other organs than lung and respiratory system. Many mouse models has developed, however; the necessity of developing and informative mouse models for lung diseases specially interstitial inflammatory lung disease haven't fulfilled. Thus, phenotypic driven genetic screen approach as an unbiased approach can result in discover of causative genes of lethal respiratory disease.

Table-3. Summery of ENU mutant identified phenotypes. Adopted from (Caruana et al., 2013).

Line	Time-point	Phenotype	Affected/Total no. embryos screened*	Affected/Total no. of embryos in affected litters	Gene ID/mapping
<i>bfb</i> [#]	18.5	skeletal (craniofacial/polydactyly)	16/149(11%)	9/46(20%)	<i>Fras1</i>
		skin		5/37 (3.5%)	
		kidney		2/21 (9.5%)	
11BC-11	18.5	Skeletal (syndactyly, craniofacial)	5/116 (4%)	5/20 (25%)	Unknown
snoopy [#]	13.5	craniofacial	8/134 (6%)	8/32 (25%)	Unknown
kanyon [#]	13.5	craniofacial, neural tube, exencephaly	12/52 (23%)	12/26 (46%)	Chr 7
<i>cauli</i> [#]	13.5	craniofacial, exencephaly, spina bifida, polydactyly, limb anomalies	15/73 (20.5%)	15/54 (28%)	<i>lft140</i>
12BC-19	18.5	Kidney, ureter	12/208 ^b (6%)	12/64 (18.8%) ^b	unknown
12BC-20	18.5	Kidney, ureter	11/198 ^b (6%)	11/42 (26%) ^b	unknown
12BCC-13	18.5	lung	7/176 (4%)	7/21 (33%)	unknown ^a
12BCC-16	18.5	lung	3/27 (11%)	3/8 (37.5%) ^s	unknown ^a
12BCC-20	13.5	gonad	7/280 ^b (2.5%)	7/36 (19%) ^b	unknown ^a
12BCC22a [#]	13.5	blood	11/136 (8%)	11/29 (38%)	<i>Lig 1</i>
12BCC-22b	13.5	spina bifida, curled tail	23/136 (17%)	23/60 (38%)	unknown
12BCC-24	18.5	curled tail	4/24 (17%)	3/15 (20%)	unknown
		fused digit		1/15 (6.7%)	
14BC-2	18.5	eye pigmentation	3/31 (10%)	3/15 (20%)	Unknown
14BC-7	18.5	Kidney, ureter	7/305 ^b (2%)	7/43 (16%) ^b	Unknown

[#] Allele names and symbols have been registered with MGI. Allele ID for *lft140^{cauli}* is MGI: 4458412. Mouse strains have been deposited into the Australian Phenome Bank repository (<http://pb.apf.edu.au/phenbank>).

^aNumber of G3 embryos screened in litters with ≥ 6 embryos/litter.

^sAffected embryos in 3 individual litters. Litter sizes were <6 embryos for this pedigree.

^aThe phenotype was not inherited by the 2nd generation males.

^bTotal numbers include male and female. Testis anomalies are only seen in males and kidney anomalies are predominately seen in males. Therefore a greater number of total embryos were screened.

2.3. Discovering of the causative gene in identified phenotype

2.3.1. Isolation of phenotypes

An extensive histological and immunohistological analysis carried on P0 and P7 pups of F1x F2 females. The detail of assays and techniques explained at chapter 3- material method. Once, the identified F2 female carrier analyzed for second time (secondary screen) and showed

same phenotype characteristics. The F2 animal identified as the carrier and F3 generation produced from it by breeding it with a WT C57BL/6J. Due to aging of F1 and F2 breeders, in some cases the secondary screen done after out crossing of F2 and producing F3. To keep the line of mutants, the F3 carriers the outbreed to produce F4 animals. Of course, it was after recovery of phenotypes in F3 generation and preparing samples for whole exome sequencing.

2.3.2. Mapping and whole exome sequencing

In past mapping of diseases induced by mutations after ENU treatment was extremely time consuming. However, by revolutionizing of next-generation sequencing the large-scale forward genetic screens and ENU mutagenesis programs all over the world become more fruitful.

Exome sequencing is a strategy where known coding and some non-coding regions of the genome are enriched by hybridization to DNA or RNA probes and the resulting enriched genomic DNA is then sequenced.

One limitation of this approach is this only applicable to the discovery of mutations within the enriched regions. Mutations in poorly or recently annotated coding sequence or in non-coding sequence will not be found.

Moreover, non-coding sequences that will not be assessed by exome sequencing include much of the UTRs, many non-coding RNA genes and regulatory sequences such as transcription factor binding sites and enhancer. However, these non-coding functional elements often reside in regions of the genome that are conserved between species. These limitations of exome sequencing could be overcome if an additional set of probe pools, designed to the noncoding conserved elements (Hubisz, Pollard, & Siepel, 2011). Thus, the custom designed probe pools for used for exome sequencing would be the reliable approach (Simon, Mallon, Howell, & Reinholdt, 2012).

Aiming to develop new animal models for lung diseases, decided to use a forward genetic screen approach. This strategy provides an unbiased method to identify genes and signaling pathways regulators which contribute to pathological conditions. The available models and knowledge regarding lethal lung disease is not comprehensive. Still to characterize the detail mechanism of such diseases new animal mouse models that their pathological conditions

humanized is required. To establish a model that recapitulate human respiratory disease condition more than one mutation and one causative gene is required. Thus, ENU forward genetic screen is an optimal approach. In addition, most of previous screening on ENU mutagenized mouse carried on embryonic age. Therefore, isolated putative mutants showed early development and patterning of the respiratory system. However, embryonic viable mutations and associated lung epithelial cell differentiation and dedifferentiation regulators left to characterize. Thus, to screen for such phenotypes, pups at postnatal day 7 (P7) isolated and a comprehensive histological and immunohistological methodology used.

Chapter 3

Materials and methods

3.1.Equipment

Disposable

Table 1.1. list of equipment used in this work.

Equipment	Model	Suppliers
Pipette PIPETMAN	F123615	Gilson International
Coverslips	24x50 mm	Menzel Gläser
Coverslips	20x 20mm	VMR
Glass slide	Super ultra plus	Thermo scientific
Reaction tubes 1,5ml; 2ml	Safe Lock Tubes	Eppendorf
Latex gloves	Powder free	ROTH
Syringe	5 ml	TERUMO
Syringe	1ml Omnifix-F	BRAUN
Needle	21G, 0.5x 16 mm	TERUMO
Butterfly needle	Ecoflo- 20mm	Dispomed
Falcon 50ml	227261	Greiner bio-one
Pipette tips	10 µl; 200 µl;1000 µl	Greiner bio-one
Thin pipette tips for kapillary filling	20 µL Physio Care Concept	Eppendorf
Cryomolds 25/20/5mm	4557	Weckert Labortechnik
Pipette 10ml, 25ml, 5ml	1V	Greiner
Pasteur-Pipetten Glas 150mm, 230 mm		VWR
Eye dropper pasteur pipette Plastic	1V	Greiner
Syringe top filter Filtropur 0.20µm		Sarstedt
Syringe top filter Filtropur 0.45 µm		Sarstedt

Non-disposables

Table 1.2: list of equipment used in this work.

Equipment	Model	Suppliers
Staining jar- Staining PMP (TPX)	631-9130	VWR
Staining from Choplin	631-9331	VWR
Staining jar with lid	631-9328	VWR
Forceps Student Dumont #5 Forceps – Inox	91500-09	Fine Science Tools(FST)
Forceps Student Dumont #5 Forceps	11252-40	Fine Science Tools(FST)
Scissors- Micros scissors- wide curved	503364	Word PrecisionInstruments(WPI)
Scissors-McPherson-Vannas-straight	14124	Word Precision Instruments(WPI)
Gerald Forceps - Serrated Curved -17cm	11015-18	Fine Science Tools
Thin pipette tips for kapillary filling20 µL		Physio Care Concept
Objekttrager-Mappe Karton 30-PI	631-0690	VWR International GmbH
Dako Pen for Immunocytochemistry	S200230-2	Dako Deutschland GmbH
Magnetic Stirring Bars, Length: 50 mm, diameter: 8 mm	442-4528	VWR International GmbH
Water bath Gfl 1003	462-5112	VWR
Mini-tumble mixer (Nutator)		VWR International GmbH
Water bath		Ju-Labo
PH Meter Five easy Fe20-Basic		Mettler-Toledo
Cryostat	CM1950	Leica
Flourescence Microscope	Imager A1	Zeiss Axio

Table 1.3: Product, type and supplier of used non-disposable materials.

Product	Supplier
BSA	SIGMA
Entelan	Merck
Paraformaldehyde	Sigma
Triton X-100	Sigma
Colorization kit Masson Trichrome-HT15	Sigma
Xylol	Roth
Alcian Blue 8GX	Sigma
Oil red O	Sigma
Ethanol	Roth
Methanol	Roth
Mowiol 4-88 Reagent	Merck
Phosphate buffer saline (PBS) tablets	Signa
Saccharose	Roth
OCT	Tissue Tek
Hematoxylin	Wadeck
Glacial acetic acid	Roth
Eosin solution	Waldeck
Glycerol	Merck Milipore
Isopropanol	Roth
Vectashield	Vector lab

3.2. Buffer and solutions

Used **buffer and solutions** in this work are listed. Unless specified otherwise the solutions were prepared in distilled and autoclaved water. Freshly prepared solutions for an application were not autoclaved.

Table 2: Compositions of buffers and solutions.

Buffer/Solution	Compositions
PFA in PBS (4%)	4 g PFA dissolve in 100 ml PBS (add few drops of NaOH). Heat at 55°C until PFA is dissolved. Cool and adjust the pH to 7.4 and store at -20°C
B-Block	2% Bovine serum Albumin(BSA) in PBST [v/v] 0.1% Tween 20 [v/v]. Store at 4°C
Acetic Acid Solution (3%)	Glacial acetic acid 3 ml in 97 ml Distilled water. Store at room temperature.
Alcian Blue Solution	1 g of Alcian blue, 8GX in 100 ml of Acetic acid 3% solution Mix well and adjust pH to 2.5. Store at room temperature.
Nuclear Fast Red (0.1%)	Dissolve 5 g of aluminum sulfate in water. Add 0.1 g nuclear fast red and slowly heat to boil and cool. Filter and add a grain of thymol as a preservative. Store at room temperature.
Oil Red O stock solution (ORO) (0.7%)	0.7g of oil red O dye mixed in 100ml of Isopropanol for 2hrs. It was then filtered using a whatman filter paper. (This solution can be stored for 6 months at room temperature)
Antigen retrieval buffer	0.1 M Tris/HCl buffer (pH 9.0)

Antibodies

Primary Antibodies

Name	Description	Company	Raised in	Dilution	Reference
Acetylated alpha-Tubulin	Monoclonal- IgG2	Sigma	Mouse	1:10000	T7451
Alpha smooth muscle actin-Cy3	Monoclonal IgG2a	SIGMA	Mouse	1:500	c6198
Anti-Pro surfactant Protein C (proSP-C)	Polyclonal IgG	Merck Millipore	Rabbit	1:600	AB3786
Anti cytokeratin 5	Polyclonal IgG	abcam	Rabbit	1:1000	ab53121
CC10(T-18)	polyclonal IgG	Santa cruz	Goat	1:200	sc9772
CGRP-KLH	Polyclonal	SIGMA	Rabbit	1:5000	C8198
E-cadherin (Decma-1)	monoclonal	abcam	Rat	1:1000	ab11512
Isolectin B4- FITC (BSI-B4)	Lectin from Bandeiraea-conjugated	SIGMA	Bandeiraea simplicifolia	1:5000	L2895
Mucin 5AC(45M1)	monoclonal IgG	abcam	Mouse	1:3000	ab3649
PCNA(PC10)	monoclonal IgG	Santa cruz	Mouse	1:300	Sc-56

Hybridoma bank antibodies

Developmetal Studies of Hybridoma Bank (DSHB) Supernatant antibodies	Antibody Name	Description	Host	Dilution
	AMF-17B/ Vimentin	Monoclonal IgG	Chicken	1:30
	G8.8/ EPCAM	IgG2a	Rat	1:10
	2.21B4/ Duct-1	IgM	Rat	1:20
	8.1.1 / T1alpha	IgG	Hamster	1:20
	2H8/ PECAM	IgG	Hamster	1:1

Secondary antibodies

Name	Company	Dilution	Reference
Alexa Fluor 488 Goat Anti-Rat IgG (H+L)	Life Technologies	1:300	11006
Alexa Fluor 488 Goat Anti-Rabbit IgG (H+L)	Life Technologies	1:300	11034
Alexa Fluor 488 Goat Anti-Mouse IgG (H+L)	Life Technologies	1:300	11029
Alexa Fluor 488 Donkey Anti-Mouse IgG (H+L)	Life Technologies	1:300	21202
Rabbit Anti-Syrian Hamster IgG H+L (DyLight® 488)	Abcam	1:300	Ab102328
Alexa Fluor 488 Donkey Anti-Rat IgG (H+L)	Life Technologies	1:300	21208
Alexa Fluor 568 Donkey Anti-Mouse IgG (H+L)	Life Technologies	1:300	10037
Alexa Fluor 488 Donkey Anti-Rabbit IgG	Life Technologies	1:300	10042
Alexa Fluor 568 Donkey Anti-Mouse IgG	Life Technologies	1:300	10037
Donkey anti-Goat IgG(H+L)-Cy3.5 conjugated	Bethyl	1:300	50-201C4
Goat anti-Syrian Hamster IgG(H+L)-Cy3 conjugated	Bethyl	1:300	140-201C3

Methods

1. Mice:

1-1.Ethics statement

All animal experiments conformed to the regulatory standards of, and were approved by German animal welfare authorities under approval number B21-1011.

1.2. ENU mutagenesis and Breeding strategy

C57BL/6J males at were injected interaperitoneally at the age of 8–10 weeks with 100 mg ENU per kg body weight weekly for three weeks. The ENU mouse has purchased from Monica Justice laboratory at Baylor College of Medicine, USA (Salinger & Justice, 2008).

Then for executing genome-wide screen; first G0 male mice are injected with ENU and crossed with untreated wild type females to produce F1 progeny. Then F1 were heterozygous for a potential mutation and they have mated with non-mutant females to yield F3 animals.

The F1 fathers are the family founders and for each family 4 to 5 F2 female animals produced. In addition, the F2 male sibling kept alive as an alternative breeder in case of F1 breeders death. Crossing of F1 animals with F2 females can produce a reproductive pressure on F1 male. Therefore, as an alternative male breeder, the F2 male animals kept alive. Once a F2 female identified, it has outcrossed with a wild type male animal to produce F3 generation. Later on, each F3 animal were back crossed with F1 founder to identify heterozygote carriers in F3. Meanwhile, during the time for growing mouse population to mature, the F2 females have re screen by F1. Actually, for each candidate first the F2 female crossed with F1 father to assure regarding the phenotype and penetration of phenotype rate. F1 and F2 back cross pups were used at postnatal seven (P7) and postnatal zero (P0) of age.

Regarding of required time to screen one F2 female per F1 male, total 21 to 22 weeks should take in consideration. In detail, 10 weeks is required to produce F1 mature (7 week old male) animals from each G0. Then if F1 males bred exactly at 7 weeks old, WT female partners yield F2 generation animals in 4 weeks. By 2 months these F2 animals were mature and back

crossed with F1 founder. Then, after three or four weeks, the P0 pups were ready for screen. In case of P7 screening one more week took to finish screening of one F2 female.

In this work to increase the pace of screen, initially two females per male breeders used. Then later three breeders per one partners used. However, this breeding strategy put female breeders at stress and result in aborted embryos or carnivores reaction. Thus, in most cases we applied 2 female per male strategy. For sake of space at animal house, at the same time 30, F1 male used and after screening first 30 founder, the second 30 F1 males and their prepared family screened.

This screening covered all 114 F1 founders in three round of non stop screening.

Once F1x F2 cross yield P7 pups, each pup checked individually for any macroscopic phenotype and weighted. In this regard, each pup's breathing pattern and skin color monitored as well. The aim was identifying any respiratory mall function as well as cyanosis due to new born respiratory syndrome. In addition, any morphological defect such as limb malformation, sub-cutaneous and sub cranial hemorrhage, limb displacement, hair and whisker loss, and cleft palate has checked. The severe morphological (catastrophic) defects just recorded since the aim was selecting significant phenotypes related with respiratory system cells differentiation. Most of gross morphological defects and pups with sever new born respiratory syndrome only revealed in dead pups or not have found due to cannibalism by mother after birth. In fact in this screen for 50 litters of P7 mouse the blood glucose and lactate measured as well as retina isolated and analyzed regarding any significant phenotypes. Later on, this screen narrowed down only to the lung lobes and trachea phenotype (Figure3).

Lung and trachea isolation

Processing and sampling of lung and trachea tissue for histology and Immunohistochemistry analysis

First each pup was anesthetized with Isofluran CP for 5 minute. Then, abdomen's skin was cut and rib cage cut at corners in order to prepare an open thoracic cavity. Then salivary glands were removed to expose the trachea. After that the heart was injected with 1 cc of distilled, deionized (DI) water with a 21 gauge needle through the right ventricle. This injection washes the blood from heart and respiratory system. According to the diameter of the trachea in pups, 1 mm,

the butterfly needle was used to infuse lungs with 2-cc of fixative, 4% paraformaldehyde (PFA) through the trachea. In addition, the thymus was removed. In P0 pups the whole respiratory system while still attached to heart was removed and placed in the 4% paraformaldehyde (PFA) in a well of sterile six well plate for one hour at 4° C (Figure 1. A, B).

In P7 pups the trachea was detached and divided into two parts. The posterior part of trachea was collected for whole mount Alcian blue staining (Figure1. C) and the anterior portion fixed in PFA for 1 hour at 4° for further histological and immunohistological analysis.

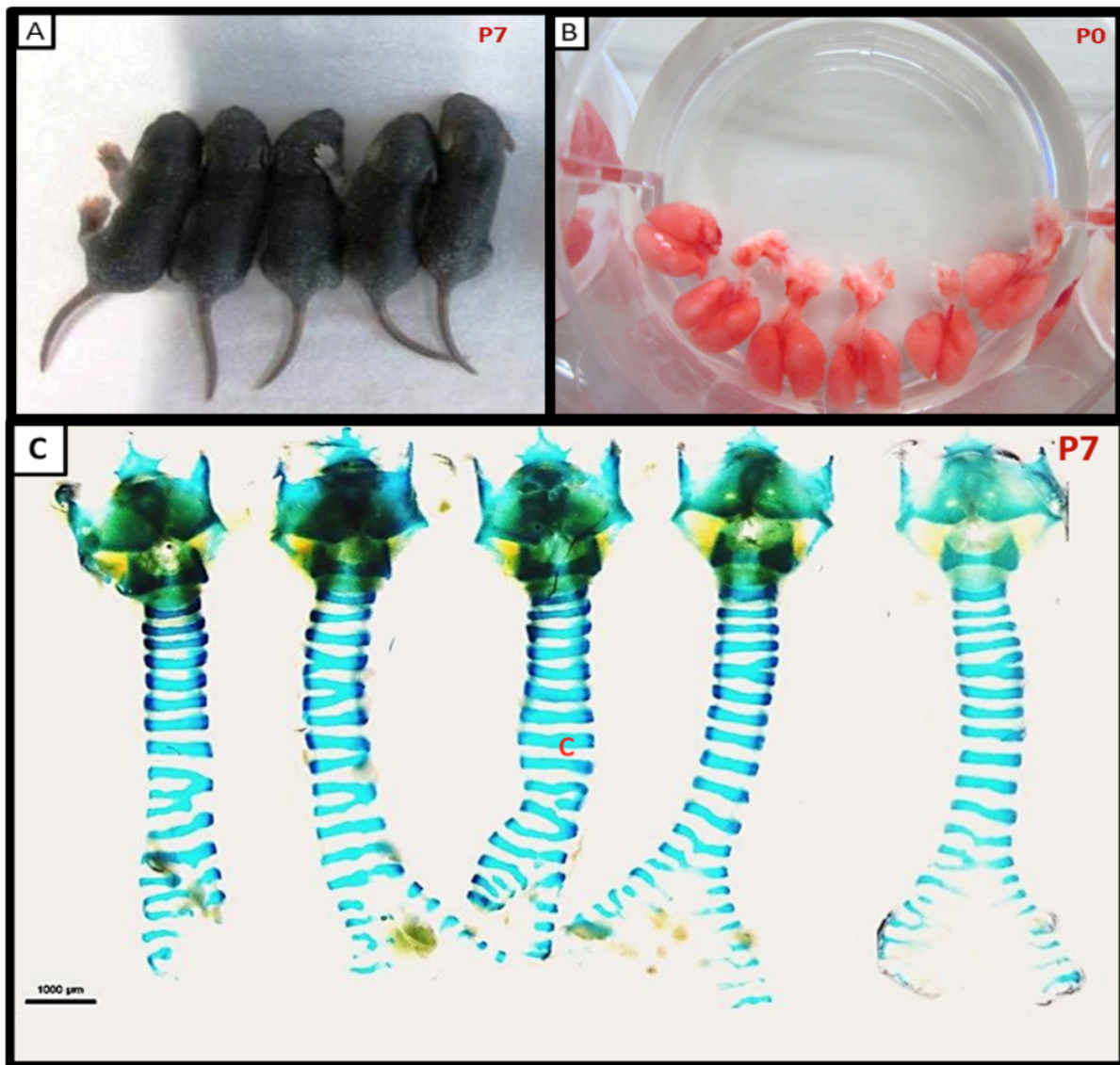


Figure 1. P7 pups and isolated whole lungs and trachea analysis. (A), (B) 1 litter of pups that the lung lobes as well as trachea isolated and fixed in 4% PFA for further analysis. (C) Alcian blue whole mount staining of trachea. The cartilage rings stained in blue (C stands for cartilage). The isolated trachea looking normal and each trachea has average 12 C shape cartilage rings in the ventral side.

1.3.2. Dissection and sampling of eye for retina whole mount staining and analysis

After isolation of lung and trachea from euthanize pup with Isofloran. The head fixed on surgery pad by pinning down on the surgery pad or putting a forceps. Then the skin that surrounds eye cut and remove to expose skull and connective tissue. By pushing down the tip of sharp curved forceps or curved scissors under the eye, the eye bulb scope out and collect by a fine forceps. First, the retina washed 1X for 5 minute in PBS to remove extraneous tissue and blood from the outside of the eye. Then fixed in 4% PFA on ice for 2 hours at 4° C. After fixation, washed 3X with PBST (PBS 1X + Tween 0.1 % for 10 minutes each and directly dissected. After fixation eyes can be stored in PBS for 1night at 4°C. The dissection steps conducted under the bright field microscope. Each eye collected by an eye droppers Pasteur pipette with the cut tip to become wider for avoiding damaging eyes. Eyes put in a 35mm dish containing 1X cold PBS. Eyes are submerged in PBS. The eye bulb fixed by pushing down the optical nerve and faced up the cornea. During dissection, the eye maintain its spherical shape and by a pairs of sharp forceps (DUMONT# 5, 11252-40,FST) gently remove as much muscle and connective tissue as possible. Then by inserting tip of a needle (27G) into the cornea and help of a fine scissors (15000-00 FST) a small hole pinched in the center of the cornea and by help of a pair of forceps cornea removed. Then, the Iris and Sclera; the black color membrane which embrace the eye retina, removed and finally the lens collected. The hyaloid vessels, located in proximal of developing retinal vessels, removed gently by forceps. In the last 4 cuts made in retina to make a 4 petals shape clover.

1.3.3. Procedure of sampling

After one hour pre-fixation of lung lobes, they washed 3 times with 1x PBS for 5 minute each. Then subsequently infiltrated with 10 % sucrose in 1x PBS, 20 % sucrose in 1x PBS each 60 minute and finally in 30 % sucrose in 1x PBS for overnight. Left lobes were mounted in O.C.T medium on one cryomold, dorsal part placed towards surface of cryomold. The dry ice used for

freezing. In addition, anterior part of trachea after post fixation and sucrose gradient treatment were placed in cryomolds with same method.

Then tissue sections were cut with 8-10 μm thickness using a cryostat machine. Sections were air dried over night or 12 hours and stored at -20°C for further use.

2. Staining

2.1 Alcian blue/Nuclear fast red staining (whole mount):

Posterior trachea was incubated in 95 % ethanol for 30 min at room temperature and then washed 1x with PBS. Followed by staining in 0.03 % Alcian blue solution (dissolved in 80 % ethanol and 20 % acetic acid) over night at room temperature.

In addition, the lung lobes with all five lobes as well as anterior portion of trachea has placed in PFA solution inside of one well of sterile six well plate for one hour at 4°C .

In next day posterior trachea washed with 80% ethanol for 3 hours at room temperature until extra connective tissues dissociate from cartilage. Then trachea washed in 2% KOH for 3 hours and finally, treated with gradient of glycerol in PBST solution 50% and 80% for 1 hours and in 100 % glycerol overnight. Then anterior trachea analyzed under light microscope regarding cartilage rings pattern in trachea (Figure 1.C).

2.2. Hematoxylin and Eosin (H & E) staining:

The cryosections were post-fixed in 4% PFA for 20 min, briefly rinsed in PBS 1x 5 minute and stained in Hematoxylin acidic meyer solution (WALDECK, Cat. No 2E-038) for 10 min. Then sections washed in running water for 5 min and put them in 2% Eosin stock solution (WALDECK, Cat. No 2C-140) for 30 seconds for counter staining of cytosol. Dehydration was done by incubating the slides in 95 % ethanol for 1 min followed by incubation in 100 % ethanol for 2 min. Clearing was done in xylene medium for 2 min followed by mounting of slides with Entellan

(MERCK). In Figure 2. A,B, D. longitudinal and transverse sections of trachea and lung that stained with H&E staining presented.

2.3. Alcian blue/Nuclear fast red staining (tissue sections):

For tissue cryosection after air drying over night or 12 hours at room temperature slides were fixed in 4% PFA for 10 minutes. Then, slides were washed 3 times for five minutes in PBS 1x. Later, for 30 minutes stained with 1% Alcian blue solution (Sigma life sciences, Cat. No A5268-10G) dissolved in 3% acetic acid for 30 minutes. Slides were washed in running tap water for 2 minutes and rinsed in distilled water. Then, slides were counterstain in 0.1% nuclear fast red solution for 5 minutes. Proceeding with wash in running tap water for 1 minute. Slides were dehydrated through 95% Ethanol and 2 times absolute alcohol and clear in xylene or xylene substitute. Slides were mounted with Enthelan mounting medium.

2.4. Masson trichrome staining

For cryosection slides after fixation with 4%PFA, the Sigma-Aldrich Trichrome Stains (Masson) kit used. To study connective tissue, muscle and collagen fibers in interesting phenotypes in lung with inflammation, fibrosis and alveolitis phenotypes. Trichrome stains used to distinguish collagen and extracellular matrix material. Tissue sections are treated with Bouin's solution to intensify the final coloration. For this purpose slides were incubated in preheated Bouin's Solution at 56°C for 15 minutes or at room temperature overnight. Then, slides cooled down in tap water and wash in running tap water to remove yellow color from sections. Then Nuclei are stained with Hematoxylin solution for 5 minutes. Wash in running tap water for 5 minutes and rinse in deionized water. Then, cytoplasm and muscle are then stained with Beibrich scarlet-acid fuchsin. After treatment with phosphotungstic and phosphomolybdic acid, collagen is demonstrated by staining with aniline blue. Rinsing in 1% acetic acid for 2 minutes and rinse slides. Dehydrate through alcohol, clear in xylene and mount.

The nuclei will be in black blue if Hematoxylin solution use, cytoplasm and muscle fibers in red and collagen in blue.

2.6. Oil red O staining

After fixation of cryosections in 4% PFA for 15-20mins. The slides were washed in PBS for 5mins. The slides were then dipped into 60% isopropanol for 5mins. Slides were then kept in the Oil Red O working solution for 15mins. The Oil Red O working solution from stock solution prepared fresh and used within 2hrs of preparation. The slides were then dipped into 60% isopropanol for 5mins to remove the excess background staining. Then, slides were washed in PBS for 5mins. Later on, slides were dipped in Hematoxylin for 1min and were washed in PBS for 5mins. For mounting, glycerol used. In this staining lipid particles would be in red and nuclei stains in blue.

2.7. Immunohistochemistry:

To study the distribution and cell differentiation of progenitor cells in lung epithelium and trachea immunohistochemistry done to visualize specific cells/tissues in interesting candidate that have been discovered by histological analysis. For cell type of interests mostly lung progenitor cells, following antibody combination has been used. In Figure 2 (C,E) the IHC on trachea and lung applied to visualized proximal and distal airways.

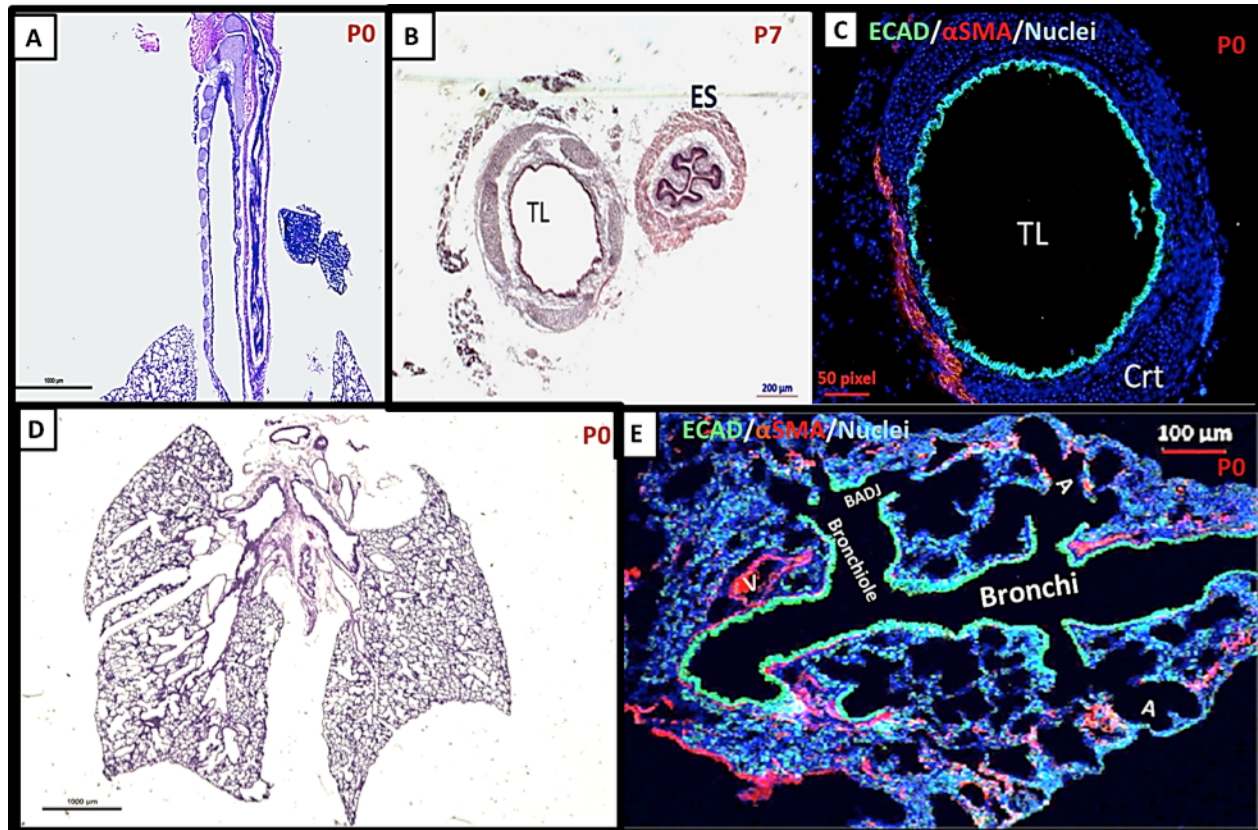


Figure 2. Histological and immunohistochemistry analysis. (A) and (B) Histological analysis of longitudinal and transvers cyosections of trachea.. H&E staining used to study morphology of trachea epithelium and cells structure as well as smooth muscle and adjacent esophagus. (C) Immunochemistry analysis of transvers trachea cyosection. The smooth muscles (alpha smooth muscle in red) located dorsal of C-shape cartilage rings (in blue). Epithelial cells at trachea lumen lined throughout the trachea lumen stained Ecadherin (ECAD in green). (D) The H&E staining to analyze P0 lung lobes histologically. The left lobe, right cranial lob as well right caudal lobes attached with together via main bronchi. (E) A higher magnification image of a right accessory stained for epithelial cells (ECAD in green) and vessels and myofibroblast (alpha smooth muscle in red).

For immunofluorescent staining of lung and trachea cryosections after air drying over night fixed with fresh 4% PFA for 20 minutes at room temperature. Slides were washed in PBS1x and were blocked by blocking solution. The 1-2 % BSA in PBS-T was used prior to primary antibodies incubation. The blocking time was 20-30 minutes depends on antibody that have used. Following antibodies were used: Anti-Pro surfactant Protein C (proSP-C) (Merck Millipore), anti alpha smooth muscle actin conjugated with Cy3 (Sigma), anti-Mucin 5AC (Abcam), anti-acetylated Tubulin (Sigma), Anti cytokeratin 5 (Abcam), CC10 (Santa cruz), anti E-Cadherin (abcam), and antibodies from Developmental studies hibrydoma bank (DSHB) such as Anti T1 alpha or podoplanin (Pdpn), EPCAM, PECAM/ CD31, Vimentin, Duct1. Sections were incubated

for over night at 4°C or 6 hours at room temperature. The next step is washing 3 times in 1x PBS-T solution (0.1 % Tween in 1x PBS) for 5 minute each.

Table of antibodies combinations

Cell types	Antibodies
Alveolar epithelial Type I + Type II	Pdpn + ProSP-C
Smooth muscle/myofibroblasts + Epithelial cells	Alpha smooth muscle actin + E-cadherin
Endothelial cells + Mesenchymal cells	PECAM + Vimentin
Epithelial cells + AEC II	EPCAM + ProSP-C
Basal cells + Ciliated cells	Cytokeratin 5 + Acetylated alpha-tubulin
Neuroendocrine cells + Epithelial cells	CGRP + EPCAM
Bronchio-Alveolar Stem Cells (BASCs)	CC10 + ProSP-C

After washing step; following secondary antibodies used. These antibodies were conjugated with Alexa Flour 488, 565 and Cy3 used. Secondary antibody (diluted in blocking solution) incubation over night at 4°C or 4 hours at room temperature. Slides were again washed three times with 1x PBS-T and counterstained the nuclei with DAPI solution (1:10,000 dilution in 1x PBS-T) followed by three times washing with 1x PBS-T for 5 minute. Then slides mounted by using Mowiol mounting medium (CALBIOCHEM, Cat. No 475904) and sealed the cover slides by using colorless nail polisher. Pictures were taken using Zeiss Axio observer A1 florescence microscope and images were analyzed with ZEN software.

2. 8. Whole mount retina

Each dissected retina incubated with FITC-LECTINBeta-1 (1:200 in PBS) for overnight; light protected at 4° C on the rotator. Also, to stain smooth muscles at arteries, the SMA-cy3 (1:5000 in PBS) antibody at 4° C used. Retina washed 3X with PBS and mounted. To collect retina a plastic Pasteur pipette carefully used. Flat mount each retina and 1 drop of Malwiol or Vectashield (vector lab) mounting medium used for mounting. The margin of retina dried with cotton tissue and mounting finished by using a cover slide. The nail polish applied around the

cover slide edges to fix cover slide. Imaging done by Axio imager A2. Retina visualized with the 480/GFP. The Figure 3 (C,D, E) shows the steps of retina isolation mounting and imaging.

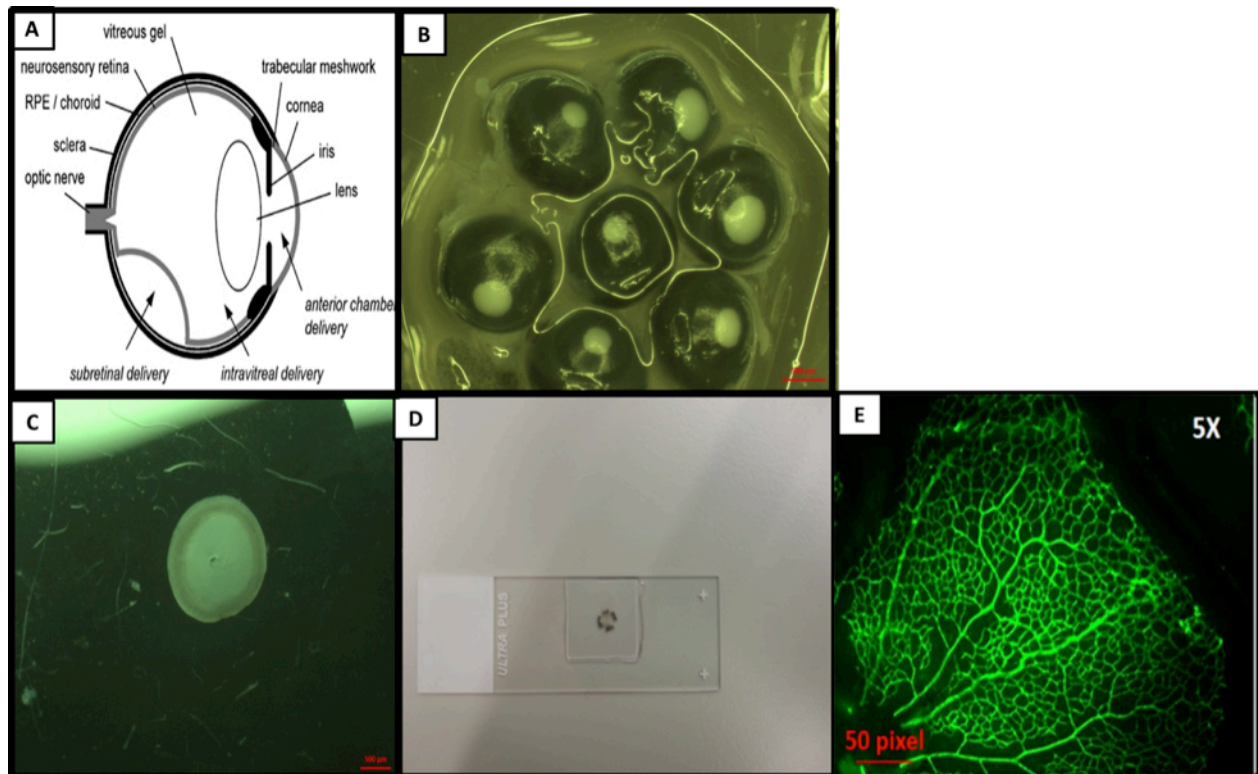


Figure 3. Retina analysis of P7 pups. (A) Side view of eye and structure. B isolated eyes prefixed in PFA 4%. (C,D) dissected retina and mounting. (E) vessels are visualized by FITC-conjugated isolectin B4 staining. The retinal vasculature stain in green.

Chapter4-Results

In my part of screen, I have analyzed the offspring of 114 F1 founders at postnatal age 7 and 0, (P 7 and P0). I identified 11 different phenotypes in 42 different F2. The type and number of discovered phenotypes described in table and graph1. From total screened primary litters; 8% were positive for inflammatory cells infiltration into the alveolar interstitium, bronchiolitis, fibrosis and myofibroblasts hyperplasia, non-classified cell mass and pulmonary nodule, defect in alveolarization and collapsed lung lobes. The less frequent lung phenotypes were accumulation of mucin in alveolar epithelium, hemorrhage, alveolar type 2 hyperplasia, broken cartilage rings and leaking lung vasculatures. Moreover, other phenotypes observed in other organs such as; cystic kidney, sub cutaneous hemorrhage, hyperglycemia, abnormal curved back bone, fatty liver, hair loss and whisker less, non asymmetric blind mouse, and cleft palate. The figure 1 and 2 shows a few phenotypes that detected in other organs or not in alveolar epithelium. Therefore, they were not follow up. In this regard, Figure.1(A,B) represents the Polycystic kidney (PDK), (C;C') increase of sub mucosal gland in middle of cartilage ring of trachea; (D) an extra cartilage element and (E) whisker and hair less pups. The PDK and whisker; hair less phenotype haven't follow up due to our interest in only lung organ phenotype. The tracheal phenotypes were no reproducible.

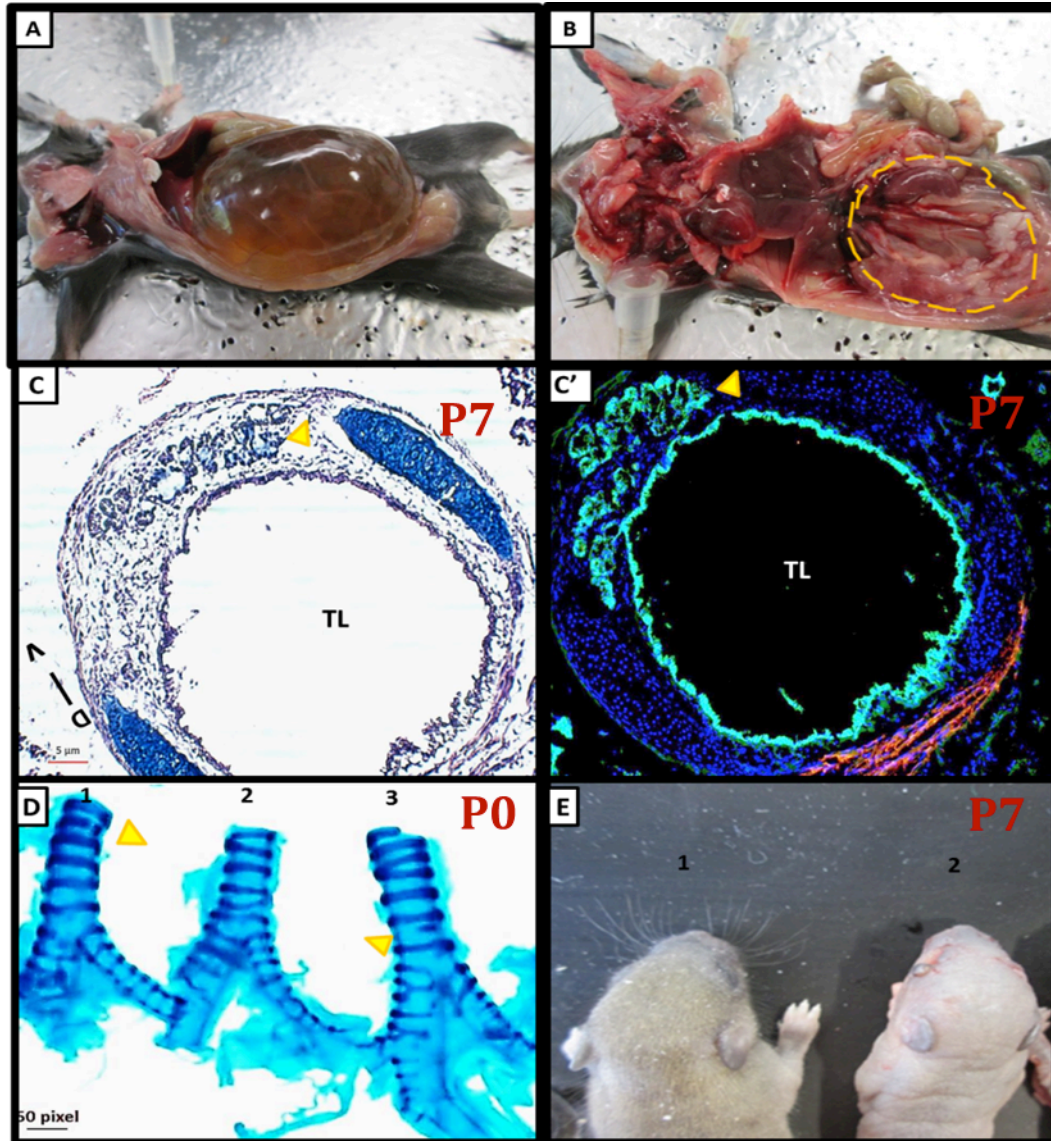


Figure 1. . Detected phenotypes in organs other than lung epithelium. (A;B) The gross morphology of cystic kidney phenotype identified in an adult F2 female mouse presumably a dominant heterozygote. The mutant showed increase in weight and abnormal abdomen inflammation, after dissection; a massive cysts (fluid-filled sacs) identified on right kidney. On the other the left kidney looked normal. The founder of this family choose for sperm freezing. (C, C') The hyperplasia of tracheal submucosal glands(SMG) in a C-shape cartilage ring. The histological (Alcian blue staining) and immunohistological analysis of a transverse cyrosection of trachea. The epithelial cells at tracheal lumen are expressing ECAD (green), C-shape cartilage ring in blue (DAPI) and tracheal smooth muscle located dorsal of trachea lumen visualized with α -smooth muscle(red). The yellow triangle points to the SMG glands that abnormally located in between of two part of a cartilage rings. This section was made from the half proximal part of the trachea that fixed in 4% PFA and sectioned with 8 μ m thickness. (D) The identified broken cartilage ring (trachea#1) and an extra element (trachea#3) between two complete C-Shape trachea rings. The yellow triangles points to trachea number 1 and 3. Whole mount Alcian blue(AB) staining carried on tracheal cartilage rings to study structures and numbers on dorsal half of the trachea. (E) A whisker and hair less phenotype at P7; (pup number1). TL: Trachea lumen

According to previous research reported the association of cleft palate phenotype in mouse and lung development defects (Kaartinen et al., 1995); in this screening the identified cleft palate phenotype (Figure.2) didn't have any lung defect.

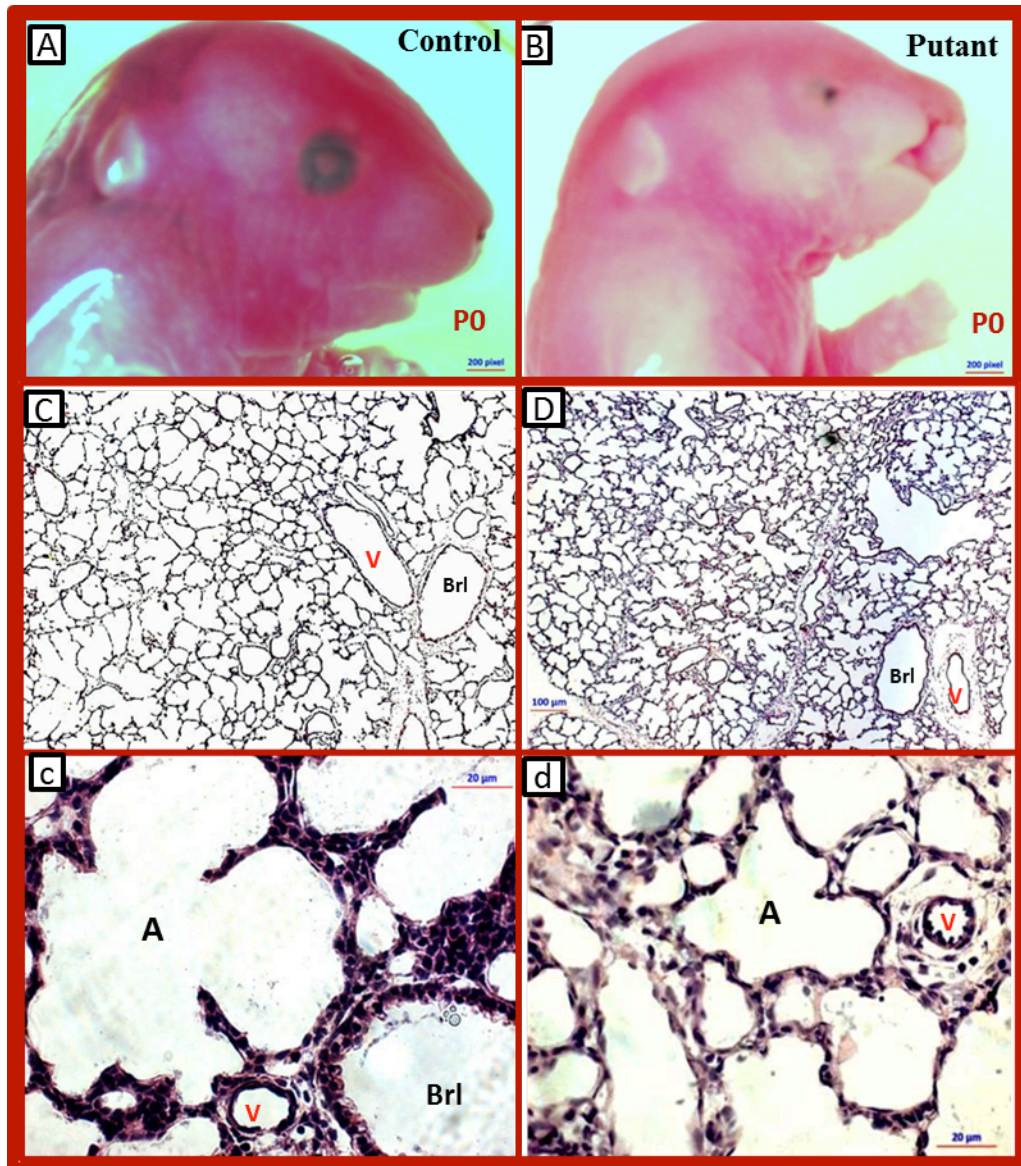
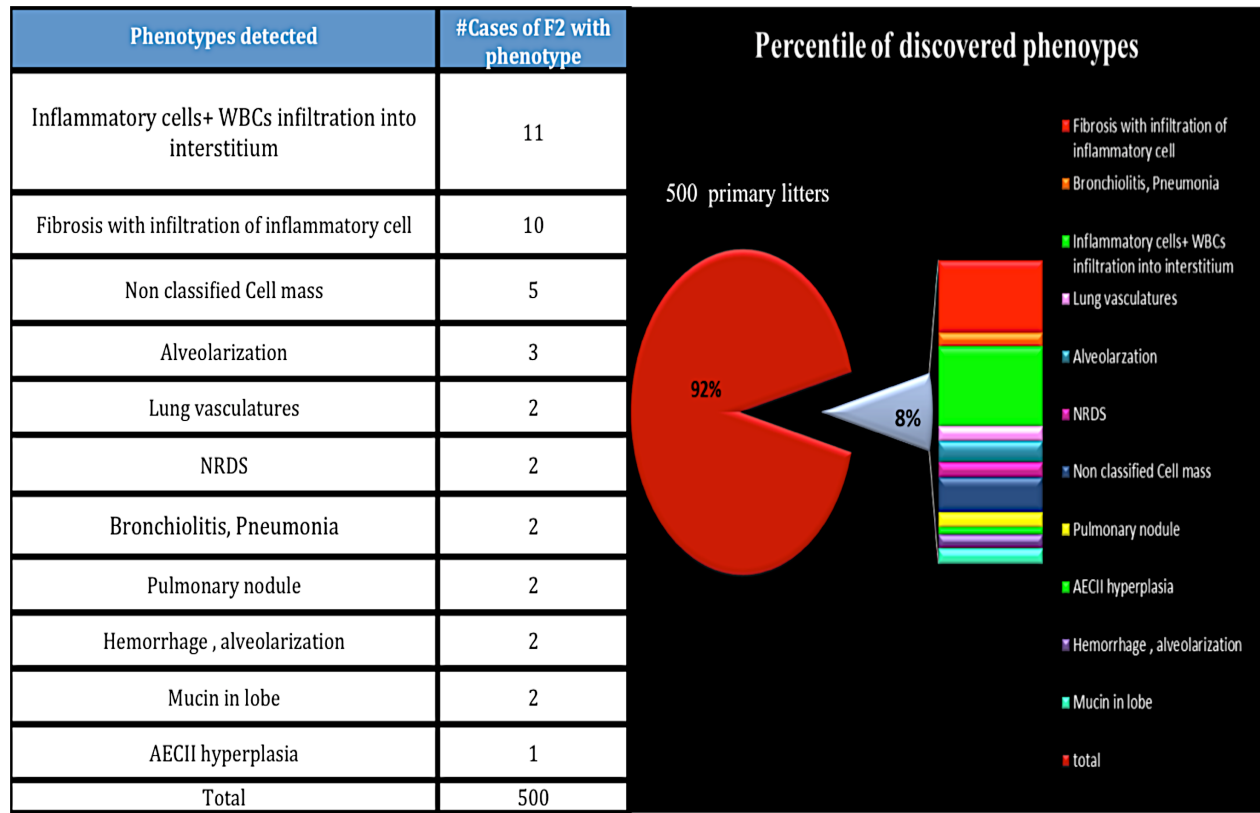


Figure 2. Cleft palate in P0 pup without any significant lung phenotype. (A and B) P0 pups with normal and cleft palate facial phenotype. (C,c; D,d) Histological analysis (H&E staining, 8µm cyrosections) of lung lobes. The alveolar structure and morphology of the airways looks normal. Alveoli units are widely developed and septa structures forms completely. A: Alveoli; Brl: Bronchiole, V: vessel

Most important discovered and recovered phenotypes in this screen are inflammation and infiltration of inflammatory cells into the intestine. The following tables demonstrate the summary of each F1 screen and further analysis of F3 generation. The F3 carriers were identified by screening their pups as a result of a back cross with heterozygote F1 founder or F2 mother. Once primary phenotype recovered from any of these crosses, the heterozygote F3 carriers interbreed to have putative progenies as well as wild type (WT) looking siblings. Histological and immunohistological analysis carried on produced pups and tail samples collected for DNA extraction. In the end two putative and two WT siblings were used for whole exome sequencing. In this work the efficiency of screening for primary screen was 83% and efficiency of screen for most significant phenotype from founder ID# 373238 is 78%.

According to longer and less possible mating times for females, just F1 male has used to cross out with wild type females and prepare F2 breeders. According to rodent gestation time each pregnancy takes 21 days to produce only 1 litter. Moreover, each female mouse can only have maximum productive 5-6 matings in her life. Therefore, having F1 females as family founders not only take longer time to screen 5 male animals per F1 founder, but also for further generations the animal production would be risky.

Table 1. The percentile of discovered phenotypes.



4.1. Inflammation, bronchiolitis, collapse lobe phenotypes

Founders with identified F3 reproducible carries

4.1.1. Most significant founder:

The most significant and reproducible phenotype has identified is interstitial inflammation and bronchiolitis from founder (Id#373238). The alveolar epithelium of lungs showed the infiltration of immune and white blood cells into the alveolar interstitium and alveolar sacs. In primary screen following the back cross of F2 female (ID:474626) with the F1 male (ID: 373238), 2 out of 5 alive pups from total 7 pups; showed the collapsed right caudal lobe and medium aggressive form of bronchiolitis. The bronchiole at collapsed lobe were accumulated by white blood cells. The figure.3 shows lung interstitium and alveolar sacs that was mainly affected with mild inflammation. The table 2.A and B summarized the history of this founder screening. As is shown in table 2.A from three F2 females 20 pups screened and 2 pups were positive for inflammation phenotype. In fact from 3 F2 female only 1 F2 female shows potential as a carrier for inflammation and infiltration of immune cells into lung interstitium. In this carrier (Id# 474626) 2 of 5 alive P0 pups were positive for inflammation phenotype and two pups died right after delivery. Generally in this screening the pups cadaver haven't analyzed due to autophagy effect post mortem effect. However, in cases of fresh cadaver it has analyzed for lung and liver phenotypes. At the second time of screening same couple the phenotype haven't observed however animal house reported 1 dead pup. I have concluded that the causative mutation may be fetal and result in death in P0 pups. Therefore, this carrier choose to cross out with a WT male animal for further analysis.

Table 2A: Screen summary of F2 female of Founder# 373238

F1 male DOB	F2 female DOB	Size/stage (DOB)	Phenotypes of F1#373238					
			Histology (H&E,VVG,AB)	IHC	Mutant	Cartilage	RANK	Status
373238 (17.09.13)	474626 (26.07.14)	5+2 /P1 (28.12.14)	Inflammation	Myofibroblasts Increase Fibrotic structures	2	Analyzed		X Out C57 5#Female , 4 male
		5+1/ P0 (27.03.14)	Analyzed	Analyzed	0	Analyzed		
	474627 (26.07.14)	4+1/P0 (23.12.14)	Analyzed	Analyzed	0	Analyzed		Alive
	474628 (26.07.14)	4/P0 (24.12.14)	Analyzed	Analyzed	0	Analyzed		Alive

Figure 2A. Summary table of F2 females (ID: 474626, 474627, 474628) back crossed to F1 male father (ID:373238). The back cross of F2 female (ID: 474626) to the F1 male (ID:373238) yielded 5 pups; and 1 pups showed inflammation; collapsed lung lobe and bronchiolitis. Further at secondary screen; 1 pup was dead with strong lung collapse and accumulation of cells of unknown lineage inside the alveolar sacs at postnatal day 0.

This F2 carrier has been crossed with a wild type male animal to produce F3 generation. After 81- 90 days (approx. 3 months) of the time of carrier's pregnancy report notification; the F3 animals were ready to cross back with the F1 founder that presumably is heterozygote for phenotype of interest.

The Figure.3 (A,B) shows difference between a wild type looking lung and a putative mutant pup. In wild type lobes, alveoli sac, bronchiole and proximal airways are quite clean and wide open. The secondary septa structure at each alveoli unit is about to form. The Figure3.C and c represent a bronchiole from a wild type looking sibling and an affected bronchiole lumen and obstructed with inflammatory cells. Hyperplasia of cuboidal epithelium containing club cells and abnormal distribution of ciliated cells observed. In addition the alveolar wall were thickened and occupied with inflammatory cells.

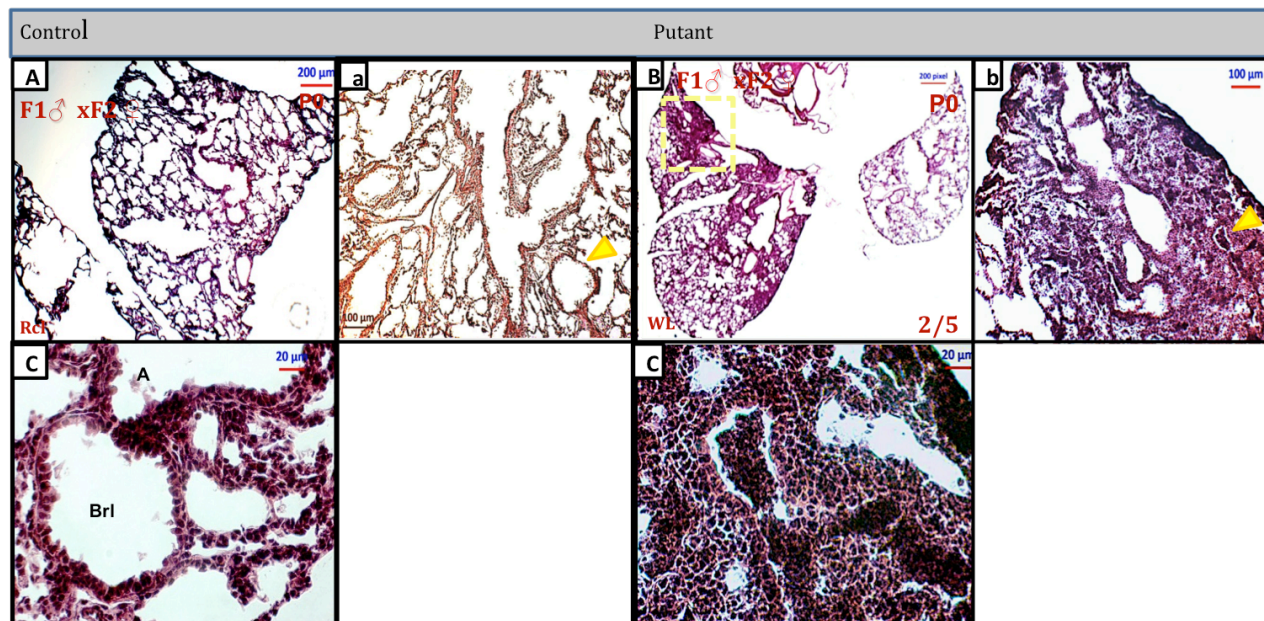


Figure 3. Figure 3. Inflammation phenotype. Multifocal inflammatory cell infiltration in the alveoli, peribronchiolar, bronchioles and perivascular regions identified by histological analysis (H&E) of longitudinal sections of whole lung P0 sample from ventral to dorsal; thickness 8 µm. (A,B) Represents the longitudinal section of Right cranial lobe (Rcl) from wild type looking sibling (WT), and Rcr; Right caudal lobe (Rcd) of putative mutant. Alveolar walls are thickened and occupied by infiltrated inflammatory cells, the bronchiole narrowed and peribronchiolar fibrosis and smooth muscle atrophy of vessels in interstitium observed. In mutant; the size of lung is also smaller relatively. The area that enclosed in yellow dashed square represents in higher magnification. (a,b) Higher magnifications of alveolar epithelium of WT and putant of alveolar epithelium. The inflammatory cells such as polymorph nuclear white blood cells as well as lymphocytes and macrophages accumulated in alveoli and bronchioles. The yellow triangles pointed to a bronchiole in dorsal lung epithelium. (C,c) Represent a bronchiole structure in WT and putant. The bronchiole in putant is not only filled with inflammatory cells but also the morphology of cells at bronchial lumen changed. In fact, cuboidal epithelium and non-ciliated cells (club cells) undergone morphological change, such as enlargement and faint decrease in number of cilia on apical side of ciliated cells.

As summarized in table 2.B, F2 carrier (474626) produced 5 female and 4 male animals as result of out cross with wild type. By the back crossing each F3 female with F1 male animal, 3 F3 female carrier with strong phenotype identified. In addition, 1 male F3 animal identified by crossing with F2 female carrier. In the primary screen the number of discovered mutant was ¼ of total litter number and according to Mendelian law the phenotype expressed in recessive manner. However, the recovered phenotype in pups from F3 and F1 male crosses shows the phenotype in dominant manner. As it shown in table 2.B, carrier 521250, 521251 and 52 had 3, 3 and 4 pups from 10, 7 and 7 total litter. The percentile of F4 putative mutants; 30%, raised a question on possibility of segregation of this phenotype in dominant manner.

Table 2B: Screen summary of F3 carriers of Founder # 373238

F1 male	F2 Female	F3 mice	Size/stage (DOB)	phenotypes of F1 #373238				
				IDing strategy	Phenotype	Mutant	Carrier	Status
373238 (17.09.13)	474626 (26.07.14)	521250 (Female)	8/P0 (04.05.15)	X F1	Hemorrhage Very weak Cell mass	1	Positive	Tail sample collected for exome sequencing –planned
			10/P1 (19.07.15)	X F1	Inflammation	3	Positive	
			6/P5 (20.08.15)	X F3 sib WT male 521255	Inflammation	1	Positive	
			10/P1 (27.09.15)	F3 sib WT male 521255	Eaten pups	-	-	
				X C57 WT	Not pregnant			
		521251 (Female)	7/P0 (04.05.15)	X F1	Inflammation	3	Positive	Produced F4 3 Female; 4 male (23.08.15)
			9/P1 (24.07.15)	XWT C57	Inflammation	3	Positive	
			6/P0 (07.11.15)	X WT C57	Inflammation	2	Positive	Carrier pups# 4. and 2
			5/P7 (09.12.15)	XWC57	Inflammation	1	Positive	Carrier pups# 3
		521252 (Female)	7/P1 (14.05.15)	X F1	Inflammation	4	Positive	XWT produced F4 1 Female. 6 Male(DOB:22.10.15)
			6/ P0 (19.07.15)	X WT C57	Inflammation	2	Positive	
			6/P4 (21.08.15)	X F3 sib WT male 521256	Inflammation	1	Positive	Sample collected
			(13.11.15)	X WT C57	Dead pups	0	Dead pups	X WT to collect sample for WES
		521253 (Female)	1/P0 (12.05.15)	lnx F3 (521256)	1 Pup born and died,	0	Dead pup	
			5/Po (03.07.15)	X F1	-	0	Negative	
		521254 (Female)	5/P2 (13.05.15)	lnx (521256)	Inflammation	1	Positive	
			5/P5 (26.08.15)	X F1	-	0	Negative	
		521255 (Male)	5 dead (29.04.15)	X F2 (474626)	5 pups dead	0		
		521256 (male)	1/P0 (12.05.15)	lnx F3 (521253)	-	0	Dead pup	
			5/P2 (13.05.15)	lnx F3 (521254)	Inflammation	1	Positive	
		521257 (Male)	-	XF2 (474626)				XF2- 3.06.15 NP 15.06- Separated
		521258 (Male)	1 Dead (05.09.15)		Dead		?	

Table 2B.Summary table of F2 female (ID: 474626) and her progenies in F3. In F3, 5 F3 female and 4 male produced and screened. From F3 females, 3 carriers identified as heterozygote for inflammation phenotype with dominant segregation.

After observing this ratio, to clarify whether or not this phenotype is dominant or recessive, the potential carrier were crossed with a wild type male animal. In this work each phenotype and relevant carriers numbered according to greatness of phenotype and chronically order. The Figure.4 summarized the histological analysis of this phenotype in identified F2 and F3 carriers as well as the rediscovery of this dominant phenotype with recessive segregation from out crossing of F3 carrier with a wild type animal. This phenotype also showed abnormal morphology of bronchiolar epithelial cells.

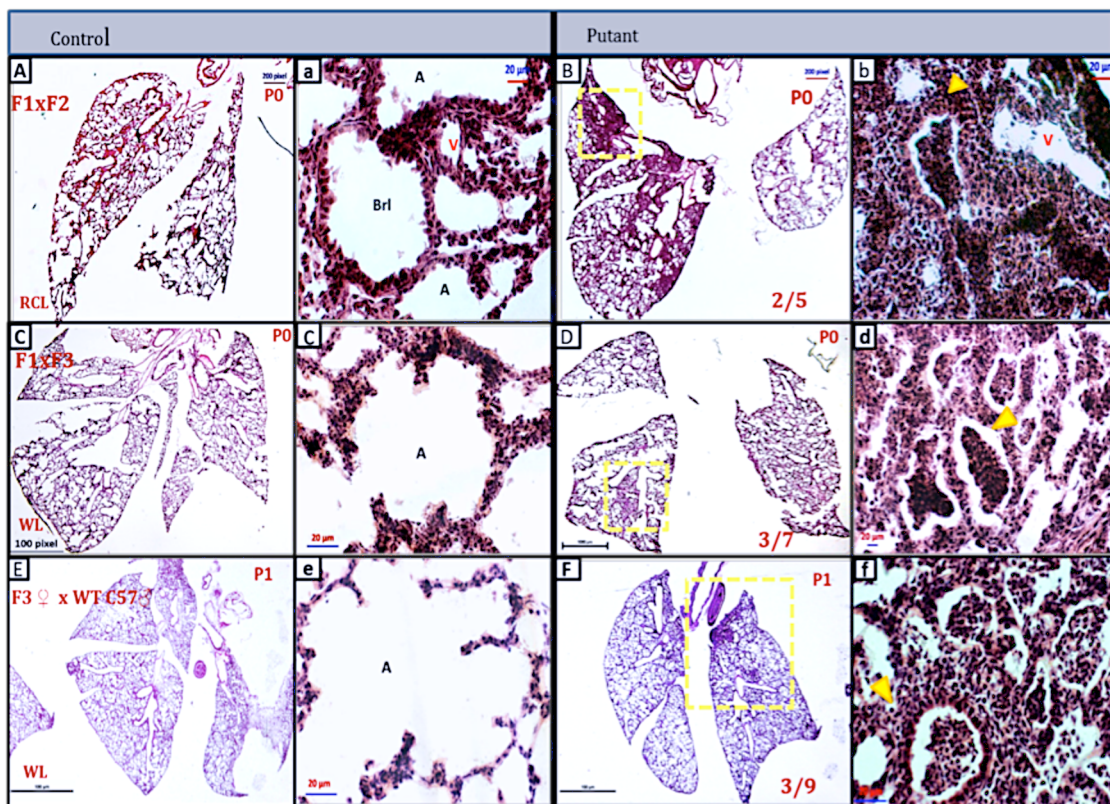


Figure 4. Summary of inflammation phenotype in F3 carrier 1. (A,a;B,b) hematoxylin and eosin (H&E) staining of cryosections section of 4% PFA fixed lung. Discovered phenotype in P0 pups at primary screen (F1 founder X F2 female) in higher and lower magnification. The segregation of phenotype was recessive. (C;c,D;d) All lung lobes of WT sibling and putant lobes stained with H&E to study structure and morphology of lung epithelium. The identified putants were from F3 carrier1 (Id# 521251) and from 7 pups at P0; 3 showed accumulation of alveolar interstitium with inflammatory cells. The yellow dashed square boxes and arrows specifies the affected area. (c,d) The magnified images from alveolar epithelium of Rcd lobe; shows a quite clean and well developed alveoli in WT in the contrast in putant alveoli units showed thickened wall and blocked with inflammatory cells. However, the inflammation foci observed in relatively smaller area than primary screen. The segregation of phenotype was aprox:30%. (E,e; F,f) The phenotype recovered in a dominant segregation in pups from F3 carrier 1 and C57/Blc6 Wt. (E,F) Whole lobes of WT with normal alveolar epithelium and wide open and empty alveoli compartment(e). (F) The recovered phenotype in 3 P0 pups from 9 pups. Inflammation were more severe and spread through whole lobe. As is specified in (F); it observed at mesothelium of left lobe as well as in the alveolar epithelium. The number of putants with same inflammation phenotype confirmed the hypothesis of dominant segregation of this phenotype from founder (Id# 373238).

Summary of inflammation phenotype in F3 career1(ID#521251) represented in Figure 4 and 5. As is represented the phenotype observed in 3 F4 pups from a litter of 9 pups. Furthermore, the hyperplasia of epithelial cells at bronchiole lumen seen (Figure6).

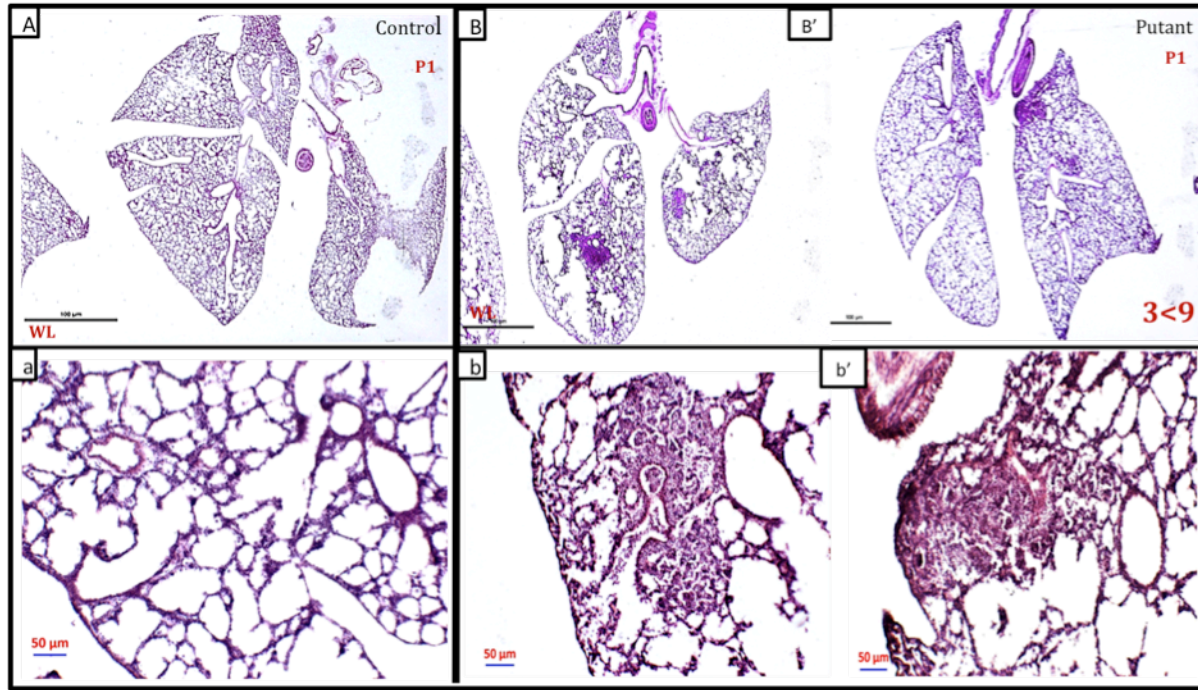


Figure 5. The recovered inflammation phenotype with dominant segregation. (A;B) hematoxylin and eosin (H&E) staining of cryosection of lung from P1 pups in F4 generation. The images shows the WT and the appearance of inflammation spots with at different alveolar interstitium. (a,b and b') Represent the manifestation of this phenotype in higher magnification. The lung tissue thickened and alveolar septa widened. The inflammatory cells composed of white blood cells infiltrates to the interstitial. In addition, fibrosis with fibroblastic foci forms at alveolar epithelium. In addition, intense inflammation and hyperplasia of myofibroblasts which are the bio marker of fibrosis observed adjacent to normal lung areas. The yellow arrow points to a bronchiole and bronchio alveolar duct junction that is obstructed with inflammatory cells and migrated these cells towards the dorsal of alveolar interstitium and mesothelium

This phenotype accompanied with abnormal ciliated cells morphology similar with inflammation phenotype induced by CeO₂ treatment (Cho et al., 2010).

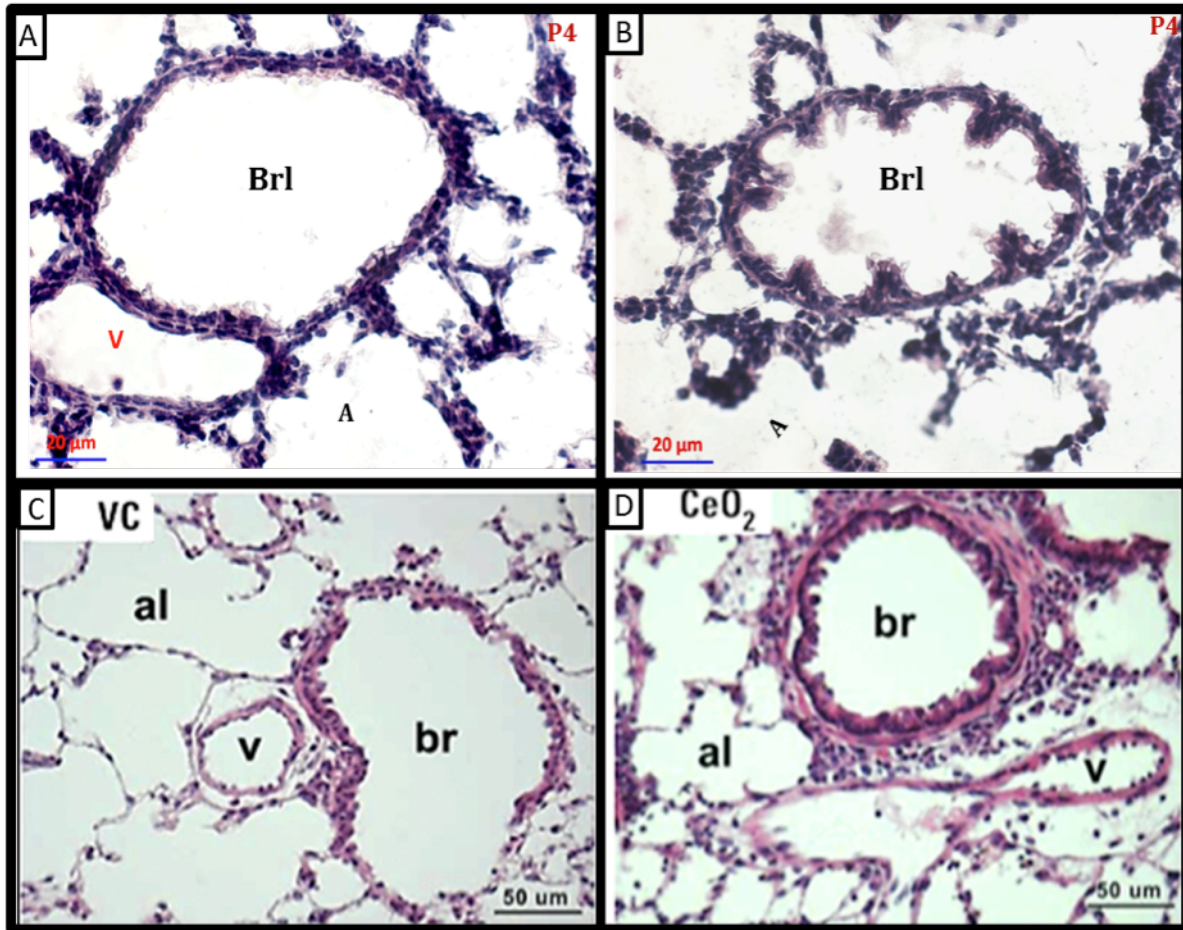


Figure 6. Hyperplasia of epithelial cells at bronchiole lumen and abnormal ciliated cells morphology similar with inflammation phenotype induced by CeO₂ treatment (Cho et al., 2010). H&E staining of a WT looking sibling and a putant. (A) and (C) Represent normal bronchiole and alveolar interstitium similar with control samples a which were demonstrated acute pulmonary toxicity after treatment with Nano Particles (NPs) such as cerium oxide (CeO₂NP). (B) and (D) The identified inflammation phenotype showed folded bronchiole lumen, remodeling of ciliated cells location in distal narrowed airways. The simple columnar/cuboidal epithelium has undergone immune response changes. Abbreviations: A:Alveoli; BrI: Bronchiole ; V:Vessels

The immunohistological analysis of this phenotype for primary screen as well as recovered phenotype in F3 back crosses and out crosses showed in Figure 7; 8 and 9. The main manifestation of inflammation phenotype was accumulation of airway sacs with immune cells. It resulted obstruction of alveoli and disorganizing alveolar interstitium. Thus, the gas exchange between alveoli and pulmonary vasculatures disrupts. In addition, presumably to compensate the oxygen exchange the pulmonary vasculatures goes under alteration. In fact, the increase and structural alteration of pulmonary vasculatures observed at inflammation areas. To clarify

regarding the role of inflammatory cells and alteration of vasculatures the immunohistological analysis done.

To visualize vasculatures and stromal cells in mutant lung, I performed an immunostaining with anti-PECAM/CD31 and Vimentin antibody. It has been reported that the Vimentin can be a specific marker for stromal and mesenchymal cells in which most abundant ones are fibroblasts. In addition, previous works suggested that this marker can use to stain the quiescent fibroblasts and myofibroblasts (Goodpaster et al., 2008). Furthermore, to investigate abundance and structure of smooth muscles in lung epithelium that incorporated with large airways and blood vessels; tips of septa structures when protruding into the alveolar duct as well as architecture of pulmonary vessels the anti alpha smooth muscle (Alpha smooth muscle actin-cy3; Sigma- c6198; 1:500) used. Besides the role of smooth muscles in forming the architecture of lung organ; smooth muscle hyperplasia reported as a marker of fibrosis and in bleomycin-treated rats (Leslie, Mitchell, Woodcock-Mitchell, & Low, 1990) and other respiratory disease conditions such asthma, COPD, and CF. Figure 8 represents structural alterations of alveolar interstitium, hyperplasia of myofibroblasts in the alveolar epithelium and smooth muscle increase at bronchiole, pibronchiole and pre pulmonary vessels. According to the important role of E-cadherin in the maintenance of tissue integrity and cell-cell junctions. Therefore, to visualize lung epithelial cells the combination of E-cadherin antibody and smooth muscle used. This immunohistological analysis provide sufficient information about epithelial cells distribution and lung distal airways structures as wells as pathological alteration of lung interstitium.

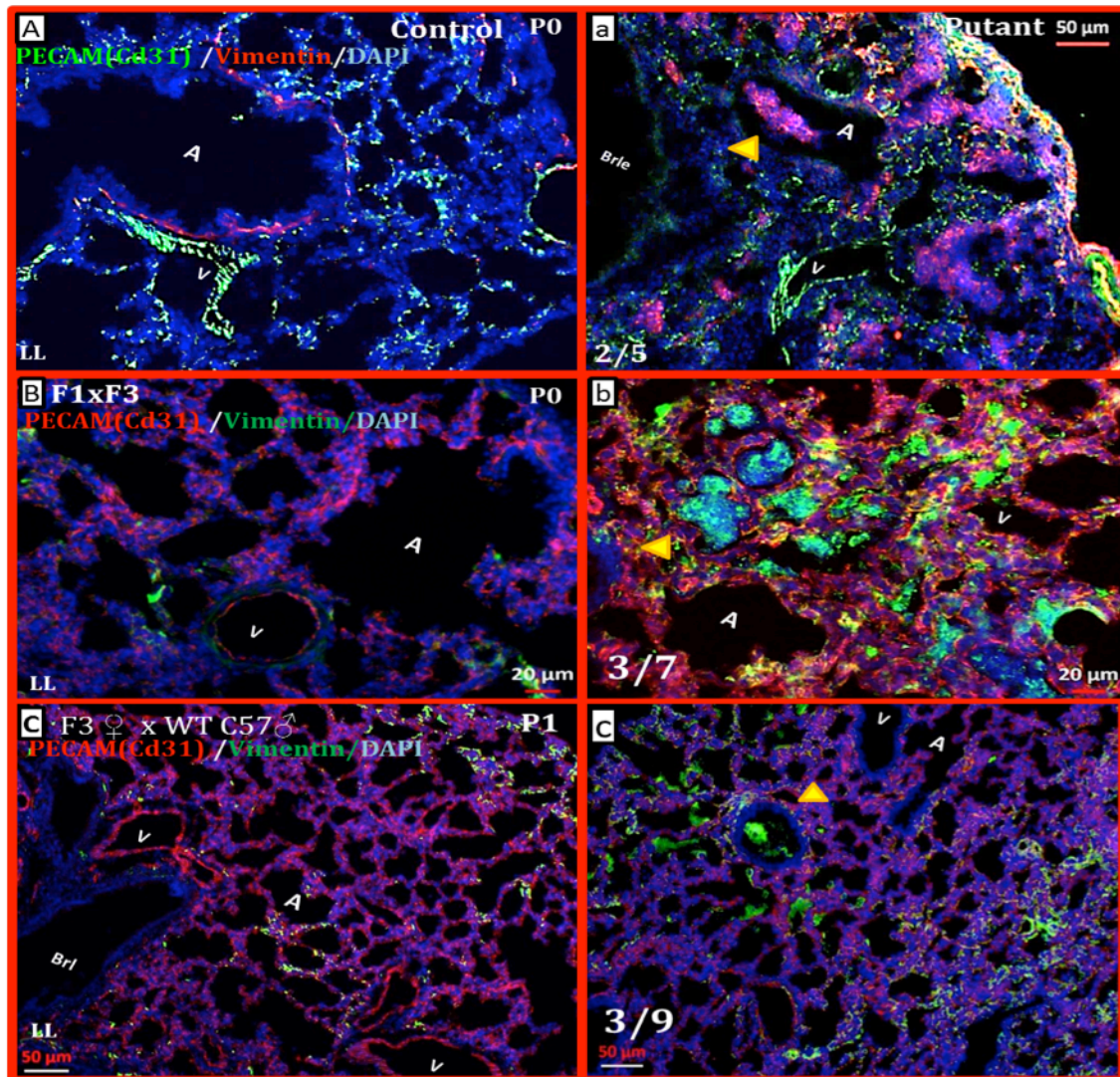


Figure 7. Inflammatory cells and fibroblast accumulation in interstitium in three different generation and the segregation of phenotype. (A) In primary screen, the WT sibling alveoli (a) represents putant left alveolar epithelium filled with inflammatory vimentin positive cells. Vasculatures stained with PECAM/ CD31 (DSHB-2H8; Hamster; 1:1) and for inflammatory cells Vimentin (DSHB-AMF-17b; chicken; 1:30) used. The yellow triangle points to inflammatory cells mass granules in alveoli epithelium. (B,b) The reproducible phenotype with significant vimentin positive and collapsed alveoli in F4 putants, identified the F3 carrier by F1x F3 backcross. (C,c) Identified putants with recessive segregation confirmed the heterozygosity of F3 carrier (Id#521251) for dominant phenotype. Abbreviations: A:Alveoli; BrI: Bronchiole ; V:Vessel

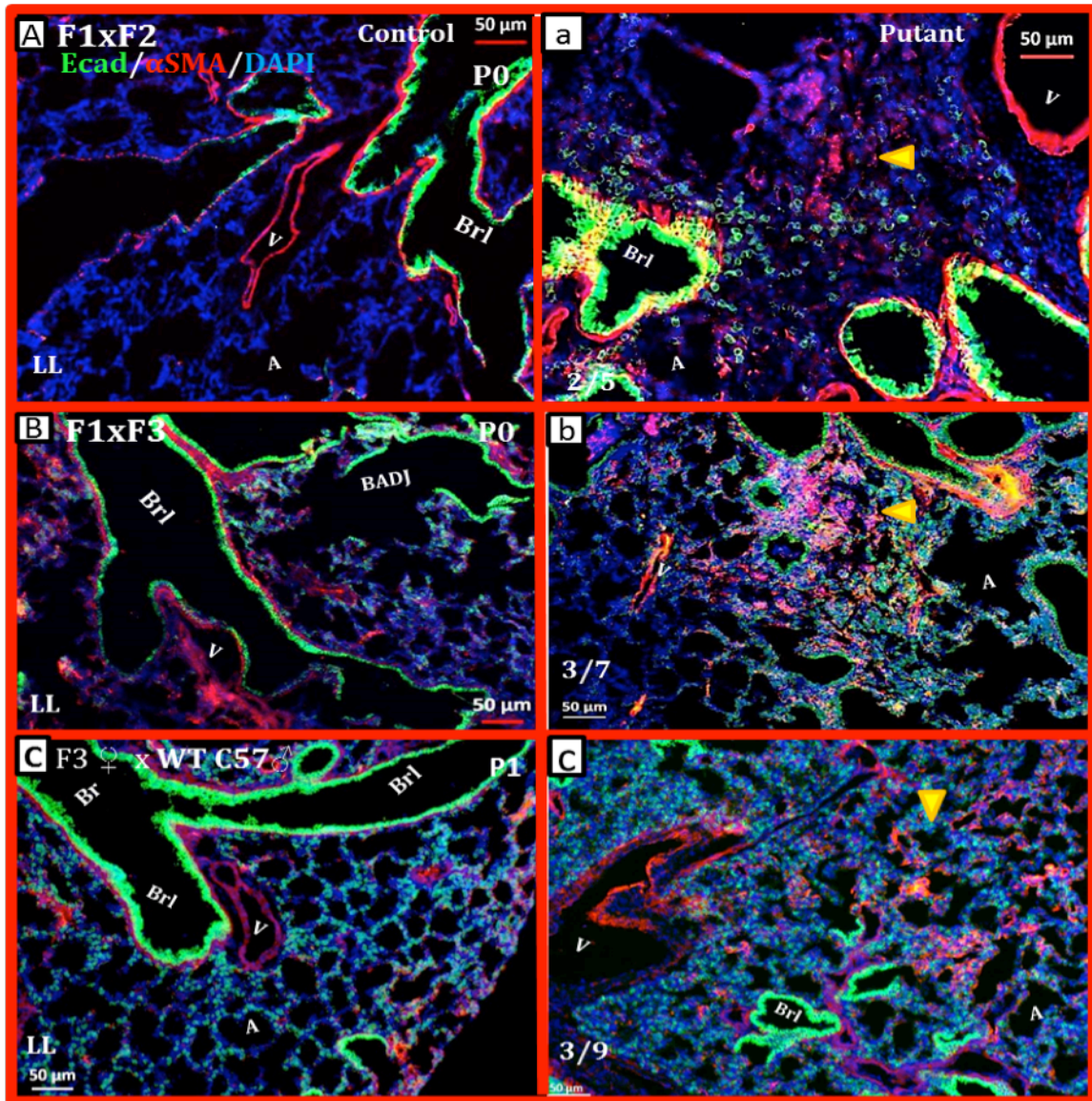


Figure 9. Inflammatory cells and fibroblast accumulation in interstitium in three different generation and the segregation of phenotype. (A) In primary screen, the WT sibling alveoli represents a left lobe of putant; filled with inflammatory vimentin positive cells. To visualize epithelial cells E-cadherin/ Decma-1 (abcam; Rat; 1:1000) and for smooth muscles and myofibroblasts, α smooth muscle actin conjugated antibody with cy3 (Sigma; mouse; 1:500) used. (B,b) Quite clean and well shaped alveoli unit in WT compared with narrowed alveolar units with myofibroblast positive inflammatory cells mass plaque. (C,c) Identified putants shows prebronchiolar area has collapsed and myofibroblast and epithelial cells increased. Abbreviations: A: Alveoli; Bronchi: B; Brl: Bronchiole BADJ: Bronchio alveolar duct junctions; V: Vessel

In addition, for investigation of alveolar epithelial cells type I and II, which are most specified cells in resident organ, the anti podoplanin /T1alpha and Anti-Pro surfactant Protein C /pro SP-C used respectively. After investigation of AEI and II cells in these putants, the identity

of cell mass in alveoli recognized as inflammation plaque. In fact, this result (Figure9) turned down the possibility of **Pulmonary alveolar proteinosis (PAP)** phenotype in which abnormal accumulation of surfactant occurs within the alveoli. In such phenotype the surfactant particles would be stained with anti SPC and visualized in green similar with AECII cell in this immunohistological analysis.

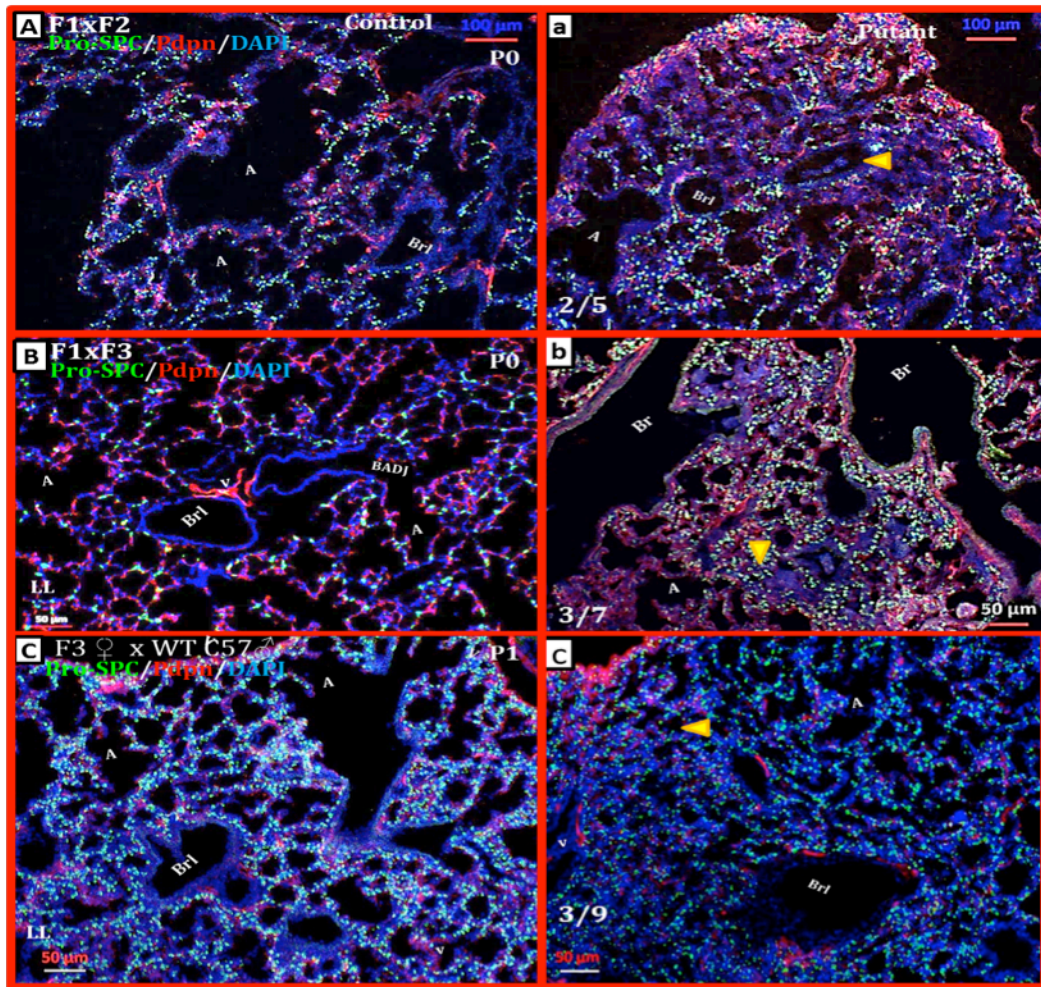


Figure 10. Immunohistochemical staining of a wild type sibling and putant to investigate number, structure and cell differentiation of specialized alveolar cells/ pneumocytes type I and II. (A) Normal Alveolar interstitium and (a) inflammation in alveolar epithelium. The yellow triangle indicates a bronchiole with an inflammatory cell mass accumulation. Alveolar epithelial cells type I (AECI) in red stained with podoplanin /T1alpha (Anti t1 α ; DSHB- 8.1.1; Hamster, 1:20) build the alveoli units. AEC II in green located at corner of alveoli walls, marked by Anti-Pro surfactant Protein C /pro SP-C (Merck/ Millipore; Rabbit; 1:600). The lymphatic vessels also stained in red. (B) Wide open alveolar units separated with septum (b) collapsed air sacs and bronchioles filled with inflammatory cells, fairly positive for T1 α (red) and negative for surfactant protein C. Thus, rules out the Pulmonary alveolar proteinosis (PAP) phenotype in which abnormal accumulation of surfactant occurs within the alveoli, interfering with gas exchange. (C,c) The air sacs narrowed in comparison with WT sibling. AECI and II looks to increase, although, it is due to collapsed lobe. Abbreviations: A: Alveoli; Bronchi: B; BrI: Bronchiole; BADJ: Bronchio alveolar duct junctions; V: Vessels

First F3 identified carrier is (521251); 3 of the 7 P0 pups showed inflammation and accumulation of immune cells into bronchiole. In the other word, one third of pups from this cross were positive for phenotype of interest and it confirmed heterozygosity of F3 carrier. The proportion of mutants versus wild type looking siblings brought up whether or not this phenotype is dominant or incomplete dominant (partial dominant). Thus, the F3 carrier has crossed with a

wild type male to investigate this hypothesis. As a result, 3 of 9 F4 pups showed the inflammation and infiltration in the alveolar interstitium. In conclusion, this phenotype for this founder identified as a dominant phenotype. To identify the causative gene the tail samples has collected and store for exome sequencing from mutants isolated from carrier#521251 and a WT male. In addition from this carrier a F4 generation produced for future analysis and sperm freezing to store the line.

The second identified and significant F3 carrier is Id#521252. In figure 10 and 11 histological examination of inflammation phenotype that recovered in F3 carrier presented. Further, in Figure 11; images from WT siblings as well as putative mutants with severe inflammation with dominant segregation in 1 litter presented to illustrate the aggressive and significant manifestation of this phenotype. From this carrier also a F4 generation produced and store to save this mouse line. The samples for whole exome sequencing collected and stored.

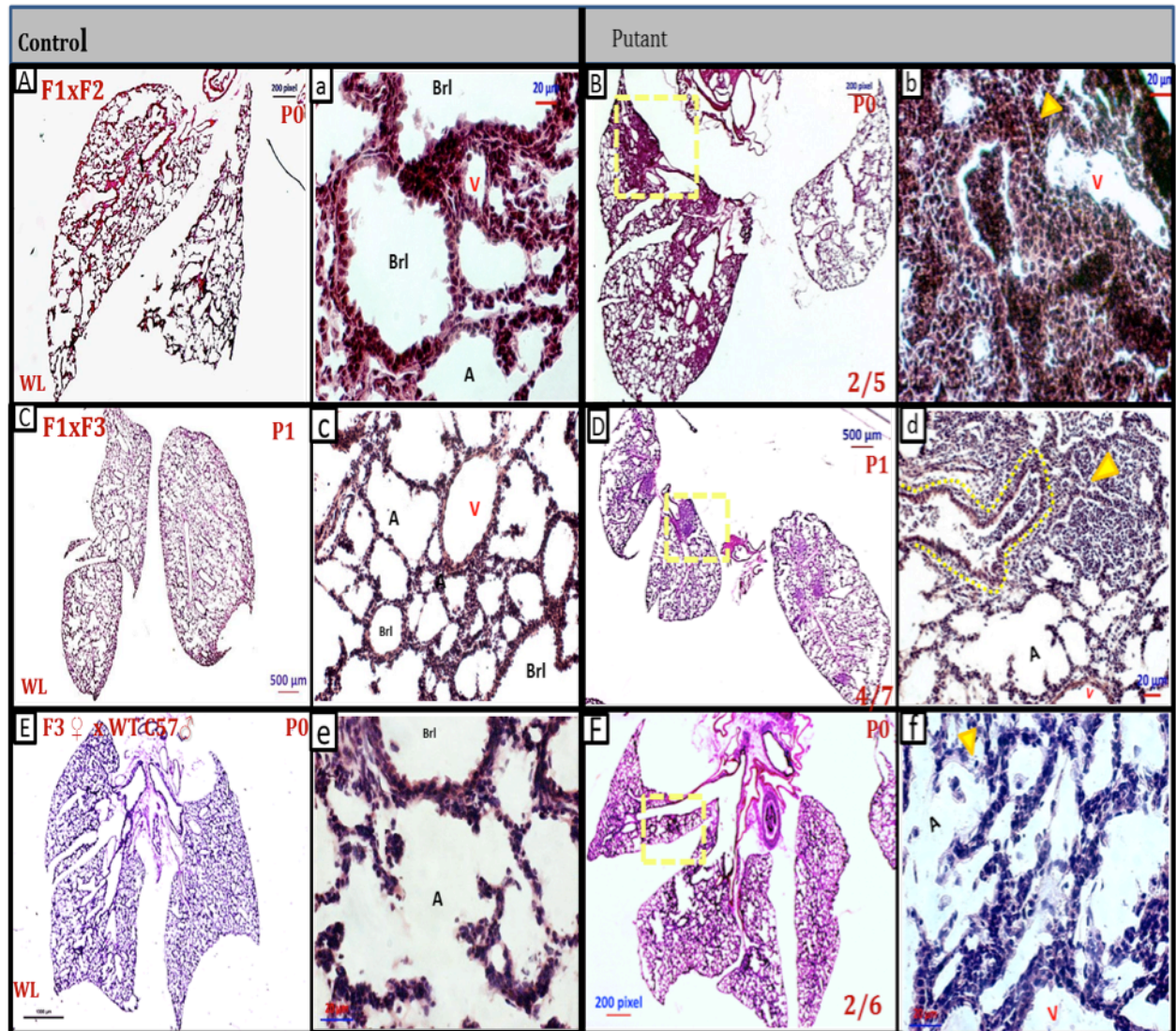


Figure 11. Summary of Histological examination of inflammation phenotype in F3 career2 (521252). H&E sections revealed infiltration of immune cells into alveoli and inflammation in alveolar interstitium, and bronchiolitis. The segregation of phenotype was dominant. H&E staining of whole lobe 4% PFA fixed; 8μm cryosections. (A,a;B,b) Discovered phenotype in P0 pups at primary screen (F1 founder X F2 female) in higher and lower magnification. The yellow dashed line square indicates inflammation foci/ granulomatous inflammation. Segregation of phenotype was recessive according to number of discovered putants. (C;c;D;d) The significant accumulation of alveolar inflammation in interstitium with large and spreads out lymphocyte and other white blood cells aggregation. The 4 of pups from total 7 showed a variety of severe interstitial lung inflammation. The F3 female (Id# 521252) identified as second strong carrier. (c,d) The magnified images from alveolar epithelium of Rcd lobe; shows a quite clean and well developed alveoli in WT in the contrast with putant with thickened alveoli wall and obstructed with inflammatory cells. The segregation of phenotype was approx. 30%. (E,e; F,f) The phenotype recovered in a dominant segregation in pups from F3 carrier 1 and C57/Blc6 Wt. (E,F) Whole lobes of WT with normal alveolar epithelium and wide open and empty alveoli compartment(e). (F) The recovered phenotype in 2 P0 pups from 6 pups. Inflammation were more severe and expanded throughout the whole lobe. As is specified in (F); it observed adjacent of mesothelium of right cranial lobe as well as distal lung. The number of putants with same inflammation phenotype confirmed the hypothesis of dominant segregation of this phenotype from founder (Id# 373238).However, the phenotype presumably become diluted and less destructive in out breed F4 pups. Abbreviations: A: Alveoli; Bronchi: B; Brl: Bronchiole; BADJ: Bronchio alveolar duct junctions; Rcd: Right caudal lobe, V:Vessels, WL: whole lobe

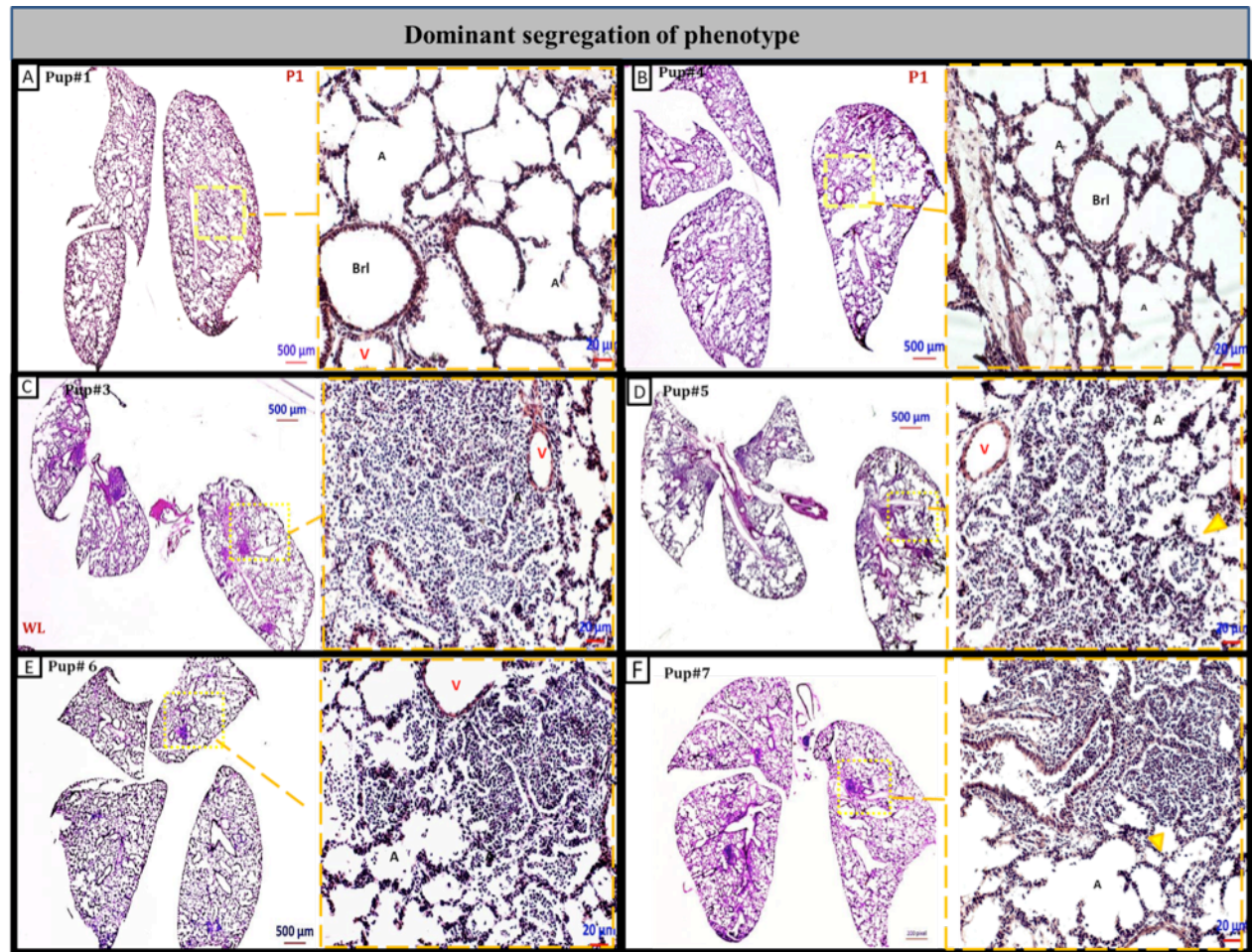


Figure 12. Summary of Histological examination of inflammation phenotype in F3 carrier2 (521252). H&E sections revealed infiltration of immune cells into alveoli and inflammation in alveolar interstitium, and bronchiolitis. The segregation of phenotype was dominant. H&E staining of whole lobe, prefixed with 4% PFA; 8μm cryosections. The multifocal inflammatory cells in interstitium and infiltration of immune cells in peribronchiolar, and perivascular regions. (A,B) Two WT sibling P1 pups. Represent the manifestation of inflammation in 4 of P1 pups (C,D,E,F). The segregation of phenotype is dominant. The F3 female (Id# 521252) identified as second strong carrier. The magnified images of alveolus full filled with white blood cells and macrophages. The yellow triangles point to inflammatory foci and effected bronchioles. Abbreviations: A: Alveoli; Bronchi: B; Brl: Bronchiole; BADJ: Bronchio alveolar duct junctions, V:Vessels, WL: whole lobe

4.1.2. Second most significant founder

The second most significance similar reproducible phenotype identified from founder (Id# 356784). The inflammation foci observed in various spots on left lobe and right caudal lobes. In

primary screen, following the back cross of 4 F2 female; 1 identified as heterozygote by analysis of F3 pups. From F2 female (ID:411095) and F1 male (ID: 356784), 2 of 10, P0 pups showed inflammation. Thus, we hypothesized that this phenotype is recessive. For more investigation this F2 carrier crossed with a wild type male animal to produce F3 generation. After 81- 90 days (approx. 3 months) of the time of carrier's pregnancy report; the F3 animals were ready to cross back with the F1 founder which presumably is heterozygote for phenotype of interest. Meanwhile, by interbreeding of F2 female carrier and F2 male siblings, the F2 male heterozygote identified.

As is summarized in table 3, the F2 carrier (411095) produced 3 female and 3 male animals as result of out cross with wild type. The F1 founder died due to mutagenizing and aging effects. By the crossing back of each F3 female with F2 male carrier animal, one F3 female carrier with strong phenotype in P0 pups discovered. In addition, one male F3 animal identified by crossing with F2 female carrier. In the primary screen the number of discovered mutant was $\frac{1}{4}$ of total litter number and according to mendelian law the phenotype express in recessive manner. However, the recovered phenotype in pups from F3 and heterozygote male cross showed the phenotype in dominant manner. As it shown in table3, carrier 515822 identified as a heterozygote. The putants number was 4 out of 9 and to confirm the dominant segregation of phenotype an out breed with male wild type carried on. The F4 out breed progenies were positive in recessive manner for inflammation phenotype.

Table 3: Screen summary of F3 carrier of Founder # 356784

F1 male	F2 female	F3 mouse (DOB)	Size/stage (DOB)	Phenotypes of F1 #356784				
				IDing strategy	Phenotype	Mutant	Carrier	Status
356784 Died (04.08.14)	411095 (30.01.14)	500181 (15.11.14) Female	5/P0 (26.02.15)	X F2(411098)	-	0	NEG	Crossed x 411098 06.07.15-----NP 23.07.15
		515822 (11.01.15) Female	5/P0 (11.04.15)	X F2(411098)	-	0		Crossed x 411098 (16.04.15)
			9/P1 (25.05.15)	X F2(411098)	inflammation	4	Carrier-Dominant	OUX C57: 2.10.15 to collect sample for sequencing NP: 19.11.15
			4/P1 (18.07.15)	OutX WTC57 male	inflammation	1	Carrier-Dominant	
			?/ P0 (11.09.15)	F3 (515824) male	Eaten	0	Carrier?	
		515823 (11.01.15) Female	8/P0 (08.04.15)	X F2(411098)	-	0	Neg	
			8/P1 (25.06.15)					
		515824 (11.01.15) Male	5/P0 (12.05.15)	X F2(411095) Female	EATEN	0	?	X 515822 (13.08.15)
			?/ P0 (11.09.15)	F3 (515822) Female	Eaten	0	Carrier?	Died 10.11.15
		515825 (11.01.15) Male	P0 (23.07.15)	X F2(411095) Female	EATEN	0	?	Back X F2(411095)- on 25.06 Deliver dead pups 23.07
		515826 (11.01.15) Male						BackX F2(411095) Crossed: 13.08.15- 19.10 NP

Table 3.Summary table of F2 female (ID: 411095) and here progenies in F3. In F3, 3 F3 female and 3 male produced and screened. From F3 females, 1 female characterized as a carrier.

The Figure.12 shows the summary of this founder screen as well as phenotype expression. The inflammation discovered first time in P7 pups with smaller inflammatory spots. The alveolar units separated sharp septum (a,c,e) and sturdy; however, in putants secondary septum either not developed or undergone abnormal alterations. The air sacs are filled with inflammatory cells in which assembly as secondary effect of scarred alveoli. The phenotype severity diluted in out bred F4 pups (Figure12.b,d,f). The out breeding of dominant heterozygote carrier results diluted phenotype. Furthermore, since pups born over night and picked up the next morning, screened P1, there is chance that putant with severe phenotype and respiratory malfunction had eaten by mother. Actually, this issue was one of the crucial obstacles of screening in this age. Due to the significant number of dead litters at P7 age; the screening of P0 and P1 litters done.

Through this strategy not only interesting phenotypes have found but also, inflammation phenotypes observed in a severe and more aggressive manner. To have sound and well conserved lung tissue, the perfusion and inflation steps skipped from preparation procedure. The pups from F3 and WT crosses collected P1. According to aggressive phenotype and small litter size, we concluded that the more effected putants born dead or with severe respiratory function.

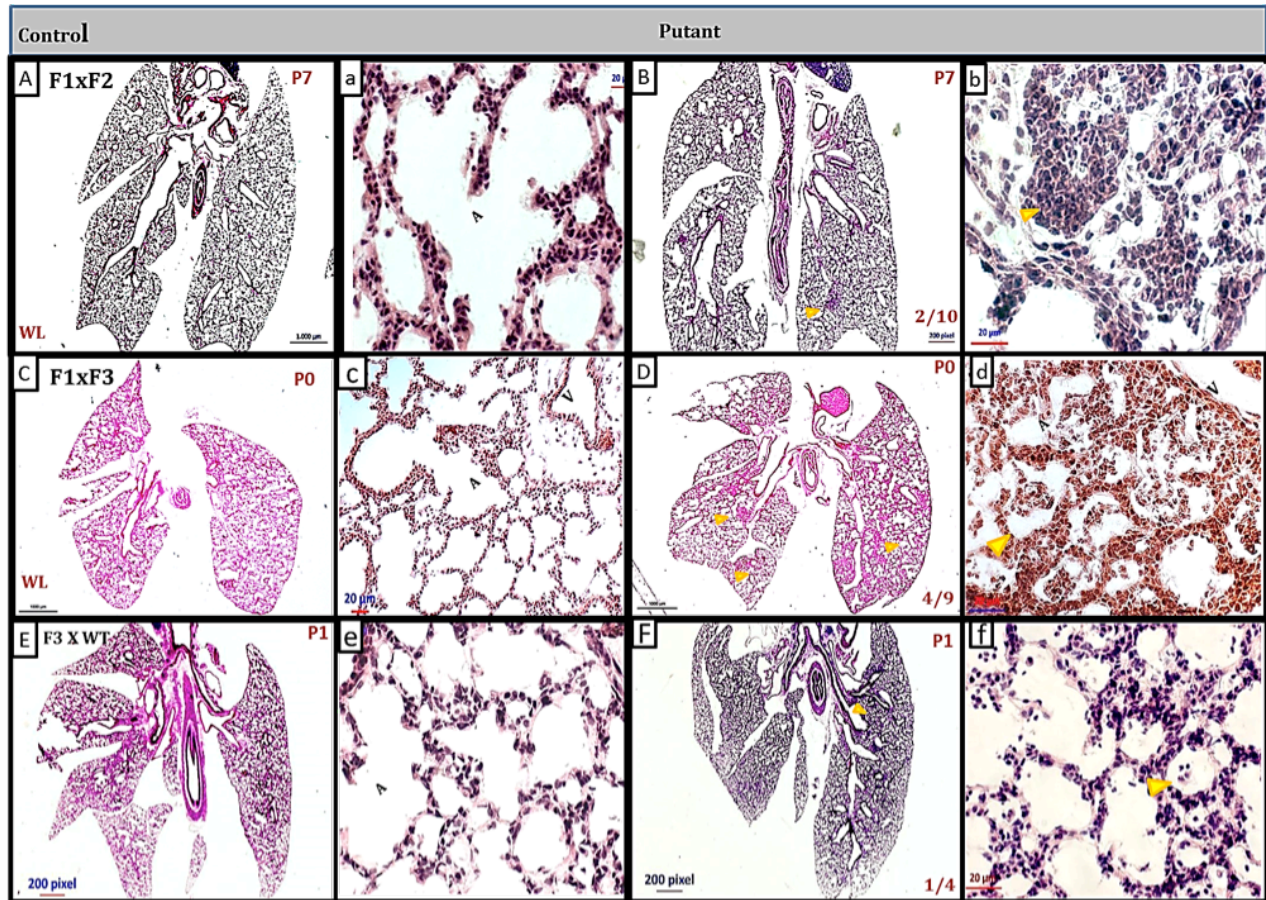


Figure 13. Summary of Histological analysis shows alveolar interstitium, and bronchiolitis inflammation from second significant founder; F1(356784). H&E staining, whole lobe 4% PFA fixed; 8μm cryosections. H&E sections revealed infiltration of immune cells into alveoli, bronchiole and deposition of extra cellular matrix in alveolar interstitium. (A,a;B,b) Primary screen, phenotype discovered in one fourth of pups. Higher magnification focused on one of inflammation foci in which air sac are obstructed with aggregated immune cells. The yellow triangle indicates a macrophages and neutrophils mass. (C;c,D;d) The reproduced phenotype in dominant segregation. From F1 heterozygote founder and F3 identified carrier 4 pups in F4 generation had inflammation and weak fibrotic lesion. (c,d) Magnified images from a healthy well divided and functional alveoli and an infected, scared alveoli units. Alveoli walls thickened and septa structures are not as sharp as WT looking sibling. lobes were collapsed as a result of extra cellular matrix and macrophage accumulation in interstitium. (E,e;F,f) Rediscovered phenotype in recessive manner. The phenotype was diluted however; still white blood cells infiltration into alveoli detected.

The Figure 13 demonstrates the observation of inflammation phenotype in 4 of 9 pups in dominant segregation.

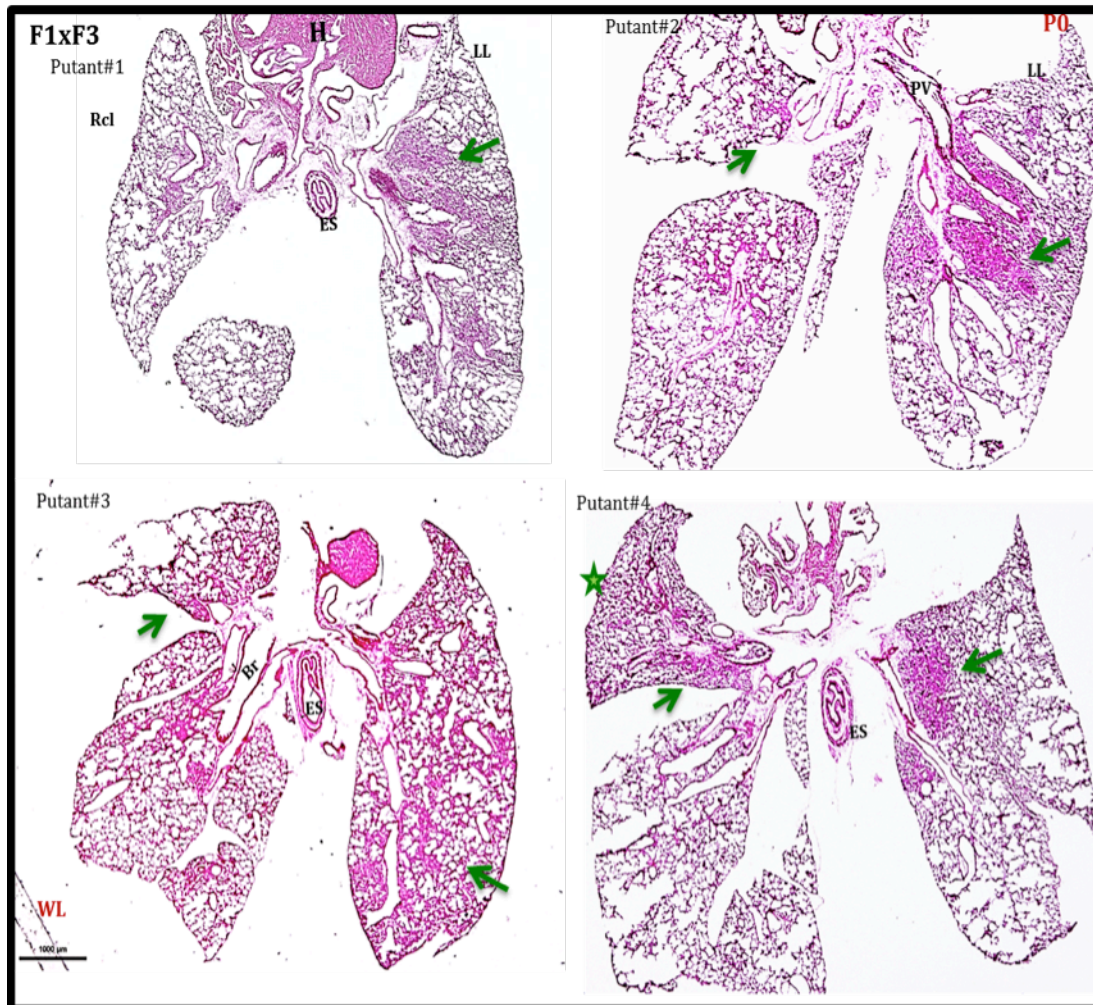


Figure 14. Severe inflammation phenotype in lung with dominant segregation. Histopathology of lung tissue shows inflammation, disordering of lung parenchymal cells, and fibrosis. All 4 putative mutants showed expanded inflammation regions on in all lung lobes. The green arrows point to inflammation foci which. Green star indicates a right cranial lobe that has collapsed presumably due to blocked bronchiole and alveoli by inflammatory cells. Abbreviation: Br: Bronchiole; ES: Esophagus; H: heart; LL: left lobe ; Rcl: right cranial lobe; PV: pulmonary vein; WL: whole lobe

The lung lobes were collapsed due to degrees of interstitial and alveolar inflammation. More likely, these inflammation granulomas and blocked bronchioles result in collapsed lobes. In addition, the immunohistological analysis of this phenotype for primary screen as well as recovered phenotype in F3 back crosses and out crosses carried on (Figure 14). In this family not only immune cells detected as main contributor of pathological condition; but also the

disarrangement of pulmonary vessels observed. Thus, gas exchange between alveoli and pulmonary vasculatures disrupts and lung lobes collapse. The immunofluorescent staining visualized the plugged bronchioles with inflammatory cell masses as well as abnormal pulmonary vasculatures. The pulmonary vessels studied with help of anti Alpha smooth muscle actin (conjugated-cy3; Sigma- c6198; 1:500). In addition, smooth muscles in structure of large airways, blood vessels, and tips of septa structures can be visualized (Figure14.A,a). The alveolar epithelium and bronchial lumens stained with anti Ecadherin. To visualized vasculatures the PECAM/ CD31 and for inflammatory cells Vimentin used (Figure14. B,b).

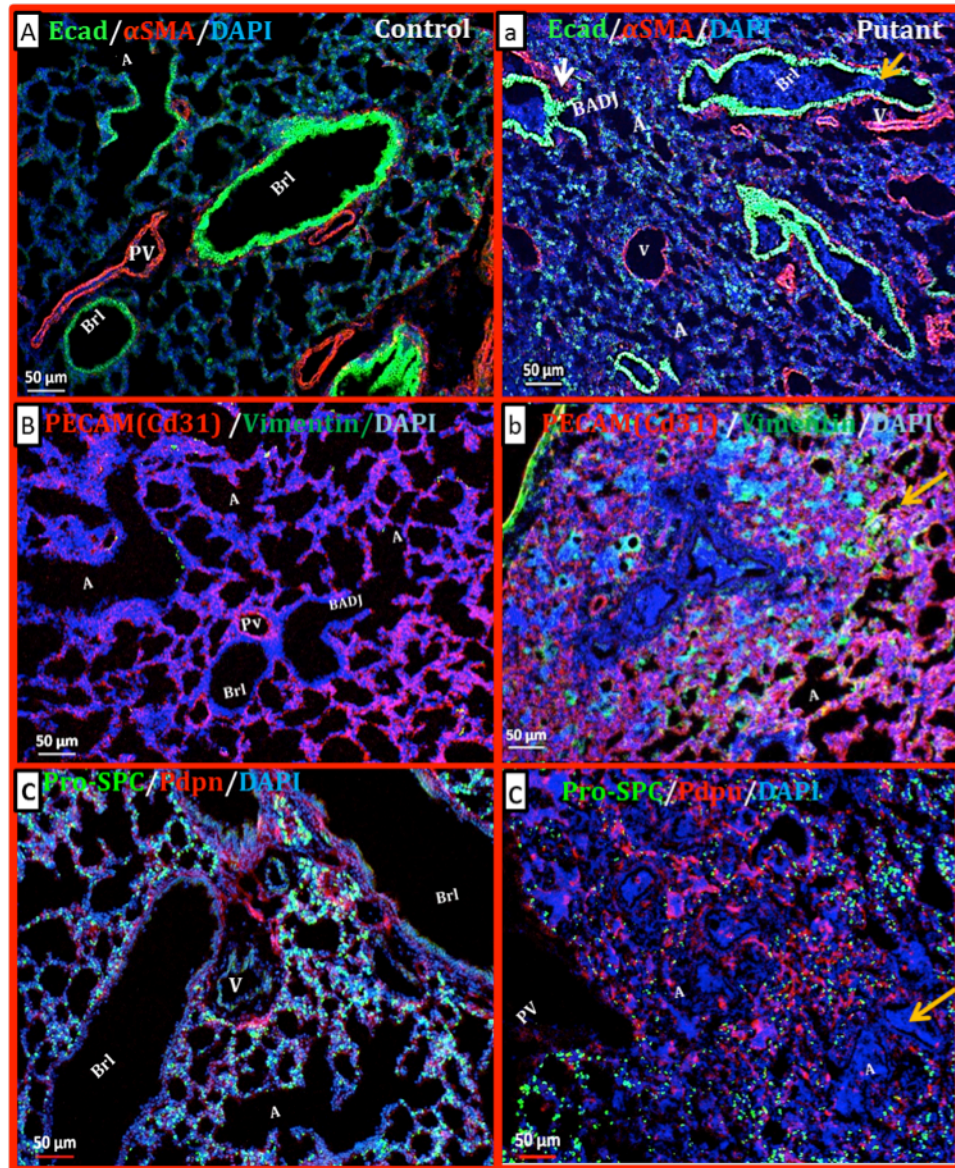


Figure 15. Immunohistological analysis of putative mutants confirmed the interstitial lung inflammation with vessel disruption. (A,a) lung epithelium and interstitial structure (in green) investigated by anti E-cadherin/ Decma-1 (abcam; Rat; 1:1000) and for pulmonary vessels and myofibroblasts ,anti α -smooth muscle actin conjugated antibody with cy3 (Sigma; mouse; 1:500) used. (A) Bronchiolar epithelial cells in green (green) coated inside of bronchiolar lumens. (a) The yellow arrows indicates affected bronchioles with inflammatory cells. The white arrow pints towards a bronchiolar duct junction (BADJ) of a bronchiol filled with inflammatory cells. The immune cells leaked into alveolar interstitium via this BADJ. The pulmonary vessels (in red) which always located close to bronchioles. The small pulmonary vessels affected and capillary loss. The , complex vascular lesions of small vessels (arterioles) undergone the structural changes .The deposition of α -smooth muscles positive seen in interstitium as well as hyperplasia of myofibroblasts. (B,b) The detail investigation of pulmonary vessel illustrated. Pulmonary vasculatures and endothelial cells stained with PECAM/ CD31 (DSHB-2H8; Hamster; 1:1) and for inflammatory cells Vimentin (DSHB-AMF-17b; chicken; 1:30) used. The yellow triangle points to inflammatory cells mass granules in alveoli epithelium. (C,c) Identified putants shows collapsed alveoli and prebronchiolar area. Alveolar epithelial cells type I (AECI) in red stained with podoplanin /T1alpha (Anti t1 α ; DSHB- 8.1.1; Hamster, 1:20). AEC II in green located at corner of alveoli walls, marked by Anti-Pro surfactant Protein C /pro SP-C (Merck/ Millipore; Rabbit; 1:600). The lymphatic vessels also stained in red. Alveoli units are obstructed with SPC negative cell types. Abbreviations: A: Alveoli; Bronchi: B; BrI: Bronchiole, BADJ: Bronchio alveolar duct junctions; PV: pulmonary Vessel

The represented area is example from scared alveoli with obstructed with polymorphonuclear neutrophils (PMNs) and fibroblasts. The endothelial cells increase and microvasculatures acquired abnormal mesh structure. The hyperplasia of myofibroblasts in the alveolar epithelium and macrophages accumulation in pribronchiole and pre pulmonary vessels area represented in Figure.15(a,b).

The thickened alveoli units visualized with anti podoplanin /T1alpha for AECl and Anti-Pro surfactant Protein C /pro SP-C for AECII . As expected cell masses in bronchiole were indeed composed of white blood cells.

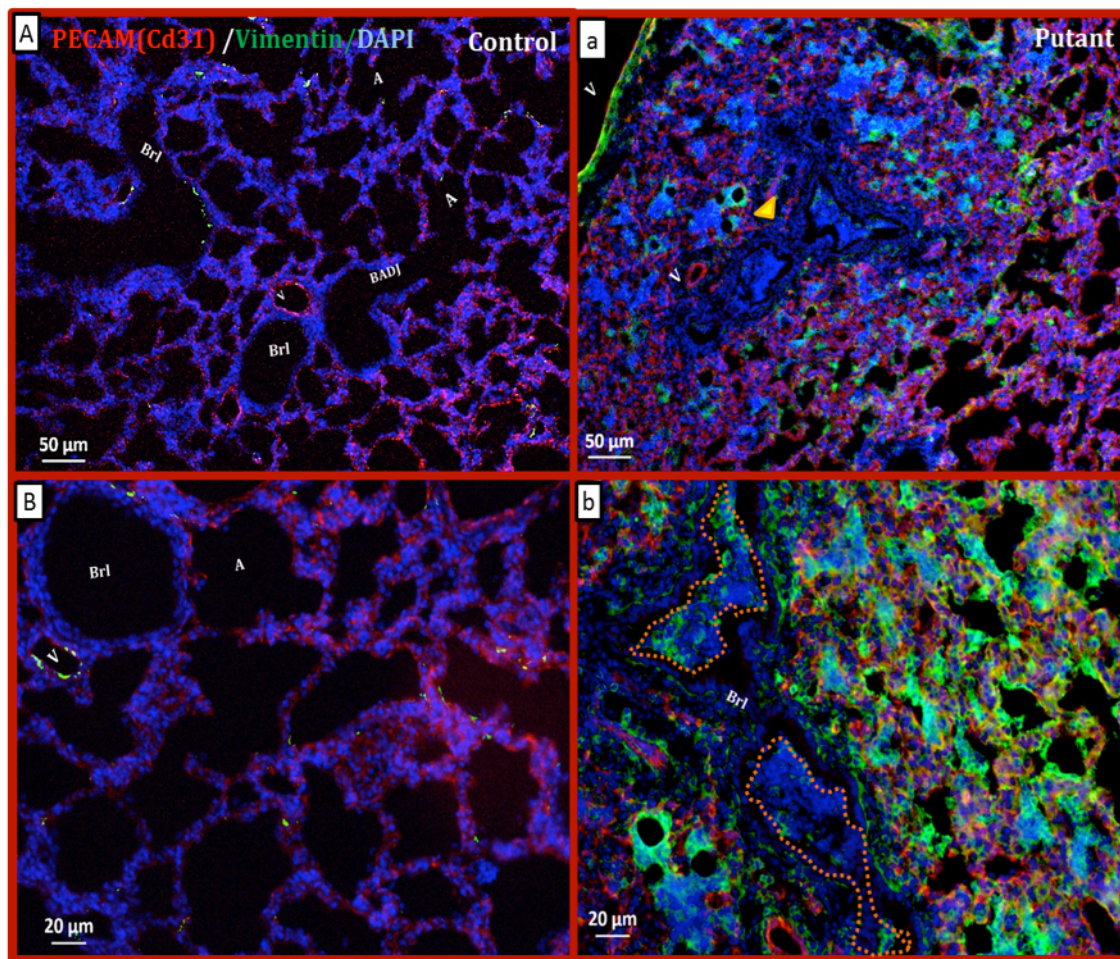


Figure 16. Clarifying the identity of cell mass in alveoli interstitium and bronchiole. Pulmonary vasculatures and endothelial cells stained with PECAM/ CD31 (DSHB-2H8; Hamster; 1:1) and for inflammatory cells Vimentin (DSHB-AMF-17b; chicken; 1:30) used. The yellow triangle points to inflammatory cells mass granules in alveoli epithelium. The yellow triangle pointed to an inflammation foci. The orange dashed line separated poly morpho nuclear cell mass in a bronchiole. Abbreviations: A: Alveoli; Bronchi: B; Br1: Bronchiole; BADJ: Bronchio alveolar duct junctions; PV: pulmonary Vessel

4.2. Identified phenotype with F3 generation

The following founders showed alveolar interstitial inflammation in recessive segregation and with slightly different expression. The table4 summarized these founders and relevant F2 carriers.

Table 4: Summary of phenotypes without identified F3 carriers

Phenotype	F1 carrier	F2 carrier	Strategy	#Putant	#F3 carrier
inflammatory cells in alveolar interstitium +Cell mass	398443	514224 515830 514229	F1xF2	2/9 3/5 1/5	568393 F3 produced 584922,23
	404656	505971	F1xF2	3/10	F3 produced

Table 4. Identified 4 F2 females from two different F1 males. The identified phenotype is alveolar interstitial inflammation in recessive segregation.

4.2.1. Founder 1(ID#398443); carriers with alveolar interstitial inflammation

From founder 398443; two F2 female carrier has identified with fairy severe phenotype and 1 with weak phenotype by histological analysis. The summary of this founder screen and the F2 identified carriers illustrated in table 5. To investigate the lung epithelial, progenitor cells alteration and identify the type of cells involve in formation of this phenotype immunohistological staining done.

Table 5: Summary of founder#398443 screen

F1 male (DOB)	F2 female (DOB) Cross type	Size/stage (DOB)	Phenotypes of F1#398443				
			Histology (H&E,VVG,AB)	IHC	Mutant	Cartilage	Status and ongoing work
398443 (24.11.13)	514224 (08.01.15) F1xF2	2/P0 (02.04.15)	Analyzed	Analyzed	0	Analyzed	Alive Produced litter (DOB: 23.06.15) (4 Female, 2 male) F3 carrier identified
		9/P0 (25.05.15)	Inflammation Fibrotic cell mass	Inflammation Myofibroblast hyperplasia	2		
	514225 (08.01.15)	3/P0 (06.04.15)	Analyzed	Analyzed	0	Analyzed	
	515827 (12.01.15)	8/P0 (14.04.15)	Analyzed	Analyzed	0	Analyzed	
		3/P0 (19.08.15)	Analyzed	Analyzed	0	Analyzed	
	515830 (12.01.15) F1xF2	5/P0 (06.05.15)	Inflammation Fibrotic cell mass	Inflammation Myofibroblast hyperplasia	3		Alive Produced F3 (DOB: 27.08.15) (4 Female, 4 male) F3 carrier to be identify
	514227 (08.01.15)	1/P0 (03.07.15)	Analyzed	Analyzed	0	Analyzed	
		2/P0 (17.08.15)	Analyzed	Analyzed	0	Analyzed	
	514230 (08.01.15)	8/P1 (13.06.15)	Analyzed	Analyzed	0	Analyzed	
	514231 (08.01.15)	7/P1 (15.06.15)	Analyzed	Analyzed	0	Analyzed	
	514228 (08.01.15)						X F1 (11.06.15) Np (15.06.15) – Died (29.06.15)
	514229 (08.01.15) F1xF2	5/P0 (03.07.15)	Inflammation Fibrotic cell mass	Inflammation Myofibroblast hyperplasia	1		Alive Out crossed with WT C57 Produced F3 (DOB: 27.08.15) (7 Female, 2 male) F3 Carrier identified

Table 5. From F1 (398443) three F2 females characterized as carrier. From these three carriers, F3 generations produced and identifying F3 carriers done. Among F2 female animals , phenotype in F2 (Id#514224) progenies was more significant.

This analysis presented in Figures 16, 17 and 18. In this phenotype infiltration of eosinophilic white blood cells and neutrophils clearly observed. In addition, wide spread aggregation of inflammatory cells and macrophage blocking alveoli units detected. Alveoli walls thickened and septum structures cracked. Moreover, the club cells and ciliated cells at bronchiolar lumen undergone morphological changes and weak hyperplasia (Figure 16.A,a;B,b). Indeed, immunohistological study, confirmed these cell masses are composed of inflammatory vimentin positive cells (Figure16-C,c) and (Figure 18.B;b). Also, these cell mass were negative for Pro surfactant protein C (Figure 19). Thus, this phenotype was similar with previous ones that identified as interstitial inflammation. In general, appearance of this phenotype in all F2 carriers, was similar.

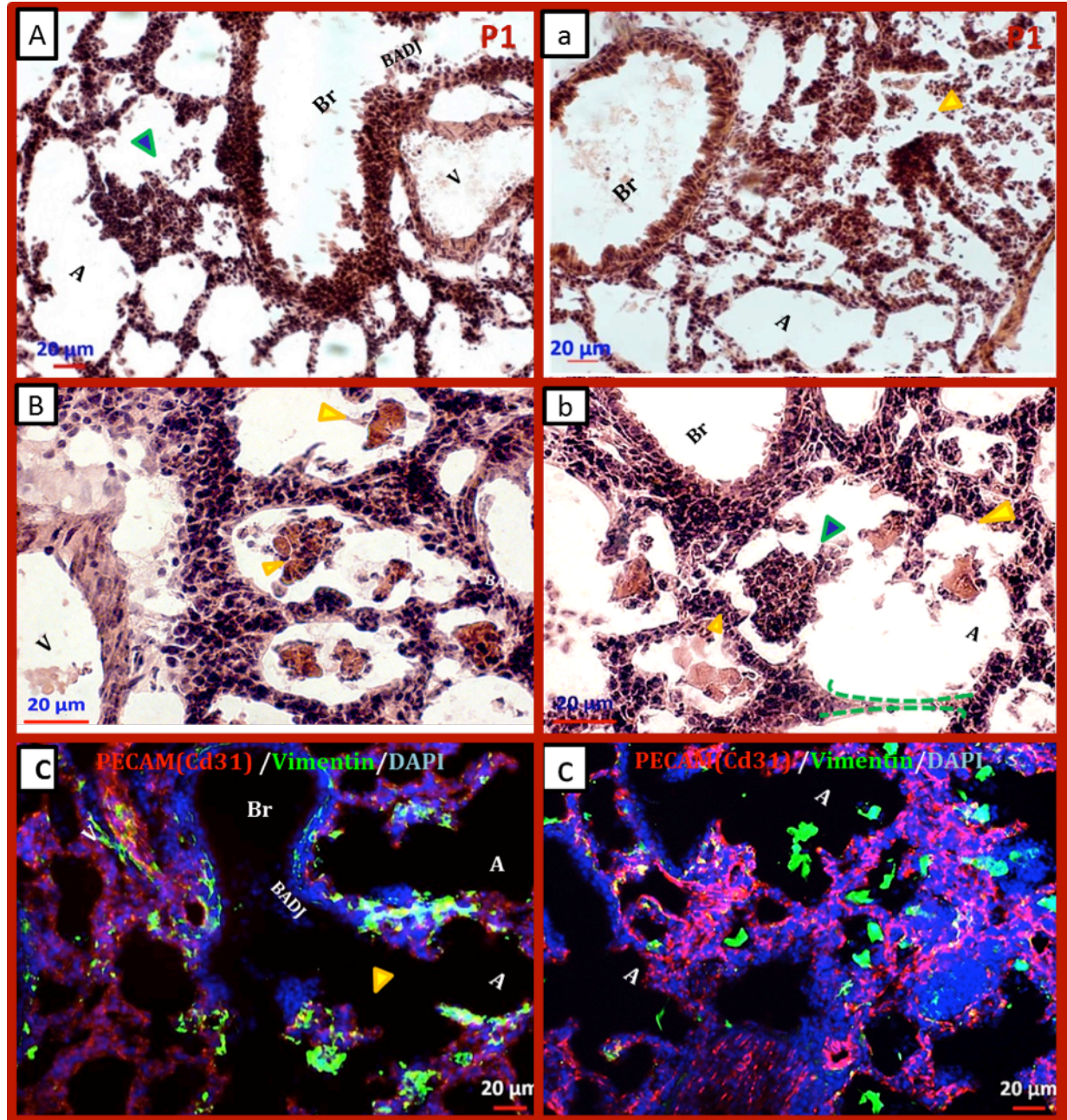


Figure 17. The inflammation in the interstitial lung phenotype, founder F1Id#(398443). This phenotype accompanied with eosinophilic and poly morpho nuclear white blood cells infiltration. (A,a;B,b) Histopathology of P0 putants with scared alveoli, inflammatory cell mass in alveoli, bronchiolitis. The green triangle points out cell mass which plugged alveoli. The yellow triangles indicate macrophages and neutrophils. (C,c). The Immunohistological analysis confirmed the inflammatory identity of these cells. The cell masses were positive for vimentin (DSHB-AMF-17b; chicken; 1:30) and vasculatures stained with PECAM/ CD31 (DSHB-2H8; Hamster; 1:1). Abbreviations: A: Alveoli; Bronchi: B; Brl: Bronchiole; BADJ: Bronchio alveolar duct junctions, V:Vessel/pulmonary vein; WL: whole lobe

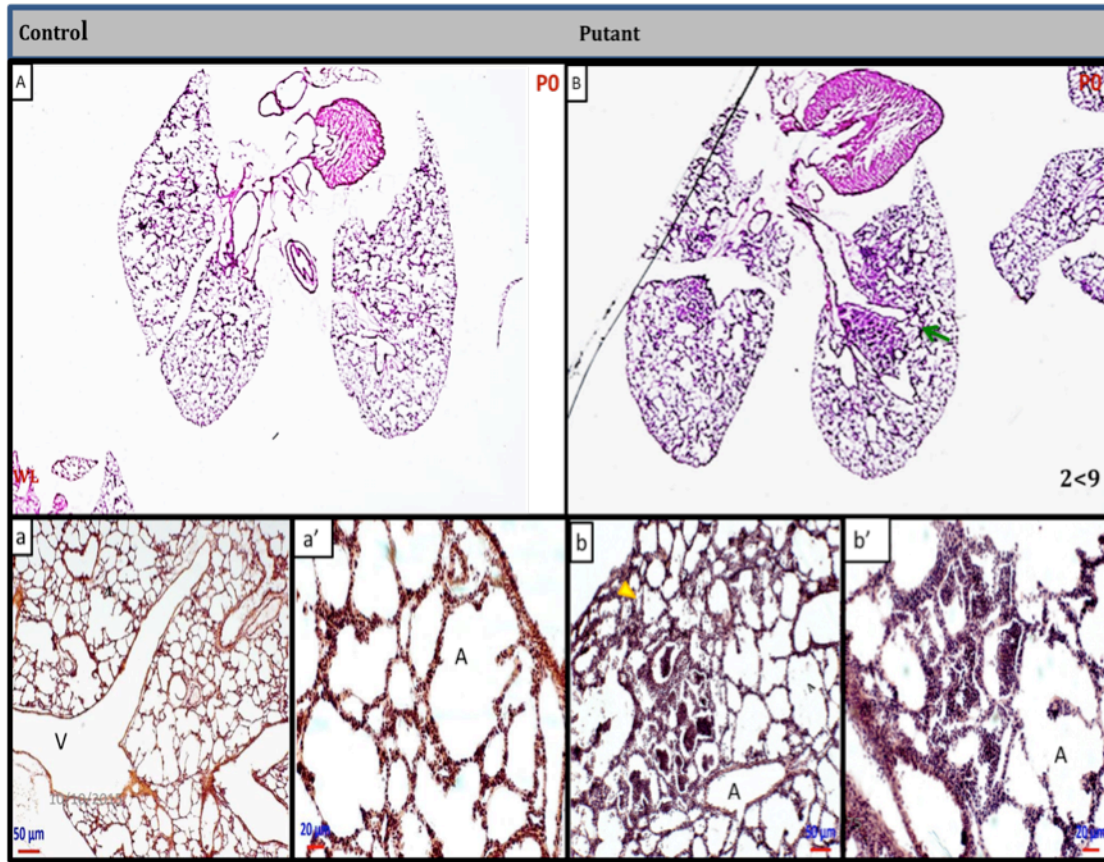


Figure 18. Histopathology of P0 pups. Inflammatory cells infiltration into alveolar interstitium, 2 from 9 pups from carrier Id#514224 showed severe phenotype with recessive segregation. The lung lobes pre fixed in 4% PFA; 8μm cryosections. (A,a; a') Whole lobes view and higher magnification of wild type looking sibling. Alveolar units and dorsal air ways look clean and void of any significant cell mass. (B,b,b') Multiple inflammatory foci observed in left, right cranial and right caudal lobe. The higher magnification images taken from one of the inflammation foci in which air sacs are obstructed with aggregated immune cells. The green arrow points to immune cells mass and collapsed alveoli.

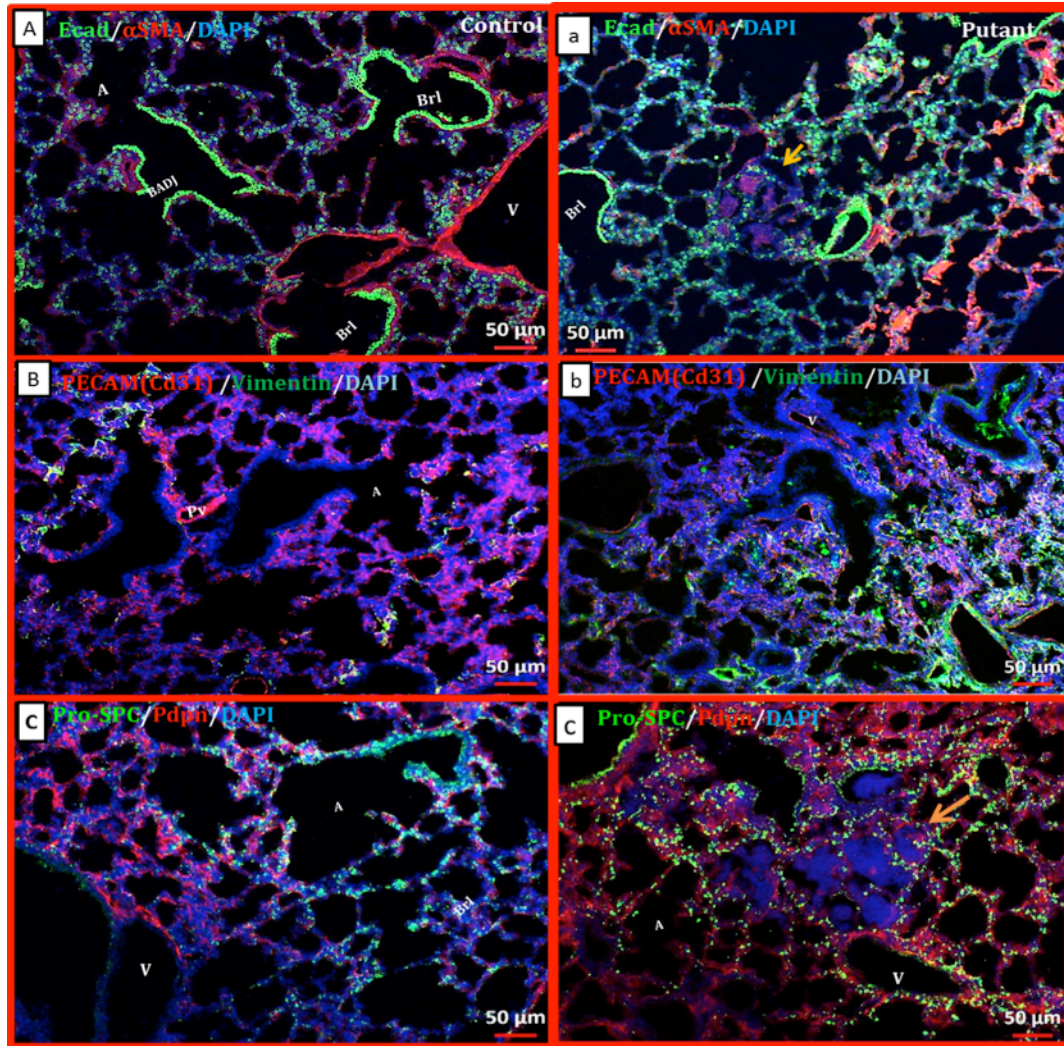


Figure 19. Immunohistological analysis of putative mutants confirmed the interstitial lung inflammation and cell mass in alveolar units. (A,a) lung epithelial cells and bronchiolar lumens cells (in green) visualized by anti E-cadherin/Decma-1 (abcam; Rat; 1:1000) antibody. The pulmonary vessels and myofibroblasts (in red) stained with anti α -smooth muscle actin conjugated antibody with cy3 (Sigma; mouse; 1:500). (A) In wild type looking sibling the distal air ways and bronchiole are clean. (a) The yellow arrow indicates inflammatory cells and myofibroblasts bulk (α SMA positive in red). Moreover, the myofibroblast seems to have increased in alveolar interstitium. In this founder, bronchiolitis and distal air ways obstruction observed. (B,b) The pulmonary vessels structure studied by PECAM/CD31 (DSHB-2H8; Hamster; 1:1) antibody (in red) and fibroblast and fibrotic foci visualized in green Vimentin (DSHB-AMF-17b; chicken; 1:30). (C,c) Identified putants shows normal distribution of AECI distribution, in red (anti podoplanin /T1alpha; DSHB- 8.1.1; Hamster, 1:20), AECII in green (anti-Pro surfactant Protein C /pro SP-C; Merck/Millipore; Rabbit; 1:600) and nuclei in blue (DAPI, 1:1000). The lymphatic vessels and other mesenchymal cells also stained in red. Alveoli units are obstructed with inflammatory cells aggregation. The dark yellow arrow pointed to these cell mass. Abbreviations: A: Alveoli; Bronchi: B; Brl: Bronchiole, BADJ: Bronchio alveolar duct junctions; PV: pulmonary Vessel

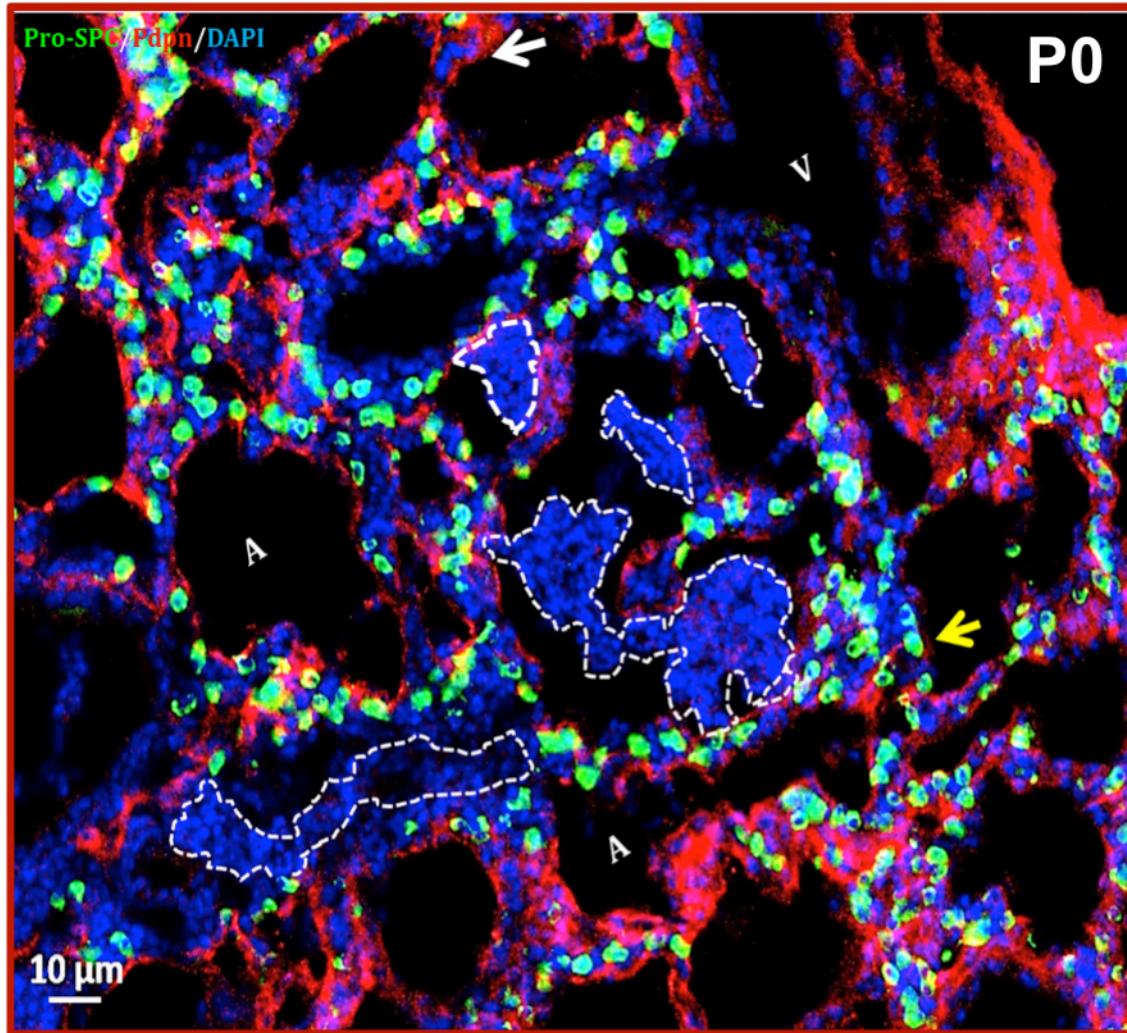


Figure 20. High magnification of cell mass aggregation in alveoli units. The white arrow indicate alveolar type 1 cells that forming alveoli walls and visualized in red (anti T1alpha; DSHB- 8.1.1; Hamster, 1:20). The yellow arrow points to alveolar type 2 cells in green which are located at corner of alveoli walls. AECII stained with (anti-pro SP-C; Merck/ Millipore; Rabbit; 1:600). The non classified cell aggregation in air sacs showed by dashed white color lines. These bulky cell aggregations occupied multiple alveoli units within the alveolar epithelium. Alveoli units are obstructed with inflammatory cells aggregation. The dark yellow arrow pointed to these cell mass. Abbreviations: A: Alveoli; Bronchi: B; Brl: Bronchiole, BADJ: Bronchio alveolar duct junctions; V:Vessel

4.2-2- Founder 2 (ID#404656); carriers with alveolar interstitial inflammation

The founders 404656 also showed same inflammation in interstitial phenotype. The summary of founder #404656 presented at table 6. As is shown in table 6. From 6 F2 female, 1 F2 carrier identified. From 10 pups, 3 putants showed very severe inflammation and collapsed lobes. In fact, 3 from 10 pups showed inflammation and according to mandelian segregation law,

we hypothesized that the F2#505971 is a heterozygote carrier for recessive phenotype. Actually, since the phenotype has identified in 30 % of progenies, and according to mendelian segregation law it was fairly more than $\frac{1}{4}$ of total. We validate our hypothesize by breeding out the F2 carrier with a C57/Bl6 WT male. From 9 pups didn't show any form of inflammation in alveolar interstitium. Thus, we concluded the F2 carrier is indeed a heterozygote for recessive phenotype. Therefore, this F2 has bred out with WT C56/Bl6 male mouse to produce F3 generation and identifying F3 carriers by crossing back to F1 founder.

Table 6: Summary of phenotypes without identified F3 carriers

F1 male DOB	F2 female DOB Cross type	Size/stage (DOB)	Phenotypes of F1#404656				
			Histology (H&E,VVG,AB)	IHC	Mutant	Cartilage	Status
404656 (28.12.13)	505968 (17.12.14) F1xF2	5/P0 (11.04.15)	Analyzed	Analyzed	0	Analyzed	
		5/P0 (02.06.15)	Analyzed	Analyzed	0	Analyzed	
	505969 (17.12.14) F1xF2	5/P0 (20.03.15)	Analyzed	Analyzed	0	Analyzed	
	505970 (17.12.14) F1xF2	No litter production	-	-	-	-	Since 23.4.15 X F1: NP; separated XF1: 31.07 NP; 16.09.15-Separated
	505971 (17.12.14) F1xF2	10/P1 (16.07.15)	Inflammation Fibrotic cell mass	Fibrotic cell mass	3		Alive Out crossed with C57Bl/6J 4 Female, 5 male F3 carrier to be identify
	515840 (15.01.15)	5/P0 (26.07.15)	Analyzed	Analyzed	0	Analyzed	
	515841 (08.01.15)	9/P0 (30.07.15)	Analyzed	Analyzed	0	Analyzed	
	515842 (15.01.15)	10/P2 (22.08.15)	Inflammation	Analyzed	1	Analyzed	

Table 6. From F1 (404656), the F2 (Id# 505971) characterized as carrier. The F3 generations produced for future analysis.

The detail histological and immunohistological analysis presented in Figure 20 and 21. These analyses revealed that the number of myofibroblasts significantly increased in area close to the accumulated cells.

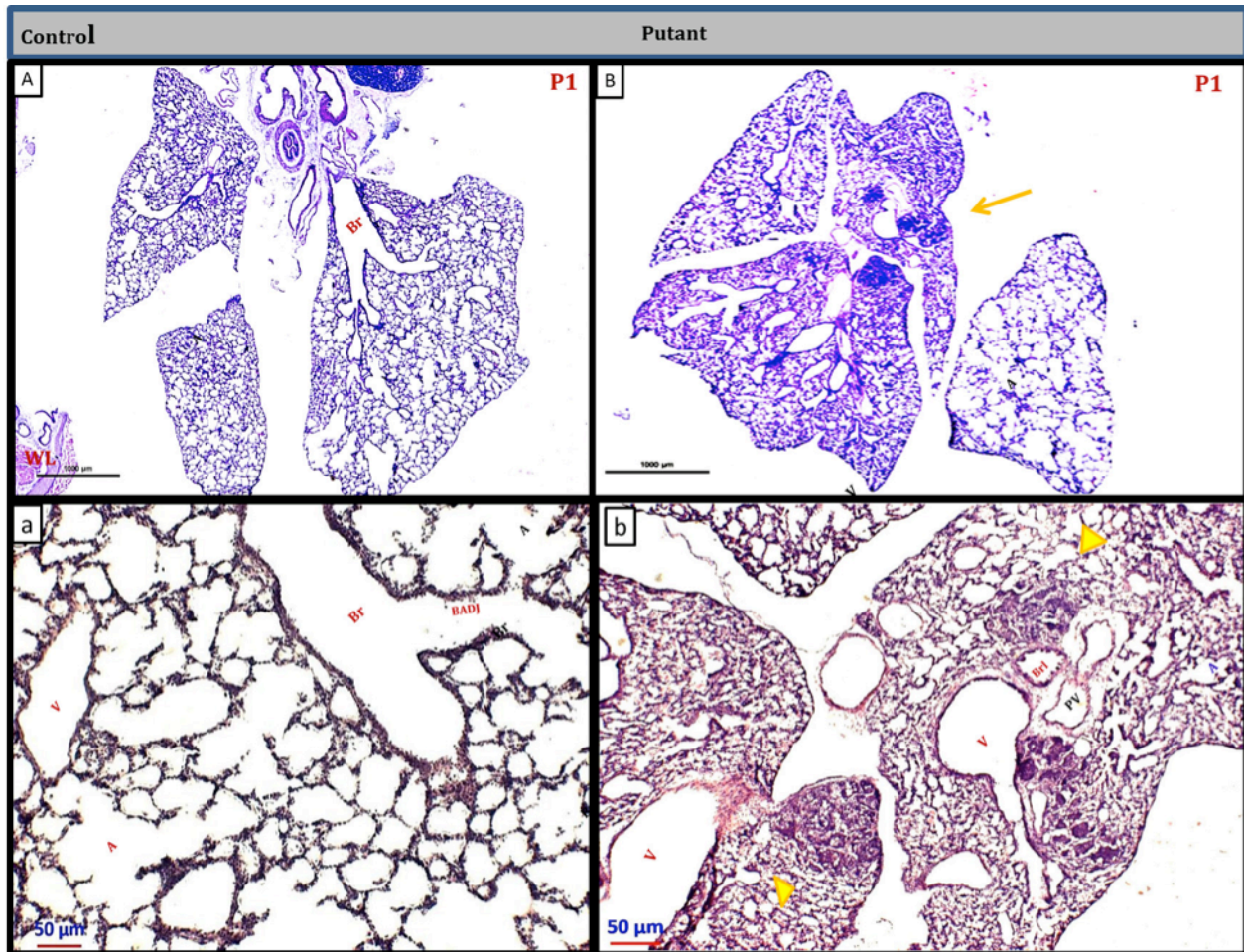


Figure 21. Histopathology of P1 pups. Inflammatory cells foci collapsed lobes. From 10 pups 3 showed same immune cells infiltration into the interstitium. The lung lobes pre fixed in 4% PFA; 8µm cryosections. (A,a) Whole lobes cryosection and stained with H&E of wild type looking sibling. Alveolar units and dorsal air ways look clean and void of any significant cell mass. (B,b) Multiple inflammatory foci observed in right cranial and right caudal lobe. The right cranial lobe, pointed by yellow arrow, collapsed and air sacs narrowed and blocked by cell accumulation. (b) The higher magnification images taken from close inflammation foci adjacent to mesothelium. The yellow triangles point to alveoli in which filled with inflammatory cells.

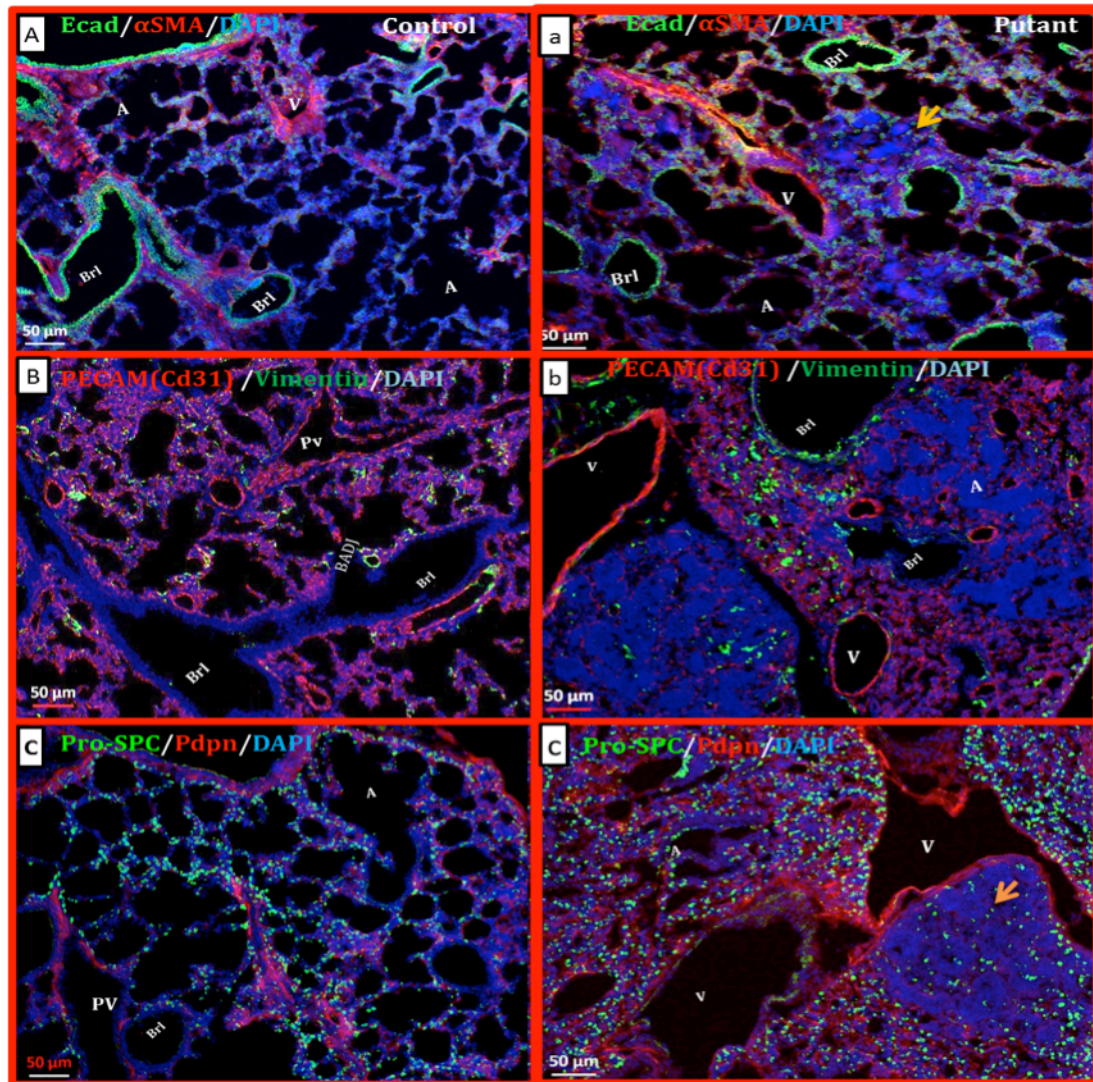


Figure 22. Immunohistological analysis confirmed the interstitial lung inflammation phenotype. (A,a) lung epithelial cells and bronchiolar lumens cells (in green) visualized by anti E-cadherin/ Decma-1 (abcam; Rat; 1:1000) antibody. The pulmonary vessels and myofibroblasts (in red) stained with anti α -smooth muscle actin conjugated antibody with cy3 (Sigma; mouse; 1:500). (A) In wild type looking sibling the distal air ways, bronchiole and alveoli are clean. (a) The yellow arrow indicates inflammatory cells aggregation in to the alveolai unit. (B,b) The pulmonary vessels structure studied by PECAM/ CD31 (DSHB-2H8; Hamster; 1:1) antibody (in red) and fibroblast and fibrotic foci visualized (in green) by Vimentin (DSHB-AMF-17b; chicken; 1:30). (C,c) Identified putants show normal distribution of AECl in red (anti podoplanin /T1alpha; DSHB- 8.1.1; Hamster, 1:20) and AEClI in green (anti-Pro surfactant Protein C /pro SP-C; Merck/ Millipore; Rabbit; 1:600); nuclei in blue (DAPI, 1:1000). Indeed, the nuclei of infiltrated cells and their coagulated mass can be seen in blue. The lymphatic vessels also stained in red. The dark yellow arrow pointed to these cell mass. Abbreviations: A: Alveoli; Bronchi: B; Brl: Bronchiole, BAdJ: Bronchio alveolar duct junctions; PV: pulmonary Vessel

The Figure.22 is a resemble of these area with mild fibrosis. Moreover, the number of epithelial cells increased and alveolar interstitium is congested. In this putant lung samples

showed interstitial lung diseases characteristic which was increase the number of myofibroblast.

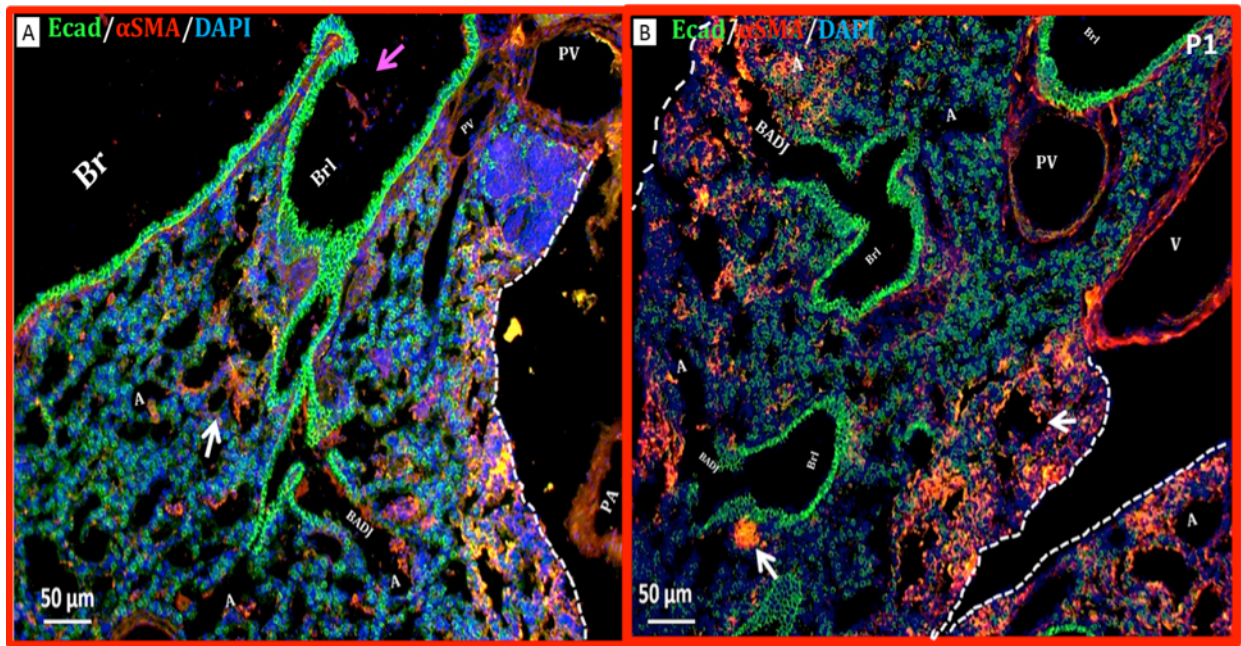


Figure 23. Increased myofibroblast and fibrosis adjacent to inflammatory cells accumulation and collapsed lobe (A,B) Higher magnification from alveolar interstitium showed aggregation and increase of α -smooth muscle actin cells at prebronchiolar, mesothelium (identified by dashed white color) and alveolar interstitium. White purple arrow indicate fibroblasts in red deposited in bronchiole, white arrows pointed to inflammatory cells mass that encompasses by alveolar epithelial cells and myofibroblasts. The alveolar epithelium under gone structural changes and collapsed. The alveoli units lost the septum structure and their wall thickened. The anti α -smooth muscle actin conjugated antibody with cy3 (Sigma; mouse; 1:500) used to stain myofibroblasts, fibroblast, pulmonary vessels (in red). The epithelial cells visualized by anti E-cadherin/ Decma-1 (abcam; Rat; 1:1000) antibody and nuclei stained by DAPI (Sigma, 1:1000). Abbreviations: A: Alveoli; Bronchi: Br; Br1: Bronchiole, BADI: Bronchio alveolar duct junctions; PA: Pulmonary artery PV: pulmonary Vessel

4.3. Phenotypes without recovered F3 carrier or with different characteristics in recovered phenotype from primary phenotype

4.3.1. lung nodule

This phenotype recovered in F3 carriers by interbreeding strategy of F3. Due to death of F1, the confirmation of F3 heterozygosity and collection of putative mutants experiment aborted. Nonetheless, two F2 female and male F3 interbred progenies showed the phenotype.

The nodule phenotype discovered in second time of this F2 carrier. This lung nodule was filled with inflammatory cells. It was similar with previous findings regarding lung nodule. Figures 23 and 24 shows the discovered nodule phenotype and the magnified images from cells that composed the nodule. In addition, in identified putant from F3 generation the serial sectioning from left lobe and right medial lobe done to investigate the structure of the nodule and cell types that participate in formation of lung nodule.

lung Nodule

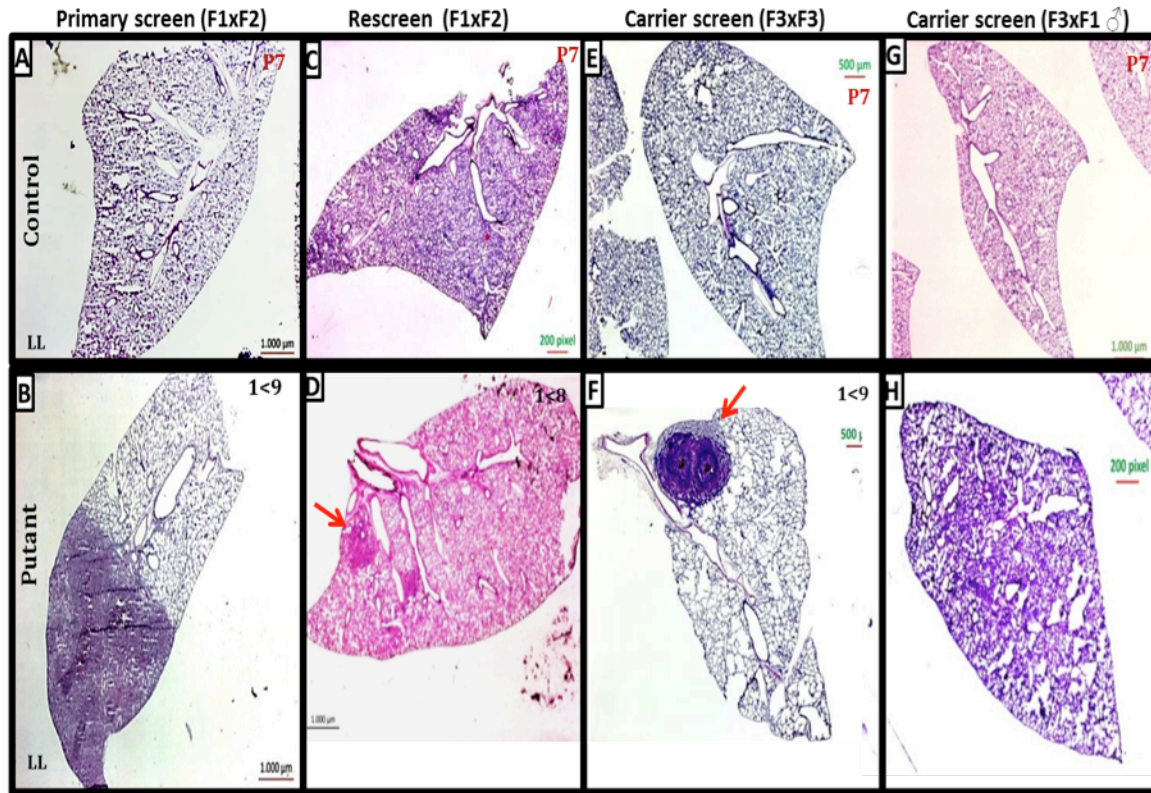


Figure 24. Histopathology of P7 pups with lung nodule and cell mass. The lung lobes inflated with PFA 4% and pre fixed ; 8µm longitudinal cryosections and stained with H&E. (A,B)The wild type sibling and a putative mutant left lobe showed cell masses and filled with various nodule structure. (C,D) At secondary screen, granuloma and nodule structure observed in three area on left lobe lung. The affected area observed was smaller. The red arrow points to alveolar epithelium that encompasses the nodule and granuloma. (E,F) The recovered phenotype by F3x F3 interbreed. The nodule made of inflammatory cells in proximal of lobes. (G,H) Wild type looking pups from back crossing of potential F3 carrier with F1 founder.

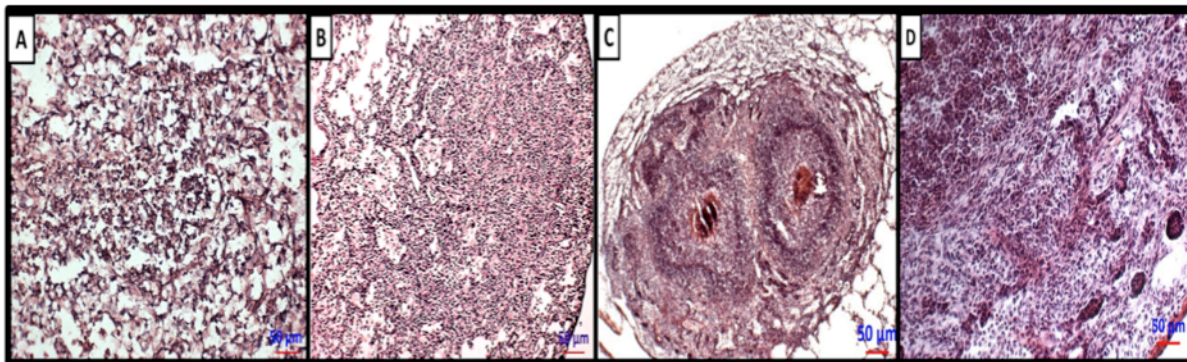


Figure 25. Higher magnification of lung nodule. Inflammatory cells composed lung lobes. Inflated P7 lobes with 4% PFA ; 8µm longitudinal cryosections and stained with H&E. (A,B) Similar phenotype manifestation from primary, secondary in F3 interbreed recovered putants (C,D). The lung nodule histopathology is similar with noninfectious benign inflammatory lung nodules. In which filled with inflammatory and extra cellular matrix deposition.

In Figure 25 the histological serial sectioning and observation of white blood cells in structure of nodule presented.

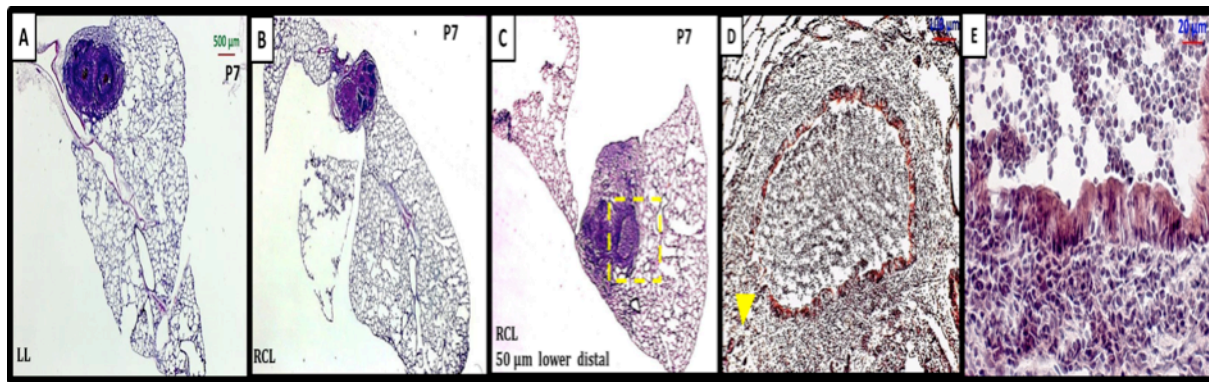


Figure 26. Histopathology of P7 putative mutant with nodule structure on proximal of left lobe and right caudal lobe. (A,B) Left lobe and right caudal lobe showed nodule structure. (C) By serial sectioning of right caudal lobe from proximal to distal. This method showed size, structure and consistency of lung nodule morphology within the alveolar epithelium. The yellow dashed square enveloped a bronchiole that under gone massive structural changes and filled with inflammatory cells. (D) A bronchi filled with inflammatory white blood cells and enveloped by collapsed air sacs in which in filtered by poly morpho nuclear white blood cells such as neutrophils. The prebronchiole area and alveoli epithelium are occupied inflammatory white blood cells accumulation. The yellow triangle pointed to bronchiole lumen that disrupted and inflammatory cells passage into alveoli interstitium. (E) Higher magnification of affected bronchiole. The lung lobes pre fixed in 4% PFA; 8µm cryosections and stained with H&E.

Furthermore, to characterize the type of lung nodule the immunofluorescent staining carried on. These analysis confirmed the nodule and cell mass structures are indeed made of inflammatory cell mass. The vimentin used as marker to identify fibroblast and lymphocytes. The vimentin found in various non-epithelial cells, especially mesenchymal cells. It is highly expressed in fibroblasts, in some expression in T- and B-lymphocytes, and little in Burkitt's lymphoma cell lines. Expressed in many hormone-independent mammary carcinoma. In addition, to study the endothelial cell and pulmonary vessels condition and relationship in nodule affected area; PECAM/ CD31 antibody used. The summary of this detail study illustrated in Figure 26 and 27. Moreover, these data showed that at the nodule cell mass not only composes of myofibroblast and white blood cells, but also these structures enveloped by fibroblasts and AECI and II cells. In addition, this structure were well enveloped by endothelial and pulmonary vasculatures as well as lymphatic vessels. Furthermore, high rate of proliferation observed in AECII cells that exclusively located around the nodule structure and were positive for Anti-PCNA antibody, a marker for proliferating cells.

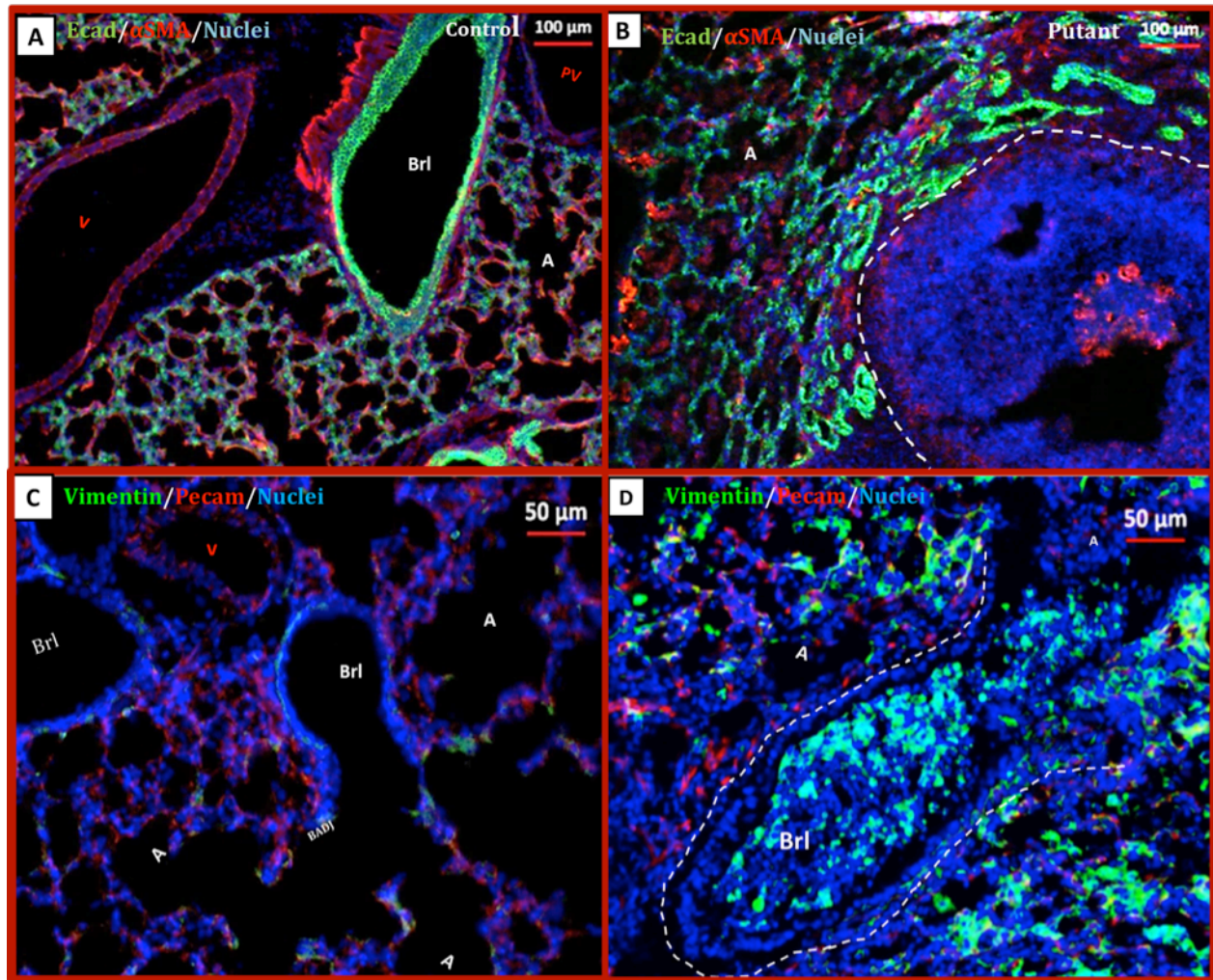


Figure 27. Immunohistological analysis of nodule confirmed the inflammatory composition of this structure. (A,B) Immunofluorescent staining for epithelial cells (in green) visualized by anti E-cadherin/ Decma-1 (abcam; Rat; 1:1000). Also, pulmonary vessels, myofibroblasts, and fibroblast stained with anti α -smooth muscle actin conjugated antibody with cy3 (Sigma; mouse; 1:500). The alveolar wall thickened and air sacs collapsed in putant in comparison with wild type sibling. The smooth muscle actin pulmonary vessels in prebronchiolar area and tips of septum observed well organized. The alveoli units are wide open. In contrast, myofibroblasts accumulated in collapsed air sacs and encapsulates the nodule. The white dashed line shows half of the nodule structure. (C,D) The pulmonary vessels structure studied by PECAM/ CD31 (DSHB-2H8; Hamster; 1:1) antibody (in red) and fibroblast and fibrotic foci visualized (in green) by Vimentin (DSHB-AMF-17b; chicken; 1:30). The alveolar epithelium and bronchioles are occupied by inflammatory cells at nodule and pre bronchiole area. The white dashed line identifies a bronchiole in which filled with inflammatory and fibroblast Vimentin positive cells adjacent o nodule area. Abbreviations: A: Alveoli; Bronchi: Br; Brl: Bronchiole, BADJ: Bronchio alveolar duct junctions; PA: Pulmonary artery , PV: pulmonary Vessel

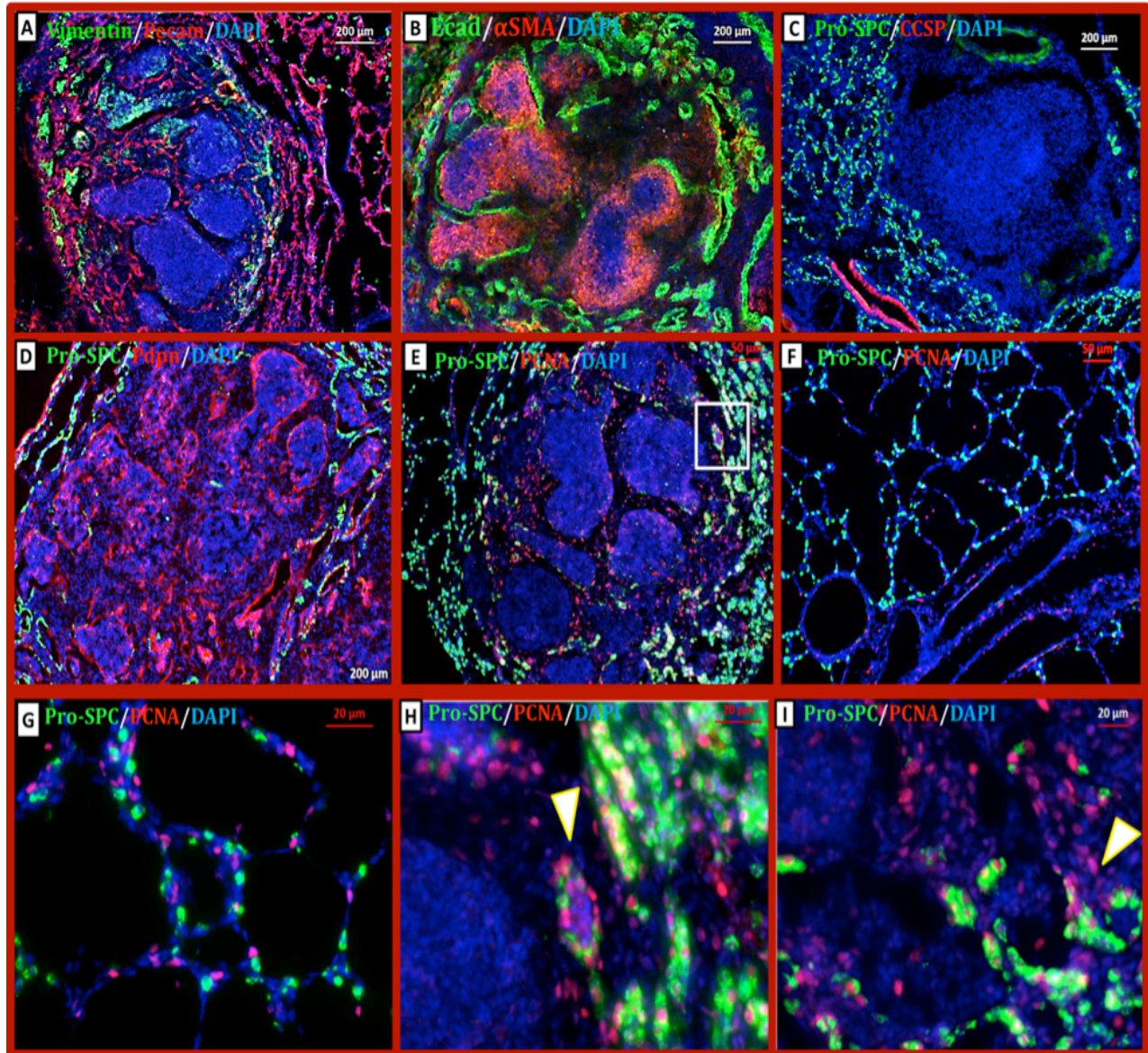


Figure 28. Immunofluorescent staining of an inflammatory nodule encompasses with proliferative Alveolar epithelial type II cells (AECII). (A) Immunofluorescent staining to visualize fibroblasts and fibrotic foci applied vimentin marker (DSHB-AMF-17b; chicken; 1:30). Multiple cell masses observed within interstitium enclosing nodule structure. Inflammatory cells (in green) in filtered into bronchiole and alveolar interstitium. Lung micro vasculatures (in red) at alveoli wall under gone structural alteration. Vessels stained with PECAM/ CD31 (DSHB-2H8; Hamster; 1:1). (B) Cell mass structures made of myofibroblast (in red) positive for anti α -smooth muscle actin Cy-3 conjugated antibody (Sigma; mouse; 1:500). Myofibroblasts aggregation separated from each other by epithelial cells (in green). Epithelial cells stained with E-cadherin/ Decma-1 (abcam; Rat; 1:1000). The nuclei observed in blue, DAPI (sigma; 1:1000). (C) The cell mass was negative for lung progenitor cells (CCSP+/ Pro SpC+). The center of nodule structure was full of nuclei of cells that were negative for lung progenitor cells. It roles out the hypothesis of carcinoma nodule. AECII cells in green stained with (anti-pro SP-C; Merck/ Millipore; Rabbit; 1:600) located at corners of alveoli walls and. The non classified cell aggregations in air sacs were DAPI positive (blue). The Club cells (in red) studied with anti CC10 (Santa cruz; Goat, 1:200) located exclusively inside of bronchiole lumen. (D) AECI and II cells were not forming the cell mass structures. AECI, (in red) forms alveoli walls and located at merge of cell masses, visualized by (anti podoplanin /T1alpha; DSHB- 8.1.1; Hamster, 1:20) and AECII in green (anti-Pro surfactant Protein C /pro SP-C; Merck/ Millipore; Rabbit; 1:600); nuclei in blue with DAPI(Sigma, 1:1000). (E) Proliferation of nodule cells investigated by Anti proliferation Marker, PCNA/PC10 (Santa cruz; mouse; 1:300).

Inflammatory cell accumulation masses were not proliferating; however, surrounding alveolar epithelium; specifically AECII (in green) identified at proliferative stage. Surfactant protein C producing cells (green cytoplasm) with PCNA/PC 10 positive (red nuclei) identified as positive cell types for proliferation. (F, G) Represents a P7 wild type looking sibling alveolar epithelium cell proliferation studied by anti-Pro surfactant Protein C /pro SP-C (Merck/Millipore; Rabbit; 1:600); PCNA/PC10 (Santa cruz; mouse; 1:300) and nuclei in blue with DAPI(Sigma, 1:1000). (H, I) lower magnification images from nodule structure, in which AECII specifically observed as positive for anti PCNA. The white arrows points toward AECII PCNA positive cells. Alveolar units are sound and undergone less proliferation at P7 age rather than collapsed air sacs with AECII hyperplasia.

History of F1(345739)

Primary screen number of tracheal basal cells (1:5 pups at P7) decreased significantly. This F2 female (Id#372125) back crossed again with F1 founder. The very severe nodule phenotype expressed in secondary phenotype and the hypoplasia of Basal cells haven't observed. According to its importance and lack of any significant change in tracheal basal cells this F2 carrier were tracked for nodule phenotype.

The lung nodule expressed in 1 from 9 pups. The number of basal cells didn't show significant decreased in comparison with wild type sibling. In fact, the sections from trachea prepared in serial section method and by observation of sections of proximal to dorsal of trachea, no significant change observed in number of basal cells. In addition, the blood glucose and lactate increased in this putant. The F2 carrier (372125) screened for the third time to validate its potential as a heterozygote for a mutation related with lung nodule. In third screen, one from 8 pups at P7 showed three cell mass and adenocarcinoma like structure in alveolar interstitium. These effected area located adjacent to bronchiole and alveoli units collapsed and filled with inflammatory cells. The summary of this founder screen presented in table 7. According to this result, the female (Id#372125) characterized as a carrier for this phenotype. Therefore, the female out bred with a C57BL/6J to produce F3 generation and identify heterozygote carriers by crossing back with F1 founder. In this regard 4 female and 7 male produced. To increase the pace of screen due to aging of F1 breeders, once F3 progenies reached 8 weeks old (2 months) 3 female back crossed with F1 male (Id#345739). Also, F3 males bred with F2 female (372125). For F3 females who couldn't cross with F1 breeder, the inter breed with F3 male sibling strategy applied.

Table 7: Summary of F1 (345739) screening

F1 male	F2 female (Fvb/Bic6)	Size	Mouse ENU-Recessive Screen Phenotypes							
			Glucose/ Lactate	Histology (H&E,IVG,AB)	IHC	Cartilage	Retina vessel	Other	Mutant	Status
345739	370180	6 P7	No measurement	Analyzed	G : ▲ 1<6	Analyzed	Analyzed		1	Killed
	370181	6 P7	G: ▲ (1<6)	Analyzed	Analyzed	Small element 1<6 Defect cartilag e rings 2<6	Analyzed		1	No phenotype recovery in 2 nd screen killed
	370182	7 P7	G: ▲ (1<3)	Analyzed	Analyzed	Analyzed	Analyzed		0	Killed
	372125	5 P7	No measurement	Analyzed	Tracheal B: ▼ 1<5	Analyzed	1 eye haven't formed		1	Out crossed X C57Bl/6J : 9 female and 11 Male Phenotype recovered by F3 inter breed The F3x F1 male and F3x F2 female Phenotype haven't recovered.
		9 P7	G: ▲ L: ▲ (1<9) (1<9)	Lung nodule	Tracheal B: ▼ 1<9 SMA ▲	Analyzed	Analyzed	proximal Left lobe occupied by nodule	1	
		8 P7	Not measured	Lung nodule Cell accumulation& cell mass	Fibrosis SMA ▲	Analyzed	Analyzed		1	

▲: Increase, ▼Decrease; (E: extended vessel; H: hemorrhage; M: migration; T:thin vessel; G: goblet cells, alpha smooth muscle: SMA
C: Ciliated cells, M: mucin , Fib: Fibroblasts, A: Alveoli, RBC: Red Blood Cells

Table 7. From 4 different F2 females, one (ID#372125) showed the lung nodule in pups of a back cross with F1 heterozygote. The F3 generations produced for future analysis.

By this strategy, the nodule phenotype observed in pups from an interbreed. Surprisingly, other F3 siblings haven't shown any significant lung epithelium phenotype by F1xF3 interbreed strategy. According to mendelian law if a phenotype segregation is recessive, therefore by out breeding a F2 heterozygote carrier with a wild type homozygote, $\frac{1}{2}$ of F3 progenies should carry the mutation related with the phenotype. In this case from 20 progenies 10 either female or male progenies should be heterozygote. In the best case scenario, it was expecting to discover a phenotype with recessive segregation in F4 pups by back crossing F3 animals with F1 founder and F2 carrier. Then by inter breeding two F3 identified sibling carriers, pups will screen and tail samples from putative mutants will collect for whole exome sequencing.

According to this project protocol, two putative mutant and two wild type sibling's DNA samples will prepare for exome sequencing. However, by this strategy in this family the nodule phenotype expressed only by interbreeding of two specific F3 siblings and didn't recovered by

F1x F3 cross strategy. Tables 8-1 and 2 summarized identification of F3 female carriers. Id#487302 interbred with F3 siblings since F1 was in cross with other F3 females. Offsprings of 487302 and 487306; from 9 pups in P7, 1 showed the lung nodule and cell accumulation phenotype.

In regard with high rate of P7 litters death and losing pups, the screening stage changed from P7 to P0 once the breeders start aging. Thus, in this family once F1 founder used for breeding with F3 the P0 litters collected and analyzed. Although, in the primary screen the phenotype manifested in P7 stage, hypothetically if the phenotype is penetrant and significant in P0 pups also should manifest and would isolate. However, P0 animals haven't express any phenotype similar with lung nodule or strong cell mass/ accumulation.

As is clearly summarized in table 8-1 and 8-2, the nodule phenotype only rediscovered in P7 pups and only from an interbreeding F3 (487302 X 487306). By this data it can conclude that the phenotype exclusively express in P7 stage.

Giving mendelian law, if F1 and F3 are heterozygotes, from 8 pups in P7; 2 should be putative mutant and express the phenotype. Such phenomenon haven't seen and unfortunately due to death of F1 breeder, the F3 (487302) couldn't back cross with F1 for this investigation.

According to my hypothesis, if F1 (345739) and F2 (372125) are heterozygotes, from each F1 and F3 cross $\frac{1}{4}$ of pups should show the phenotype in recessive segregation. To clarify if my experimental data (number of putative mutants in P7 stage) do fit with my expectations according to mendelian law, a critical value as a probability value $p = 0.05$ used. To compare observed data with data that I was expecting the Chi-square used. To calculate Chi-square in this case; the differences between observed putative mutants and expected putants measured and powered to 2 and divided to expected number of putants. The Chi square was equal to 1. Given to commonly used P value: 0.05 ; if $p > 0.05$. Thus, I concluded that my hypothesis is true regarding heterozygosity of this F3.

In this case the Chi square is 1 and indeed it is greater than P value. Therefore, the hypothesized and screening strategy for F3 (487302) and F1, F2 founders cannot be rejected.

$$\text{Chi-square} = \sum \frac{(o-e)^2}{e} \quad \text{O= Observed} \quad \text{E= Expected}$$

Thus, to have the conclusion regarding this F3 female, more screening need to be done to have greater study population at P7. In the other word; as sample size increases, the average deviation from the expected fraction or ratio should decrease.

Thus, a larger sample size reduces the impact of chance deviation on the final outcome.

Table 8-1: Summary of female F3 progenies screening

F1 male (DOB)	F2 female (DOB)	F3 females (DOB)	Size/stage (DOB)	F3 Female animals screening to identify carriers from F1 #345739				
				Iding strategy	Phenotype	Mutant	Carrier	Status
345739 (15.06.13)	372125 (09.09.2013)	487295 (04.10.14)	5/P0 (24.12.14)	X F1	-	0	Neg	
			7/P7 (4.02.15)	X 458019	Weak cell mass	1	Carrier Different phenotype	
			7/P7 (25.03.15)	X F1	-	0	Neg	
		487296 (04.10.14)	5/P7 (12.12.14)	X F1	-	0	Carrier Different phenotype	
			7/P0 (31.01.15)	X F1	Weak cell mass	1		
			6/P0 (10.12.14)	X 458022				
		487297 (04.10.14)	10/P8 (06.02.15)	X F1	-	0	Neg	
			8/P0 (12.12.14)	X 458023	-	0	Neg	
		487299 (04.10.14)	4/P0 (12.12.14)	X 458024	-	0	Neg	
			8/P7 (08.02.15)	X F1	-	0	Neg	
		487300 (04.10.14)	8/P0 (11.01.15)	Inx 458025	-	0	Neg	Eaten pups Dead mother after delivery
			Pups eaten (12.03.15)	Inx 487305		0	Neg	
		487301 (04.10.14)	8/P0 (12.12.14)	x 458026	-	0	Neg	
			8/P7 (02.02.15)	X 487304	Thickened Alveolar, inflammatory cells	2	Carrier	
			10/P0 (12.03.15)	X F1	-	0	Neg	
			Dead (17.11.15)	X 487306	-	-		
		487302 (04.10.14)	7/P0 (15.12.14)	X 487304	-	0	Neg	Inter breed Carrier found
			9/P7 (26.01.15)	X 487306	Lung nodule Cell accumulation & cell mass	1	Carrier	
			7/P0 (12.03.15)	X F1	-	0	Neg	Crossed back with F1 for P7 but pregnancy was not productive
								Out X to have F4 –to keep line
			8/P7 (30.04.15)	X F1	Nodule negative weak cell mass	2	Weak positive	
			9/P7 (01.06.15)	X 487306	Eaten pups	0	Eaten pups	Eaten pups P7 screening not successful
			10/P0 (04.08.15)	X 487306	No significant cell mass and lung nodule	0	Neg	
			Eaten (21.11.15)	X 487306	Eaten at P4			
		487303 (04.10.14)	10/P0 (10.12.14)	X 487305	-	0	Neg	
			5/P0 (6.02.15)					
			7/P7 (1.04.15)	X F1	-	0	Neg	

Table 8-1. From the heterozygote F2 females (ID#372125), 9 F3 female produced by a out cross with wild type male. The F3 heterozygotes through a back cross with F1 heterozygote identified.

Table 8-2: Summary of male F3 progenies screening

F1 male (DOB)	F2 Female (DOB)	F3 Males (DOB)	Size/stage (DOB)	F3 male animals screening to identify carriers from F1 #345739				
				Iding strategy	Phenotype	Mutant	Carrier	Status
345739 (15.06.13)	372125 (09.09.13)	458019 (10.07.14)	7/P7 (28.01.15)	x487295	Weak cell mass	1	Carrier Different phenotype	
		458020 (10.07.14)	5/P0 (17.02.15)	X F2	-	0	NEG	
		458021 (10.07.14)	7/P7 (31.01.15)	x 487296	-	0	Neg	XF2 female Not pregnancy
		458022 (10.07.14)	6/P0 (10.12.14)	x 487297	-	0	Neg	
			10/P8 (06.02.15)	X F2	-	0	Neg	
		458023 (10.07.14)	8/P0 (12.12.14)	x 487297	-	0	Neg	F2 female Not pregnancy
		458024 (10.07.14)	5/P0 (13.12.14)	x 487299	-	0	Neg	F2 female Not pregnancy
		458025 (10.07.14)	8/P0 (11.01.15)	x 487300	-	0	Neg	
			5/P7 (17.02.15)	X F2	-	0	Neg	
		458026 (10.07.14)	8/P0 (12.12.14)	X 487301	-		Neg	
		487304 (04.10.14)	7/P0 (15.12.14)	X 487302	-	0	Carrier Different phenotype	
			8/P7 (02.02.15)	X 487301	Thickened Alveolar, Inflammatory cells	2		
		487305 (04.10.14)	10/P0 (10.12.14)	X 487303	-		Neg	
			05/P7 (60.02.15)	X 487303	-		Neg	
		487306 (04.10.14)	9/P7 (26.01.15)	X 487302	Lung nodule Cell accumulation& cell mass	1	Carrier	Sent Back cross for F2 Np 19.03-15.04
			9/P7 (01.06.15)	X 487302	Eaten pups	0	Eaten pups	Eaten pups P7 screening not successful
			10/P0 (04.08.15)	X 487302	No significant cell mass and lung nodule	0	Neg	X WT57BL/6J To save the line
			Eaten (21.11.15)	X 487302	Eaten at P4			X WT57BL/6J To save the line To be done

Table 8-2. From the heterozygote F2 females (ID#372125), 11 F3 male produced by a out cross with wild type male. The F3 (487306) progenies showed the lung nodule phenotype as a out come of an interbreeding strategy.

4.3.2. Abnormal AECI distribution and interstitial inflammatory cell mass and sub cutaneous hemorrhage

The primary and secondary screen showed disorganized alveolar epithelium as well abnormal distribution of AECI and AECII. The F2 carrier out crossed to produce F3 animals. The

F1 founder were crossed with 3 F3 female and meanwhile 1 more F3 female were inter cross with a F3 male sibling to identify. From 4 F3 female, one identified as a potential carrier. From F3x F3 cross these animals identified as heterozygote Figure 28. One from 8 pups showed very severe disorganized lung epithelium as well as inflammatory cells accumulation in air sacs and AECI and II morphological change in alveolar sacs. Then the F3 female carrier (Id#451303) crossed again F1 male. As a result, 4 pups produced and analyzed in P0. Non of the P0 pups were positive for a severe cell accumulation in alveoli. However; one from 4 showed a weak white blood cells infiltration into the epithelium.

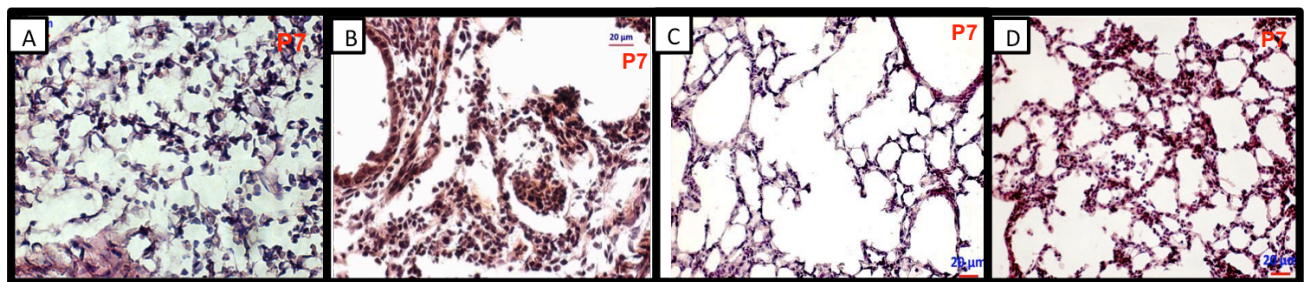


Figure 29. Histopathology of P7 putative mutant with disorganized alveolar epithelium and interstitial immune cells cell mass. (A) The primary screen showed collapsed alveoli units and in filtered white blood cells. (B) The screening of F3 female and F1 male, shows significant immune cells mass in alveoli. (C) The interbreeding F3 female carrier and male carrier showed very weak immune cells accumulation in lung. (1:10). (E) Same F3 partners screened for second time, from 11 pups no pups were positive for alveolar interstitium phenotype. The lung lobes pre fixed in 4% PFA; 8μm cryosections and stained with H&E.

Through screening of F3 females of this F2 carrier (Id#370233), all F3 females and 4 F3 male screened. The primary phenotype haven't recovered by F1 or F2 cross with F3 animals. The alveolar interstitium was void of significant inflammatory cell mass. In Figure 28, primary phenotype and summary of observed lung phenotypes in secondary and F3 interbreeds presented.

The sub cranial hemorrhage in P0 pups and disrupted pulmonary vessels observed in interbreeding of F3 animals (Figure 29. A-C). The interbreeding with sub cranial hemorrhage and disrupted vessels observed in progenies of a particular F3 male; Id#(451305). Therefore, we concluded that the F3 male (451305) is definitely heterozygote for a mutation that probably express in dominant pattern. This male animal under gone sperm freezing for future studies.

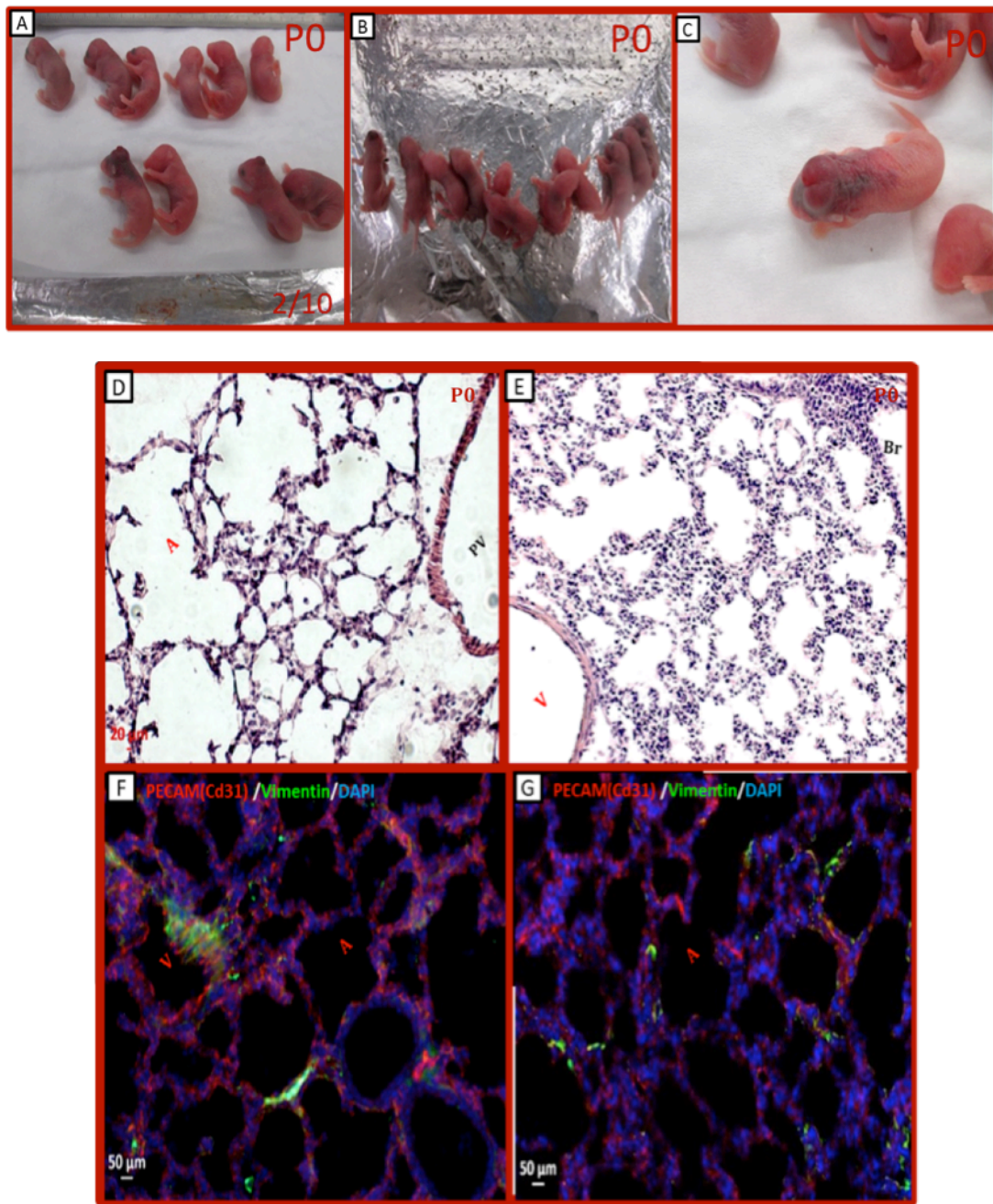


Figure 30. The sub cranial hydrocephaly phenotype (A,B,C). The histological analysis of lung lobes from a pup with normal head and a pup with under cutaneous hydrocephaly (D,E). No significant change observed in lung vessels. The immune histochemical analysis also confirm the healthy lung vasculatures PECAM/ CD31 (DSHB-2H8; Hamster; 1:1) antibody (in red) and fibroblast visualized (in green) by Vimentin (DSHB-AMF-17b; chicken; 1:30) in pups without and with sub cutaneous hemorrhage (F,G). Abbreviations: A: alveoli, Br: Bronchi, BrI: Bronchiole, PV: Pulmonary vessel, V:Vessel,

The summary of detail screening of F3 female and males of F2 (370233) illustrated at table 9. From interbreed of F3 female (451301) and (451303) with F3 (451305) no vascular defects observed in alveolar epithelium. Presumably sub cranial hemorrhage could be the result of vascular defects; however, the vasculature of the mutants appeared to initiate normally. histological analysis (Figure 29 has investigated it in D, E) and by staining for the PECAM-1 (CD31 antigen). This result presented in (Figure 29. F, G).

Table 9. Summery of characterizing F3 carriers

F1 male	F2 female	F3 mice	Size/stage (DOB)	Phenotypes of F1# 345742				
				Iding strategy	Phenotype	Total pups screened	Mutant for primary phenotype	Carrier for primary phenotype
345742	370233	Female	4/P0 (6.09.14)	XF1	-	10# (F1x F3)	0	Negative
		451300	6/P0 (10.11.14)	X F3(451305)		6# (F3x F3)		
			6/P0 (21.02.15)	X F1				
		451301	4/P0 (5.09.14)	XF1	-	6# (F1x F3)	0	Negative
			2/P0 (13.12.14)					
			10/P0 (23.01.15)	X F3(451305)	Sub cranial hemorrhage 2/10	10#(F3xF3)	0	Sub cranial hemorrhage positive
			5/P0 (3.03.15)	XF1	-	10#(F1xF3)	0	Negative
			5/P0 (6.04.15)					
		451302	6/P0 (25.09.14)	X F3(451304)	-	6#(F3x F3)	0	Negative
			4/P0 (29.10.14)	X F3(451305)	-	4#(F3x F3)		
			8/P0 (29.01.15)	X F1	-	14#(F1x F3)	0	Negative
			6/P0 (21.04.15)					
		451303	8/P7 (27.09.14)	X F3(451305)	Infiltration of inflammatory cells in interstitium	19#(F3x F3)	1	Positive
			11/P0 (24.12.14)		Sub cranial hemorrhage 2/11		0	Sub cranial hemorrhage positive
			4/P0 (12.01.15)	X F1	Infiltration of inflammatory cells in interstitium	4#(F1x F3)	1	Weak positive
		Male	6/P0 (25.09.14)	X F3(451304)	-	6#(F3x F3)	0	Negative
		451304						
		451305	8/P7 (27.09.14)	X F3(451303)	Infiltration of inflammatory cells in interstitium	19#(F3x F3)	1	Positive
			11/P0 (24.12.14)		Sub cranial hemorrhage 2/11			Sub cranial hemorrhage positive
			4/P0 (29.10.14)	X F3(451302)	-	4#(F3xF3)	0	Negative
			6/P0 (10.11.14)	X F3(451300)	-	6#(F3xF3)	0	Negative
			2/P0 (09.01.15)	X F2	-	2#(F2xF3)	0	Negative
			10/P0 (23.01.15)	X F3(451301)	Sub cranial hemorrhage 2/10	10#(F3xF3)	0	Negative
		451307	3+2/P0 (12.11.14)	X F2	-	10#(F3xF3)	0	Negative
			5/P0 (04.01.15)					
		451308		X F2	-		0	Not productive pregnancy

Table 9. From 4 F3 female and 4 F3 male; 1 male (Id# 451305) and 1 females (Id# 451303) showed the weak infiltration of inflammatory cells and thickening of interstitium. A new phenotype observed among pups from inter breeding F3 (Id# 451305) and (Id#451301 and Id# 451303). The primary phenotype hasn't observed in significantly. The F3 male animal (Id#451305) identified as a heterozygote for a sub cranial hemorrhage and used for sperm freezing.

4.3.3. Leaking vessel phenotype

In most reported cases, leaking lung vessels reported either as a complication of heart muscle failure or in immune system and inflammatory cells response in bacterial or viral pulmonary infections. These immune cells migrate from blood into the infected tissue in order to release a cocktail of pro-inflammatory proteins. Through this inflammatory response, the blood vessel barrier becomes “leaky.” Once the infection resolves, the integrity of the blood vessel barrier will recover. In fact, something that make. The importance of leakiness is in severe pneumonia cases, leaky vessels result in the Acute Respiratory Distress Syndrome (ARDS). The mortality rate of ARDS is yearly up to 40%. The ARDS with massive leakiness in lung vessels leads to the accumulation of fluids which covers the cells and disrupt exchanging of oxygen and carbon dioxide. Patients usually require mechanical ventilators to force oxygen into the lungs in order to survive. Moreover, Ebola patients the leakiness is also often cause severe blood pressure drops and shock.

If the heart muscle cannot pump effectively, the back-up of blood returning from the lungs to the heart. Therefore, pressure within the blood vessels of the lung increased and resulting in excess fluid leaking from the blood vessels into lung tissue. It can produce the pulmonary edema and indeed it is a common complication of **atherosclerotic (coronary artery) disease**.

This phenotype detected once in P7 pups in recessive segregation. One from 11 pups showed few leaky vessels and infiltration of blood cells into the alveolar epithelium. However, this phenotype haven't recovered in secondary screen of F1 and F2 female. In Figure 30 the manifestation of this phenotype presented.

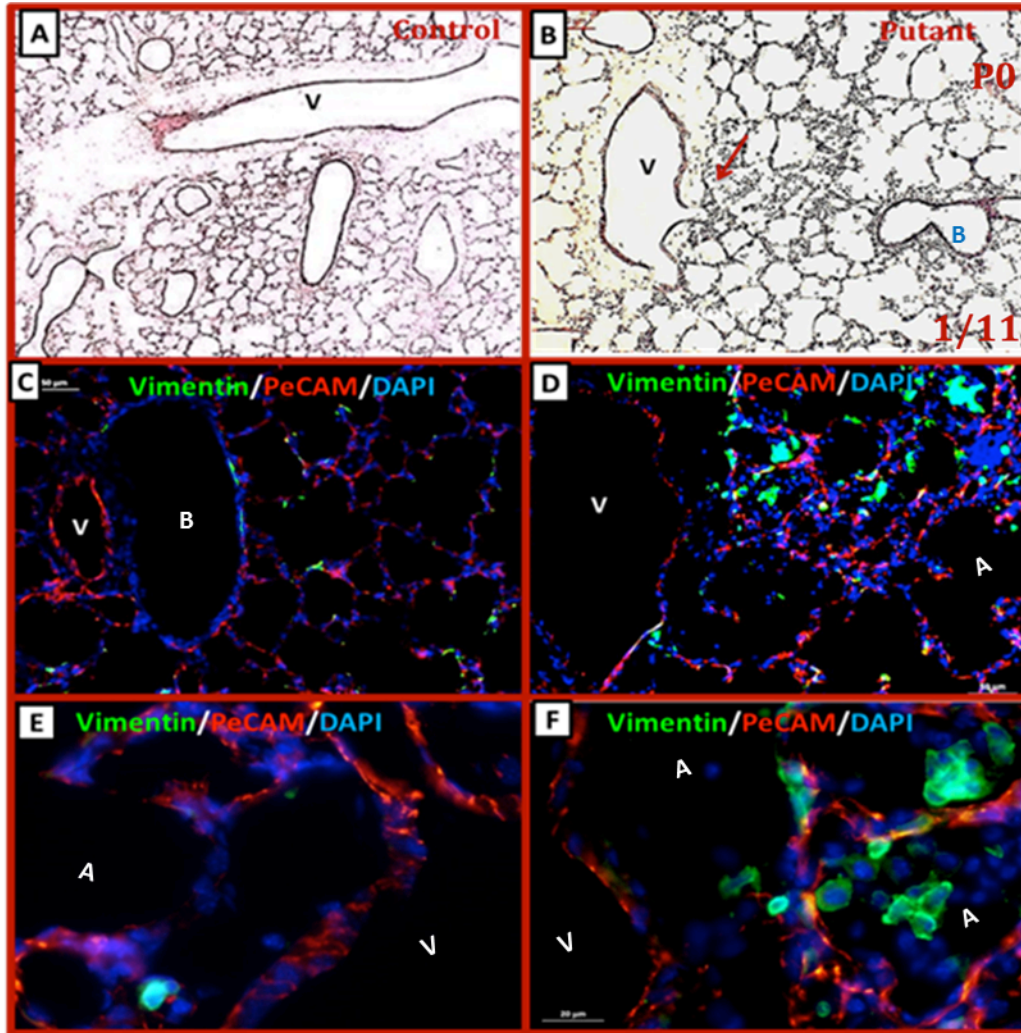


Figure 31. Histological and Immunohistological analysis of ruptured pulmonary vessel. (A,B) H&E staining of WT sibling and a putant. The pulmonary vessel that ruptured and white blood cells infiltrated into alveolar interstitium. The red arrow pointed to the ruptured vessel. (C-F) Images from WT sibling with healthy vessels and putant that inflammatory cells infiltrated into alveoli units. The pulmonary vessels structure studied by PECAM/CD31 (DSHB-2H8; Hamster; 1:1) antibody (in red) and fibroblast visualized by Vimentin (DSHB-AMF-17b; chicken; 1:30). Abbreviations: PA: Pulmonary artery, PV: pulmonary Vessel, V: Vessel

4.3.4. Tracheal Goblet cells hyperplasia and accumulation of mucus in distal airways

Given to important role of Goblet cells in formation of various respiratory disease, by observing changes in number of Goblet cells and abnormal secretion of mucus in alveolar epithelium; the potential carrier chose to rescreen by backcrossing F1x F2 discovered female. Irritation of the respiratory system causes both inflammation of the air passages and a notable increase in mucus secretion. Mucous cell metaplasia; goblet cells, induced in response to harmful

insults and provides front line protection to clear the airway of toxic substances and cellular debris. In chronic airway diseases mucous metaplasia persists and results in airway obstruction mortality. Mucus hypersecretion involves increased expression of mucin genes, and increased mucin production. The most well known and lethal respiratory disease related with hyperplasia of mucin secreting Goblet cells and deposition of mucus in alveolar epithelium is Cystic Fibrosis (CF). The mucus hyper production typifies CF and many evidences reported regarding an indirect connection between CFTR expression and mucin it is related the lack of CFTR expression in most mucin-secreting (goblet, mucous) cells (Kreda, Davis, & Rose, 2012).

In addition, in neonatal lung injuries and alveolar development arrest is often accompanied by goblet cell hyperplasia. Genes that regulate alveolarization and inflammation are likely to contribute to susceptibility to neonatal lung injury (Lan et al., 2009). Although, this phenotype looked very significant, it didn't recovered in secondary screen.

The immunohistological analysis of this phenotype presented in Figure31.

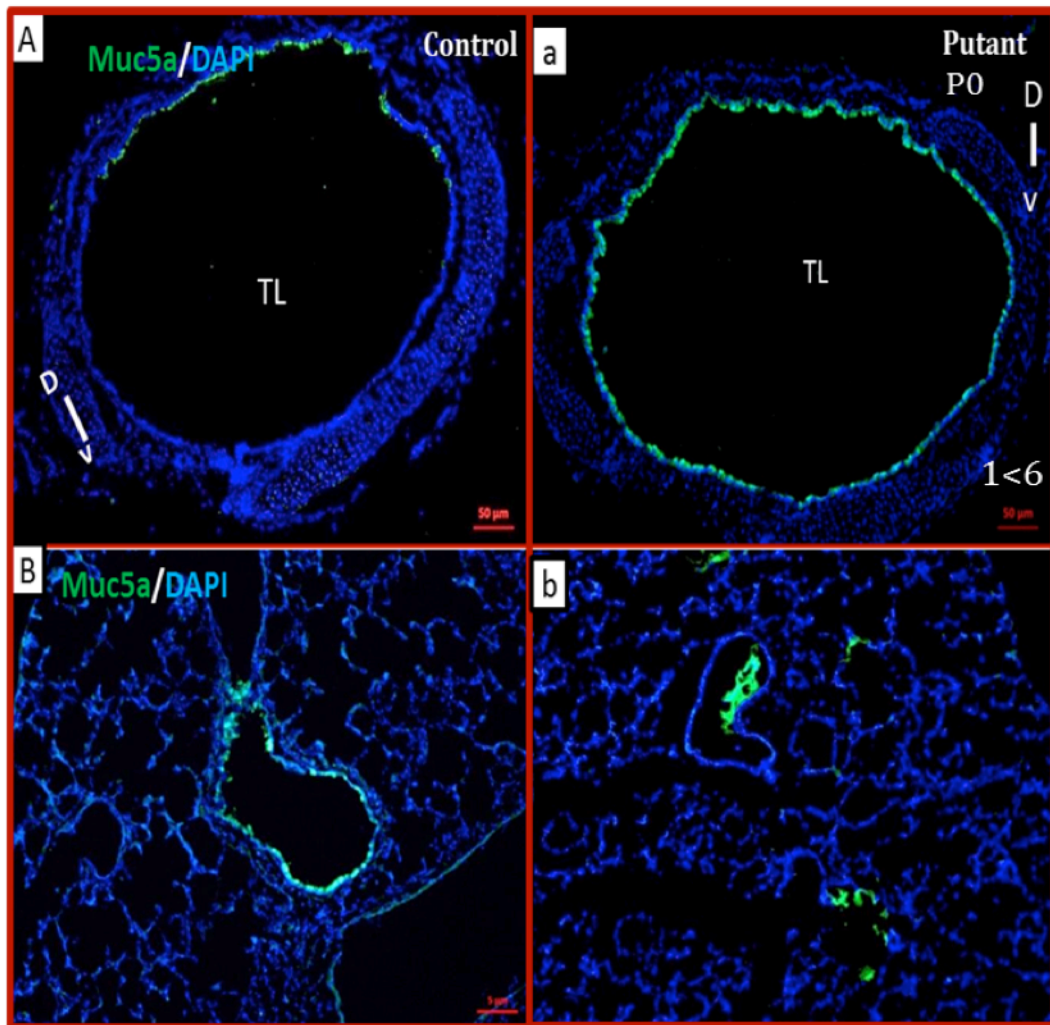


Figure 32. Immunohistological analysis of trachea and left lobe of potential putative mutant (A,a) WT sibling and a putant trachea sections. From 6 pups, one has shown mucin accumulation in dorsal bronchioles. 4 slide from different layers of lung and trachea has check. Goblet cells in green (B,b) Images from WT sibling alveolar epithelium and distal airways goblet cells distribution. In putant mucous excrete into bronchiole and alveoli epithelium. For goblet cells and mucin molecules Mucin 5AC(45M1) (abcam;mouse, 1:3000) and DAPI(Sigma, 1:1000) for nuclei used. Abbreviations: TL: Trachea lumen

Thrachea and left lobe of potential putative mutant sectioned and studied from proximal to distal. By observation of mucin depletion in bronchiole and increase of goblet cells, 4 different section from different layers of tissue investigated regarding the number of goblet cells and distribution of depleted of mucin particles. From 6 pups, one has shown mucin accumulation in

distal bronchioles. For goblet cells and mucin molecules Mucin 5AC(45M1) (abcam;mouse, 1:3000) and DAPI(Sigma, 1:1000) for nuclei used.

4.3.5. Alveolar collapse, Neonatal respiratory distress syndrome (NRDS)

Other non recovered phenotype in F3 generation that was also significant is NRDS. The **Neonatal respiratory distress syndrome (NRDS)** is when lungs aren't fully developed and surfactant in the lungs is not sufficient. This syndrome mostly occur in premature infants in human cases. Therefore the lungs cannot be inflated very well and air sacs collapsed. Thus, babies with NRDS shows cyanosis, abnormal breathing and are light weighted. It also called hyaline membrane disease and it is correlating with structural and functional lung immaturity. Yearly only in the United States 24,000 infants born with this syndrome(Hermansen & Lorah, 2007). Moreover, lung collapse due to surfactant protein B dysfunction and reduction of the superficial tension in alveoli reported (Yin et al., 2013).

In the primary screen 2 F2 female showed the phenotype. In a more sever case, from 10 pups 1 was dead and 2 pups were cyanotic. Their skin turned into blue color, the breathing pattern was abnormal, in the other word, they had shortness of breath, and stop in breathing (apnea). These putative mutants showed unusual breathing movements, for example drawing back of the chest muscles with breathing and shortness of breath. In addition, their weight was lighter than other siblings. The blood glucose and lactate measurement was higher than average of this litter. After observing these macroscopic analysis, the trachea and lung lobes collected for histological analysis. From 9 alive pups, 2 pups showed fairy smaller lung lobes, collapsed lungs and alveolar wall. Alveoli units are smaller and haven't formed septum structure. In addition with histological analysis on cryosection, the immunohistological analysis applied. In general a combination of 12 different antibodies used to investigate alveolar epithelial cells, pulmonary vessels and smooth muscle as well as secretory cells. To study the specialized alveolar epithelium cell types, AECI and AECII as well as goblet cells and other secretory cells, antibodies for their markers used. AECI marker: podoplanin /T1alpha, AECII marker: Pro surfactant Protein C as well as anti MUC5A for goblet cells, Club cells: CC10. The Figure 32 presented the macroscopic study and histological analysis of this phenotype.

In Figure 32 (F,G) the different distribution of AECl and AEcII cells in wild type and putant can appreciated. AEcII located at corners of alveoli units and alveoli are wide open. In contrast the putant with collapsed lung shows very compact alveoli structures.

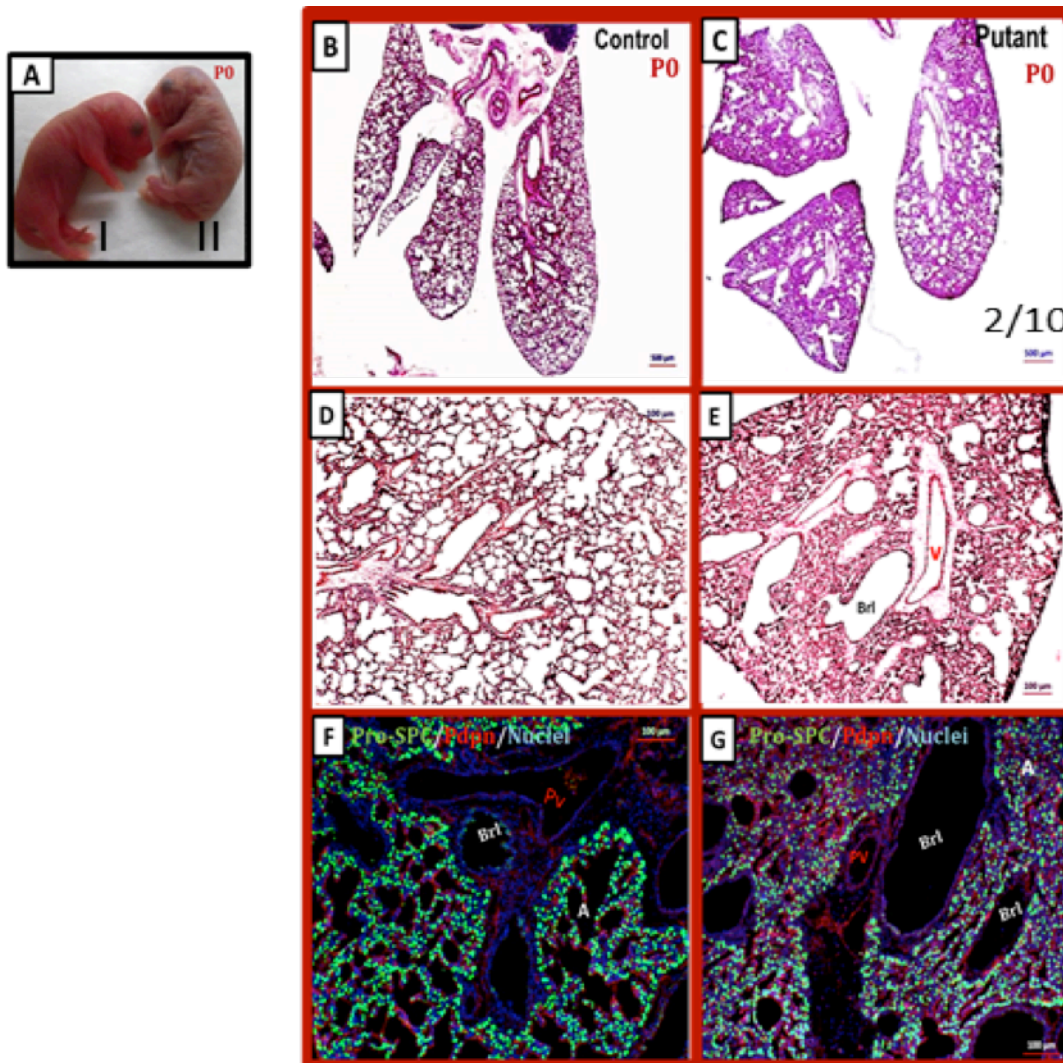


Figure 33. New born respiratory distress syndrome. From 10 pups (P0); 2 showed shortness of breath, draw back shoulder, apnea and cyanosis. Pup number I resemble a WT looking and pup number II is a putative mutant with cyanosis and defect breathing. (B-E) Histological analysis of the WT sibling and putant. Lung lobes collapse. H&E staining of prefixed cryosections. (C,E) Abnormally compact lungs with poorly developed alveoli units. (F;G) Distribution and morphology of AECl, AEcII in alveolar epithelium investigated. Immunohistological analysis of WT and putant whole lung. The alveoli units are smaller and haven't formed septum structure. Air sacs are smaller in comparison with wild type sibling. The number of AEcII looks higher due to smaller air sacs and collapsed alveolar epithelium. The AECl in red (anti podoplanin /T1alpha; DSHB- 8.1.1; Hamster, 1:20) and AEcII in green (anti-Pro surfactant Protein C /pro SP-C; Merck/ Millipore; Rabbit; 1:600); nuclei in blue (DAPI, 1:1000). Abbreviations: A: Alveoli; Bronchi: Br; Brl: Bronchiole, PV: pulmonary vessel

Chapter 5

Discussion and outlooks

We describe our recent work on ENU forward genetic screen mutagenesis in the mouse to uncover novel alleles and phenotypes in a particular tissue of interest, which was lung and trachea. We used a morphological and histological analysis of the P0 and P7 pups.

The aim of this project was to discover novel genes and genetic regulators of lung cell differentiation. Most identified phenotypes expressed inflammation, fibrosis and pathological changes in alveolar epithelium similar with interstitial lung disease.

In total 114 F1 founder screened in this work. Among various observed phenotypes in lung epithelium, one phenotype was recovered in F3 generation and samples collected for whole exome sequencing and future analysis. In four different families the inflammation; inflammatory cells infiltration in lung interstitium and weak fibrosis observed. In general the alteration of the alveolar epithelium, bronchial, pre-bronchial area obstruction by inflammatory cells mass, disorganized pulmonary microvasculatures structure similar with Idiopathic pulmonary fibrosis (IPF) detected. It has been confirmed by histological and immunohistological analysis that this phenotype is not PAP and definitely is inflammation and bronchiolitis.

The inflammation generally is a response against invasion of microorganisms, external toxins and inhaled allergens. The inflammation accompanied by increased mucus secretion to protect the mucosal surface of the airways (Peter J Barnes, 2000). Following of inflammatory reactions a repair process occurs in which damaged epithelial cells proliferates and airways structure changes (Hajnalka, 2005). In inflammation generally Mast cells, macrophages, dendritic cells, eosinophil, neutrophil and basophil granulocytes, T- and B-lymphocytes, and platelets involve although the precise role of each cell type is not yet certain.

The alveolar epithelial cells also maybe involve in initiation and formation of alveolar inflammation. It has been reported that granular pneumocytes, alveolar epithelial cells type II (AEC II) are responsible for epithelial reparation after injury and ion transport and are very active immunologically by contribution to lung defense by secreting antimicrobial factors.

Moreover, AEC II secrete cytokines and chemokines that are involved in activation and differentiation of immune cells. Also, AECII cells present antigens to specific T cells.

Another important cell type in lung defense is the pulmonary macrophage (PuM). In regard with Chuquimia et al, report AEC may play a role in conveying signals from the external to the internal compartment and modulate the activity of PuM. Interstitial pulmonary macrophages (PuM) have close contact with other immune cells in the lung interstitium and alveolar macrophages exist more in bronchioalveolar lavage (Chuquimia, Petursdottir, Periolo, & Fernández, 2013). They suggested that AEC-derived factors are fundamental in providing micro environmental signals and modify functional behavior of incoming and tissue-resident immune cells.

The possible mechanisms associated with phenotype

Previous research on pulmonary diseases by using animal models and human samples revealed reactivation of lung developmental programs and embryonic signaling pathways in initiation and formation of respiratory disease such as IPF and cancer, specially non small cell lung cancer (NSCLC). Indeed, we hypothesized that the ENU induced mutation presumably altered these developmental and signaling pathways. Therefore, in mutant animal we expect to observe phenotypes similar with lung pathological conditions. In this work by identifying inflammation phenotype, we hypothesize that the immune reaction and inflammatory responses pathway may be affected by ENU mutagenesis. In particular activation of macrophages and attracting other immune cells. As a result, white blood cells mobilized to alveolar epithelium and infiltrate into alveolar sacs. In histological analysis the cell mass accumulation in alveolar sacs and infiltrated immune cells observed (chapter4-Figure3,4,5). In addition, the bronchiolar lumen undergoes alterations (Chapter4-Figure6); by these observations we can conclude the role of immune cells as well as alveolar and bronchiolar epithelial cells in progression of this phenotype. The figure.1, clearly shows polymorphonuclear neutrophils and immune cells such as lymphocytes as well as alveolar macrophages contribution in formation of this phenotype.

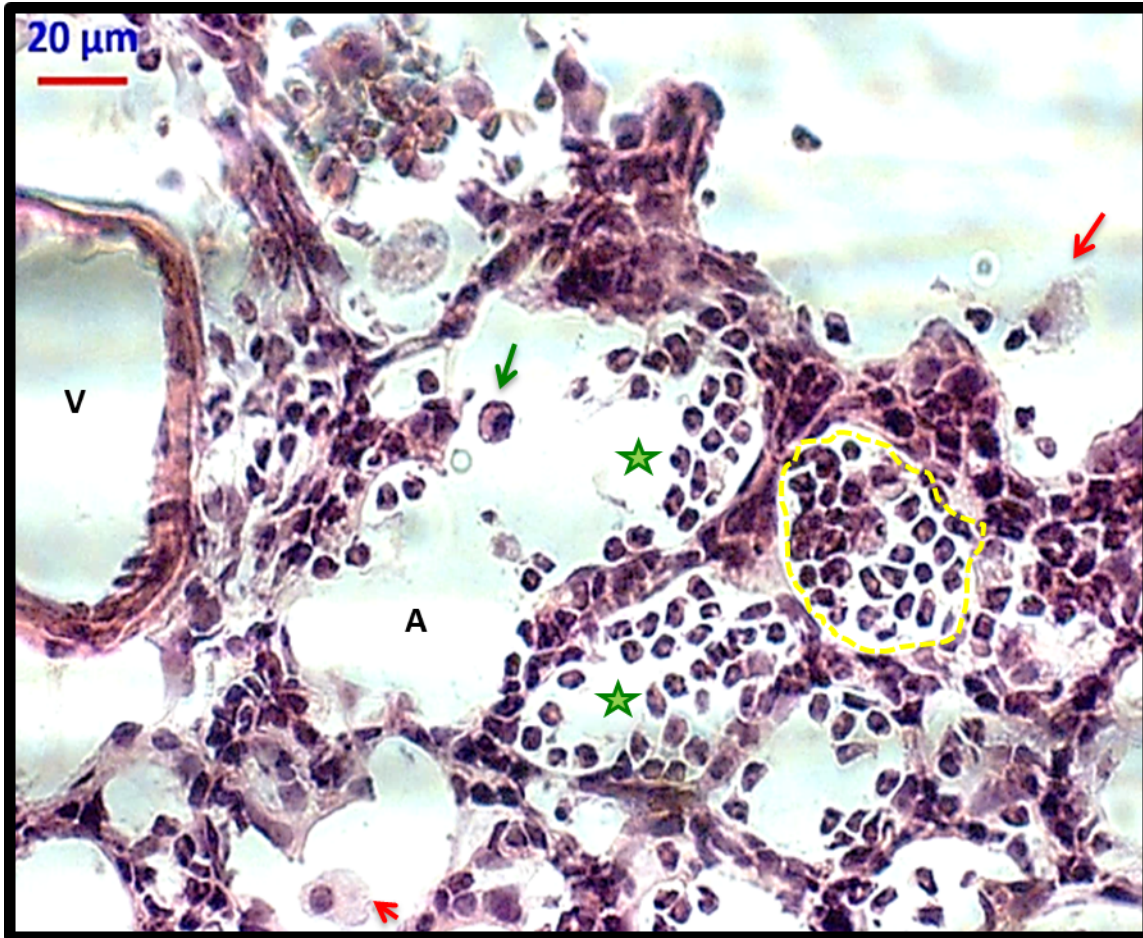


Figure 1. An affected alveoli epithelium. Red arrows pointed to pulmonary macrophages. The green stars adjacent with neutrophils. The green arrow pointed to a lymphocyte.

In addition, as is presented in Figure 1, and Chapter-4. Figure 7; 8 and 9; in formation and developing of this phenotype: inflammatory Vimentin positive cells characterized in alveolar cell mass. It has reported that Vimentin is marker for stromal and mesenchymal as well as quiescent fibroblasts and myofibroblasts (Goodpaster et al., 2008). In addition, myofibroblasts increased and smooth muscle hyperplasia in the alveolar epithelium and at bronchiole, peribronchiole and pre pulmonary vessels observed. In fact, these analysis rolled out **Pulmonary alveolar proteinosis (PAP)** phenotype, abnormal accumulation of surfactant occurs within the alveoli (chapter 4- Figure 8).

Thus, hyperplasia of myofibroblasts (fibrosis bio marker) and vimentin positive cells infiltration, lead us to characterize this phenotype as interstitial inflammation accompanied by

weak fibrosis. In addition, the identified phenotype is sharing pathological manifestation with Idiopathic Pulmonary Fibrosis (IPF). Regarding the IPF mechanism and associated signaling pathways; the reactivation of developmental programs, including the WNT signaling pathway, reported (Königshoff & Eickelberg, 2010)

Furthermore; given to previous studies; by secretion of high content of TGF β , CCL18, resistin-like secreted protein in inflammatory zone the alveolar interstitium undergo structural changes. In detail, the α v β 6 integrin also expressed in inflamed alveolar epithelial cells binds to latent TGF β and induces a conformational change in TGF β . Among these mediators TGF- β has recommended as a major factor in fibrosis.

In fact, TGF β is a multifunctional cytokine that involved in development, the immune system, matrix production, angiogenesis, and control of proliferation (Figure.2). Basically all cells express TGF- β and have TGF- β receptors. The activated TGF- β initiates a wide range of pro-fibrotic processes. In addition to its direct effects, TGF- β upregulates other pro-fibrotic molecules such as platelet-derived growth factor, ROS, and connective tissue growth factor (Dani S. Zander MD, 2008).

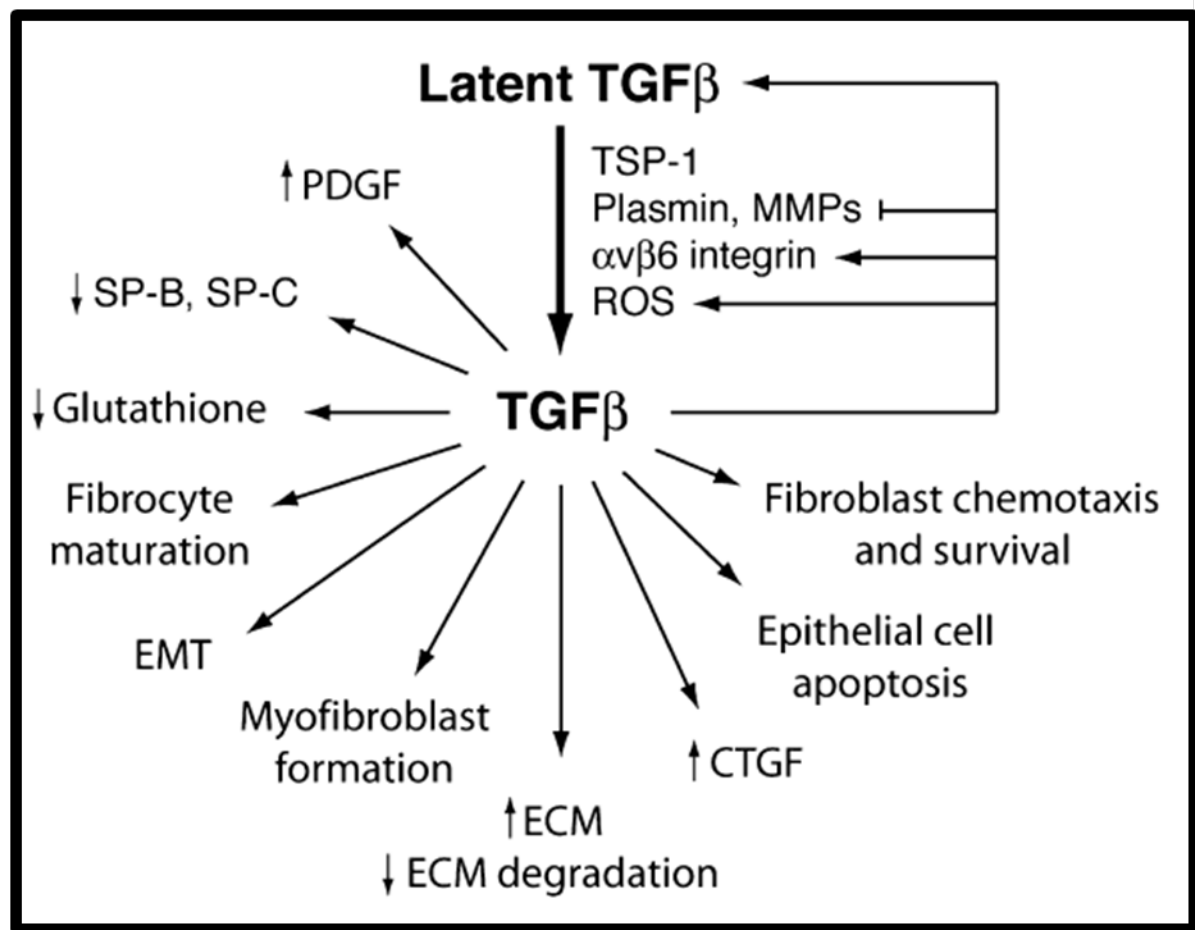


Figure 2. The transforming growth factor- β (TGF- β) plays a central role in lung fibrosis. TGF- β is activated by thrombospondin-1 (TSP-1), $\alpha\text{v}\beta 6$ integrin, proteases or reactive oxygen species (ROS). The TGF- β also regulates its own signaling by up-regulating two activation mechanisms (ROS and $\alpha\text{v}\beta 6$ integrin) (Dani S. Zander MD, 2008).

Macrophages derive from blood monocytes and produce pro-inflammatory ($\text{TNF-}\alpha$, IL-1 β , IL-6) and anti-inflammatory (interleukin 10 and 12; IL-10 and IL-12) cytokines. Macrophages also act as antigen-presenting cells and process allergens for presentation to T-lymphocytes (Peter J. Barnes, 2003).

Presumably, the infiltrated immune cells and altered alveolar structure, end in development of fibrosis foci as a secondary complication of this phenotype. Hypothetically if progenies of these lines study in older stages, more spread out and developed fibrosis foci and severe epithelial damage will observe. In other words, the inflammation, cell masses and chemokines perhaps contribute to EMT and form a fibrosis foci.

The *epithelial- mesenchymal transition* (EMT) is a process in that epithelial cells undergo a trans-differentiation to form fibroblasts and then myofibroblasts. In this processes epithelial cells lose their characteristic markers such as E-cadherin and zona occludens-1 and acquire mesenchymal markers such as fibroblast-specific protein-1 and α -SMA . Moreover, Kapanci et al, reported AEC II store TGF beta 1 and TNF alpha. These cytokines, besides their involvement in fibrogenesis, play an important role in the expression of alpha-SM actin by alveolar myofibroblasts (Kapanci, Desmouliere, Pache, Redard, & Gabbiani, 1995).

All in all, there is a close relationship between fibrocytes, alveolar epithelium, myofibroblasts and mechanism of fibrosis and pro inflammatory factors. The figure 3 summarized the available model on relationship and origin of myofibroblasts involve in idiopathic pulmonary fibrosis mechanism and its association with cytokines and growth factors.

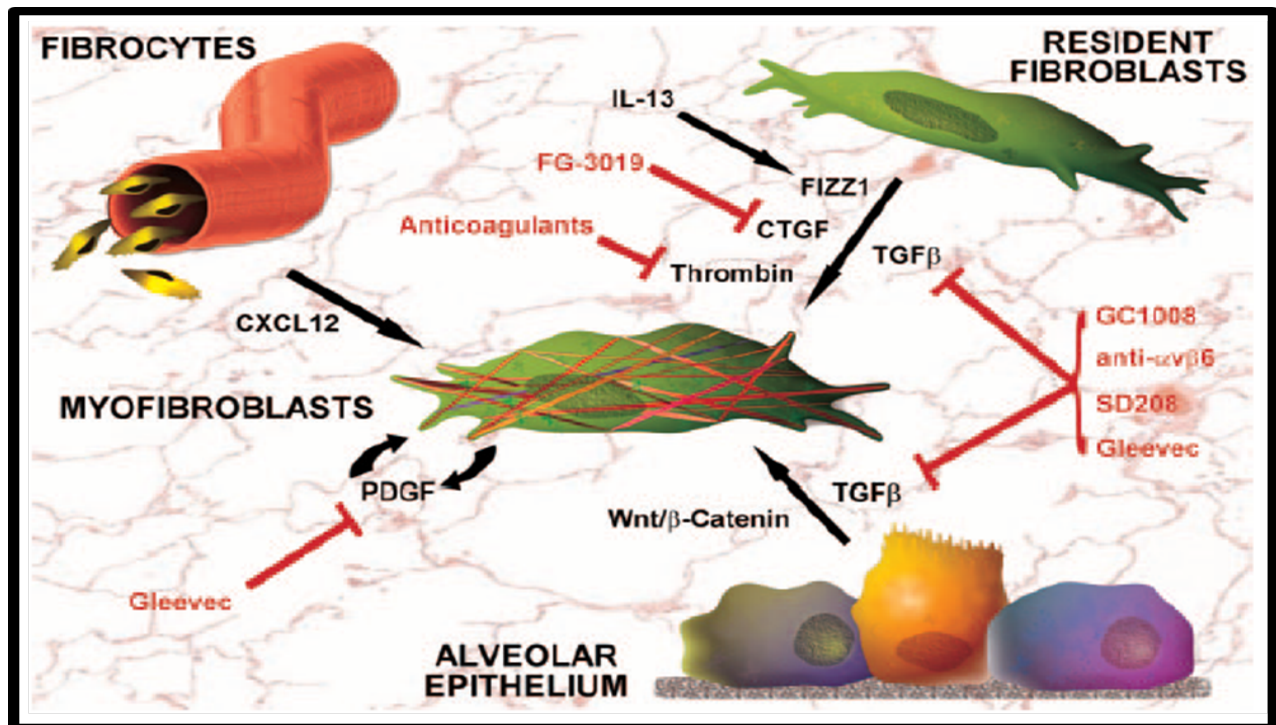


Figure 3. The Origins of myofibroblasts. Myofibroblasts are the key cell type in IPF and thought to arise from the three sources. (1) proliferation and differentiation of resident fibroblasts; (2) epithelial-mesenchymal transition; or (3) recruitment of circulating fibrocytes. Various cytokines, growth factors, and signaling pathways are able to mediate these events (black arrows). The potential therapeutic strategies (shown in red) are under development. The figure adopted from (Scotton & Chambers, 2007).

As is mentioned in above, alveolar macrophages and inflammatory cells would be main players of initiation inflammatory foci.

The initial step in activation of macrophages and other immune cells is manage by **Toll-like receptors (TLRs)**. Toll-like receptors (TLRs), with their co-receptors such as MD2 and CD14, recognize pathogen molecules, and inflammatory cytokines, such as tumour necrosis factor (TNF), interleukin-1 β (IL-1 β) and interferon- γ , propagate inflammation.

Also, bronchial or alveolar epithelial cells interactions deliver inhibitory signals to alveolar macrophages through CD200 receptor (CD200R). The CD200 is on the respiratory epithelium and by recruiting of RAS GTPase-activating protein RASA2 (also known as RASGAP), the inflammatory pathways: extracellular signal-regulated kinase (ERK), p38 mitogen-activated protein kinase (MAPK) and JUN N-terminal kinase (JNK) will block. In contrast, increased expression of the negative regulators and inhibition of TLR signaling pathways, leads to suppression of alveolar macrophages (Hussell & Bell, 2014).

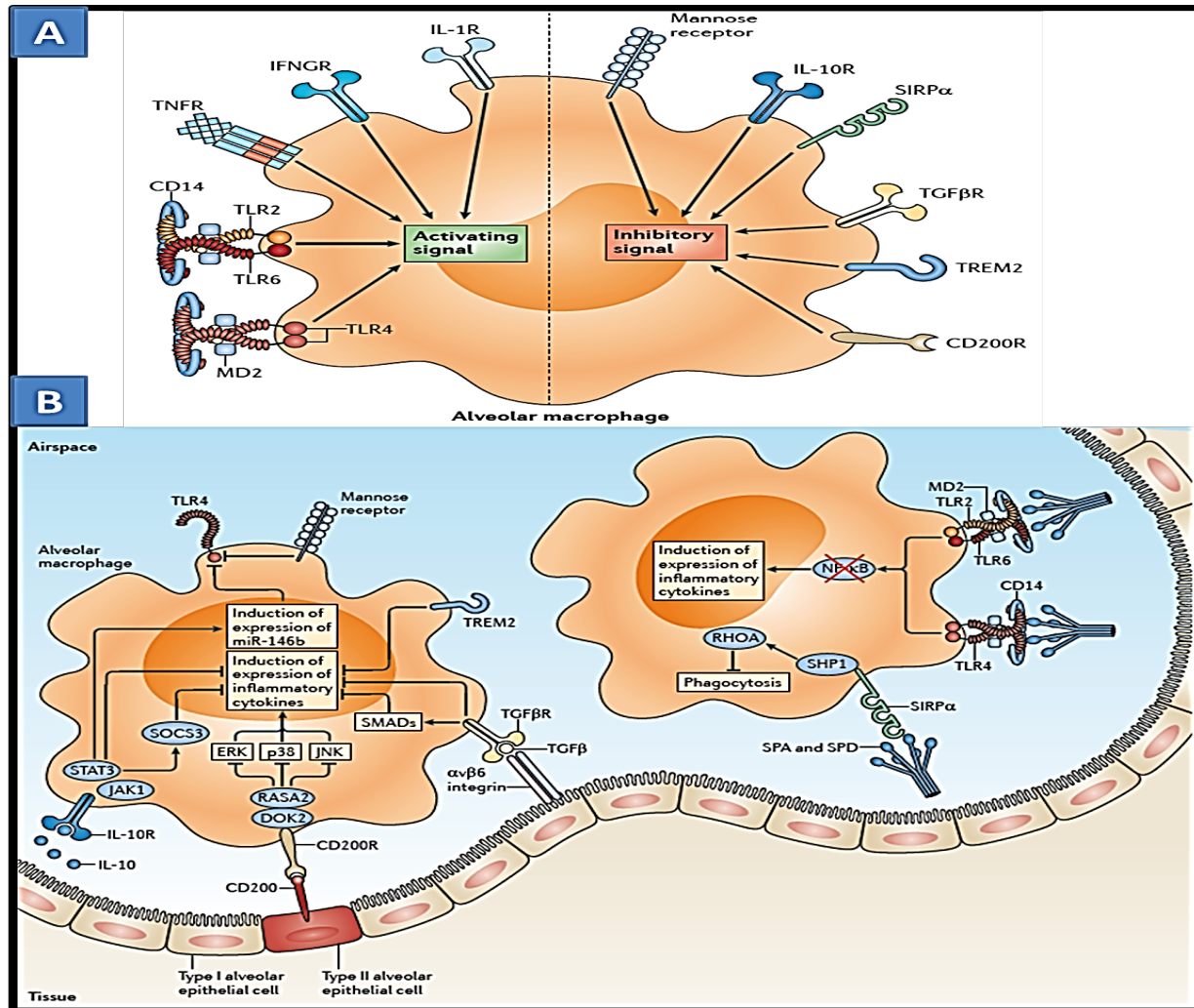


Figure 4. A. The balancing act of macrophage activation. B. Inhibitors of alveolar macrophage activation. The CD200 receptor (CD200R) interacts with CD200 on the respiratory epithelium, RAS GTPase-activating protein RASA2 (also known as RASGAP), which blocks the extracellular signal-regulated kinase (ERK), p38 mitogen-activated protein kinase (MAPK) and JUN N-terminal kinase (JNK) inflammatory pathways. Pulmonary surfactant-associated protein A (SPA) and SPD block TLR2 and TLR4 interactions with their respective ligands, as well as their interactions with the TLR co-receptors MD2 and CD14, which prevents the activation of nuclear factor- κ B (NF- κ B) and the initiation of the inflammatory response. Binding of surfactant proteins to signal-regulatory protein- α (SIRP α) recruits SH2 domain-containing protein tyrosine phosphatase 1 (SHP1) and activates RHOA, which inhibits phagocytosis. IL-10R, IL-10 receptor. Adopted from (Hussell & Bell, 2014)

Dendritic cells are specialized macrophage-like cells which able to induce a T-lymphocyte mediated immune response during the development of asthma. Other white blood cells that observed in infiltrated cell accumulation in alveolar sacs; are Eosinophil, neutrophils. The eosinophils are characteristic feature of allergic inflammation

Eosinophil recruitment involves adhesion of eosinophils to vascular endothelial cells, their migration into the submucosa and subsequent activation. Eosinophils also contribute to the structural changes and secretion (TGF- β). Neutrophils recruited in severe conditions of asthma into the airways.

A complex network of pro- and anti-inflammatory cytokines and chemokines play a major role in mediating, amplifying, and perpetuating inflammatory-induced lung injury (Goodman et al., 2003). It has been reported that many inflammatory cells (macrophages, mast cells, eosinophils and lymphocytes) and structural (epithelial cells, airway smooth muscle and endothelial cells) cells synthesizing and releasing these proteins (Hajnalika, 2005).

According to recent studies on mechanism of lung fibrosis and COPD, the main signaling pathway associated with activated macrophages, and presumably are main players of this phenotype is Wnt signaling.

It has been reported that WNT signaling not only has role in normal embryonic and adult lung development but also involve in pulmonary disease such as lung cancer and pulmonary fibrosis and pulmonary arterial hypertension. Also, it plays role in mesenchymal development.

Indeed, by microarray analysis studies for IPF disease on human and animal models specific gene expression characterized. Among them, genes associated with Wnt/ β -catenin pathway was found. In addition, up-regulation of developmental relevant genes included several members of transcription factor families such as forkhead box observed (Pardo et al., 2005), (Studer & Kaminski, 2007).

(For complete datasets see <http://www.dom.pitt.edu/pacem/Genomics/data.html>).

Also, an active tissue remodeling program, including extracellular matrix and a large number of myofibroblast/smooth muscle cell-associated and epithelial cell-related genes identified (Selman, Pardo, & Kaminski, 2008). Resident fibroblasts in lung respond signaling that leads to fibroblast-to myofibroblast differentiation by WNT signaling (Königshoff & Eickelberg, 2010). In addition, these data support a role of WNT signaling on profibrotic phenotypes of lung fibroblasts—in particular, via paracrine effects of epithelium derived WNT ligands.

In general, the canonical Wnt signaling pathway involves the binding of Wnt proteins (cysteine-rich secreted glycoproteins) to frizzled-cell surface receptors or low density lipoprotein co-receptors. In brief, by inhibition of glycogen synthase kinase-3 and the consequent hypophosphorylation of β -catenin; this cytoskeletal protein can then translocate to the nucleus, where its binding to the lymphoid enhancer-binding factor and converts them from transcriptional repressors to activators (Morrissey, 2003). Wnt proteins can also signal via protein kinase C (the Wnt/Ca²⁺ pathway) or c-Jun N-terminal kinase. It is known also as the planar cell polarity pathway.

In addition, in mononuclear cells including T-cells and surrounding resident tissue cells activation of Toll-like receptors by pathogens leads to activation of nuclear factor- κ B (NF- κ B) and upregulation of Wnt5a and cytokines (George, 2008). Therefore, increased levels of Wnt5a activate the noncanonical pathway via calcium/calmodulin dependent kinase II (CAMKII). Then, inflammatory cytokines including: IL-12, IL-6, IL-8, IL-1 β upregulate as well as macrophage inflammatory protein-1 β (MIP-1 β) either in (NFAT)-dependent or independent manner.

A group of possibilities can be discuss regarding in initiation, progression and failed resolution of inflammation in alveolar interstitium. More likely, by induction of inflammatory cues in alveolar epithelial cells; specially alveolar type 2 cells, alveolar macrophages activated and alveolar walls and epithelial cells damage as well as basement membrane injured. Then, profibrotic mediators (TNF α , TGF β) and cytokines/ growth factors released. Then, immune cells infiltrate into alveolar sacs. In second step, presumably by activation of Wnt signalling by Toll-like receptors and later nuclear factor- κ B (NF- κ B), inflammatory cytokines including IL-12, IL-6, IL-8, IL-1 β , and nuclear factor of activated T-cells (NFAT)-dependent release and may affect other mononuclear cells including T-cells and surrounding resident tissue cells.

In the third step, epithelial to mesenchymal transition program in response to Wnt signaling and TGF- β signaling occurs and EMT will develop the inflammation area. In addition, Dendritic cells and circulating fibrocytes or hematopoietic stem cells which are attracted inside the lungs following secretion of soluble factors and chemokines like CSCL12; from the injured epithelium; transdifferentiates into myofibroblasts while promoting fibrosis.

Conclusion

The goal of this large forward genetic screening project was discovering genes that contribute to lung epithelial cells differentiation or dedifferentiation that leads to respiratory system structural changes. Indeed, the aim of phenotyping mice in this work is to isolate phenotypes that mimicking most lethal human respiratory diseases pathology. Further, novel genes and genetic regulators will be identify by mapping and whole exome sequencing analysis on characterized carriers. Moreover, the animal model with discovered gene/genes would be design to characterize the detail mechanism of such disease. As a result, new drugs and therapies could develop for lung diseases which the only available treatment for its patients is lung transplantation with maximum 4.6 years survival.

It has been hypothesized ENU treatment of a C57BL/6J male mice, will induce point mutations in genome that manifest in lung organ and respiratory system by formation of pathological conditions induction of cell differentiation. The progenies of ENU mutagenized animals are homozygosed through a 2 generation breeding scheme, and F2 pups are screened. ENU is an alkylating agent and transfers its ethyl group to nucleophilic nitrogen or oxygen sites on each of the four deoxy ribonucleotides. The ENU induces random point mutations. Almost 85% of all nucleotide substitutions are either A-T to T-A transversions or A-T to G-C transitions (Acevedo-Arozena et al., 2008). It has been suggested that ENU mutagenizing produce roughly 32 loss-of-function mutations per genetic line.

Most identified human molecular mutations, function largely in hypomorphic manner or dominant and semi-dominant. ENU mutagenesis mechanism produces less polymorphism. Therefore, forward genetic is better approach to discover novel proteins genes which are relevant with human disease (Weber et al., 2000). Thus, ENU phenotypic driven screening approach lead scientist to generate novel mouse models of human disorders. In regard with the organ of interest in this screening, trachea and lung lobes isolated to study respiratory system development and cell differentiation, eyes to investigate the development of vasculatures, blood to evaluate glucose and lactate measurement was used as well.

Given to interest in isolation of phenotypes with recessive segregation. The breeding scheme established to produce heterozygote F2 generation from F1 heterozygote male animals. By a back crossing strategy, F2 female progenies produced and screened. To have the optimum

efficiency from each F1 heterozygote animal, minimum 4 daughters crossed and their progenies screened. In this regard the frequency of heterozygotes in F3 generation would be 25% of all F3 pups.

As mentioned in material and method chapter each F3 litter of animals studied macroscopic first and later by histological and immunohistological analysis. The blood's glucose and lactate measurement conducted to investigate the metabolic abnormalities for 40 litters. This part of screening canceled after observation of very high variation rate among pups due to feeding times by the mother. Although, the retina of 50 litters P7 analyzed, to investigate development of vasculatures. Due to lack of association between lung and retinal defect phenotypes, this part of screen also was canceled. Therefore, screening narrowed down to only isolation of phenotypes in lung and trachea that expressing most common respiratory diseases and pathological conditions. According to available data on initiation and mechanism of most common lung disease such as COPD and IPF, developmental pathways can be reactivated and induce lung disease. Hypothetically ENU treatment, mutagenize mouse genome in each allele linked to signaling pathways and proteins which play role in lung pathogenesis. Thus, by conducting the breeding scheme explained in material and methods chapter; one fourth of pups would express phenotypes similar with lung disease. From 114 F1 screened families; 11 different phenotypes observed. To isolate these phenotypes at least for each litter of animals 8 different antibody combination used.

The most frequent and penetrant phenotype in lung organ was inflammatory cells infiltration into the alveolar interstitium and prebronchiolar tissue; bronchiolitis, fibrosis and myofibroblasts hyperplasia. In addition, non-classified cell mass accompanied alveolar interstitium inflammation with mild fibrosis. In fact, the alveolar interstitium phenotype is most significant discovered and characterized phenotype of this work. From 11 different phenotypes the inflammation in alveolar interstitium chose to follow up. This phenotype identified in 4 different F1 families with semi dominant and recessive segregation. The samples from identified carriers have collected and F4 generation produced for further analysis. The common features of this phenotype among identified lines are accumulation of airway sacs with white blood cells and assembly of immune cells. Alveolar macrophages number increase in alveolar sacs. Polymorph nuclear white blood cells obstructed alveoli. The infiltration of inflammatory cells and production of ECM thickened the alveolar wall and secondary septum effected. Beside fibroblast deposition in inflammatory area; they have transdifferentiated into myofibroblasts and become activated

myofibroblasts. These cells play an important role in EMT process. Inflammatory cell mass interrupted normal gas exchange in lung and lung lobes start to collapse. Moreover, the pulmonary vasculatures undergone structural changes to compensate the defect O₂/CO₂ exchange between AECI and vessels. To investigate the identity of cells that involve in cell mass accumulation and differentiation of lung progenitor cells, AECII (Pro-SPC+) and Club cells (Scgb1a1+), the immunohistological analysis conducted. These cell masses haven't expressed any lung epithelial or bronchiolar markers. In addition, no evidence from depletion of surfactant protein C observed in blocked alveoli.

The detail of inflammation mechanisms in lung is unknown. However according to previous research on IPF and fibrosis models in lung and respiratory disease following mechanism is suggested.

In general abnormal recapitulation of developmental pathways and epigenetic changes involve with inflammatory cues. First alveolar epithelial cell microinjuries and apoptosis occur by injury like or inflammatory cues. Then, neighboring epithelial cells activated and inflammatory cells, mesenchymal cells recruit to the inflammation lesion. Moreover, alveolar macrophages and alveolar progenitor cells become activated.

The abnormal activated alveolar epithelial cells (AECs) produce inflammatory mediators. The resident mesenchymal cells proliferate and maybe transdifferentiate into myofibroblasts. In the next step, myofibroblasts secrete excessive amounts of extracellular matrix that scars and destroys alveoli walls and lung architecture (King Jr, Pardo, & Selman). In addition, alveolar macrophages through their interaction with AECII cells become activated and release TGF β and inflammatory mediators. Through Wnt and Shh signaling activation in alveolar macrophages, inflammatory cytokines such as IL1, IL6, IL8, and IL15, TNF α and intercellular adhesion molecule-1 (ICAM-1) (Di Stefano et al., 1994) would be released. The expression of ICAM in the epithelium recruits other leukocytes. In addition, IL8 secreted from the bronchial epithelium attracts neutrophils. Neutrophils and macrophages both contribute to the pathogenesis of inflammatory tissue. They reactivate oxygen metabolites and release proteinase.

Moreover, tissue matrix metalloproteinases (MMP-s) increased and induce tissue destruction. The MMP gene association with both pro-inflammatory cytokines and canonical Wnt signaling reported. The precise mechanism is not clear (Pongracz & Stockley, 2006). Therefore, detail of Wnt and Shh signaling pathway regulators during inflammation in lung epithelium yet to be clarify.

In parallel with epithelial cells and alveolar interstitial changes, pulmonary vasculatures undergo structural changes and remodeling as well as vascular smooth muscle hyperplasia.

All these processes results in expansion of inflammatory foci and development of the fibrosis. In the end fibroblastic foci secrete high amounts of extracellular matrix components that destroy the lung parenchyma. Thus, for future study on carrier animals the MRI technique can use to monitor the development of inflammation lesion.

This work results in discovery of a phenotype similar with human lung interstitial diseases. This phenotype is reproducible and causative factor is genetically heritable. The expression of this phenotype is recessive in three families and in another family is dominant or semi-dominant. By analysis of whole exome sequencing from identified carriers the causative gene/es and genetic regulators will be discover. This project facilitates designing drugs and developing new therapies for IPF and other interstitial lung disease.

Another aspect of this work suggests that disease and phenotypes induced with ENU mutagenesis may involve with more than one causative gene. In fact, some pups from characterized heterozygote F2 animals through the screening were phenodeviant and showed deviation from expected phenotypes. This observation gave rise to the idea of linked genes role in expression of such phenotypes. In the other words, the single gene disorder or simple Mendelian diseases is not realistic concept. Presumably a group of random point mutations induced a multiple genes disorder and a complex trait. Nevertheless, assembly of one gene play the primary role in pathogenesis, with one or more independently inherited modifier genes that influence the phenotype (Dipple & McCabe, 2000). Therefore, for further analysis and mapping study on identified carriers; effects of modifier and linked genes should take to consideration. Actually these phenomena for lung heritable disorders reported before. The phenotypic differences between individuals with CF; one of most lethal and common lung disease; showed effects of single recessive modifier or multiple modifier loci (Zielenski et al., 1999) and (Blackman et al., 2006). Thus, there is no such absolute correlation between phenotype and genotype.

In conclusion, the phenotypic driven screen is an efficient unbiased approach to establish a population of animals that carry a reproducible phenotype. Indeed, this approach is practical to produce phenotypes similar with human diseases. By further analysis and exome sequencing of

carrier animals a reliable animal model could be designed and use as the main tool in field of *in vivo* studies on lung diseases.

Future direction

Mapping Whole Exome Sequencing

Once the samples were collected from recovered interesting phenotype in F4 animals, DNA from 2 WT and 2 putative mutant pups from the same F3 parents, send to BGI for whole exome sequencing. Then, the coding sequence SNPs and the genomic regions linked to the mutation analyze.

To identify the genomic region that contains the mutation of interest; sequencing PCR products of the SNP will conduct. Then by genotyping 10 mutant (MT) animals (F4 or F5), the genomic region that contains the mutation of interest identify. If only one coding SNP in the genomic region linked to the phenotype recognized, then we investigate whether or not this mutation indeed produce the discovered phenotype.

In case of previous published work on mutation in the gene of interest; the complementation studies would be the best strategy for further work. However, if there was not any available mouse line for candidate gene, best approach to proceed is by CRISPRs technology make a mutation candidate gene. Furthermore, after designing a mouse model for identified gene, the molecular analysis and rescue assay would be consider.

In the case of identifying more than one coding SNP in the genomic region, the linkage analysis and complementation studies apply. The linkage analysis requires enough number of mutant animals either F4 or F5 for genotyping. The genotyping can be done by sequencing, HRMA or RFLP analysis. In the mouse to differentiate between coding SNPs that are close together many MT animals will need to be generated and genotyped.

In cases of identifying a couple of candidate causative genes, first of all by insitu hybridization we can confirm the expression of these genes in lung epithelium.

Indeed, linkage analysis in mouse is a problematic and time consuming work due to small litter size, aging the carriers and maximum productivity time of each female mouse; which is 5 times.

Moreover, to fully investigate phenotypes and further studies, F4 and F5 animals of identified carriers would be analyzed in embryonic and older age. For example, for phenotypes with leaky vessels and neonatal respiratory distress syndrome the embryonic analysis of respiratory system will be optimal choice. For inflammatory cell mass accumulation, developing nodule, fibrosis the MRI can be a good approach to investigate the progression of disease.

For the main phenotype of this work which is inflammation, using the MRI to investigate the development and progression of inflammation and fibrosis has been considered. In addition, after identifying candidate causative genes to validate any changes in expression of these genes, the quantitative analysis and molecular assay such as western blot can guide us to validate our hypothesis regarding the identified candidate genes and expression of inflammatory regulators and cytokines. Moreover, in vitro assays on cell lines can help us to micro investigate the identified gene relevant proteins. Another approach is flow cytometry assay to isolate and study cell types involved in formation of inflammation nodules. In this regard particular cells such as pulmonary macrophages or white blood cells can be isolated by using transgene line for mesenchymal cells and flow cytometry assays. Investigating the RNA molecules content presents at infiltrated white blood cells can lead us to identify the precise genetic regulators. Moreover, the carrier can cross with available transgene mouse lines that express inflammatory cytokines under lung epithelial cell promoters.

In the end from each family one identified male carrier will be chosen for sperm freezing for future studies.

ZUSAMMENFASSUNG

Die Identifizierung der Regulationsmechanismen der Lungenzellendifferenzierung durch eine „vorwärts-gerichtete-Screeningmethode in Mäusen

Das Atmungssystem spielt eine wichtige Rolle in der Evolution terrestrischer Lebewesen. Die Lunge umfasst mehr als 40 verschiedene Zellarten, angefangen bei Epithelzellen bis zu residenten Mesenchymzellen. Diese Zellen stammen aus dem Vorderdarmentoderm im Embryonalstadium 9.5d und differenzieren in spezialisierte Zelltypen, die den Atmungsapparat ausbilden. Das komplette Atmungssystem setzt sich zusammen aus den proximal gelegenen zuführenden Luftröhren und dem distal gelegenen Alveolarraum, in welchem der Gasaustausch stattfindet. Verschiedenste in-vivo und in-vitro Studien am Modellorganismus *mus musculus* (Maus) haben schon wertvolle Informationen über Lungenzellabstammung und ihre Differenzierung bzw. Dedifferenzierung während der Entwicklungsphase unter pathologischen Bedingungen gezeigt. Jedoch sind die molekularen Wege, denen diese Differenzierungsprozesse unterliegen, kaum bekannt und könnten auch eine Rolle für pathologische Bedingungen spielen.

Nach Angaben der Weltgesundheitsorganisation (WHO) sind nur begrenzte Möglichkeiten der Behandlungen und Therapien verfügbar, während die Anzahl der Atemwegserkrankungen stetig ansteigt. Für die meist tödlich verlaufenden und am weitesten verbreiteten Lungenerkrankungen wie die Zystische Fibrose (CF), COPD (chronic obstructive pulmonary disease), Idiopathic Pulmonary Fibrosis (IPF) und Lungenkrebs ist im Verlauf keine weitere Behandlung mehr möglich als die Lungentransplantation. Diese Methode ist natürlich beschränkt einsetzbar wegen fehlender Organe und der Immunreaktion, die oftmals zur Abstoßung des transplantierten Organs führt. Die Überlebensrate von Patienten mit Organtransplantation beträgt 4,6 Jahre („What are the risks of lung transplant“). Deshalb besteht eine immer größere Notwendigkeit nach neuen Medikamenten und alternativen Therapien. Die Entwicklung neuer Therapien wird angekurbelt durch die Entdeckung neuer wichtiger Faktoren, die involviert sind in die pathologische und physiologische Lungenzellendifferenzierung. Bedingt durch die komplexen anatomischen Strukturen der Lungenorgane und die Einbeziehung unterschiedlichster Zelllinien in

die Entwicklung und Aufrechterhaltung des Atmungsapparates wären in vivo Studien die beste Option. Um dies zu erreichen, wurden schon viele Anstrengungen unternommen und verschiedenste Tiermodelle erstellt. Tiermodelle stellen das ideale Arbeitsgerät dar, um diese Innovationen voranzutreiben. So gesehen, gibt es zum Beispiel für Cystic Fibrosis (CF) ungefähr 11 CF –Mausmodelle. Die meisten dieser Modelle sind gegen das cystic fibrosis transmembrane conductance regulator (CFTR) Gen gerichtet. Aber auch diese Modelle sind nicht optimal (Mall, Grubb, Harkema, O'Neal, & Boucher, 2004).

Zusätzlich gilt, wenn man ein effizientes IPF-Modell designt, sollte man strukturelle, biochemische und molekulare Charakteristika menschlicher IPF berücksichtigen. Um ein Modell für eine neoplastische Lungenerkrankung zu erstellen, muss man auch eine Kombinationen onkogener Faktoren in Betracht ziehen. Die Herstellung genetisch veränderter Tiere dauert lange, ist teuer und stimmt nicht immer mit der Humanbiologie überein. Im Falle von COPD wurden Tiermodelle durch eine Kombination veränderter Gene erstellt und die Tiere wurden dem Zigarettenrauch ausgesetzt. Jedoch gibt es Unterschiede zwischen der Lunge von Menschen und Mäusen durch chronischem Zigarettenrauchkontakt. Zusätzlich wurde berichtet, dass Veränderungen bedingt durch Zigarettenrauch auch stammabhängig sind. Nichtsdestoweniger werden uns Nagetiermodelle und die Integration dieser Modellsysteme dabei helfen, Erkrankungen und die Behandlung derselben zu verstehen (Kwon & Berns, 2013).

Mit dem Ziel neue Tiermodelle für Lungenerkrankungen zu entwickeln, haben wir uns für einen vorwärts-gerichteten Screeningansatz entschieden. Diese Strategie ermöglicht eine unverfälschte Methode um Gene zu identifizieren, die zu pathologischen Bedingungen führen können. Im Einzelnen wurden männliche Mäuse mit *N*-ethyl-*N*-nitrosourea (ENU) mutagenisiert. Um mutagene Tiere zu kreieren, eignen sich adulte männliche Tiere besser als weibliche, da in den Oozyten aktive DNA- Reparatur stattfindet. ENU mutagenisiert die Ursamenzellen und die Stammzellen der Ovarien. ENU ist ein alkalisiertes Reagenz, welches Punktmutationen verursacht, meistens Transversionen von A nach T, seltener dagegen G/C zu C/G oder kleinere Deletionen der DNA. Während der DNA-Replikation werden die methylierten Basenpaare falsch abgelesen und führen zu Punktmutationen. ENU erzeugt hypomorphe Mutationen, die auch oft bei menschlichen Erkrankungen gefunden werden (Cordes, 2005). Die Dosierung und Wiederholung der ENU-Gabe kann so eingestellt werden, dass man durchschnittlich eine Mutation in jeder 1-5 Megabase (Mb)

oder ungefähr 3000 Veränderungen im haploiden Genom induziert. Tatsächlich befinden sich davon ca. 1,6% in codierenden Regionen (Concepcion, Seburn, Wen, Frankel, & Hamilton, 2004). ENU-Mutagenisierung wirkt sich anders als bei der Bestrahlung, auf den einzelnen Locus aus (Kile & Hilton, 2005). Deshalb trägt jeder mutagene F1-Nachwuchs weniger als 100 mögliche funktionelle Mutationen. Diese Mutationen passieren in Stammzellen der Spermien und werden auf die folgende Generation übertragen nach den Mendel'schen Vererbungsgesetzen. Viele durch ENU verursachte Mutationen führen homozygot im Embryonalstadium zum Tod. Andererseits sind heterozygote oft lebensfähig nach der Geburt. Deshalb wurde das postnatale Stadium ausgesucht, um Phänotypen mit rezessiver Segregation zu isolieren.

Ergebnisse von mutagenisierten Tieren mit ENU zeigten, dass 63% der Mutationen „missense“ waren und bei 26% verursachte es abnormales Splicing. Die restlichen 10% ergaben „nonsense“-Mutationen und 1% verursachten sog. „make-sense“-Mutationen, indem ein Stop-Codon in eine Aminosäure-bindende-Region eingebaut wurde (Noveroske, Weber & Justice, 2000). Vorhergehende Arbeiten mit ENU-Mutagenisierung berichteten von ca. 25 Mutationen mit funktionellen Folgen bei F1-Tieren. Diese Mutationen zeigen hauptsächlich hypomorphe Allele anstelle von Allelen mit hypermorphen (wachsenden), neomorphen (neuen), oder antimorphen (dominant negativ) Funktionen (Cordes, 2005).

Wir interessieren uns eher für Mutationen, die in die Zelldifferenzierung einfließen als mit solchen, die die Frühentwicklung betreffen und die Strukturierung des Atmungssystems. Mit anderen Worten ist es unser Ziel embryonale lebensfähige Mutationen zu isolieren, um die Lugenzelldifferenzierung zu untersuchen. Deshalb entschieden wir uns nach Phänotypen im Atemwegssystem in der F3-Generation postnatal Tag 7 (P7) zu screenen. Wir haben eine umfangreiche histologische und immunhistologische Methodik etabliert um nach Phänotypen zu screenen.

Das folgende Verpaarungsschema nutzten wir um Tierlinien mit heterozygoten Foundern herzustellen. Zuerst wurden männliche C57BL/6 Tiere mit ENU behandelt. Anschließend wurden diese Tiere mit weiblichen C57BL/6 verpaart um die F1-Generation zu bekommen. Diese F1-Männchen sind die Founder. Diese wurden mit Wildtypweibchen C57BL/6 verpaart um die F2-Generation zu bekommen. Durch diesen Ansatz war die Hälfte der F2-Mäuse heterozygot in Bezug auf die durch ENU-induzierten Mutationen, die in den F1-Tieren vorhanden waren. Dann wurden

die F2-Weibchen zurückgekreuzt mit den F1-Founder, um F3-Nachwuchs zu erhalten. Nach dem Mendel'schen Vererbungslehregesetz für einzelne Mutationen gilt folgendes: wenn das F1-Tier und die F2 Eltern heterozygot sind, werden 25% (1:4) der F3 Nachkommen homozygot. Falls diese Mutation folglich einen Effekt auf den Lungenentwicklungssignalweg und auf genetische Regulatoren hat, würden sich bei 25% der F3-Nachkommen Phänotypen entwickeln, die zelluläre und strukturelle Veränderungen der Lunge und des Atemsystems zeigen.

Histologische Analysen wurden auf transversalen und longitudinal verlaufenden Cryoschnitten der Lunge und Trachea durchgeführt. Im P7 Wurf wurden die Tiere zuerst mit PBS durch eine Injektion in den linken Ventrikel perfundiert und die Lungen wurden aufgefüllt mit einem Fixativ mittels einer Infusion über die Trachea. Die proximale Hälfte der Trachea-Proben wurden für histologische und immunhistologische Analysen verwendet und die dorsale Hälfte für eine whole mount-Färbung mit Alzianblau, um die Knorpelspannen der Trachea darstellen zu können. Der linke Lungenlappen wurde für histologische und IHC-Analysen verwendet und der übrige Teil wurde eingefroren. Bei Proben von P0-Tieren wurden alle Lungenlappen, die dem Herzen anhängen, mit 4% PFA (Paraformaldehyd) fixiert, bevor sie in mit OCT gefüllten Kryoeinbetterschälchen bei -80 °C weggefroren wurden. Von jeder weggefrorenen Probe wurden 8µm dicke Kryoschnitte gemacht. Diese Kryoschnitte wurden mit 4% PFA fixiert und anschließend mit Hämatoxylin und Eosin (H&E) gefärbt. Um die Zellverteilung und die Differenzierung der Zellen proximal und dorsal in den Lungenorganen zu sehen, wurden auch immunhistologische Methoden angewendet. Es wurden viele unterschiedliche Marker für Lungen-, Tracheaepithel- und Vorläuferstammzellen, als auch für mesenchymale Zellen benutzt. Zum Beispiel wurden Basalzellen, sogenannte Lungenstammzellen durch eine Färbung mit Cytokeratin 5 sichtbar gemacht. P63 ist gegen Club cells, anti CC10 gegen ciliated cells, anti Acetylated Tubulin zeigt goblet cells, anti Muc5a, AEC1's werden durch T1- alpha erkennbar und für AEC2's benutzt man anti- surfactant protein-C/SP-C. Zusätzlich noch für Endothelzellen Pecam (CD31) und alpha-smooth muscle actin gegen Myofibroblasten. EpCAM- und E-cadherin- Marker wurden verwendet um zu unterscheiden zwischen Fibrosen und Zelltumoren oder dem Phänotyp der Zellanhäufung. Außerdem wurde noch der Vimentinantikörper zur Erkennung von Fibroblasten, mesenchymalen Zellen, die während einer Entzündung eindringen, eingesetzt. Für jeden Nachkommen wurde eine Kombination von mindestens acht verschiedenen Antikörpern für acht unterschiedliche Zellmarker verwendet. Erstens wurde durch eine H&E-Färbung mutmaßliche Mutanten gesammelt.

Als zweites wurde eine IHC-Analyse durchgeführt, um alle Zelltypen zu charakterisieren, die einen Phänotyp bilden.

Außerdem wurde auch eine whole mount Retina-Färbung parallel für 50 Würfe im Alter von P7 durchgeführt, um einen vaskulären Defekt während der Entwicklung zu untersuchen, der durch die ENU Mutagenisierung verursacht wurde.

In meinem Screen etablierte ich 114 Familien und beobachtete 11 verschiedene Phänotypen in 42 unterschiedlichen F2 Weibchen. In jeder Familie wurden mindestens vier F2 - Weibchen pro Founder analysiert. Insgesamt habe ich 500 Würfe im Alter von P0 oder P7 mit durchschnittlich 7 Jungtieren gescreent. Schwere Defekte im Atmungssystem können sich negativ auf das Überleben der Mäuse nach der Geburt auswirken.

Apnoe und Neugeborenenatemstresssyndrom (new born distress syndrome, NRDS), sehr stark entzündete Lungenknötchen, all dies sind Funktionsstörungen, an denen die Neugeborenen im frühen Stadium sterben. Deshalb würde man diese Phänotypen bei P7-Mäusen nicht mehr auffinden. Also werden Familien, die eine hohe Sterblichkeitsrate der Neugeborenen zeigen, nochmals im Stadium P0 gescreent. Von allen gesichteten Würfen waren 8% positiv für Entzündungszellen, die in das alveolare Interstitium eindringen, für Bronchiolitis, Fibrosen, myofibroblastische Hyperplasie, nicht klassifizierbare Zellansammlung, Lungenknötchen, Defekten in der Alveolarisierung und kollabierte Lungenlappen. Die weniger häufigen Lungenphänotypen bestanden in einer Akkumulation von Mucin im alveolaren Epithelium, Hämorrhagie, Alveolar Typ2 Hyperplasie, unterbrochenen Knorpelringen und löchrigem Lungengewebe. Darüberhinaus konnte man in anderen Organen weitere Phänotypen sehen, wie z. B. Zystische Nieren, subkutane Hämorrhagie, Hyperglycemia, abnormal gebogener Rückenknochen, Fettleber, Haarlosigkeit und fehlende Schnurrhaare, asymmetrische blinde Mäuse und Gaumenspalten. Von all diesen Phänotypen wurden diejenigen untersucht, die am signifikantesten, schwerwiegendsten und penetrantesten waren wie z. B. Entzündung und die Infiltration von Entzündungszellen in das Interstitium. Dieser Phänotyp wurde in vier verschiedenen F1-Familien mit semi-dominanter und rezessiver Segregation identifiziert. Die Proben identischer Träger wurden eingesammelt und weitere Analysen sollen mit der F4-Generation weitergeführt werden. Die üblichen Merkmale dieses Phänotyps unter den identifizierten Linien ist die Infiltration von Entzündungszellen in die Alveolen, Akkumulation des

Luftsackes mit weißen Blutzellen. Die Anzahl der alveolaren Makrophagen steigt in den Alveolarsäcken an und die Produktion von ECM verdickt die Alveolarwand und das Sekundärseptum ist beeinträchtigt. Außerdem kommt es zu einer Ablagerung von Fibroblasten in der Entzündungsregion. Sie haben sich transdifferenziert zu Myofibroblasten und werden zu aktivierten Myofibroblasten. Diese Zellen spielen eine wichtige Rolle im EMT Prozess. Die Entzündungszellmasse unterbricht den normalen Gasaustausch in der Lunge und die Lungenflügel fangen an zu kollabieren. Weiterhin verändert sich das Lungengewebe strukturell, um den Defekt des O₂/CO₂-Austausches zwischen AECI und Gefäßen zu kompensieren. Als letztes, durch kreuzen von F3-Carriern, wurden je zwei Proben von möglicherweise mutanten und wildtyp Geschwistern verwendet, um für jede Linie eine komplette Exomsequenzierung auszuführen. In dieser Arbeit war die Screeningeffizienz für den ersten screen 83%.

Alles in allem dienen diese Ergebnisse der Identifizierung sehr interessanter Phänotypen ähnlich der Erkrankung der interstitiellen Lungenentzündung. Diese Phänotypen kann man durch whole exome sequencing nachverfolgen. Nach dem Mapping und der Entdeckung der möglichen Mutationen kann ein Tiermodell erstellt werden, um die Mechanismen des Phänotyps im Detail zu erforschen. Wenn erst einmal die Proben von entdeckten interessanten Phänotypen der F4 Tiere gesammelt wurden, wird die DNA zweier WT und zweier vermutlicher Mutanten der gleichen F3 Eltern ins BGI für whole exome sequencing geschickt. Dann werden die SNPs aus der codierenden Region und der genomischen Regionen, die in direktem Zusammenhang mit der Mutation stehen, analysiert.

Um die genomische Region, die die gewünschte Mutation enthält, zu identifizieren, werden sequenzierte PCR-Produkte der SNP durchgeführt. Durch Genotypisierung von 10 mutierten Tieren (MT) F4 oder F5, wird die genomische Region, die die gewünschte Mutation beinhaltet, identifiziert. Wenn nur ein codierendes SNP in der genomischen Region, verknüpft mit dem Phänotyp bekannt ist, dann untersuchen wir, ob diese Mutation den entdeckten Phänotyp produziert oder nicht. Im Falle von schon veröffentlichten Arbeiten über entdeckte Gene zeigte sich, dass Komplementationsstudien die beste Strategie für zukünftige Arbeiten sind. Jedoch, wenn es keine geeignete Mauslinie für das Kandidatengen gibt, ist der beste Ansatz, diese mit der CRISPR/Cas9-Technik herzustellen. Wenn man mehr als ein codierendes SNP in der Genomregion identifiziert, sind die linkage-Analysen und die Komplementationsstudien bewährte Strategie um

voranzukommen. Zusätzlich kann die Expression identifizierter Kandidatengene und Proteine im Lungenepithel durch quantitative molekulare Assays untersucht werden. Zur vollständigen Untersuchung der Entwicklung von Phänotypen könnten identifizierte Carrier sowohl im Embryonalstadium als auch im späteren Stadium analysiert werden. Beispielsweise kann eine Akkumulation von Entzündungszellen und Fibrosen mittels MRT untersucht werden.

Ein anderer Ansatz ist der Flow Cytometry Assay, um Zellarten zu isolieren und zu untersuchen, die in die Entzündungskaskade involviert sind. In diesem Zusammenhang können spezielle Zellen wie Lungenmakrophagen oder weiße Blutzellen isoliert werden, indem man eine transgene Linie für Mesenchymalzellen und Flow Cytometry Assay benützt. Untersuchungen der RNA von infiltrierten weißen Blutzellen kann uns bei der Identifizierung der genetischen Regulatoren helfen. Weiterhin kann der Carrier mit verfügbaren Mauslinien, die entzündliche Cytokine unter dem Epithelzellpromotor exprimieren gekreuzt werden. Am Ende der Untersuchung einer Familie wird der Samen des männlichen Carrier für eventuelle weitere Analysen eingefroren.

Das Ziel dieses großen “vorwärts-gerichteten Screening”-Projektes war es, Phänotypen zu isolieren, die die Pathologie der meist tödlich verlaufenden humanen Atemwegserkrankungen nachahmen, verursacht durch die Mutagenisierung mit ENU. Tatsächlich wurde durch dieses Projekt eine Mauslinie etabliert, die solch eine Krankheit exprimiert. Weiterhin werden neue Gene und genetische Regulationswege durch Mapping und whole exome sequencing identifiziert durch charakterisierte Carrier. Tiermodelle für entdeckte Gene werden entwickelt, um Mechanismen und Details bestimmter Krankheiten zu charakterisieren. Als Ergebnis davon könnten neue Medikamente und Therapien für Lungenkrankheiten entwickelt werden, deren jetzige einzige Möglichkeit der Behandlung in einer Lungentransplantation mit einer maximalen Überlebensrate von 4,6 Jahren besteht. Zusätzlich validieren die Beobachtungen von phänotypabweichenden Carriern das Konzept der verknüpften Gene und der vielen Gene, die eine Funktion haben bei Lungenerkrankungen. Tatsächlich dürften Genveränderungen und verknüpfte Gene verantwortlich sein für die Expression von Phänotypen mit unterschiedlichsten Merkmalen.

Reference

- Acevedo-Arozena, A., Wells, S., Potter, P., Kelly, M., Cox, R. D., & Brown, S. D. (2008). ENU mutagenesis, a way forward to understand gene function. *Annu Rev Genomics Hum Genet*, 9, 49-69.
- Aoshiba, K., Tsuji, T., Itoh, M., Semba, S., Yamaguchi, K., Nakamura, H., & Watanabe, H. (2014). A murine model of airway fibrosis induced by repeated naphthalene exposure. *Experimental and Toxicologic Pathology*, 66(4), 169-177. doi: <http://dx.doi.org/10.1016/j.etp.2014.01.001>
- APF.
- Barnes, P. J. (2000). Endogenous Inhibitory Mechanisms in Asthma. *American Journal of Respiratory and Critical Care Medicine*, 161(supplement_2), S176-S181. doi: 10.1164/ajrccm.161.supplement_2.a1q4-6
- Barnes, P. J. (2003). Cytokine-directed therapies for the treatment of chronic airway diseases. *Cytokine & Growth Factor Reviews*, 14(6), 511-522. doi: [http://dx.doi.org/10.1016/S1359-6101\(03\)00058-3](http://dx.doi.org/10.1016/S1359-6101(03)00058-3)
- Barth, K., Bläsche, R., & Kasper, M. (2010). T1α/Podoplanin Shows Raft-Associated Distribution in Mouse Lung Alveolar Epithelial E10 Cells. *Cellular Physiology and Biochemistry*, 25(1), 103-112.
- Bartnikas, T. B., Steinbicker, A. U., Campagna, D. R., Blevins, S., Woodward, L. S., Herrera, C., . . . Fleming, M. D. (2013). Identification and characterization of a novel murine allele of Tmprss6. *Haematologica*, 98(6), 854-861. doi: 10.3324/haematol.2012.074617
- Beutler laboratory from <http://www.utsouthwestern.edu/labs/beutler/>
- Blackman, S. M., Deering-Brose, R., McWilliams, R., Naughton, K., Coleman, B., Lai, T., . . . Sibling, S. (2006). Relative Contribution of Genetic and Non-genetic Modifiers to Intestinal Obstruction in Cystic Fibrosis. *Gastroenterology*, 131(4), 1030-1039. doi: 10.1053/j.gastro.2006.07.016
- Brandl, K., Tomisato, W., Li, X., Nepl, C., Pirie, E., Falk, W., . . . Beutler, B. (2012). Yip1 domain family, member 6 (Yipf6) mutation induces spontaneous intestinal inflammation in mice. *Proc Natl Acad Sci U S A*, 109(31), 12650-12655. doi: 10.1073/pnas.1210366109
- Bridges, J. P., Wert, S. E., Noguee, L. M., & Weaver, T. E. (2003). Expression of a human surfactant protein C mutation associated with interstitial lung disease disrupts lung development in transgenic mice. *J Biol Chem*, 278(52), 52739-52746. doi: 10.1074/jbc.M309599200
- Brown, S. D., & Nolan, P. M. (1998). Mouse mutagenesis-systematic studies of mammalian gene function. *Hum Mol Genet*, 7(10), 1627-1633.
- Brusselle, G. G., Bracke, K. R., Maes, T., D'Hulst, A. I., Moerlose, K. B., Joos, G. F., & Pauwels, R. A. (2006). Murine models of COPD. *Pulmonary Pharmacology & Therapeutics*, 19(3), 155-165. doi: <http://dx.doi.org/10.1016/j.pupt.2005.06.001>
- Caruana, G., Farlie, P. G., Hart, A. H., Bagheri-Fam, S., Wallace, M. J., Dobbie, M. S., . . . Bertram, J. F. (2013). Genome-Wide ENU Mutagenesis in Combination with High Density SNP Analysis and Exome Sequencing Provides Rapid Identification of Novel Mouse Models of Developmental Disease. *PLoS ONE*, 8(3), e55429. doi: 10.1371/journal.pone.0055429

- Chen, F., Desai, T. J., Qian, J., Niederreither, K., Lü, J., & Cardoso, W. V. (2007). Inhibition of Tgf β signaling by endogenous retinoic acid is essential for primary lung bud induction. *Development*, 134(16), 2969-2979. doi: 10.1242/dev.006221
- Chen, G., Korfhagen, T. R., Xu, Y., Kitzmiller, J., Wert, S. E., Maeda, Y., . . . Whitsett, J. A. (2009). SPDEF is required for mouse pulmonary goblet cell differentiation and regulates a network of genes associated with mucus production. *J Clin Invest*, 119(10), 2914-2924. doi: 10.1172/JCI39731
- Cho, W.-S., Duffin, R., Poland, C. A., Howie, S. E. M., MacNee, W., Bradley, M., . . . Donaldson, K. (2010). Metal Oxide Nanoparticles Induce Unique Inflammatory Footprints in the Lung: Important Implications for Nanoparticle Testing. *Environmental Health Perspectives*, 118(12), 1699-1706. doi: 10.1289/ehp.1002201
- Chua, F., Gauldie, J., & Laurent, G. J. (2005). Pulmonary Fibrosis. *American Journal of Respiratory Cell and Molecular Biology*, 33(1), 9-13. doi: 10.1165/rcmb.2005-0062TR
- Chuquimia, O. D., Petursdottir, D. H., Periolo, N., & Fernández, C. (2013). Alveolar Epithelial Cells Are Critical in Protection of the Respiratory Tract by Secretion of Factors Able To Modulate the Activity of Pulmonary Macrophages and Directly Control Bacterial Growth. *Infection and Immunity*, 81(1), 381-389. doi: 10.1128/IAI.00950-12
- Cole, T. J., Blendy, J. A., Monaghan, A. P., Kriegstein, K., Schmid, W., Aguzzi, A., . . . Schutz, G. (1995). Targeted disruption of the glucocorticoid receptor gene blocks adrenergic chromaffin cell development and severely retards lung maturation. *Genes Dev*, 9(13), 1608-1621.
- Concepcion, D., Seburn, K. L., Wen, G., Frankel, W. N., & Hamilton, B. A. (2004). Mutation Rate and Predicted Phenotypic Target Sizes in Ethylnitrosourea-Treated Mice. *Genetics*, 168(2), 953-959. doi: 10.1534/genetics.104.029843
- Cordes, S. P. (2005). N-Ethyl-N-Nitrosourea Mutagenesis: Boarding the Mouse Mutant Express. *Microbiology and Molecular Biology Reviews*, 69(3), 426-439. doi: 10.1128/MMBR.69.3.426-439.2005
- Dani S. Zander MD, H. H. P. M., Jaishree Jagirdar MD, Abida K. Haque MD, Philip T. Cagle MD, Roberto Barrios MD (2008). *Molecular Pathology of Lung Diseases* (Vol. 1): Springer New York.
- Di Stefano, A., Maestrelli, P., Roggeri, A., Turato, G., Calabro, S., Potena, A., . . . Sietta, M. (1994). Upregulation of adhesion molecules in the bronchial mucosa of subjects with chronic obstructive bronchitis. *Am J Respir Crit Care Med*, 149(3 Pt 1), 803-810. doi: 10.1164/ajrccm.149.3.7509705
- Dipple, K. M., & McCabe, E. R. B. (2000). Modifier Genes Convert “Simple” Mendelian Disorders to Complex Traits. *Molecular Genetics and Metabolism*, 71(1–2), 43-50. doi: <http://dx.doi.org/10.1006/mgme.2000.3052>
- Dobbs, L. G., & Johnson, M. D. (2007). Alveolar epithelial transport in the adult lung. *Respiratory Physiology & Neurobiology*, 159(3), 283-300. doi: <http://dx.doi.org/10.1016/j.resp.2007.06.011>
- Domyan, E. T., Ferretti, E., Throckmorton, K., Mishina, Y., Nicolis, S. K., & Sun, X. (2011). Signaling through BMP receptors promotes respiratory identity in the foregut via repression of Sox2. *Development (Cambridge, England)*, 138(5), 971-981. doi: 10.1242/dev.053694
- Dove, W. F. (1987). Anecdotal, Historical and Critical Commentaries on Genetics Molecular Genetics of *Mus musculus*: Point Mutagenesis and Millimorgans. *Genetics*, 116(1), 5-8.

- Dow, L. E., & Lowe, S. W. (2012). Life in the Fast Lane: Mammalian Disease Models in the Genomics Era. *Cell*, 148(6), 1099-1109. doi: 10.1016/j.cell.2012.02.023
- George, S. J. (2008). Wnt pathway: a new role in regulation of inflammation. *Arterioscler Thromb Vasc Biol*, 28(3), 400-402. doi: 10.1161/atvbaha.107.160952
- Ghosh, M., Brechbuhl, H. M., Smith, R. W., Li, B., Hicks, D. A., Titchner, T., . . . Reynolds, S. D. (2011). Context-Dependent Differentiation of Multipotential Keratin 14–Expressing Tracheal Basal Cells. *American Journal of Respiratory Cell and Molecular Biology*, 45(2), 403-410. doi: 10.1165/rcmb.2010-0283OC
- Giangreco, A., Reynolds, S. D., & Stripp, B. R. (2002). Terminal Bronchioles Harbor a Unique Airway Stem Cell Population That Localizes to the Bronchoalveolar Duct Junction. *The American Journal of Pathology*, 161(1), 173-182.
- Goodpaster, T., Legesse-Miller, A., Hameed, M. R., Aisner, S. C., Randolph-Habecker, J., & Collier, H. A. (2008). An Immunohistochemical Method for Identifying Fibroblasts in Formalin-fixed, Paraffin-embedded Tissue. *Journal of Histochemistry and Cytochemistry*, 56(4), 347-358. doi: 10.1369/jhc.7A7287.2007
- Hajnalka, S. (2005). *REGULATION OF PROTEOLYTIC ACTIVITY IN LUNG INFLAMMATION: CYTOKINE-INDUCED CHANGES IN PULMONARY EPITHELIAL CELLS*. (PhD), University of Szeged,.
- Hermansen, C. L., & Lorah, K. N. (2007). Respiratory distress in the newborn. *Am Fam Physician*, 76(7), 987-994.
- Hogan, B. L. M., Barkauskas, C. E., Chapman, H. A., Epstein, J. A., Jain, R., Hsia, C. C. W., . . . Morrissey, E. E. (2014). Repair and regeneration of the respiratory system: complexity, plasticity, and mechanisms of lung stem cell function. *Cell Stem Cell*, 15(2), 123-138. doi: 10.1016/j.stem.2014.07.012
- Hooper, S. B., & Wallace, M. J. (2006). Role of the physicochemical environment in lung development. *Clin Exp Pharmacol Physiol*, 33(3), 273-279. doi: 10.1111/j.1440-1681.2006.04358.x
- Hubisz, M. J., Pollard, K. S., & Siepel, A. (2011). PHAST and RPHAST: phylogenetic analysis with space/time models. *Briefings in Bioinformatics*, 12(1), 41-51. doi: 10.1093/bib/bbq072
- Huijbers, I. J., Krimpenfort, P., Berns, A., & Jonkers, J. (2011). Rapid validation of cancer genes in chimeras derived from established genetically engineered mouse models. *Bioessays*, 33(9), 701-710. doi: 10.1002/bies.201100018
- Hussell, T., & Bell, T. J. (2014). Alveolar macrophages: plasticity in a tissue-specific context. *Nat Rev Immunol*, 14(2), 81-93. doi: 10.1038/nri3600
- Initial sequencing and comparative analysis of the mouse genome. (2002). *Nature*, 420(6915), 520-562. doi: http://www.nature.com/nature/journal/v420/n6915/supinfo/nature01262_S1.html
- Jonathan Ewbank, E. V. (2008). *Innate Immunity (Methods in Molecular Biology)*: Humana press.
- Kaartinen, V., Voncken, J. W., Shuler, C., Warburton, D., Bu, D., Heisterkamp, N., & Groffen, J. (1995). Abnormal lung development and cleft palate in mice lacking TGF-beta 3 indicates defects of epithelial-mesenchymal interaction. *Nat Genet*, 11(4), 415-421. doi: 10.1038/ng1295-415
- Kapanci, Y., Desmouliere, A., Pache, J. C., Redard, M., & Gabbiani, G. (1995). Cytoskeletal protein modulation in pulmonary alveolar myofibroblasts during idiopathic pulmonary fibrosis. Possible role of transforming growth factor beta and tumor necrosis factor alpha.

- American Journal of Respiratory and Critical Care Medicine*, 152(6), 2163-2169. doi: 10.1164/ajrccm.152.6.8520791
- Karlinsky, J. B., & Snider, G. L. (1978). Animal models of emphysema. *American Review of Respiratory Disease*, 117(6), 1109-1133.
- Kearney, J. A., Plummer, N. W., Smith, M. R., Kapur, J., Cummins, T. R., Waxman, S. G., . . . Meisler, M. H. (2001). A gain-of-function mutation in the sodium channel gene *Scn2a* results in seizures and behavioral abnormalities. *Neuroscience*, 102(2), 307-317.
- Kile, B. T., & Hilton, D. J. (2005). The art and design of genetic screens: mouse. *Nat Rev Genet*, 6(7), 557-567.
- King Jr, T. E., Pardo, A., & Selman, M. Idiopathic pulmonary fibrosis. *The Lancet*, 378(9807), 1949-1961. doi: [http://dx.doi.org/10.1016/S0140-6736\(11\)60052-4](http://dx.doi.org/10.1016/S0140-6736(11)60052-4)
- Königshoff, M., & Eickelberg, O. (2010). WNT Signaling in Lung Disease. *American Journal of Respiratory Cell and Molecular Biology*, 42(1), 21-31. doi: 10.1165/rcmb.2008-0485TR
- Kreda, S. M., Davis, C. W., & Rose, M. C. (2012). CFTR, Mucins, and Mucus Obstruction in Cystic Fibrosis. *Cold Spring Harbor Perspectives in Medicine*, 2(9), a009589. doi: 10.1101/cshperspect.a009589
- Kwon, M.-c., & Berns, A. (2013). Mouse models for lung cancer. *Molecular Oncology*, 7(2), 165-177. doi: <http://dx.doi.org/10.1016/j.molonc.2013.02.010>
- Lan, J., Ribeiro, L., Mandeville, I., Nadeau, K., Bao, T., Cornejo, S., . . . Kaplan, F. (2009). Inflammatory cytokines, goblet cell hyperplasia and altered lung mechanics in *Lg11(+/-)* mice. *Respiratory Research*, 10(1), 83-83. doi: 10.1186/1465-9921-10-83
- Leslie, K. O., Mitchell, J. J., Woodcock-Mitchell, J. L., & Low, R. B. (1990). Alpha smooth muscle actin expression in developing and adult human lung. *Differentiation*, 44(2), 143-149.
- Mall, M., Grubb, B. R., Harkema, J. R., O'Neal, W. K., & Boucher, R. C. (2004). Increased airway epithelial Na⁺ absorption produces cystic fibrosis-like lung disease in mice. *Nat Med*, 10(5), 487-493. doi: 10.1038/nm1028
- Mason, R. J. (2006). Biology of alveolar type II cells. *Respirology*, 11, S12-S15. doi: 10.1111/j.1440-1843.2006.00800.x
- McCulley, D., Wienhold, M., & Sun, X. (2015). The pulmonary mesenchyme directs lung development. *Current Opinion in Genetics & Development*, 32, 98-105. doi: <http://dx.doi.org/10.1016/j.gde.2015.01.011>
- Metzger, R. J., Klein, O. D., Martin, G. R., & Krasnow, M. A. (2008). The Branching Program of Mouse Lung Development. *Nature*, 453(7196), 745-750. doi: 10.1038/nature07005
- Morrissey, E. E. (2003). Wnt Signaling and Pulmonary Fibrosis. *The American Journal of Pathology*, 162(5), 1393-1397.
- Morrissey, E. E., & Hogan, B. L. M. (2010). Preparing for the First Breath: Genetic and Cellular Mechanisms in Lung Development. *Developmental Cell*, 18(1), 8-23. doi: <http://dx.doi.org/10.1016/j.devcel.2009.12.010>
- Mulugeta, S., Nguyen, V., Russo, S. J., Muniswamy, M., & Beers, M. F. (2005). A Surfactant Protein C Precursor Protein BRICHOS Domain Mutation Causes Endoplasmic Reticulum Stress, Proteasome Dysfunction, and Caspase 3 Activation. *American Journal of Respiratory Cell and Molecular Biology*, 32(6), 521-530. doi: 10.1165/rcmb.2005-0009OC
- Nolan, P. M., Peters, J., Strivens, M., Rogers, D., Hagan, J., Spurr, N., . . . Hunter, J. (2000). A systematic, genome-wide, phenotype-driven mutagenesis programme for gene function studies in the mouse. *Nat Genet*, 25(4), 440-443. doi: 10.1038/78140

- Noveroske, J. K., Weber, J. S., & Justice, M. J. (2000). The mutagenic action of N-ethyl-N-nitrosourea in the mouse. *Mamm Genome*, 11(7), 478-483.
- Pardo, A., Gibson, K., Cisneros, J., Richards, T. J., Yang, Y., Becerril, C., . . . Kaminski, N. (2005). Up-Regulation and Profibrotic Role of Osteopontin in Human Idiopathic Pulmonary Fibrosis. *PLoS Medicine*, 2(9), e251. doi: 10.1371/journal.pmed.0020251
- Pauwels, P. R. A., & Rabe, K. F. (2004). Burden and clinical features of chronic obstructive pulmonary disease (COPD). *Lancet*, 364(9434), 613-620. doi: 10.1016/S0140-6736(04)16855-4
- Peifer, M., Fernandez-Cuesta, L., Sos, M. L., George, J., Seidel, D., Kasper, L. H., . . . Thomas, R. K. (2012). Integrative genome analyses identify key somatic driver mutations of small-cell lung cancer. *Nat Genet*, 44(10), 1104-1110. doi: <http://www.nature.com/ng/journal/v44/n10/abs/ng.2396.html> - supplementary-information
- Pongracz, J. E., & Stockley, R. A. (2006). Wnt signalling in lung development and diseases. *Respiratory Research*, 7(1), 15-15. doi: 10.1186/1465-9921-7-15
- Rawlins, E. L., Clark, C. P., Xue, Y., & Hogan, B. L. M. (2009). The Id2(+) distal tip lung epithelium contains individual multipotent embryonic progenitor cells. *Development (Cambridge, England)*, 136(22), 3741-3745. doi: 10.1242/dev.037317
- Rawlins, E. L., & Hogan, B. L. M. (2006). Epithelial stem cells of the lung: privileged few or opportunities for many? *Development*, 133(13), 2455-2465. doi: 10.1242/dev.02407
- Rawlins, E. L., Okubo, T., Xue, Y., Brass, D. M., Auten, R. L., Hasegawa, H., . . . Hogan, B. L. M. (2009). The role of Scgb1a1(+) Clara cells in the long-term maintenance and repair of lung airway, but not alveolar, epithelium. *Cell Stem Cell*, 4(6), 525-534. doi: 10.1016/j.stem.2009.04.002
- Rawlins, E. L., Ostrowski, L. E., Randell, S. H., & Hogan, B. L. M. (2007). Lung development and repair: Contribution of the ciliated lineage. *Proceedings of the National Academy of Sciences of the United States of America*, 104(2), 410-417. doi: 10.1073/pnas.0610770104
- Reynolds, S. D., Giangreco, A., Power, J. H. T., & Stripp, B. R. (2000). Neuroepithelial Bodies of Pulmonary Airways Serve as a Reservoir of Progenitor Cells Capable of Epithelial Regeneration. *The American Journal of Pathology*, 156(1), 269-278.
- Rock, J., & Königshoff, M. (2012). Endogenous Lung Regeneration. *American Journal of Respiratory and Critical Care Medicine*, 186(12), 1213-1219. doi: 10.1164/rccm.201207-1151PP
- Rock, J. R., Onaitis, M. W., Rawlins, E. L., Lu, Y., Clark, C. P., Xue, Y., . . . Hogan, B. L. M. (2009). Basal cells as stem cells of the mouse trachea and human airway epithelium. *Proceedings of the National Academy of Sciences of the United States of America*, 106(31), 12771-12775. doi: 10.1073/pnas.0906850106
- Rudin, C. M., Durinck, S., Stawiski, E. W., Poirier, J. T., Modrusan, Z., Shames, D. S., . . . Seshagiri, S. (2012). Comprehensive genomic analysis identifies SOX2 as a frequently amplified gene in small-cell lung cancer. *Nat Genet*, 44(10), 1111-1116. doi: <http://www.nature.com/ng/journal/v44/n10/abs/ng.2405.html> - supplementary-information
- Russell, L. B., Hunsicker, P. R., Cacheiro, N. L., Bangham, J. W., Russell, W. L., & Shelby, M. D. (1989). Chlorambucil effectively induces deletion mutations in mouse germ cells. *Proceedings of the National Academy of Sciences of the United States of America*, 86(10), 3704-3708.
- Salinger, A. P., & Justice, M. J. (2008). Mouse Mutagenesis Using N-Ethyl-N-Nitrosourea (ENU). *CSH Protoc*, 2008, pdb prot4985. doi: 10.1101/pdb.prot4985

- Schittny, J. C., & Burri, P. H. (2008). Development and growth of the lung. *Fishman's pulmonary diseases and disorders*, 1, 91-115.
- Scotton, C. J., & Chambers, R. C. (2007). Molecular targets in pulmonary fibrosis*: The myofibroblast in focus. *Chest*, 132(4), 1311-1321. doi: 10.1378/chest.06-2568
- Selman, M., Pardo, A., & Kaminski, N. (2008). Idiopathic Pulmonary Fibrosis: Aberrant Recapitulation of Developmental Programs? *PLoS Medicine*, 5(3), e62. doi: 10.1371/journal.pmed.0050062
- Shannon, J. M., & Hyatt, B. A. (2004). Epithelial-Mesenchymal Interactions in the Developing Lung. *Annual Review of Physiology*, 66(1), 625-645. doi: 10.1146/annurev.physiol.66.032102.135749
- Shapiro, S. D. (2000). Animal models for chronic obstructive pulmonary disease: age of klotho and marlboro mice. *Am J Respir Cell Mol Biol*, 22(1), 4-7. doi: 10.1165/ajrcmb.22.1.f173
- Siggs, O. M., Xiao, N., Wang, Y., Shi, H., Tomisato, W., Li, X., . . . Beutler, B. (2012). iRhom2 is required for the secretion of mouse TNFalpha. *Blood*, 119(24), 5769-5771. doi: 10.1182/blood-2012-03-417949
- Simon, M. M., Mallon, A.-M., Howell, G. R., & Reinholdt, L. G. (2012). High throughput sequencing approaches to mutation discovery in the mouse. *Mamm Genome*, 23(0), 499-513. doi: 10.1007/s00335-012-9424-0
- Studer, S. M., & Kaminski, N. (2007). Towards Systems Biology of Human Pulmonary Fibrosis. *Proceedings of the American Thoracic Society*, 4(1), 85-91. doi: 10.1513/pats.200607-139JG
- Sutherland, L. M., Edwards, Y. S., & Murray, A. W. (2001). Alveolar type II cell apoptosis. *Comparative Biochemistry and Physiology Part A: Molecular & Integrative Physiology*, 129(1), 267-285. doi: [http://dx.doi.org/10.1016/S1095-6433\(01\)00323-3](http://dx.doi.org/10.1016/S1095-6433(01)00323-3)
- Tadokoro, T., Wang, Y., Barak, L. S., Bai, Y., Randell, S. H., & Hogan, B. L. M. (2014). IL-6/STAT3 promotes regeneration of airway ciliated cells from basal stem cells. *Proceedings of the National Academy of Sciences of the United States of America*, 111(35), E3641-E3649. doi: 10.1073/pnas.1409781111
- UT Mutagenetix center. from <http://mutagenetix.utsouthwestern.edu/>
- Volckaert, T., & De Langhe, S. (2014). Lung epithelial stem cells and their niches: Fgf10 takes center stage. *Fibrogenesis & Tissue Repair*, 7, 8-8. doi: 10.1186/1755-1536-7-8
- W.E. Crusio , R. T. G. (1999). *Hand Book of Molecular Genetics Techniques for Brain and behavior reserach* (Vol. 13): ELSEVIER.
- Wansleeben, C., van Gurp, L., Feitsma, H., Kroon, C., Rieter, E., Verberne, M., . . . Meijlink, F. (2011). An ENU-Mutagenesis Screen in the Mouse: Identification of Novel Developmental Gene Functions. *PLoS ONE*, 6(4), e19357. doi: 10.1371/journal.pone.0019357
- Watson, Julie K., Rulands, S., Wilkinson, Adam C., Wuidart, A., Ousset, M., Van Keymeulen, A., . . . Rawlins, Emma L. Clonal Dynamics Reveal Two Distinct Populations of Basal Cells in Slow-Turnover Airway Epithelium. *Cell Reports*, 12(1), 90-101. doi: 10.1016/j.celrep.2015.06.011
- Weber, J. S., Salinger, A., & Justice, M. J. (2000). Optimal N-Ethyl-N-nitrosourea (ENU) doses for inbred mouse strains. *genesis*, 26(4), 230-233. doi: 10.1002/(SICI)1526-968X(200004)26:4<230::AID-GENE20>3.0.CO;2-S
- Yin, X., Meng, F., wang, Y., Xie, L., Kong, X., & Feng, Z. (2013). Surfactant protein B deficiency and gene mutations for neonatal respiratory distress syndrome in China Han ethnic population. *International Journal of Clinical and Experimental Pathology*, 6(2), 267-272.

- Zheng, D., Limmon, G. V., Yin, L., Leung, N. H. N., Yu, H., Chow, V. T. K., & Chen, J. (2013). A Cellular Pathway Involved in Clara Cell to Alveolar Type II Cell Differentiation after Severe Lung Injury. *PLoS ONE*, 8(8), e71028. doi: 10.1371/journal.pone.0071028
- Zielenski, J., Corey, M., Rozmahel, R., Markiewicz, D., Aznarez, I., Casals, T., . . . Tsui, L. C. (1999). Detection of a cystic fibrosis modifier locus for meconium ileus on human chromosome 19q13. *Nat Genet*, 22(2), 128-129. doi: 10.1038/9635

Link

<https://science.nichd.nih.gov/confluence/display/zcore/Zebrafish+mutants+vs.+mouse+mutants%3A+a+comparison>

Acknowledgements

I sincerely thank Professor Dr. Didier Stainier for giving me the opportunity to study and work as a doctoral student and research assistant in his laboratory and for his continuous support, patience and motivational advice. I would like to acknowledge Dr. Hyun-Taek Kim, Dr. Wenguang Yin and Dr. Zacharias Kontarakis, for their advices, guidance and productive inputs in my project. I also would like to acknowledge Dr. Markus Bussen for his collaborations and advice regarding the ENU forward genetic screening and Dr. Dong Yao and Carmen Bütner who also were participating and collaborate in screening. In addition, I express my sincere gratitude to Prof. Dr. Anna Starzinski Powitz. I would also like to express my gratitude to Dr. Bilge Reishauer for her advice regarding my PhD studies. Finally, I would like to thank my father and family for their continuous support and I dedicate this work to my father and my family, who have supported and motivated me.

CURRICULUM VITAE

Ziba Jaberansari

Date of Birth: 10.Sep.1984 Place of Birth: Tehran, Iran

Home address: Kurstrasse 19, Bad Nauheim, Hessen, Germany, 61213

Home Phone: + 49 (0)60323079024 Cell phone: +49 (0)176 84169086

Email: ziba.jaberansari@mpi-bn.mpg.de jaber011@umn.edu

Web page: <http://www.mpi-hlr.de/index.php?id=748>

LinkedIn: <https://de.linkedin.com/in/ziba-jaberansari-39156a37>

Education and Training

**PhD candidate; Developmental Genetics, Dep. III. Prof. Stainer
Goethe University, Am Main Frankfurt , Faculty of life sciences**

Expected graduation: March 2016

M.S. in Stem Cell Biology, Medical school, University of Minnesota, USA

Sep 2010 -May 2012

B.S. in Laboratory Sciences Shaheed Beheshti University Medical Sciences, Iran May2008

Research Experience

Max Planck Institute for Heart and Lung Research, Developmental Genetics Jan.2013-Dec 2015

PhD research: An ENU forward genetic screening in mouse to identify regulators of lung cell differentiation

PI and supervisor: Prof. Dr. Didier Stainier

Stem Cell Institute, University of Minnesota, MN,USA

July2012-Dec2012

Research: Studying impacts of VEGF on Myoblast growth and differentiation

PI and supervisor: Dr. Atsushi Asakura

University of Minnesota, Masonic Cancer Center Dr. Angela Panoskaltsis Mortari Lab

Jan.2011-May 2012

Master's Thesis Project:

DECELLULARIZED LUNG MATRIX AS A SCAFFOLD FOR MOUSE LUNG STEM CELLS

PI and supervisor: Dr. Angela Panoskaltsis Mortari

BS in Laboratory Sciences

October2006- May 2008

Shaheed Beheshti University of Medical Sciences, Paramedical College, Tehran, Iran

-Study of usefulness of Ratio Free/Total PSA in Prostate cancer diagnosis

Advisor: Dr. Houshang Amirrasouli

AA in Clinical Laboratory Sciences

October 2003-Jan. 2006

Islamic Azad University, Medical Sciences branch, Tehran, Iran

Internship

October 2006-June 2008

Clinical Labs in: 1) Labbafi Nejhad Hospital (Ophthalmology center), 2) Mofid *Children* Hospital, 3) Gholestan *General* Hospital, 4) Naft *General* Hospital, and 5) Iranmehr *General* Hospital, Tehran, Iran

Science Lab Skills and Experience

Histology techniques:

Histological and immunohistological analysis as a main screener and lung morphologist, Cryosection and Immunohistochemistry staining and other tissue staining; Light and Fluorescent microscopes, Confocal microscope with supervision, animal surgery, Dissecting and handling rodents; mouse retinal dissection and whole mount staining, biopsy and preparation of mouse samples and histology techniques,

Cell culture and stem cell isolation techniques:

Stem cell culture and sterile technique and 3D cell cultures; mammalian and lung progenitor cells and Myoblasts cell culture, Decellularizing organ and 3-D bioscaffold, designing a bio reactor, isolation of progenitor cells; Flow cytometry (LSRII) and FlowJo software; lung progenitor cell culture in a bio 3D scaffolds

Molecular biology techniques:

DNA and RNA extraction, PCR; gel electrophoresis and analysis; RT-PCR

Other skills:

Familiar with scientific documentation, animal surgery; bio ethics and animal regulation, design and setting up a screening project, managing mouse colony and familiar with mouse husbandry, familiar with isolation of myoblasts,

Clinical Lab Skills:

Hematology lab: proficient morphologist, experienced in drawing blood, preparing blood cell slides, and working with a light microscope and cell counter.

-Serology and Immunology and Biochemistry lab: blood bank and blood transfusion analysis; familiar with Elisa, vis. absorption spectrophotometer and flame photometer.

-Microbiology lab: culturing bacteria in various media, preparing media, culturing blood for analyzing blood-borne bacteria; as a clinical laboratory student expert in virology and parasitology lab.

Workshops, conferences and certificates:

Talk and posters:

Presented at annual Retreat of International School of Max Planck Institute Research School
(IMPRS-HLR) **2013-2015**

-Poster presented at Excellence Cluster Cardio Pulmonary System (ECCPS) **June 2015**

-Course on
laboratory animals; Federation of European Laboratory Animal Science Associated
(FELASA)

Max Planck Institute for heart and lung research, Bad Nauheim, Germany **Spring 2015**

-Participated in
The 1st International Summer School: Developmental Biology and Stem Cells.
Royan Institute, Iran (www.royaninstitute.org) **July 2010**

Talks at Journal clubs:

-Journal club of Department III; Max planck Institute for Heart and Lung Research
Bad Nauheim, Germany, 2013-2015

-Journal club of Stem Cell Institute of University of Minnesota, Minneapolis, MN,
September 2010-October 2011

-Attended workshop of culture, harvest & banding of peripheral blood lymphocyte
chromosomes July 2010

-Attended workshop of introduction to elementary molecular methods.
June 2010

Royan Institute, Iran (www.royaninstitute.org)

Others:

A PhD committee member and representative from Dep:III at Max Planck Institute for
Heart and lung research, Bad nauheim 2014-2015

International Max Planck Research school for heart and lung research (IMPRS-HRL)
<http://imprs.mpi-hlr.de/> **Graduated: Spring 2015**

Consultant and member of Persian Students Organization of University of Minnesota, USA
<http://www.tc.umn.edu/~psom/> **2011-2013**

Language skills: Native Persian, Proficient English, Beginner in Deutsch

